Naphthobipyrrole derived novel π-extended porphyrinoids: Synthesis, structure and optical properties

A Thesis Submitted for the Degree of

DOCTOR OF PHILOSOPHY

By
Tridib Sarma

School of Chemistry
University of Hyderabad
Hyderabad-500 046
INDIA

September 2013

Dedicated

to

My Parents

CONTENTS

DECLARATION

I hereby declare that the matter embodied in the thesis entitled **"*Naphthobipyrrole derived novel π-extended porphyrinoids: Synthesis, structure and optical properties*"** is the result of investigations carried out by me in the School of Chemistry, University of Hyderabad, Hyderabad, India under the supervision of **Dr. Pradeepta K. Panda** and it has not been submitted elsewhere for the award of any degree or diploma or membership, etc.

In keeping with the general practice of reporting scientific investigations, due acknowledgements have been made wherever the work described is based on the findings of other investigators. Any omission or error that might have crept in is sincerely regretted.

September 2013 **Tridib Sarma**

UNIVERSITY OF HYDERABAD

Central University (P.O.), Hyderabad-500046, INDIA

Dr. Pradeept K Panda
Associate Professor
School of Chemistry

Tel: 91-40-23134818 (Office)
Fax: 91-40-23012460
E-mail: pkpsc@uohyd.ernet.in
pradeepta.panda@uohyd.ac.in
pradeepta.panda@gmail.com

CERTIFICATE

This is to certify that the work described in this thesis entitled "***Naphthobipyrrole derived novel π-extended porphyrinoids: Synthesis, structure and optical properties***" has been carried out by Mr. Tridib Sarma under my supervision and the same has not been submitted elsewhere for any degree.

Dean
School of Chemistry
University of Hyderabad
Hyderabad-500 046
India

Dr. Pradeepta K Panda
(Thesis supervisor)

PREFACE

The present thesis entitled "Naphthobipyrrole derived novel π-extended porphyrinoids: Synthesis, structure and optical properties" has been divided into seven chapters. Basically it describes synthesis and exploration of various conformationally rigid annulated π-extended porphyrinoids derived from alkylated naphthobipyrroles. In comparison to porphyrins, π-extension in other porphyrinoids viz. isomeric, contracted or expanded porphyrins are rarely explored. A bunch of π-extended porphyrins that has been synthesized till date reviewed very recently by Sessler and coworkers, which clearly reflects that most of the π-extended porphyrinoids has been reported in last few years. Thus, the chemistry of π-extended isomeric and expended porphyrinoids is evolving very rapidly. A brief outline of the content included in the thesis is presented below.

In **chapter 1** a very concise description of isomeric, contracted and expanded porphyrins, with a special emphasis on expanded porphyrin and its π-extended annulated analogue has been presented. **Chapter 2** gives a brief account of the methods and materials used in our investigation. C**hapter 3** provides a general route towards synthesis of alkylated naphthobipyrroles along with synthesis of dinaphthoporphycenes derived from these alkylated naphthobipyrroles. Detail chemistry of dinaphthoporphycenes is also deliberated. **Chapter 4** deals with the synthesis and characterization of cyclo[4]naphthobipyrroles. Their photophysical properties are discussed along with few very interesting aspects of these macrocycles are pointed out. In **chapter 5**, syntheses of alkylated naphthosapphyrins that possess alkyl substitution in all β-pyrrolic positions, along with one which bears alkyl substituents in all β-pyrrolic positions except the ones on the pyrrole moiety opposite to the bipyrrolic unit, are outlined. A previously unknown analogous octaalkylsapphyrin derivative with an unsubstituted pyrrole ring is also synthesized. A comparative discussion of spectral properties of this molecule has been made with those of naphthosapphyrins. In **chapter 6** π-extended BODIPY dyes derived from alkylated naphthobipyrrole are discussed. Finally, **chapter 7** summarizes the findings of the present investigation along with the future scope.

September 2013 **Tridib Sarma**

Acknowledgement

No serious effort in life is totally accomplished by one self. This dissertation work is no exception. Consequently a large number of people involved in the whole process that helped me directly or indirectly to carry out my PhD work smoothly during my 6 years long (!) stay in HCU. It is virtually impossible for me to memorize and name each and every person at this moment. I would like to express my apology in advance to those that falls in this category. It's a reflection of my inadequate memory, not your contribution.

First and foremost, I would like to take this golden opportunity to thank my supervisor Dr. Pradeepta K. Panda for his generous support over the years and for giving me the opportunity to explore this exciting field of chemistry.

I would like to thank the former and present Dean, School of Chemistry, for their constant inspiration and for allowing me to use the available facilities. I am extremely thankful individually to all the faculty members of the School for their kind help and cooperation at various stages of my stay in the campus. I thank all the non-teaching staff of the School of Chemistry and CIL for their assistance on various occasions.

Council of Scientific and Industrial Research (CSIR), India is gratefully acknowledged for providing me a fellowship.

I am also grateful to our collaborators who helped make the present work much better. Dr. S. Venugopal Rao, ACRHEM, University of Hyderabad and his research group, particularly P. T. Anusha and Debasish Swain are gratefully acknowledged for carrying out all NLO studies included in the thesis. I would also like to thank Prof. J.-i. Setsune (Kobe University, Japan) for being part of our collaboration.

My sincere thanks also extends to Prof. A. Samanta, Prof. M. Durga Prasad, School of Chemistry, UOHYD; Prof. S. N. Kaul, School of Physics, UOHYD and their respective groups for their help during PhD work.

A special mention regarding my lab mates is a must, I would say. I have been fortunate enough to enjoy each of your company like a family member. A big thank to all of you: Naren, Sanjeev, Ritwik, Brijesh, Nandakishore, Anup, Sathish, Obaiah, Vikranth, Prameela, Dr. Raju, Sandip, Prity, Dr. Balakrishna, Dr. Santhosh, and Dr. Manashi. I would also wish to thank Kiran Kumar, Chinnaayyaswamy, Shamimul, Rajesh, Promod, Rajasekhar, Samatha, Sathish, Mahesh, Vidyasagar, Shantimoy, Sauradip, Srinivas, Preety, Sabhapati, Suganya, Archana, Sanjib, Arghya, Pramit, Bilash, Arpita, Subham, Sreedhar, Shravani, Gopi Sudheer, Ramprasad, Swayam P and Sravan kumar who came at different time as a project students during my stay.

My pleasant association with some friends and seniors inside and outside UOH such as Ranjit, Sanjeev, Anoop Gurung, Abdul, Pabitra, Gauranga, Bipul Da, Naba Da, Anil da, Gautam da, Binoy da, Bipul, Satya, Prasenjit, Alankar, Jahnu, Debabrot, Moushumi, Barnali, Monima,

Swapan, Tiken, Kamble, Taya, Jayanta, Milan, Gokul, Bhokti, Debanath, Sumit, Nobojyoti, Amir, Purbalakshmi, Deep Jyoti, Sulendar, Lucky Bhai, Tapan Bhai, Chetan sir, Sanjeev bhai and Bhanu is unforgettable.

I would like to thank my school of chemistry seniors and friends Malay da, Abhijit da, Prashant da, Bhaswati di, Teja bhai, Sashi, Santhos, Kumar, Ganesh, Shrinivas, Ravindra, Naveen, Manoj, Ramana, Vanaja, Saktivel, Tamil, Sudhanshu, Dinu, Satyajit, Raja, Nayan, Satpal, Rajeswar, Arindam, Arun, Sandeep, Mehboob, Arjun, Anish, Ganesh, Vignesh, Dharavath, Sridevi, Ram babu, Yashin, Krishnachary, Tanmoy, Praveen, Sanatan, Srinivas, Karunakar, Sekhar, Gupta, Hari, Rajgopal, Sugato, Rudra, Sathish, Suman, R. Kishore, Kishore, Ramesh, Anand, Sudalai, Palash, Seshadri, Venu, Suryanayaran, Rajesh, Ramesh, Anji, Srinivas, D. K., Krishnachaitanya, Bharat, Supratim, Pramiti, Chandrasekhar, Ragavaiah, Lingaiah, Ramu, Koushik, Nabendu, Malkappa, Babu and all others whose names are not mentioned due to limited space.

I would like to thank Dr. Diganta Choudhury and Prof. D. K. Kakati for their constant support. I am also grateful to all other faculty members of the Department of Chemistry, B. Barooah College and Gauhati University. All my school teachers are hereby gratefully acknowledged.

My friends and seniors whom I met at different level of my educational life is sincerely acknowledged. Dhruba, Rupam, Debajit, Indrajit, Monima, Moushumi, Mridusmita, Deepnakar, Harjoyti, Pranab, Saranga, Amar, Pradyut da, Pankaj da, Hiten da, Anindita ba, Utpal da, Anshuman, Bijoy, Ajanta, Tun Tun, Kamal, Shymalee, Mouchumi, Mandakini, Ganesh da, Dhruba da, Priyanka, Sujata, Bapan, Prasenjit, Sohan Raben da, Medhi, Diganta, Manoj, Bijiyeta, Anshumala, Hemanta, Pranjit to name a few them.

I wish to thank my juniors Bidyut, Kashyap, Bilash, Prajwalita, Anamika, Upama, Rupinder, Neha and who visited our department under different programmes with whom I spent some unforgettable moment.

Finally, I would like to express my love and gratitude to my parents and my sister for their unconditional love and blessings. They made me what I am today and I owe everything to them. Dedicating this thesis to them is a minor recognition for their relentless support and love.

September 2013 **Tridib Sarma**

University of Hyderabad
Hyderabad-500 046
India

List of abbreviations

Anhyd.	anhydrous
2D	Two-dimensional
2PA	Two photon-absorption
3PA	Three photon-absorption
BODIPY	Boron-dipyrromethene
br	Broad
Calcd.	Calculated
Conc.	Concentaration
Cy	Cyanine
D	Doublet
DBU	1,8-Diazabicyclo[5.4.0]undec-7-ene
DCM	Dichloromethane
DCB	1,2-Dichlorobenzene
DCE	1,2-Dichloroethane
DDQ	2,3-Dichloro-5,6-dicyano-1,4-benzoquinone
DMSO	Dimethylsulfoxide
DMF	N,N-Dimethylformamide
DMAc	N,N-Dimethylacetamide
DOTC-I	3,3´-Diethyloxatricarbocyanine iodide
EPR	Electron paramagnetic resonance
fs	femto second
Equiv.	Equivalent
FDA	Food and Drug Administration
HRMS	High resolution-mass spectrometry
HOMO	Highest occupied molecular orbital
h	Hour (s)
KFL	Keio Fluors
LUMO	Lowest unoccupied molecular orbital

LCMS	Liquid chromatography mass spectrometry
m	Multiplet
m	Meta
m/z	Mass/charge
min	Minute (s)
naph	Naphthalene
Ph	Phenyl
Py	Pyrrole
NMR	Nuclear magnetic resonance
NOESY	Nuclear Overhauser effect spectroscopy
NLO	Non-linear optics
NIR	Near infra-red
o	Ortho
ORTEP	Oak Ridge Thermal Ellipsoid Program
p	Para
ps	Pico second
i-Pr	*iso*-Propyl
n-Pr	*n*-Propyl
s	Singlet
TBAF	Tetrabutylammonium fluoride
TFA	Trifluoroacetic acid
THF	Tetrahydrofuran
TLC	Thin layer chromatography
t	Triplet
p-TsOH	para-Toluene sulfonic acid
TEA	Triethylamine
UV-Vis	Ultraviolet-Visible
UV-Vis-NIR	Ultraviolet-Visible-Near infrared
XRD	X-Ray diffraction

CHAPTER 1

Introduction

1.1 Background

Porphyrins are naturally occurring tetrapyrrolic macrocycles that are ubiquitous in nature and often referred to as pigments of life.[1] This is because life depends on many biological processes that are performed or catalyzed by proteins containing porphyrin or its derivatives. For instance chlorophyll containing a reduced Mg(II)-porphyrin, plays a vital role in photosynthesis, which converts light to chemical energy, producing oxygen. This oxygen is transported, stored, and reduced in various ways by heme containing proteins, viz. hemoglobin, myoglobin, hemerythrin etc. in many organisms including mammals. In addition, porphyrins function as an excellent metal-complexing ligand. Therefore, porphyrins remain of fundamental interest to researchers and arguably the most widely studied macrocycle among all ring system present.[2] Consequently

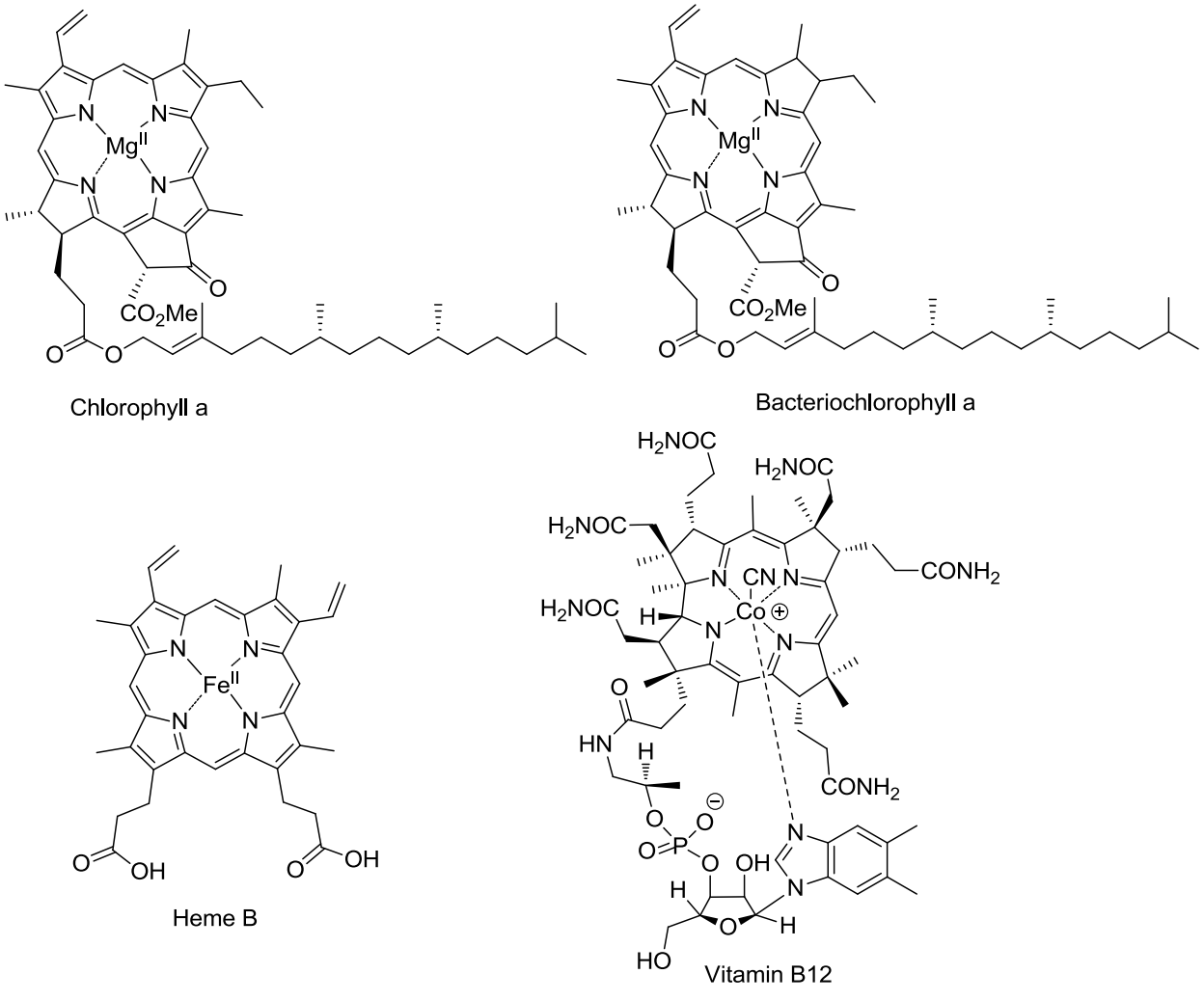

Figure 1.1 Some of the naturally occurring porphyrinoids of biological importance.

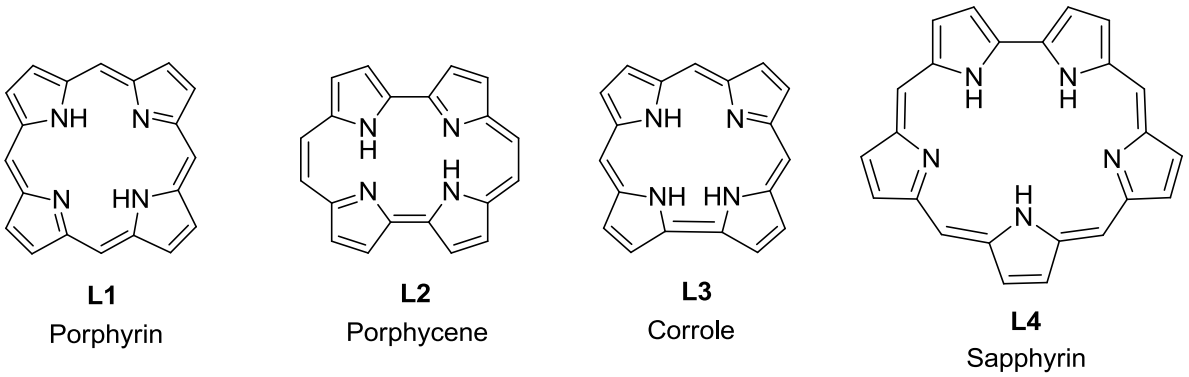

Figure 1.2 Examples of isomeric, contracted and expanded porphyrins.

the rich chemistry of porphyrin stimulates interest among the researcher to study non-porphyrin polypyrrolic macrocycles.[3] As a result a new area of research emerged where principal objective is to generate synthetic systems that bear structural resemblance to naturally occurring porphyrins while being chemically quite different. Thus three major direction of research evolved involving synthesis of expanded, contracted and isomeric porphyrinoids (Figure 1.2).

1.2 Contracted and isomeric porphyrins

Among the contracted isomers of porphyrin the corrole **L3** is the most notable one.[4] Corrole can be considered as an intermediate between porphyrin and corrin, the chromophoric constituent of vitamin B_{12}. First synthesis of corrole was achieved by A. W. Johnson in 1964.[4a] Free-base corrole, like porphyrin is an 18π aromatic macrocycle. Unlike porphyrin, corroles are strong acids and forms stable anions with aqueous alkali. Corrole also acts as a trianionic ligand and stabilizes metal ions in high oxidation state.[2a,3b] However, chemistry of corrole remains underdeveloped compared to porphyrin owing to formidable synthetic challenges. In 1999, research group of Zeev Gross reported a facile synthetic route towards stable *meso*-triaryl corrole.[5] This triggered interest in corrole, which was reflected in large number of scientific reports appeared thereafter describing synthesis of new corroles and their versatile applications including catalysis, dye sensitized solar cell, sensors and medicinal applications.[6] The most widely studied isomer of porphyrin is the porphycene **L2** reported by Vogel in 1986.[7] A detail description about this macrocycle is presented in chapter 3 of this thesis.

1.3 Expanded porphyrins

According to definition put forwarded by Sessler in his review paper, an expanded porphyrin is

defined as a macrocyclic compound containing pyrrole, thiophene, furan or other heterocyclic subunit connected directly or through one or more spacer unit in such a way that internal ring pathway contains at least 17 atoms.[8] The history of expanded porphyrin begins with serendipitous discovery of sapphyrin (**L4**) during the synthesis of vitamin B_{12} by Woodward and coworkers. He briefly mentioned about the formation of a blue color compound during the synthesis of vitamin B_{12} at the aromaticity conference in Sheffield, UK, 1966 and subsequently characterized as sapphyrin and published the synthetic detailed in 1983 only.[9] However, the first authentic work describing synthesis of sapphyrin was published much before by Johnson's group

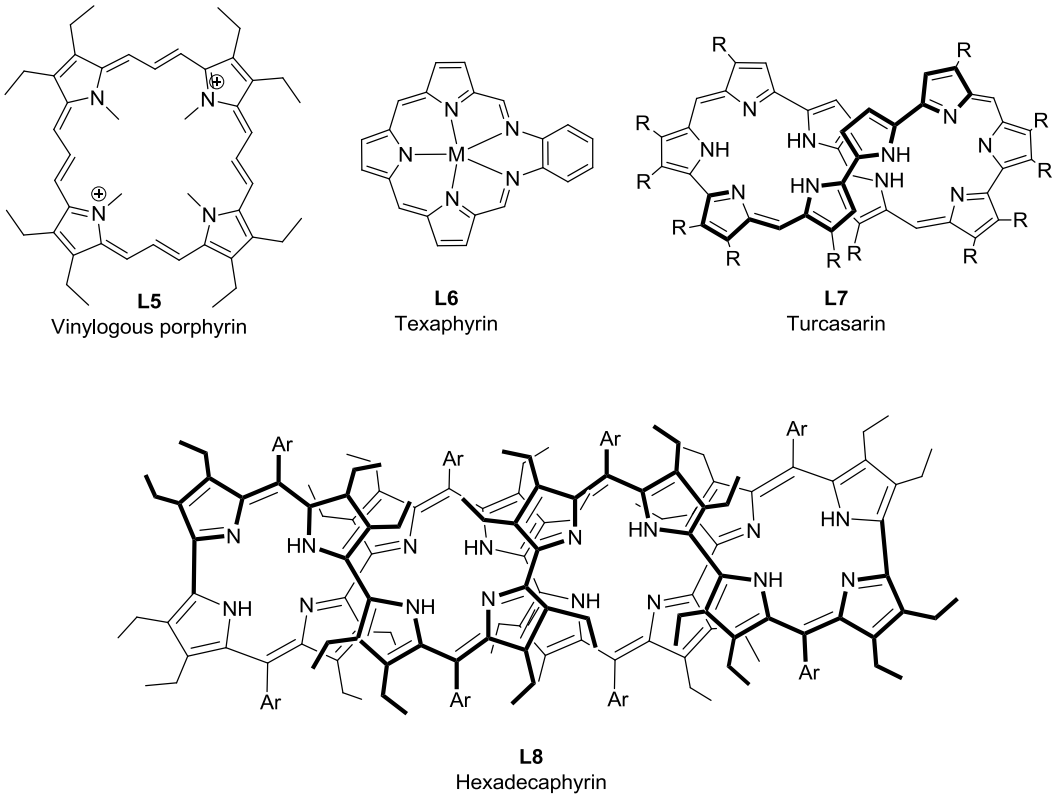

Figure 1.3 Some of the important expanded porphyrins of historical importance.

in 1972.[9b] In 1990 Sessler and coworkers published a report regarding the improved synthesis of sapphyrin and its unexpected anion binding behavior in the deprotonated state.[10] Further details about this macrocycle is presented in chapter 5 of this thesis.

In the early stage studies of extended π-conjugated system such as vinylogous porphyrins (also known as platyrins), expanded aromatic tetrapyrrolic macrocycles lead to anticipation that

enlargement of the π-conjugation would give rise to unusual physical and chemical properties to the expanded porphyrin. For instance N,N′,N″,N‴-tetramethyl[26]porphyrin-(3.3.3.3) **L5** and its tetraoxa derivative shows record molar extinction coefficient (λ_{max} = 528 nm, ε = 1-1.6 x 10^6 $M^{-1}cm^{-1}$).[11]

Another noteworthy example in the area of expanded porphyrin is the synthesis of texaphyrins **L6**, a hybrid schiff-base aromatic macrocycle by Sessler and coworkers.[12] Texaphyrin displays diverse metalation chemistry, unlike sapphyrin and other expanded porphyrin. In fact water-soluble Gd(III)-complex of texaphyrin referred to as motexaphin gadolinium (MGd) is a promising anticancer reagent that allows clear MRI contrast.[12]

A very important addition to expanded porphyrin by Sessler group is the serendipitous discovery of turcasarin **L7** during the synthesis of pentapyrrolic macrocycle, the first expanded porphyrin to display figure eight structure both in solid and solution states. Turcasarin is a decapyrrolic 40 π-nonaromatic system that exists in two interconvertible limiting helical conformations.[13] In 1995 in another report, again through serendipity, Vogel and coworkers synthesized the first octapyrrolic expanded porphyrin, [32]octaphyrin(1.0.1.0.1.0.1.0), during the synthesis of corrole and was found to adopt a chiral figure-eight conformation both in solution and in the solid states.[14] These reports began to attract interest of researchers towards figure eight motifs. Subsequently, it was noticed in general larger expanded porphyrins often adopt figure-eight conformations probably as a consequence of conformational flexibility and effective intramolecular hydrogen-bonding interactions.

Setsune and coworkers succeeded in synthesizing expanded porphyrins with up to 24 pyrrole rings using sterically hindered benzaldehyde derivatives with bipyrrole and subsequently, using bis(azafulvene) as a building block, to carry out the condensation under neutral condition. Among them 16 pyrrole ring containing [64]hexadecaphyrin(1.0.1.0.1.0.1.0.1.0.1.0.1.0.1.0) **L8** have been characterized by X-ray diffraction analysis, which still remains the largest structurally characterized expanded porphyrin.[15]

Interestingly, figure-eight conformations are found to be basically chiral, however they interconvert rapidly between two enantiomeric forms owing to their structural flexibility. In 1999, Vogel and coworkers succeeded in separation of β-alkyl octaphyrins **L9** and bis-Pd^{II}

complex of **L10** to their corresponding enantiomers.[16] Recently, Setsune and coworkers used octaphyrin(1.0.1.0.1.0.1.0) as an effective sensor for the direct determination of absolute configuration of a variety of chiral carboxylic acids at mM concentrations based on CD exciton chirality method.[17]

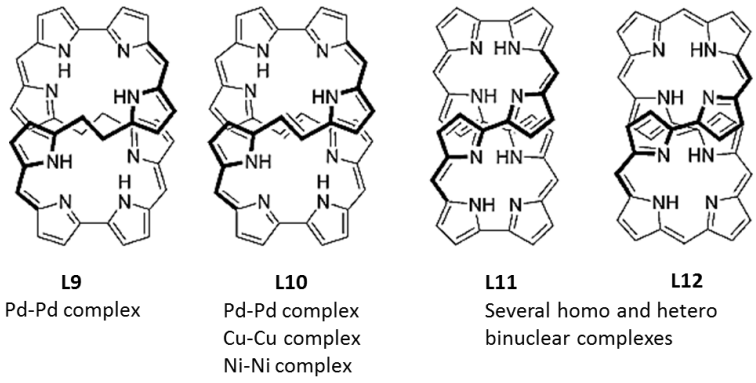

Figure 1.4 Figure eight octaphyrins (β-alkyl substitutions are omitted for clarity).

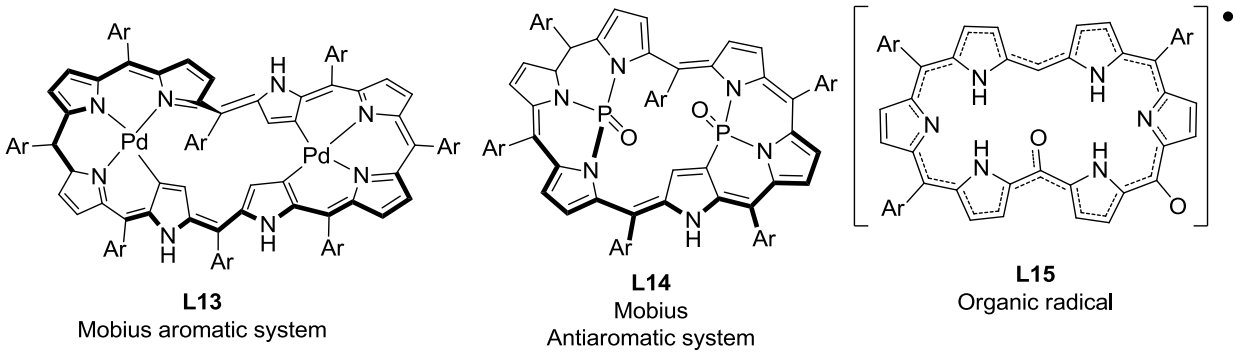

Figure 1.5 Recent examples of some of the important expanded porphyrins.

Another important role played by expanded porphyrin is to provide test bed for addressing various issues of aromaticity. Particularly in recent years, expanded porphyrins have been recognized as an effective platform to realize various stable Möbius aromatic and anti-aromatic systems which are very difficult to synthesize for other annulenes. Möbius aromaticity is the concept that predicts aromatic characters for $4n$ π cyclic conjugated systems based on a singly twisted Möbius topology.[18] This concept, was introduced first by Heilbronner in 1964 and by Zimmerman in 1966.[19] Heilbronner predicted on purely theoretical grounds that cyclic molecules with the topology of a Möbius band—a ring constructed by joining the ends of a rectangular strip

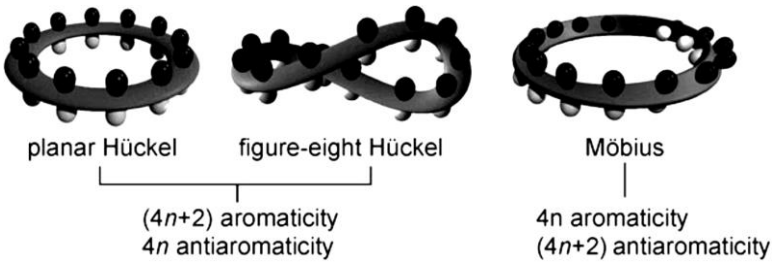

Figure 1.6 Schematic representations of topologies of π-conjugated systems.

after having given one end half a twist, should be aromatic if they contain 4n, rather than 4n + 2 π electrons. Thus the major difficulty to synthesize Möbius system is that it needs to merge two conflicting structural elements i.e. the fully conjugated cyclic electronic network and twisted topology of π systems, in a single molecule. Much later in 2003, Herges and coworkers reported a [16]annulene that has a twisted Möbius topology and moderate aromatic character.[19d] In 2007, Latos-Grażyński and coworkers reported a dynamic Hückel–Möbius system, di-*p*-benzi[28]hexaphyrin that undergoes solvent and temperature-dependent conformational changes between Hückel and Möbius structures.[20] This stimulated interest to study expanded porphyrins in this context. Subsequently, Osuka group reported the first stable Möbius aromatic system, bis-palladium complex of [36]Octaphyrin(1.1.1.1.1.1.1.1) **L13.** Infact many of the metal complexes of hexaphyrin reported earlier by Osuka group could be realized in terms of Möbius aromaticity thereafter.[21]

Although there exists increasingly large number of Möbius aromatic molecules, existence of Möbius antiaromatic molecules are still rare. Again it was Latos-Grażyński and coworkers, who reported cationic Pd^{II} vacataporphyrin exhibiting a weak paratropic ring current, which was ascribed to an 18π antiaromatic species based on the calculated Möbius structure.[22] However, first structurally characterized Möbius antiaromatic system was reported by Osuka and coworkers for a bisphosphorus [30]hexaphyrin **L14**.[23]

Another noteworthy contribution from Osuka's group is the synthesis and characterization of stable organic radicals derived from expanded porphyrin. For instance oxygenated product of 5,20-*meso*-free hexaphyrin **L15** assigned as the first example of stable monoradical based on expanded porphyrin.[24] Delocalization of an unpaired electron through extended conjugation in expanded porphyrin probably causes unusual stability in these radicals.

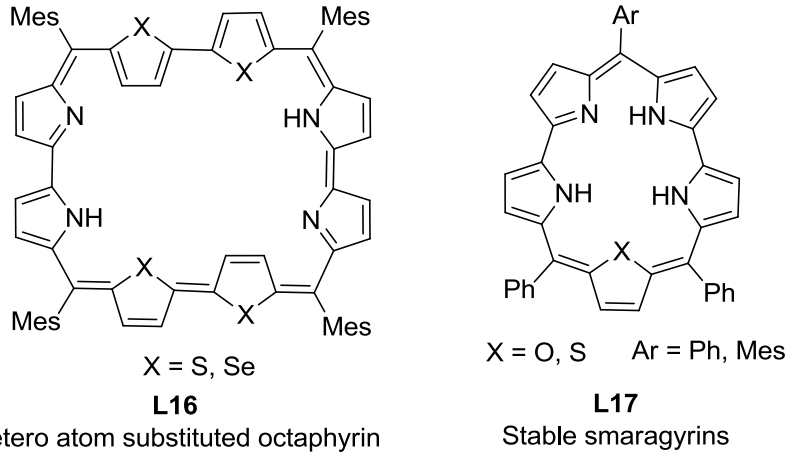

Figure 1.7 Few core modified expanded porphyrins.

Expanded porphyrin containing heteroatoms other than nitrogen are of great importance because of their unusual structural as well as photophysical properties in comparison to their nitrogen analogue. Contribution from Chandrashekar group in the development of this interesting area of research is noteworthy.[25] In general larger expanded porphyrin such as octaphyrin(1.0.1.0.1.0.1.0) are found to exist in figure eight conformation and shows non-aromatic behavior. In 2001, Chandrashekar and coworkers reported first core modified planar 34π octaphyrin **L16** that displays aromatic character.[25c] Subsequently, they reported a planar core modified aromatic dodecaphyrin that exhibits record two photon absorption cross section (σ_2 = 108000 GM).[26] In another important contribution, Chandrasekar group reported synthesis of core modified stable smaragdyrins **L17** which made possible for further exploration of this 22π aromatic macrocycle in detail.[27] Much of this later development was done by the same research group.[28a] Recently, Ravikanth group reported synthesis of boron complexes of smaragdyrins and evaluated them as fluoride ion sensor.[28b] The same group also reported the synthesis of porphyrin-expanded porphyrin dyads and especially, the porphyrin–smaragdyrin dyad was found to be an efficient fluorescent anion sensor.[28c,d] They also synthesized a series of covalently linked trichromophoric systems composed of BODIPY, smaragdyrins and porphyrin.[28e] Efficient energy transfer from central BODIPY to macrocycle was observed in these triads, hence holds great promise in the design and synthesis of suitable multichromophoric systems for material application.[28e]

1.4 π-Extended porphyrinoids

Annulated porphyrins, wherein additional aromatic rings are fused onto the porphyrin periphery, have received much attention recently. Extension of π-conjugation through additional aromatic ring often leads to bathochromically shifted absorption spectra relative to their non-annulated counterpart.[29] Thus these materials are promising for various applications such as dye stuffs, optical materials, nonlinear optics, organic semiconductors, photosensitizers for photodynamic therapy (PDT), and dye-sensitized solar cells.[30] Fused systems are generally synthesized by

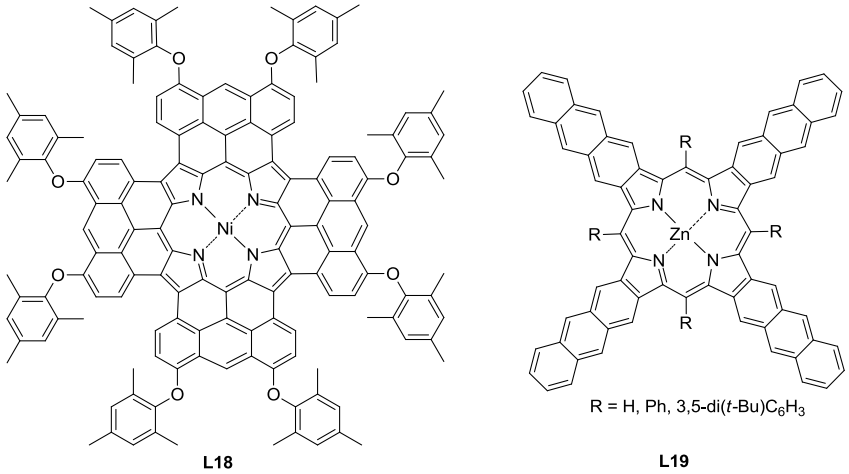

L18 L19

Figure 1.8 Examples of π-extended porphyrins.

oxidative fusion of porphyrin with aryl moiety at the periphery or by using annulated pyrrolic precursors. For instance fused tetraanthracenylporphyrin **L18** synthesized by $FeCl_3$ mediated oxidative ring closure reaction shows exceptionally small HOMO-LUMO gap with a λ_{max} extending up to 1417 nm.[31] Similarly tetraanthroporphyrins **L19** synthesized via the retro-Diels-Alder reaction of bicyclo-[2.2.2]octadiene-fused precursors have strong absorption and emission in the near-IR region.[32] However, π-extension in isomeric and expanded porphyrins is still in its infancy stage. Only a few examples appear very recently.[33] Nonetheless these molecules show unprecedented optical and structural properties compared to their non-annulated counterparts. It has been well documented that electronic, optical, and coordination properties of expanded porphyrins are dependent upon their conformations and hence control over their conformations is very crucial. Use of rigid fused bipyrrolic precursor or fusion of aromatic ring on periphery of expanded porphyrin has twofold advantages, because this not only increases π-conjugation but

also imparts structural rigidification to the resulting macrocycle. For example rosarin i.e. hexaphyrin(1.0.1.0.1.0) with 24π electrons are formally expected to be antiaromatic. However, rosarin **L20** derived from simple bipyrrole exhibit very weak antiaromatic character owing to non-planarity of this molecule as it is conformationally flexible. However, rosarin **L21** derived from naphthobipyrrole is planar and is antiaromatic.[34] Another interesting feature displayed by **L21** is that it undergoes proton coupled reduction to produce its corresponding 26π aromatic cationic counterpart when exposed to proton source. In this process an intermediate 25π-radical

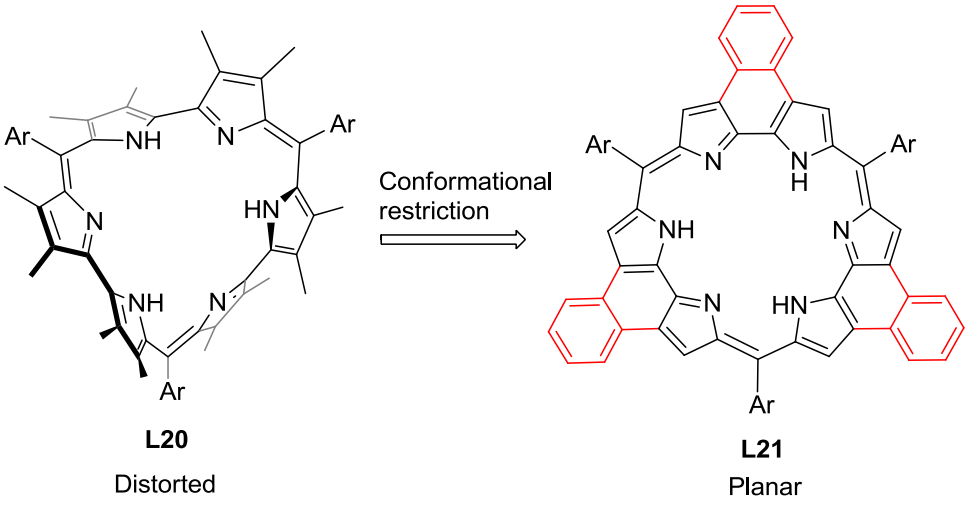

Figure 1.9 Conformationally flexible and rigid rosarins.

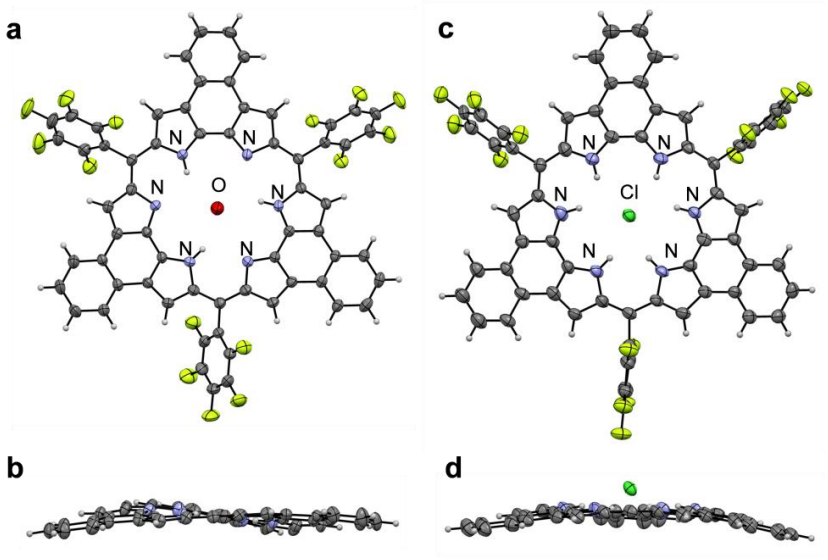

Figure 1.10 X-ray structure of **L21** (a, b) and its aromatic cationic counterpart (c, d).

dicationic species was also isolated and characterized. This interconversion between antiaromatic, radical and aromatic forms of **L21** are reversible. However, similar treatment with **L20** does not show this kind of behavior. Recently, Osuka and coworkers reported bis(Au^{III}) complex of [26]hexaphyrin fused to two anthracenes, which displays a remarkably red-shifted and sharp Q-band-like band at 1467 nm, multicharge storage ability, and a large TPA cross-section value owing to its flat and elongated rectangular conjugated network.[35] Similar π-extension in expanded porphyrins, in particular in cyclo[8]pyrrole and sapphyrin systems will be discussed in chapter 4 and 5 of this thesis.

1.5 References

1. Battersby, A. R.; Fookes, C. J. R.; Matcham, G. W. J.; McDonald, E. *Nature* **1980**, *285*, 17.
2. (a) *The Porphyrin Handbook* (Eds.: K. M. Kadish; K. M. Smith; R. Guilard) Academic Press, San Diego, **2000**. (b) *Handbook of Porphyrin Science* (Eds.: K. M. Kadish; K. M. Smith; R. Guilard) World Scientific Publishing, Singapore, **2010**.
3. (a) Jasat, A.; Dolphin, D. *Chem. Rev.* **1997**, *97*, 2267. (b) Sessler, J. L.; Weghorn, S. J. *Expanded, Contracted and Isomeric Porphyrins* Pergamon, New York, **1997**.
4. (a) Johnson, A. W.; Kay, I. T. *Proc. Chem. Soc. London* **1964**, 89. (b) Johnson, A. W.; Kay, I. T. *J. Chem. Soc*. **1965**, 1620. (c) Johnson, A. W.; Kay, I. T. *Proc. R. Soc. London, Ser. A: Math. Phys. Sci.* **1965**, *288*, 334. (c) Harrison, H. R.; Hodder, O. J. R.; Hodgkin, D. C. *J. Chem. Soc. B* **1971**, 640.
5. (a) Gross, Z.; Galili, N.; Saltsman, I. *Angew. Chem., Int. Ed.* **1999**, *38*, 1427. (b) Gross, Z.; Galili, N.; Simkhovich, L.; Saltsman, I.; Botoshsnsky, M.; Blaser, D.; Boese, R.; Goldberg, I. *Org. Lett*. **1999**, *1*, 599.
6. (a) Aviv, I.; Gross, Z. *Chem. Commun*. **2007,** 1987. (b) Aviv-Harel, I.; Gross, Z. *Chem. Eur. J.* **2009**, *15*, 8382. (c) Flamigni, L.; Gryko, D. T. *Chem. Soc. Rev.* **2009**, *38*, 1635. (d) Paolesse, R.; Jaquinod, L.; Nurco, D. J.; Mini, S.; Sagone, F.; Boschi, T.; Smith, K. M. *Chem. Commun*. **1999**,1307.
7. Vogel, E.; Köcher, M.; Schmickler, H.; Lex, J. *Angew. Chem., Int. Ed. Engl.* **1986**, *25*, 257.
8. Sessler, J. L.; Siedel, D. *Angew. Chem. Int. Ed.* **2003**, *42*, 5134.

9. (a) First mentioned by R. B. Woodward in Aromaticity: An International Symposium, Sheffield, U.K., **1966**. (b) Broadhurst, M. J.; Grigg, R.; Johnson, A.W. *J. Chem. Soc. Perkin Trans. 1* **1972**, 1124. (c) Bauer, V. J.; Clive, D. L. J.; Dolphin, D.; Paine, J. B.; Harris, F. L.; King, M. M.; Loder, J.; Wang, S.W. C.; Woodward, R. B. *J. Am. Chem. Soc.* **1983**, *105*, 6429.
10. Sessler, J. L.; Cyr, M.; Lynch, V.; McGhee, E. Ibers, J. A. *J. Am. Chem. Soc.* **1990**, *112*, 2810.
11. (a) Gosmann, M.; Franck, B. *Angew. Chem. Int. Ed. Engl*. **1986**, *25*, 1100. (b) Knübel, G.; Franck, B. *Angew. Chem. Int. Ed. Engl.* **1988**, *27*, 1170. (c) Wessel, T.; Franck, B.; Möller, M.; Rodewald, U.; Läge, M. *Angew. Chem. Int. Ed. Engl.* **1993**, *32*, 1148. (d) Franck, B.; Nonn, A.; Fuchs, K.; Gosmann, M. *Liebigs Ann. Chem*. **1994**, 503.
12. (a) Sessler, J. L.; Murai, T.; Lynch, V.; Cyr, M. *J. Am. Chem. Soc.* **1988**, *110*, 5586. (b) Sessler, J. L.; Hemmi, G.; Mody, T. D.; Murai, T.; Burrell, A.; Young, S. W. *Acc. Chem. Res.* **1994**, *27*, 43. (c) Young, S.W.; Fan, Q.; Harriman, A.; Sessler, J. L.; Dow, W. C.; Mody, T. D.; Hemmi, G. W.; Hao, Y.; Miller, R. A. *Proc. Natl. Acad. Sci. USA* **1996**, *93*, 6610. (d) Sessler, J. L.; Miller, R. A. *Biochem. Pharmacol*. **2000**, *59*, 733. (e) Hannah, S.; Lynch, V.; Guldi, D. M.; Gerasimchuk, N.; MacDonald, C. L. B.; Magda, D.; Sessler, J. L. *J. Am. Chem. Soc*. **2002**, *124*, 8416. (f) Wei, W.-H.; Wang, Z.; Mizuno, T.; Cortez, C.; Fu, L.; Sirisawad, M.; Naumovski, L.; Magda, D.; Sessler, J. L. *Dalton Trans.* **2006**, 1934. (g) Evans, J. P.; Xu, F.; Sirisawad, M.; Miller, R.; Naumovski, L.; Ortiz de Montellano, P. R. *Mol. Pharmacol.* **2007**, *71*, 193. (h) Zahedi Avval, F.; Berndt, C.; Pramanik, A.; Holmgren, A. *Biochem. Biophys. Res. Commun*. **2009**, *379*, 775.
13. Sessler, J. L.; Weghorn, S. J.; Lynch, V.; Johnson, M. R. *Angew. Chem. Int. Ed. Engl.* **1994**, *33*, 1509.
14. (a) Vogel, E.; Bröring, M.; Fink, J.; Rosen, D.; Schmickler, H.; Lex, J.; Chan, K.W. K.; Wu, Y.-D.; Plattner, D. A.; Nendel, M.; Houk, K. N. *Angew. Chem. Int. Ed. Engl*. **1995**, *34*, 2511. (b) Bröring, M.; Jendrny, J.; Zander, L.; Schmickler, H.; Lex, J.; Wu, Y.-D.; Nendel, M.; Chen, J.; Plattner, D. A.; Houk, K. N.; Vogel, E. *Angew. Chem. Int. Ed. Engl.* **1995**, *34*, 2515.
15. (a) Setsune, J.-i.; Katakami, Y.; Iizuna, N. *J. Am. Chem. Soc.* **1999**, *121*, 8957. (b) Setsune, J.-i.; Maeda, S. *J. Am. Chem. Soc*. **2000**, *122*, 12405.

16. Werner, A.; Michels, M.; Zander, L.; Lex, J.; Vogel, E. *Angew. Chem. Int. Ed*. **1999**, *38*, 3650.
17. Lintuluoto, J. M.; Nakayama, K.; Setsune, J.-i. *Chem. Commun*. **2006**, 3492.
18. (a) Rzepa, H. S. *Chem. Rev.* **2005**, *105*, 3697. (b) Herges, R. *Chem. Rev*. **2006**, *106*, 4820. (c) Yoon, Z. S.; Osuka, A.; Kim, D. *Nat. Chem*. **2009**, *1*, 113.
19. (a) Heilbronner, E. *Tetrahedron Lett.* **1964**, *5*, 1923. (b) Zimmerman, H. E. *J. Am. Chem. Soc.* **1966**, *88*, 1564. (c) Mauksch, M.; Gogonea, V.; Jiao, H.; Schleyer, P. von R. *Angew. Chem. Int. Ed.* **1998**, *37*, 2395. (d) Ajami, D.; Oeckler, O.; Simon, A.; Herges, R. *Nature* **2003**, *426*, 819. (e) Schleyer, P. von R.; Jiao, H. *Pure Appl. Chem*. **1996**, *68*, 209.
20. Stępień, M.; Latos-Grażyński, L.; Sprutta, N.; Chwalisz, P.; Szterenberg, L. *Angew. Chem. Int. Ed*. **2007**, *46*, 7869.
21. (a) Tanaka, Y.; Saito, S.; Mori, S.; Aratani, N.; Shinokubo, H.; Shibata, N.; Higuchi, Y.; Yoon, Z. S.; Kim, K. S.; Noh, S. B.; Park, J. K.; Kim, D.; Osuka, A. *Angew. Chem. Int. Ed.* **2008**, *47*, 681. (b) Park, J. K.; Yoon, Z. S.; Yoon, M.-C.; Kim, K. S.; Mori, S.; Shin, J.-Y.; Osuka, A.; Kim, D. *J. Am. Chem. Soc.* **2008**, *130*, 1824. (c) Sankar, J.; Mori, S.; Saito, S.; Rath, H.; Suzuki, M.; Inokuma, Y.; Shinokubo, H.; Kim, K. S.; Yoon, Z. S.; Shin, J.-Y.; Lim, J. M.; Matsuzaki, Y.; Matsushita, O.; Muranaka, A.; Kobayashi, N.; Kim, D.; Osuka, A. *J. Am. Chem. Soc.* **2008**, *130*, 13568. (d) Kim, K. S.; Yoon, Z. S.; Ricks, A. B.; Shin, J.-Y.; Mori, S.; Sankar, J.; Saito, S.; Jung, Y. M.; Wasielewski, M. R.; Osuka, A.; Kim, D. *J. Phys. Chem. A* **2009**, *113*, 4498. (e) Saito, S.; Shin, J.-Y.; Lim, J. M.; Kim, K. S.; Kim, D.; Osuka, A. *Angew. Chem. Int. Ed.* **2008**, *47*, 9657. (f) Tokuji, S.; Shin, J.-Y.; Kim, K. S.; Lim, J. M.; Youfu, K.; Saito, S.; Kim, D.; Osuka, A. *J. Am. Chem. Soc.* **2009**, *131*, 7240. (g) Inoue, M.; Kim, K. S.; Suzuki, M.; Lim, J. M.; Shin, J.-Y.; Kim, D.; Osuka, A. *Angew. Chem. Int. Ed.* **2009**, *48*, 6687. (h) Koide, T.; Youfu, K.; Saito, S.; Osuka, A. *Chem. Commun*. **2009**, 6047; (i) Lim, J. M.; Shin, J.-Y.; Tanaka, Y.; Saito, S.; Osuka, A.; Kim, D. *J. Am. Chem. Soc*. **2010**, *132*, 3105.
22. Pacholska-Dudziak, E.; Skonieczny, J.; Pawlicki, M.; Szterenberg, L.; Ciunik, Z.; Latos-Grażyński, L. *J. Am. Chem. Soc.* **2008**, *130*, 6182.
23. Higashino, T.; Lim, J. M.; Miura, T.; Saito, S.; Shin, J.-Y.; Kim, D.; Osuka, A. *Angew. Chem. Int. Ed.* **2010**, *49*, 4950.

24. Koide, T.; Kashiwazaki, G.; Suzuki, M.; Furukawa, K.; Yoon, M.-C.; Cho, S.; Kim, D.; Osuka, A. *Angew. Chem. Int. Ed*. **2008**, *47*, 9661.
25. (a) Chandrashekar, T. K.; Venkatraman, S. *Acc. Chem. Res.* **2003**, *36*, 676. (b) Misra, R.; Chandrashekar, T. K. *Acc. Chem. Res.* **2008**, *41*, 265. (c) Anand, V. G.; Pushpan, S. K.; Venkatraman, S.; Dey, A.; Chandrashekar, T. K.; Joshi, B. S.; Roy, R.; Teng, W.; Senge, K. R. *J. Am. Chem. Soc.* **2001**, *123*, 8620. (d) Anand, V. G.; Venkatraman, S.; Rath, H.; Chandrashekar, T. K.; Teng, W.; Senge, K. R. *Chem. Eur. J*. **2003**, *9*, 2282. (e) Rath, H.; Sankar, J.; PrabhuRaja, V.; Chandrashekar, T. K.; Nag, A.; Goswami, D. *J. Am. Chem. Soc.* **2005**, *127*, 11608. (f) Kumar, R.; Misra, R.; Chandrashekar, T. K.; Nag, A.; Goswami, D.; Suresh, E.; Suresh, C. H. *Eur. J. Org. Chem*. **2007**, 4552.
26. Rath, H.; Prabhuraja, V.; Chandrashekar, T. K.; Nag, A.; Goswami, D.; Joshi, B. S. *Org. Lett.* **2006**, *8*, 2325.
27. Narayanan, S. J.; Sridevi, B.; Chandrashekar, T. K.; Englich, U.; Ruhlandt-Senge, K. *Org. Lett*. **1999**, *1*, 587.
28. (a) Pareek, Y.; Ravikanth, M.; Chandrashekar, T. K. *Acc. Chem. Res.* **2012**, *45*, 1801. (b) Rao., M. R.; Ravikanth, M. *J. Org. Chem.* **2011**, *76*, 3582. (c) Rao, M. R.; Ravikanth, M. *Eur. J. Org. Chem*. **2011**, 1335. (d) Pareek, Y.; Ravikanth, M. *Eur. J. Org. Chem*. **2011**, 5390. (e) Khan, T. K.; Ravikanth, M. *Eur. J. Org. Chem*. **2011**, 7011
29. Mori, H.; Tanaka, T.; Osuka, A. *J. Mater. Chem. C* **2013**, *1*, 2500.
30. (a) Lash, T. D. *The Porphyrin Handbook*; Academic Press: New York, **2000**; Vol. *2*. (b) Zhi, L.; Müllen, K. *J. Mater. Chem.* **2008**, *18*, 1472.
31. Davis, N. K. S.; Thompson, A. L.; Anderson, H. L. *J. Am. Chem. Soc*. **2011**, *133*, 30.
32. Yamada, H.; Kuzuhara, D.; Takahashi, T.; Shimizu, Y.; Uota, K.; Okujima, T.; Uno, H.; Ono, N. *Org. Lett*. **2008**, *14*, 2947.
33. Roznyatovskiy, V. V.; Lee, C.-H.; Sessler, J. L. *Chem. Soc. Rev.* **2013**, *42*, 1921.
34. (a) Ishida, M.; Kim, S.-J.; Preihs, C.; Ohkubo, K.; Lim, J. M.; Lee, B. S.; Park, J. S.; Lynch, V. M.; Roznyatovskiy, V. V.; Sarma, T.; Panda, P. K.; Lee, C. H.; Fukuzumi, S.; Kim D.; Sessler, J. L. *Nat. Chem*. **2013**, *5*, 15. (b) Sessler, J. L.; Weghron, S. J.; Morishima, T.; Rosingana, M.; Lynch, V.; Lee, V. *J. Am. Chem. Soc.* **1992,** *114*, 8306.
35. Naoda, K.; Mori, H.; Aratani, N.; Lee, B. S.; Kim, D.; Osuka, A. *Angew. Chem. Int. Ed.* **2012**, *51*, 9856.

CHAPTER 2

Materials and methods

In this chapter, the materials used and the procedures employed during the course of our investigation are outlined. Purification procedures adopted for the chemicals and the solvents are described. A brief outline of the various physicochemical techniques used in the present study has also been provided.

2.1 General Experimental

2.1.1 Solvents

2.1.1.1 Solvent for reactions[1]

Pyrrole was distilled before use. Dichloromethane and 1,2-dichloroethane were dried by distillation over calcium hydride. Tetrahydrofuran and diethyl ether were dried by passage through columns of activated alumina, followed by refluxing with sodium metal, in presence of benzophenone. Ethanol and methanol were dried by using activated magnesium turnings. $CHCl_3$ was dried by passing GR grade $CHCl_3$ over basic alumina. Toluene was refluxed with sodium and benzophenone until blue color and distilled before use. $POCl_3$ was distilled before use.

2.1.1.2 NMR solvents

Chloroform-d_1, acetonitrile-d_3, D_2O and DMSO-d_6 were purchased from Acros Organics/Cambridge isotope Inc. Toluene-d_8 was purchased from E-Merck, India and used as such.

2.1.1.3 Solvents for optical measurement

DMSO, $CHCl_3$, CH_2Cl_2, methanol, DMF, toluene, acetonitrile and hexane (spectroscopy grade) were purchased from Merck and used as such.

2.1.2 Reagents

Pyrrole was purchased from Sisco research laboratories (SRL). Cuprous chloride, triethyl orthoformate, Pd/C, benzyl acetoacetate, KO^tBu, Et_3N, $BF_3.OEt_2$, TFA, $Ni(acac)_2$, $Cu(OAc)_2.H_2O$, $Pd(OAc)_2$, 2,3-dihydroxynaphthalene, $AlCl_3$ and all alkyl bromides were purchased from Sigma-Aldrich® and used as such. THF, nitrobenzene and acetonitrile were purchased from Finar chemicals. GR grade Toluene, acetic acid, 1,2-dichloroethane, DMF, DCM, $CHCl_3$, DMSO, MeOH, diethyl ether, ethylene glycol and *i*-propanol were purchased from Merck. Zn and $TiCl_4$ were purchased from Finar chemicals. All the inorganic salts, mineral acids, acetyl acetone, CH_3I, hydrazinium sulfate, hydrazine hydrate, P_2O_5, NaOH, KOH and

solvents used for the routine laboratory work, were purchased from Merck. *p*-TsOH, $FeCl_3$ and $POCl_3$ were purchased from Loba Chemie. Mg-turnings, I_2, diethyl oxalate, basic and neutral alumina were purchased from Sisco Research Laboratories.

2.2 Chromatography

Thin layer chromatography was performed on TLC Silica gel 60 F_{254} aluminum sheet, purchased from Merck. Column chromatography was carried out on silica gel (100-200 mesh) purchased from Merck.

2.3 Characterization and instrumentation

NMR spectra were obtained on Bruker 400 MHz and 500 MHz FT-NMR spectrometer operating at ambient temperature. TMS was used as internal standard for ^1H NMR spectra.

Mass spectral determinations were carried out by Autoflex III Smartbeam Bruker Daltonics, MALDI-TOF mass spectrometer, LCMS were carried out by Shimadzu-LCMS-2010 mass spectrometer and HRMS data were recorded with Bruker Maxis spectrometer.

Elemental analyses were obtained through Thermo Finnigan Flash EA 1112 analyzer. EPR measurements were done on Bruker EMX microX spectrometer. Melting points were determined by open capillary tubes on a BIO-TECH, India apparatus. IR spectra were recorded on a JASCO FTIR model 5300 and NICOLET 5700 FT-IR spectrometer.

UV-Vis spectra were recorded on Perkin Elmer Lambda 35 and UV 3600 Shimadzu UV-VIS-NIR spectrophotometer. Fluorescence spectra were recorded on Horiba Zobin Yovan Fluoromax-4 instrument. Fluorescence lifetime measurements were carried out using a time correlated single-photon counting (TCSPC) spectrometer (Horiba Jobin Yvon IBH). Nano LED source (λ_{exc} 639 nm) was used as the excitation source and an MCP photomultiplier (Hamamatsu R3809U-50) as the detector. The pulse repetition rate of the laser source was 1MHz. The width of the instrument response function, which was limited by the fwhm of the exciting pulse, was around 100 ps. The lamp profile was recorded by placing a scatterer (dilute solution of Ludox in water) in place of the sample. The time resolved emission decay profiles were collected at steady state emission maxima. Decay curves were analyzed by nonlinear least-squares iteration procedure using IBH DAS6 (Version 2.2) decay analysis software. The quality of the fit was ass-

essed by inspection of the χ^2 values and the distribution of the residuals.

Some of the crystallographic data were collected on BRUKER SMART-APEX CCD diffractometer. Mo−K_α (λ = 0.71073 Å) radiation was used to collect X-ray reflections from the single crystal. Data reduction was performed using Bruker SAINT[2] software. Intensities for absorption were corrected using SADABS[3] and refined using SHELXL-97[4] with anisotropic displacement parameters for non-H atoms. Hydrogen atoms on O and N were experimentally located in difference electron density maps. All C−H atoms were fixed geometrically using HFIX command in SHELX-TL. A check of the final CIF file using PLATON[5] did not show any missed symmetry. Remaining other crystallographic data was collected on Oxford Gemini A Ultra diffractometer with dual sources. Mo-K_α (λ = 0.71073 Å) radiation was used to collect the X-ray reflections of the crystal. Data reduction was performed using CrysAlis^{Pro} 171.33.55 software.[6] Structures were solved and refined using Olex2-1.0, with anisotropic displacement parameters for non-H atoms. Hydrogen atoms on N were located from the Fourier map in all of the crystal structures. All C–H atoms were fixed geometrically. Empirical absorption correction was done using spherical harmonics, implemented in SCALE3 ABSPACK scaling algorithm. A check of the final CIF file using PLATON[5] did not show any missed symmetry.

2.3.1 2PA and 3PA measurements

2.3.1.1 Picosecond (ps) Z-Scan at 800nm

The Z-scan measurements were performed using ~2 ps (FWHM), 800 nm pulses with a repetition rate of 1 kHz from an amplified Ti:sapphire system (Legend, Coherent). The amplifier was seeded with pulses of duration ~15 fs (FWHM, spectral bandwidth of ~50-60 nm) from the oscillator (Micra, Coherent). The pulses were nearly transform limited and this was confirmed from the bandwidth and pulse duration measurements performed using an external auto-correlation experiment using a 2-mm thick BBO crystal in the non-collinear geometry. A quartz cuvette (1 mm thick) containing the sample solution was traversed in the focusing geometry enabled by an achromat lens of 200 mm focal length. The beam waist ($2\omega_0$) at focal plane was estimated to be 60±4 μm (FW1/e^2M) with a corresponding Rayleigh range (Z_r) of 3.5±0.4 mm ensuring the validity of thin sample approximation. The Z-scan was performed over a distance of $10Z_r$ on a high-resolution linear translation stage (Newport ILS250PP) by recording the sample transmittance using a power sensor (Coherent PS19). A LabVIEW program was

designed and used for automating the data acquisition of the Z-scan experiments. Typical energies in the range of 1-10 μJ, corresponding to peak intensities in the range of 70–400 GW/cm^2, were used for all the experiments. The closed aperture scans were performed at peak intensities <100 GW/cm^2.

2.3.1.2 Ps Z-Scan at other than 800nm

Z-scan measurements were performed at 560, 580, 600, 640, 680 and 700 nm using ~1.5 ps (FWHM) pulses with a repetition rate of 1 kHz from TOPAS (Light Conversion) pumped with an amplified Ti:sapphire system (LEGEND, Coherent). The amplifier was seeded with pulses of duration ~15 fs (FWHM, ~60 nm bandwidth) from an oscillator (Micra, Coherent). A quartz cuvette (1 mm thick) containing the sample solution was traversed in the focusing geometry enabled by an achromat lens of 200 mm focal length. The beam waist (2ω0) at focal plane was estimated to be 60±4 μm (FW1/e^{2}M) with a corresponding Rayleigh range (Zr) of 3.5±0.4 mm ensuring the validity of thin sample approximation.

The open aperture z-scan data have been fitted using the relation obtained by Sheik Bahae et al.[7] by time integration of sample transmittance assuming a Gaussian temporal profile. The two photon absorption fitting is done using the equation (1) and three photon absorption fitting was done using equation (2): Where T(z) is the normalized transmittance as a function of z, $q_0 = \alpha_2 l_{eff} I_0$, $p_0 = (2\alpha_3 l_{eff} I_0^2)^{1/2}$, α_2 = 2PA coefficient and α_3 = 3PA coefficient, I_0 is the peak intensity at focus.

$$T(z, S=1) = \frac{1}{\sqrt{\pi} q_0(z,0)} \int_{-\infty}^{\infty} \ln\left[1 + q_0(z,0) e^{-\tau^2}\right] d\tau \qquad (1)$$

$$T(z, S=1) = \frac{1}{\sqrt{\pi} p_0(z,0)} \int_{-\infty}^{\infty} \ln\left[\sqrt{\ln(1 + p_0^2 \exp(-2\tau^2))} + p_0(z,0) \exp(-\tau^2)\right] d\tau \qquad (2)$$

Effective path lengths in the sample of length L for 2PA and 3PA are given as $L_{eff} = \frac{1 - e^{-\alpha_0 L}}{\alpha_0}$, $L'_{eff} = \frac{1 - e^{-2\alpha_0 L}}{2\alpha_0}$, α_0 = linear absorption coefficient.

2.3.2 Excited state life time study

2.3.2.1 Femtosecond pump-probe at 600nm

The fs degenerate pump-probe experiments were performed at 600 nm. The liquid sample was taken in a 5mm thick glass cuvette. The molecules were excited by pulses from 1 kHz optical parametric amplifier (TOPAS-C, Light Conversion, Coherent) delivering pulses of 60 fs duration pumped by a Ti:Sapphire regenerative amplifier. Pump pulses in the energy range of 5–50 μJ were used. The probe beam diameter was 2 mm, and pump beam diameter was 4 mm. The pulse-width at the sample in our fs experiments was estimated (taking into account the optics and lenses involved) to be 70 fs. The pump beam was focused using a 150 mm lens, while the probe beam was focused using a longer focal length lens (500 mm). Typical pump beam intensity was 0.3–3 TW/cm^2, while the probe beam intensity was 5 GW/cm^2. The ratio of pump to probe intensities was at least 60. The pump beam was modulated at 100 Hz with the help of a chopper, and the change in probe transmitted intensity was measured with a combination of a photodiode (SM05R/M, Thorlabs) and a lock-in amplifier (7265, Signal Recovery). The polarization of pump and probe beams was perpendicular in both the cases to avoid diffraction effects leading to coherent artefacts.

2.3.2.2 Picosecond pump-probe at 800nm

In the ps pump-probe set up, the pump and probe beam diameters were 4 and 2mm, respectively. The molecules were excited by pulses from 1 kHz Ti:Sapphire regenerative amplifier (LEGEND, Coherent) delivering pulses of ~2 ps duration .The pump and probe beams were focused using single 200 mm lens. Typical peak intensities of pump and probe beams were 150 GW/cm^2 and 2–4 GW/cm^2, respectively. The ratio of pump to probe intensities was at least 75. The focusing in both the cases was such that the probe beam diameter was ensured to be slightly smaller than the pump beam diameter.

The transmitted probe data was fitted using the equation given below. For the case of single decay, it was observed only τ_1, for double decay, τ_1 and τ_2, and for triple exponential decay, τ_1, τ_2, and τ_3 were used. $\Delta T(t)$ is the time dependent change in probe transmission, induced by the pump at time "t" after the pump excitation, and T is the probe transmission in the absence of pump.[8]

$$\frac{\Delta T(t)}{T} = y_0 + A_1 e^{-(t-t_0)/\tau_1} + A_2 e^{-(t-t_0)/\tau_2} + A_3 e^{-(t-t_0)/\tau_3}$$

2.4 Preparation of starting materials

The following compounds were prepared by following literature method, in order to utilize them as the starting material for our investigation. Their identification was further confirmed, by matching the analytical data with that reported in the literature.

2.4.1 Synthesis of PPE (Polyphosphate Ester)[9]

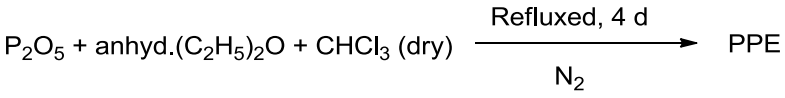

Scheme 2.1 Synthesis of PPE.

Phosphorus(V) oxide (150 g) is added to a solution of anhyd. ether (300 mL) and alcohol-free chloroform (150 mL). The reaction mixture is refluxed under dry nitrogen for 4 d and the resulting clear solution decanted from a small amount of residue. The solution is concentrated to a colorless syrupy mass in a rotary evaporator; residual traces of solvent are removed by heating the syrup for 36 h at 40 °C in vacuum.

2.4.2 Synthesis of unsubstituted naphthobipyrrole[10]

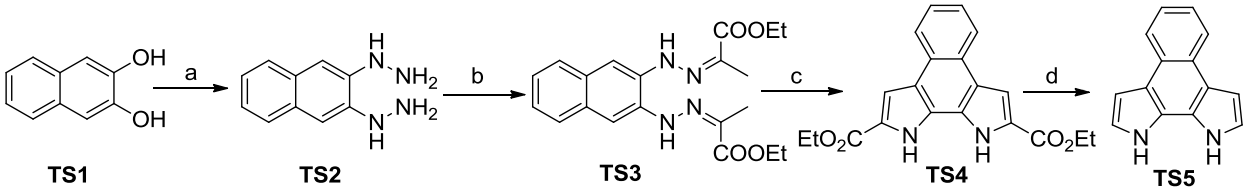

Scheme 2.2 Synthesis of unsubstituted naphthobipyrrole. a) $NH_2NH_2.H_2SO_4$, $NH_2NH_2.H_2O$, EtOH, reflux, 10 h. b) CH_3COCO_2Et, EtOH, rt, 1 h. c) PPE, 100 °C, 1h. d) NaOH, ethylene glycol, reflux, 2 h.

2.4.2.1 Synthesis of 2,3-naphthalenedihydrazene TS2[10a]

2,3-dihydroxynaphthalene **TS1** (30g, 187.3 mmol) were mixed with hydrazinium sulfate (10g, 77 mmol). To this, mixture of absolute alcohol (15 mL) and hydrazine hydrate (30 mL) were added in a round bottom flask. The mixture was heated to reflux. After 2-4 h a clear greenish brown color crystalline material starts depositing. The reaction was completed after another 3-4 h. The precipitate was filtered under suction and washed with alcohol for several times, dried under vacuum. Yield: 21g, 61 %.

2.4.2.2 Synthesis of ethyl pyruvate 2,3-naphthalenehydrazone TS3[10b]

To a suspension of 2,3-naphthalenedihydrazine (6g, 32 mmol) in abs. ethanol (50 mL), a solution of ethyl pyruvate (12 mL, 108 mmol) in abs. ethanol (5 mL) was added. Resultant reaction mixture was stirred for 1 h to obtain a yellow precipitate. It was filtered under suction and dried. Yield: 10.52 g, 86 % (lit. 87 %).

2.4.2.3 Synthesis of 2,9-Diethoxycarbonylnaphthobipyrrole TS4[10b]

Ethyl pyruvate 2,3-naphthalenedihydrazone (4g, 10.4 mmol) **TS3** was heated with polyphosphate ester (28 mL, 8.9 mmol) at 100 °C for 1 h and poured into ice cold water. The resultant brown color precipitate was filtered under suction, washed with water 3-4 times and finally washed with $CHCl_3$ till the filtrate become colorless. Product dried under high vacuum. Yield: 2.5 g, 68 %.

^{1}H NMR (400 MHz, DMSO-d_6, δ in ppm): 11.8 (s, 2H, NH), 8.3 (m, 2H, CH-naph), 7.8 (s, 2H, CH-naph), 7.4 (m, 2H, CH-naph), 4.4 (q, J = 7.2 Hz, 4H, CH_2-ester), 1.4 (t, J = 7.2 Hz, 6H, CH_3-ester).

2.4.2.4 Synthesis of 2,9-Diethoxycarbonylnaphthobipyrrole TS5[10b]

Naphthobipyrrole diesters **TS4** (2 g, 5.7 mmol), ethylene glycol (60 mL), and NaOH (2.5 g, 63 mmol) were taken in a round bottomed flask and kept under high vacuum for 1 h. The mixture was then heated at reflux for 3 h under N_2 atmosphere, cooled to 100 °C and degassed water (90 mL) was added. The reaction mixture was stirred for 5 min, cooled to r.t. and the white-green coloured precipitate thus formed was filtered under suction and washed thoroughly with water to remove the excess ethylene glycol, dried under vacuum to obtain the desired product in almost quantitative yield. (lit. 22 % in two steps).

^{1}H NMR (400 MHz, DMSO-d_6, δ in ppm): 11.0 (brs, 2H), 8.21-8.15 (m, 2H), 7.38-7.32 (m, 2H), 7.24 (t, J = 2.67 Hz, 2H), 7.03-7.01 (m, 2H).

2.4.3 Synthesis of *N,N*-dimethylamides[11]

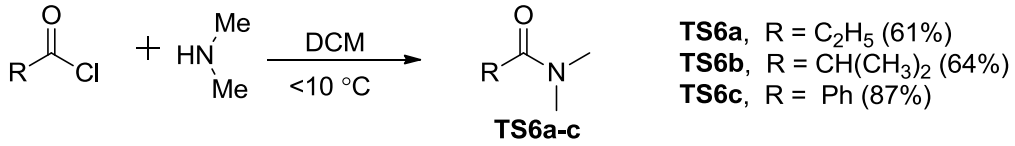

Scheme 2.3 Synthesis of *N,N*-dimethylamides.

General procedure: To a solution of dimethylamine (40% aqueous solution, 2 equiv.) in dichloromethane, a solution of acyl chloride (1 equiv.) was added, while keeping the temperature of the reaction mixture below 10 °C. Reaction mixture was stirred at room temperature for another 5 h, after addition is over. Organic layer was separated and washed with 1N HCl, followed by water, dried over anhyd. sodium sulfate and concentrated under reduced pressure.

TS6a: Yield: 61 %, ^{1}H NMR (400 MHz, $CDCl_3$, δ in ppm): 1.15 (t, J = 7.6 Hz, 3H, CH_3), 2.33 (q, J = 7.2 Hz, 2H, CH_2,), 2.95 (3H, 3H, CH_3, N-methyl) 3.01 (3H, CH_3, N-methyl).^{13}C NMR (100 MHz, $CDCl_3$, δ in ppm) 9.42, 26.64, 35.49, 37.21, 173.94.

TS6b: Yield: 64 %, ^{1}H NMR (400 MHz, $CDCl_3$, δ in ppm): 1.11 (d, J = 6.4 Hz, 6H, CH_3), 2.82 (m, 1H, CH), 2.95 (s, 3H, CH_3), 3.05 (s, 3H, CH_3).^{13}C NMR (100 MHz, $CDCl_3$, δ in ppm) 19.35, 30.33, 35.74, 37.19, 177.19.

TS6c: Yield: 87 %, ^{1}H NMR (400 MHz, $CDCl_3$, δ in ppm): 2.97 (s, 3H, CH_3), 3.10 (s, 3H, CH_3), 7.45-7.35 (m, 5 H, Ph).

2.4.4 Synthesis of α-keto esters[12]

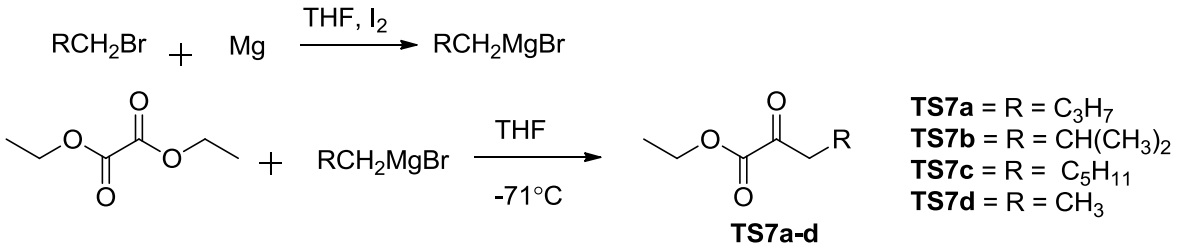

Scheme 2.4 Synthesis of α-keto esters.

General procedure: Magnesium turnings (4 equiv.) and iodine (small amount) were taken in dry nitrogen filled round bottom flask and stirred for 2 h. Dry THF was added to this, followed by slow addition of the alkyl bromide (1.2 equiv.) with continuous stirring. After complete addition, the mixture was stirred for another 1 h to get the desired alkyl magnesium bromide. This was then added slowly through a cannula to a solution of diethyl oxalate (1.1 equiv.) in twice of its volume of THF at -70 $^{\circ}$C, over one hour period. The reaction mixture was stirred for another 4 h, quenched with 3M HCl till final pH of the solution becomes 4. The aqueous layer was extracted with an equal volume of methylene chloride. The combined organic layers were dried over anhyd. $MgSO_4$ and solvent was evaporated to obtain a light yellow liquid, which was further purified by distillation under reduced pressure. Yield: 80-90 %.

TS7a: Yield: 85 %; ^{1}H NMR (400 MHz, $CDCl_3$, δ in ppm): 0.92 (t, J = 7.2 Hz, 3H, CH_3,), 1.35 (m, 5H, CH_3, CH_2), 1.62 (m, 2H, CH_2), 2.83 (t, 2H, J = 7.2 Hz, CH_2,), 4.33 (m, 2H, CH_2 ester).

TS7b: Yield: 80 %; ^{1}H NMR (400 MHz, $CDCl_3$, δ in ppm): 0.87 (d, J = 6.8, 6H, CH_3,), 1.27 (m, 3H, CH_3), 2.09 (m, 1H, CH), 2.62 (d, J = 6.8, 2H, CH_2,), 4.22 (m, 2H, CH_2 ester).

TS7c: Yield: 85 %; ^{1}H NMR (400 MHz, $CDCl_3$, δ in ppm): 0.85 (t, J = 7.2 Hz, 3H, CH_3,), 1.19–1.30 (m, 6H, CH_2), 1.32 (m, 3H, CH_3), 1.63 (m, 2H, CH_2), 2.78 (t, J = 7.2, 2H, CH_2), 4.27 (m, 2H, CH_2 ester).

TS7d: Yield: 90 %; ^{1}H NMR (400 MHz, $CDCl_3$, δ in ppm): 1.14 (t, J = 7.2 Hz, 3H, CH_3,), 1.39 (m, 3H, CH_3), 2.87 (q, J = 7.2 Hz, 2H, CH_2,), 4.34 (m, 2H, CH_2 ester).

2.4.5 Synthesis of tripyrrane diacid TS11[13]

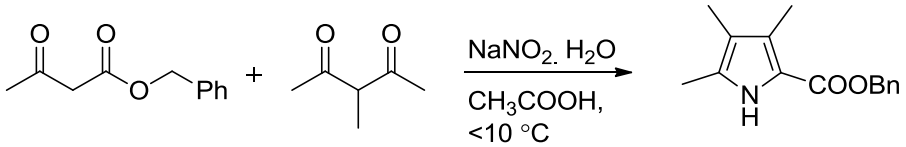

TS8

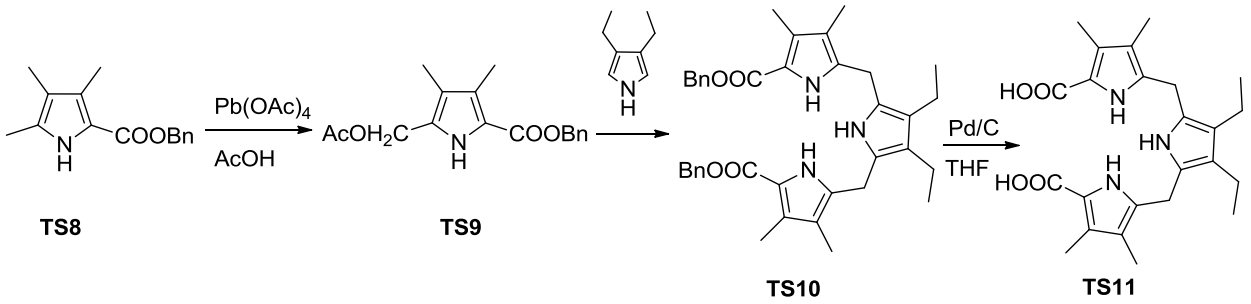

Scheme 2.5 Synthesis of tripyrrane diacid **TS11**.

2.4.5.1 Synthesis of benzyl-3,4,5-trimethylpyrrole-2-carboxylate TS8[13a]

Benzyl acetoacetate (2.1 mL, 12.26 mmol) was taken in glacial acetic acid (5 mL), to this a solution of $NaNO_2$ (1 g, 14.7 mmol) in water was added with stirring during 30 min. below 10 °C. The reaction mixture was further stirred for 4 h and kept overnight at room temperature. To this solution, 3-methylpentane-2,4-dione (1.4 g, 12.26 mmol) in acetic acid was added followed by addition of zinc dust (1.6 g, 24.47 mmol). The internal temperature of the reaction mixture was kept above 10 °C during addition. The reaction mixture was heated under reflux for 15 min. and poured into crushed ice. White precipitate thus obtained was filtered under suction, washed with water and dried under vacuum. Yield: 1.5 g, 51 % (lit. 45.5 %).

^{1}H NMR (400 MHz, $CDCl_3$, δ in ppm): 1.93 (s, 3H, CH_3), 2.25 (s, 3H, CH_3), 2.29 (s, 3H, CH_3), 5.31(s, 2H, CH_2-benzyl), 7.44-7.32 (m, 5H, Ph), 8.58 (brs, 1H, NH).

2.4.5.2 Synthesis of benzyl 5-(acetoxymethyl)-3,4-dimethylpyrrole-2-carboxylate TS9[13c]

$Pb(OAc)_4$ (3.86 g, 8.71 mmol) was added to a solution of benzyl-3,4,5-trimethylpyrrole-2-carboxylate (2 g, 82.2 mmol) **TS8** in acetic acid (20 mL) and acetic anhydride (2 mL, 20.3 mmol) and the reaction mixture was stirred at room temperature for 3 h and poured into ice water. The resultant precipitate was filtered and washed well with water, dried under vacuum. Yield: 2.3 g, 92 % (lit. 88 %).

^{1}H NMR (400 MHz, $CDCl_3$, δ in ppm): 2.00 (s, 3H, CH_3), 2.06 (s, 3H, CH_3), 2.28 (s, 3H, CH_3), 5.01 (s, 2H, OCH_2), 5.31 (s, 2H, CH_2-benzyl), 7.40 (m, 5H, Ph), 9.90 (brs, 1H, NH).

2.4.5.3 Synthesis of tripyrrane dibenzylester TS10[13b-d]

3,4-Diethylpyrrole (41 mg, 0.34 mmol) and benzyl 5-(acetoxymethyl)-3,4-dimethylpyrrole-2-carboxylate **TS9** (200 mg, 0.66 mmol) were dissolved in 2-popanol and acetic acid (64 μL). The resulting solution was stirred and refluxed under an atmosphere of N_2 for 16 h. The mixture was allowed to cool to room temperature and further cooled in an ice bath. The resulting precipitate was filtered, washed with cold ethanol and dried in vacuum overnight to get the tripyrrane **TS10**. Yield: 124 mg, 61.6 %.

^{1}H NMR (400 MHz, $CDCl_3$, δ in ppm): 1.15 (t, J = 7.2 Hz, 6H, CH_3), 1.82 (s, 6H, CH_3), 2.18 (s, 6H, CH_3), 2.49 (q, *J* = 7.2 Hz, 4H, CH_2), 3.57, (s, 4H, *meso*-CH_2), 4.37 (s, 2H, CH_2-benzyl), 7.00 (m, 4H, Ph), 7.24 (m, 6H, Ph), 8.79(1H, brs, NH), 11.14 (2H, brs, NH).

2.4.5.4 Synthesis of tripyrrane diacid TS11[13b-d]

Tripyrrane dibenzylester **TS10** (100 mg, 0.17 mmol) was dissolved in freshly distilled dry THF (10 mL) and placed in a round bottom flask. The solution was diluted with methanol (5 mL) and to this, 10% Pd (25 mg, 0.022 mmol) on activated carbon was added, air was flashed from the vessel with H_2 and the reaction mixture was stirred under the atmosphere of H_2 for 16 h. After completion of the reaction, the catalyst was removed by suction filtration over celite pad and the solvent evaporated under reduced pressure (below 30 °C). The product was dried under high vacuum and used directly in the next step.

2.4.6 Synthesis of tetraethyl bipyrrole dialdehyde TS13[14]

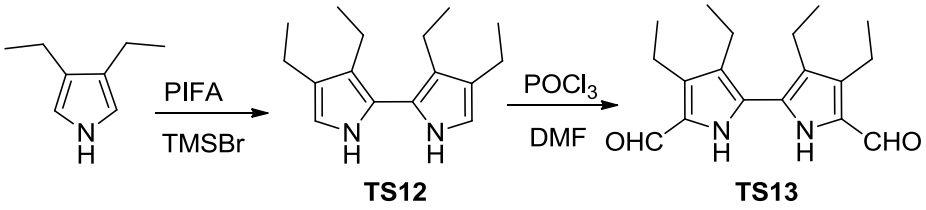

Scheme 2.6 Synthesis of tetraethyl bipyrrole dialdehyde **TS13**.

2.4.6.1 Synthesis of tetraethyl bipyrrole TS12[14a]

To a stirred solution of 3,4-diethylpyrrole[14c] (700 mg, 5.67 mmol) in CH_2Cl_2, PIFA (phenyliodine bis(trifluoroacetate)) (813 mg, 1.9 mmol) and TMSBr (bromotrimethylsilane) (0.52 mL, 3.8 mmol) were added quickly at -78 °C. The reaction mixture was then stirred for 1 h

while the reaction temperature was maintained below -40 °C. To the reaction mixture, sat. aq. $NaHCO_3$ (ca. 130 mL) was added and stirred for an additional 10 min at ambient temperature. The organic layer was separated and the aqueous phase was extracted with CH_2Cl_2. The combined extract was dried with anhyd. Na_2SO_4 and evaporated to dryness and distilled under reduced pressure to obtain the desired bipyrrole **TS12**. Yield: 350 mg, 76 % (lit. 75 %).

^{1}H NMR (400 MHz, $CDCl_3$, δ in ppm): 1.05 (t, J = 7.8 Hz, 4H), 1.25 (t, J = 7.8 Hz, 4H), 2.42 (q, J = 7.8 Hz, 4H), 2.52 (q, J = 7.8 Hz, 4H), 6.53 (bs, 2H), 7.58 (bs, 2H).

2.4.6.2 Synthesis of tetraethyl bipyrrole dialdehyde TS13[14b]

Dry DMF (0.65 mL, 7.0 mmol) was taken in a two necked round bottomed flask under N_2 atmosphere. Cooled to 0°C, freshly distilled $POCl_3$ (0.55 mL, 7.0 mmol) was then added slowly to it with continuous stirring. After complete addition, the mixture was again stirred at room temperature for 1 h. To this mixture a solution of tetraethyl bipyrrole **TS12** (350 mg, 1.4 mmol) in dichloroethane was added at room temperature, under N_2 atmosphere. Subsequently, the reaction mixture was refluxed in a preheated oil bath for 2 h, cooled to room temperature and quenched with sat. NaOAc (70 mmol) solution and again refluxed for 1 h. The reaction mixture was cooled to room temperature, diluted with $CHCl_3$ and organic layer was separated and washed with water, dried with anhyd. Na_2SO_4 and evaporated to dryness. The crude product was purified by column chromatography (silica, ethyl acetate/hexane 1:4). Yield: 165 mg, 41 %.

^{1}H NMR (400 MHz, $CDCl_3$, δ in ppm): 1.09 (t, J = 7.6 Hz, 4H), 1.29 (t, J = 7.6 Hz, 4H), 2.55 (q, J = 7.6 Hz, 4H), 2.80 (q, J = 7.6 Hz, 4H), 9.13 (bs, 2H, NH), 9.65 (s, 2H, -CHO).

2.5 Summary

A brief account of various solvents, chemicals used in the synthesis and different spectrometers and other physical and computational methods employed for characterization in our investigation, is given in this chapter. Syntheses of the already reported compounds, which are employed as starting materials for the dissertation work, were also described here.

2.6 References

1. Armarego, W. L. F.; Chai, C. In *Purification of laboratory chemicals*; sixth edition, Elsevier, Burlington**, 2003**.

2. SAINT, version 6.45 /8/6/03, Bruker AXS, **2003**.
3. Sheldrick, G. M.; *SADABS, Program for Empirical Absorption Correction of Area Detector Data,* University of Göttingen, Germany, **1997**.
4. Sheldrick, G. M.; *SHELXS-97* and *SHELXL-97, Programs for the Solution and Refinement of Crystal Structures,* University of Göttingen, Germany, **1997**.
5. (a) Spek, A. L.; *PLATON, A Multipurpose Crystallographic Tool*, Utrecht University, Utrecht, The Netherlands, **2002**; (b) Spek, A. L. *J. Appl. Cryst.* **2003**, *36*, 7.
6. Oxford Diffraction. CrysAlis CCD and CrysAlis RED. Versions 1.171.33.55. Oxford Diffraction Ltd, Yarnton, Oxfordshire, England, **2008**.
7. Sheik-Bahae, M.; Said, A. A.; Wei, T.-H.; Hagan, D. J.; Van Stryland, E. W. *IEEE J. Quantum Electron.* **1990**, *26*, 760.
8. (a) Swain, D.; Anusha, P. T.; Prashant, T. S.; Tewari, S. P.; Sarma, T.; Panda, P. K.; Rao, S. V. *Appl. Phys. Lett*. **2012**, *100*, 141109. (b) Anusha, P. T.; Swain, D.; Hamad, S.; Giribabu, L.; Prashant, T. S.; Tewari, S. P.; Rao, S. V. *J. Phys. Chem. C* **2012**, *116*, 17828.
9. Dixon, L. A. (April 15, **2001**). PPE. In *Encyclopedia of Reagents for Organic Synthesis*. John Wiley & Sons, Ltd. DOI: 10.1002/047084289X.rp185, onlinelibrary.wiley.com/o/eros/articles/rp185/frame.html.
10. (a) Franzen, H. *J. Pract. chem.* **1907**, *76*, 205. (b) Samsoniya, Sh. A.; Trapaidze, M. V.; Kuprashvili, N. A.; Kolesnikov, A. M.; Suvorov, N. N. *Khim. Geterotsikl. Soedin.* **1985**, 1222.
11. (a) Park, S.; Brookhart, M. *J. Am. Chem. Soc.* **2012**, *134*, 640. (b) Oxley, P. M.; Partridge, W. T.; Robson, D.; Short, W. F. *J. Chem. Soc.*, **1946**, 763.
12. (a) Weinstock, L. M.; Currie, R. B.; Lovell, A. V. *Synth. Commun.* **1981**, *11*, 943. (b) Kelly, N. M.; Reid, R. G.; Willis, C. L.; Winton, P. L. *Tetrahedron Letters*, **1995**, *36*, 8315.
13. (a) Johnson, A. W.; Markham, E.; Price, R.; Shaw, K. B. *J. Chem. Soc.* **1958**, 4254. (b) Sessler, J. L.; Johnson, M. R.; Lynch, V. *J. Org. Chem.* **1987**, *52*, 4394. (c) Jiao, W.; Lash, T. D. *J. Org. Chem.* **2003**, *68*, 3896. (d) Panda, P. K.; Kang, Y.-J.; Lee, C.-H. *Angew. Chem. Int. Ed.* **2005**, *44*, 4053.

14. (a) Dohi, T.; Morimoto, K.; Maruyama, A.; Kita, Y. *Org. Lett.* **2006**, *8*, 2007. (b) Vogel, E.; Koch, P.; Hou, X.-L.; Lex, J.; Lausmann, M.; Kisters, M.; Aukauloo, A. M.; Richard, P.; Guilard, R. *Angew. Chem., Int. Ed. Engl.* **1993**, *32*, 1600. (c) Sessler, J. L.; Mozaffari, A.; Johson, M. R. *Org. Synth*. **1998**, *Coll. Vol. 9*, 242.

CHAPTER 3

Dinaphthoporphycenes

3.1 Introduction

3.1.1 Background

Porphycene **L2** is the first constitutional isomer of porphyrin to be reported by Vogel in 1986.[1] Among the other isomers of porphyrin, porphycene is also regarded as the most stable one.[2] Hence its chemistry has been widely studied particularly as a ligand;[3] again the corresponding metal complexes are explored in terms of many applications such as catalysis,[4] material chemistry,[5] protein mimicry[6] etc. It can be formally derived from porphyrin by replacing two alternate *meso* carbons with a direct pyrrole-pyrrole linkage and inserting two carbon atoms at the remaining two *meso* positions. The name porphycene arises from its similarity to both porphyrins and acenes, which is also referred to as [18]porphyrin-(2.0.2.0).[7] Reduced symmetry of porphycene in comparison with porphyrin causes bathochromic shift in absorption spectra, particularly Q-like transitions are more intense than (λ > 600 nm, ε > 50000 $M^{-1}cm^{-1}$) porphyrin, which stimulates interest among the researcher to explore its ability as a potential photosensitizer for photo dynamic therapy (PDT) of cancer[8] and photoinactivation of viruses and bacteria.[9]

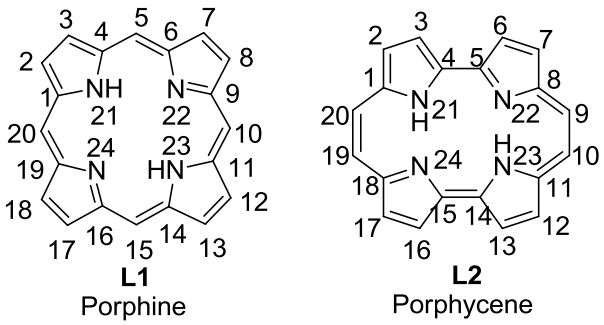

Figure 3.1 General structures of porphine and porphycene with atom numbering scheme.

In his seminal paper, Vogel reported the synthesis of porphycene from 2,2′-bipyrrole dialdehyde **L22** via McMurry type coupling to effect reductive dimerization **L23**, which in turn oxidized spontaneously by atmospheric O_2, resulting in the formation of an 18 π-electron aromatic macrocycle **L2** (Scheme 3.1).[1] The evidence of aromatic nature of porphycene **L2** first came from its proton NMR data, for instance the internal NH protons suffers a significant upfield shift (δ = 3.15 ppm) relative to simple pyrrolic NH protons. At the same time β-pyrrolic protons experiences a down field shift. These shifts were taken as an indication of presence of diamagnetic ring current in the macrocycle. Further support for aromatic nature of **L2** came from UV-Vis spectral analyses. The absorption spectrum of **L2** recorded in benzene was found to be similar in many ways to unsubstituted porphyrin. For

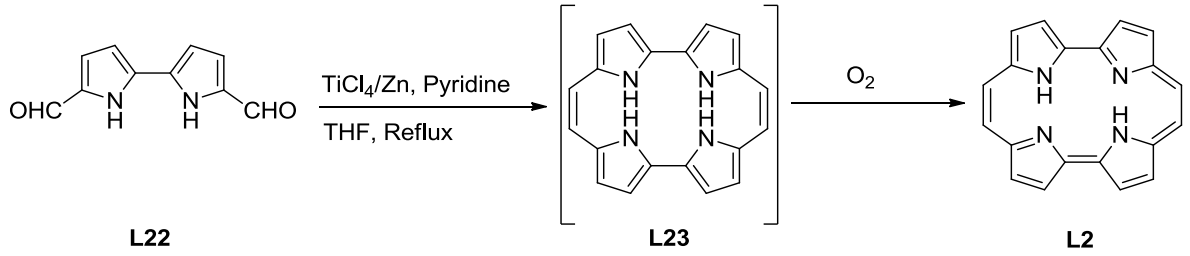

Scheme 3.1 Vogel's synthesis of porphycene.

instance, a split Soret like band was observed in the near UV region (λ_{max} = 358 and 370 nm) along with three Q-type transition in the visible region (λ_{max} = 558, 598 and 560 nm). These observations support the basic notion that compounds of porphycene class are best regarded as true aromatic isomer of porphyrin.

3.1.2 Synthesis of substituted porphycenes

Albeit, diverse range of porphycenes made till date, the general strategy employed by Vogel i.e. McMurry coupling[10] of bipyrrole dialdehyde remains the most versatile one for the synthesis of porphycene, with very few exception used to make some specific system. For instance, Srinivasan and coworkers employed acid catalyzed oxidative coupling strategy for the synthesis of 9,10,19,20-tetraaryl porphycene **L25** (Scheme 3.2).[11] Therefore, synthesis of functionalized porphycene remains largely dependent on synthesis of novel bipyrroles. Among the various methods available for synthesis of bipyrrole,[12] Ullmann coupling of iodo-

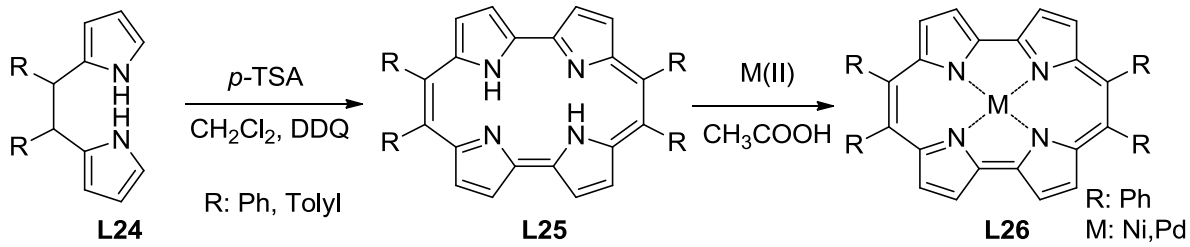

Scheme 3.2 Synthesis of *meso*-tetraaryl porphycene following acid mediated oxidative coupling.

pyrrole **L27**[13] remains most attractive as it permits to synthesize diverse range of bipyrroles having *β*-pyrrolic substituents. Shortly after the synthesis of unsubstituted porphycene **L2**, Vogel and coworkers synthesized alkylated porphycenes, bearing alkyl chains mainly at 2,7,12,17-positions to improve the solubility and crystallinity of the macrocycle (Scheme 3.3), so as to make them suitable for further studies.[14] Several methodologies were developed

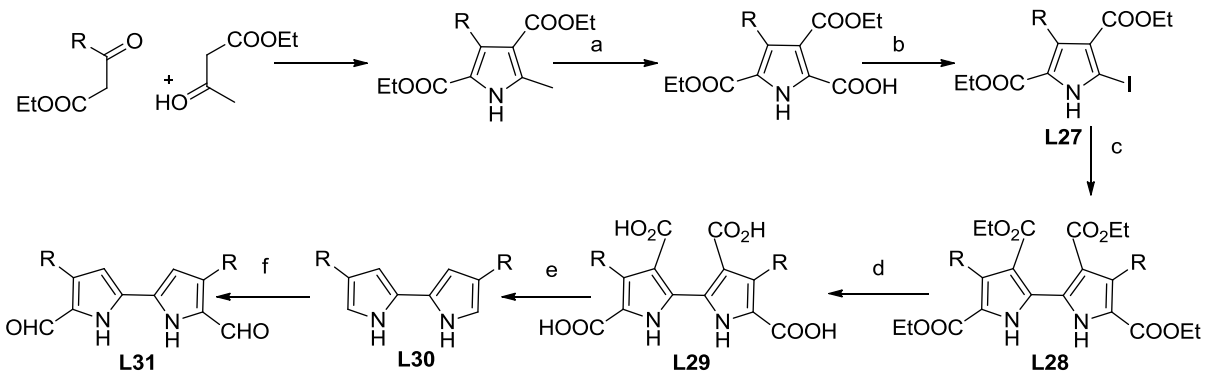

Scheme 3.3 Synthesis of *β*-alkylated porphycenes: (a) Br_2, SO_2Cl_2, AcOH/HCOOH, 0 °C. (b) KI/I_2, EtOH/H_2O, 75 °C. (c) Cu, DMF, 20 °C. (d) NaOH, EtOH/H_2O, reflux. (e) Sublimation. (f) $POCl_3$, DMF.

to improve the synthesis of substituted bipyrroles in order to access porphycene for photophysical studies. In this direction, contribution from Nonell group is noteworthy. Specifically single step decarboxylation,[15] non-decarboxylative method[16] and use of thienyl bipyrrole[17] are notable. Improved synthesis of bipyrroles, allows synthesis of novel porphycenes having interesting photophysical properties. For example, 2,7,12,17-tetraphenylporphycene[15] shows bathochromic shift (30 nm) in absorption spectrum compared to that of unsubstituted porphycene. Thus, it was suggested that absorption spectra of porphycene, particularly in the Q-band region could be modulated by placing appropriate substituent at the periphery, thereby allowing optimization of optical properties desirable for PDT application.[18]

3.1.3 *Meso-*, etio- and dodeca- substituted porphycenes - Effect of substitutions on core geometry

Geometry of unsubstituted and those of 2,7,12,17- alkylated porphycenes core were found to be rectangular (short and long N-N distance typically in the range 2.6 and 2.9 Å respectively).[14] Metal complexation ability of porphycenes is less efficient compared to porphyrins. Because of its rectangular core, lone pairs on nitrogens are not properly oriented towards the metal centre. However, it was observed that geometry of porphycene core could be modulated[19] by introducing steric hindrance through the substituents at the periphery, particularly -9,-10,-19,-20 (*meso*)[20] positions as well as in the -3,-6,-13,-16 (inner *β*-) positions. This latter species bear structural similarity to etioporphyrin and known as etioporphycene.[21]

Meso-tetraalkylated porphycene was first synthesized again by Vogel in 1989,[20] via McMurry coupling of diacylated bipyrroles (Scheme 3.4).[22] X-ray structure determination of **L34** (R = C_3H_7) derivative shows a planar skeleton, but due to repulsion of the propyl group there is a

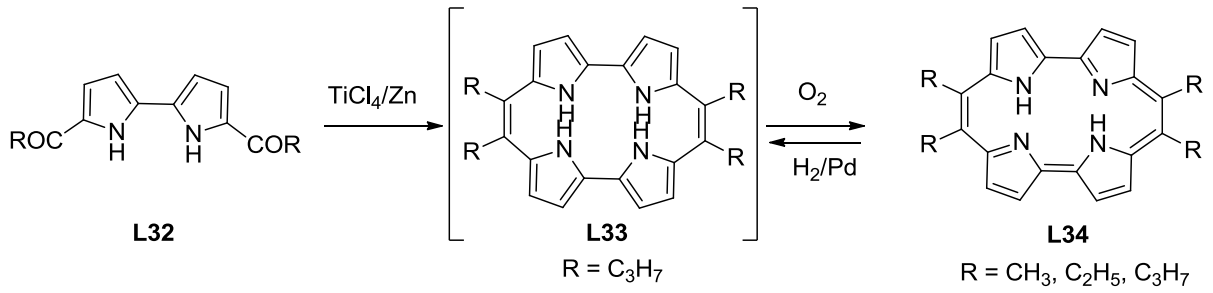

Scheme 3.4 Synthesis of *meso*-tetraalkylated porphycenes.

convergence of the oppositely disposed nitrogen atoms resulting in rather smaller N-N distance compared to unsubstituted porphycene (2.5 Å vs. 2.6Å) and geometry of the core now becomes decidedly rectangular.[20a] Another interesting observation in *n*-propyl derivative is that catalytic hydrogenation of this allows isolating its intermediate form (**L33)**. X-ray structure of this intermediate form revealed a cyclophane-type conformation in which each bipyrrole moiety rotated out of the plane in opposite direction. It was assumed that the steric

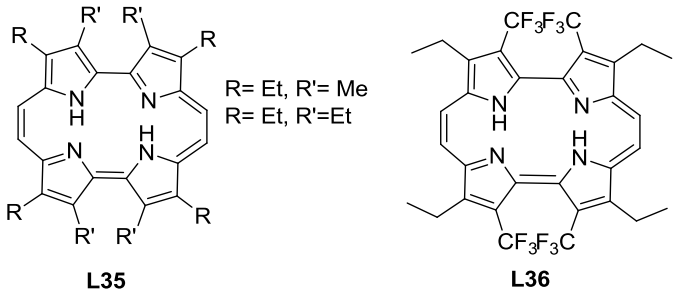

Figure 3.2 *β*-Octasubstituted porphycenes.

interactions between the adjacent alkyl chains drastically slow down the rate of pyrrole ring rotation, which in turn provides kinetic barrier against adopting a planar conformation in order to undergo easy oxidation. However, *β*-octasubstituted porphycenes (Figure 3.2) show rather square type core and thus capable of accommodating larger metal ions.[21] For example, the more open cavity of etioporphycene was rationalized in terms of steric interaction of the *β*-substituents which force the molecule to adopt a square core. The required pyrroles for the synthesis of *β,β′*-substituted bipyrroles are generally obtained by Zard-Barton method.[23]

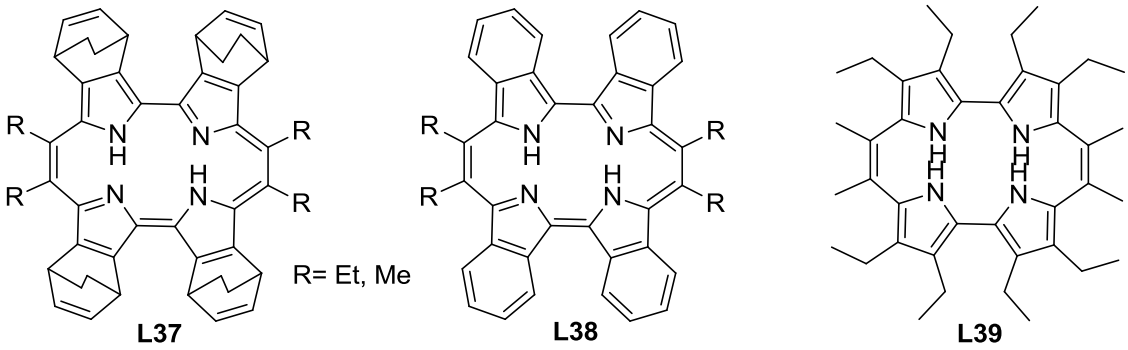

Figure 3.3 Dodecasubstituted porphycenes.

Very recently dodecasubstituted porphycenes, i.e. *meso*-tetra-*β*-octasubstituted derivatives are reported by Yamada and coworkers (Figure 3.3).[24] This involves use of bicyclo[2.2.2]octadiene (BCOD) fused bipyrrole. McMurry coupling of acylated BCOD fused bipyrrole leads to the formation of *meso*-tetraalkyl BCOD fused porphycene **L37**, which was subsequently converted quantitatively to the corresponding tetrabenzoporphycene **L38** by heating at 220 °C under vacuo. X-ray structure of BCOD fused derivative **L37** (R = Et) shows saddle type structure with a rectangular core comparable to unsubstituted porphycene. *Meso*-free analogue of BCOD fused porphycene **L72** also shows a somewhat rectangular type core (2.7 and 2.8Å), instead of a square core obtained for octaethylporphycene.[25] This indicates comparatively less bulkiness of BCOD fused derivative. However, attempt to obtain open chain dodecasubstituted derivative remains so far unsuccessful, and resulted in the formation of *N,N′*-dihydro intermediate **L39**, which could not be oxidized to porphycene, unlike in the case of *β*-tetraethyl-*β*-tetra(trifluoromethyl) porphycene **L36**.[26]

3.1.4 Functionalization of porphycene

Reactions at porphycene periphery are very important in order to obtain functionalized porphycenes that are having improved photochemical properties and pharmacological efficacy. Halogenation of alkylated porphycene **L40** (R = C_3H_7) provides up to tetra-substituted species as readily isolable products **L41**.[27] Mono bromination or iodination could be achieved using solid support **L43**.[27a] However, in case of unsubstituted porphycene **L2** (R = H) halogenation takes place exclusively at 2-position (**L42**).

Sulfonation of porphycene (Scheme 3.6) with fuming sulfuric acid gives mixture of mono-, di- and tri-sulfonated products **L44**.[28] The sodium salts of these sulfonated products are water

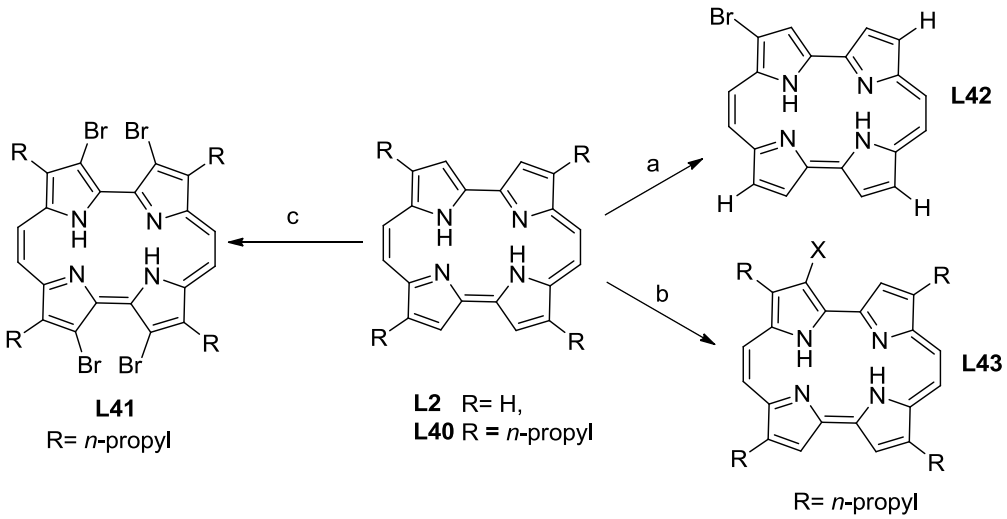

Scheme 3.5 Halogenation of porphycenes: (a) NBS, $CHCl_3$, (b) (X = I) Amberlyst A-26, bromoform, CH_2Cl_2, AcOH, 0 °C. (X=I) I_2, 0 °C. (c) Br_2, CCl_4, NaOAc/H_2O.

soluble thereby making them useful for biological application. Similarly, sulfonyl chloride group can be introduced at 3-position of porphycene **L40** by treating with sulfonyl chloride (**L45**).[29] This latter species can be further converted to its sulfonamide derivatives **L46** and **L47** by reacting with appropriate amines. These water soluble sulfonamides have been reported as an effective mitochondrial localizer.[29]

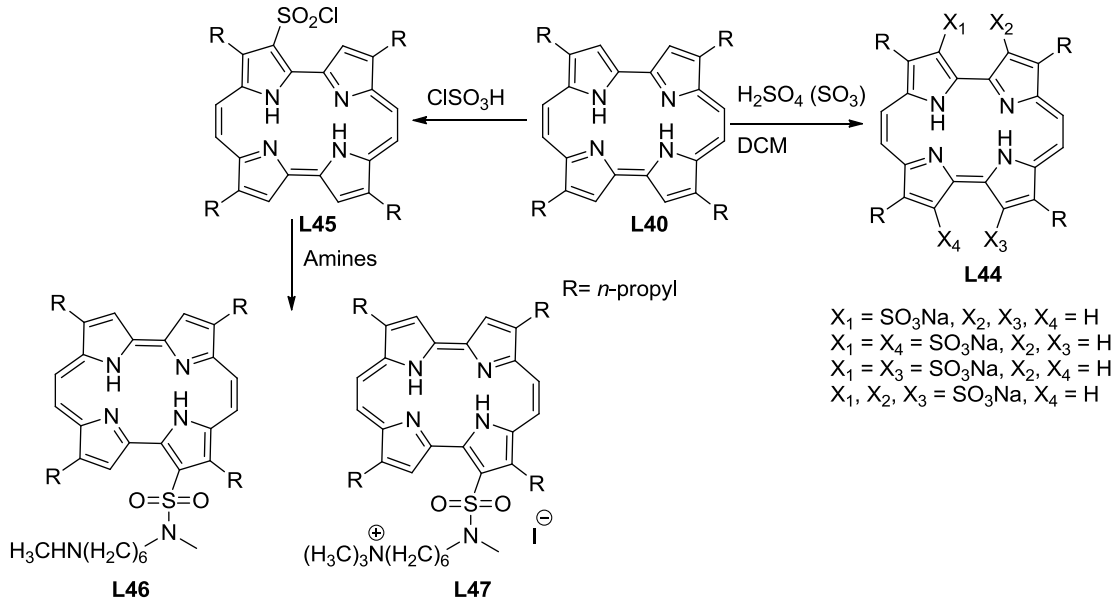

Scheme 3.6 Sulfonation of porphycene and its further derivatizations.

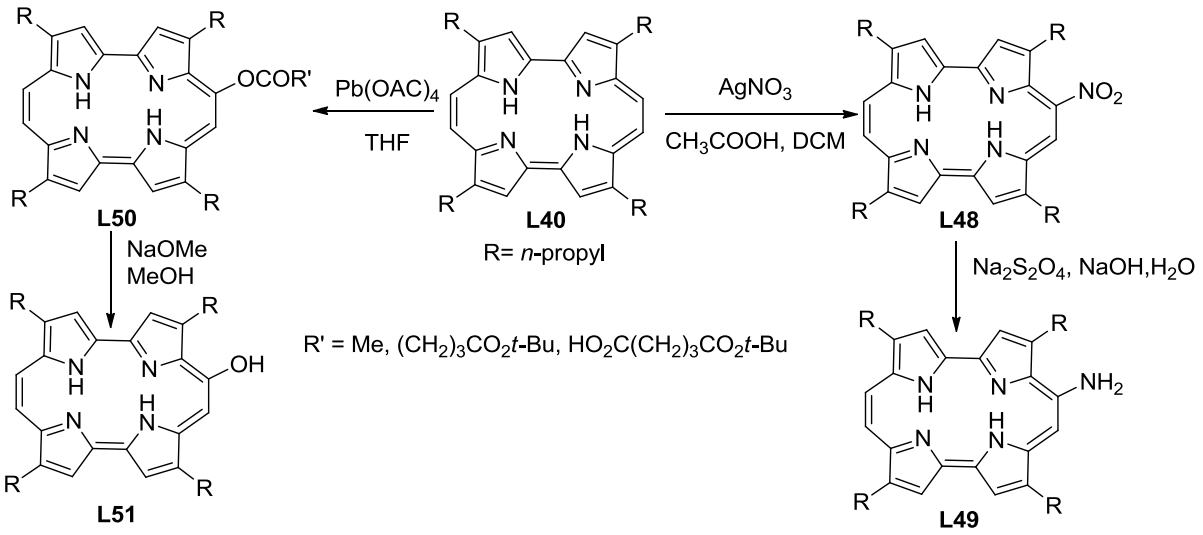

Scheme 3.7 *Meso*-functionalizations of porphycene.

Unlike halogenation and sulfonation reactions of porphycene, which take place at *β*-pyrrolic position, nitration of porphycene occurs at *meso*-position (Scheme 3.7).[30] This nitro group at 9-position (**L48**) can further be reduced to its corresponding amine (**L49**).[31] Similar functionalization at *meso* positions includes formation of acyloxy-derivative (**L50**), which can be further hydrolyzed to yield 9-hydroxyporphycene (**L51**).[30] These 9-substituted porphycenes are important starting materials for the preparation of a variety of derivatives and conjugates, studied extensively for PDT application.[32]

Functional group interconversion at porphycene side chain (Scheme 3.8) leads to an array of peripherally functionalized compounds that are studied widely for PDT application. 2,7,12,17-tetramethoxyethyl porphycene **L52** plays a pivotal role in this regard.[33] Removal of methyl ether protection using Lewis acid such as BBr_3 affords the corresponding alcohol (**L53**), which can be further interconverted to different functional groups viz. mesylate (**L54**), cyano (**L55**) and carboxylate (**L56**).[32] On the other hand, using BBr_3 in presence of boric acid provides bromo derivative (**L57**) instead of the hydroxyl-counterpart. Mono-, di-, tri-, or tetra-brominated products could be isolated depending upon the amount of Lewis acid used. This can be further converted to vinylporphycenes (**L58**, **L59**), upon treatment with DBU.[32] Mono-vinylporphycene undergoes Diels-Alder reaction upon treatment with dimethyl acetylenedicarboxylate to provide mono-benzoporphycene **L60**, which is studied widely as a potential PDT photosensitizer.[33,34]

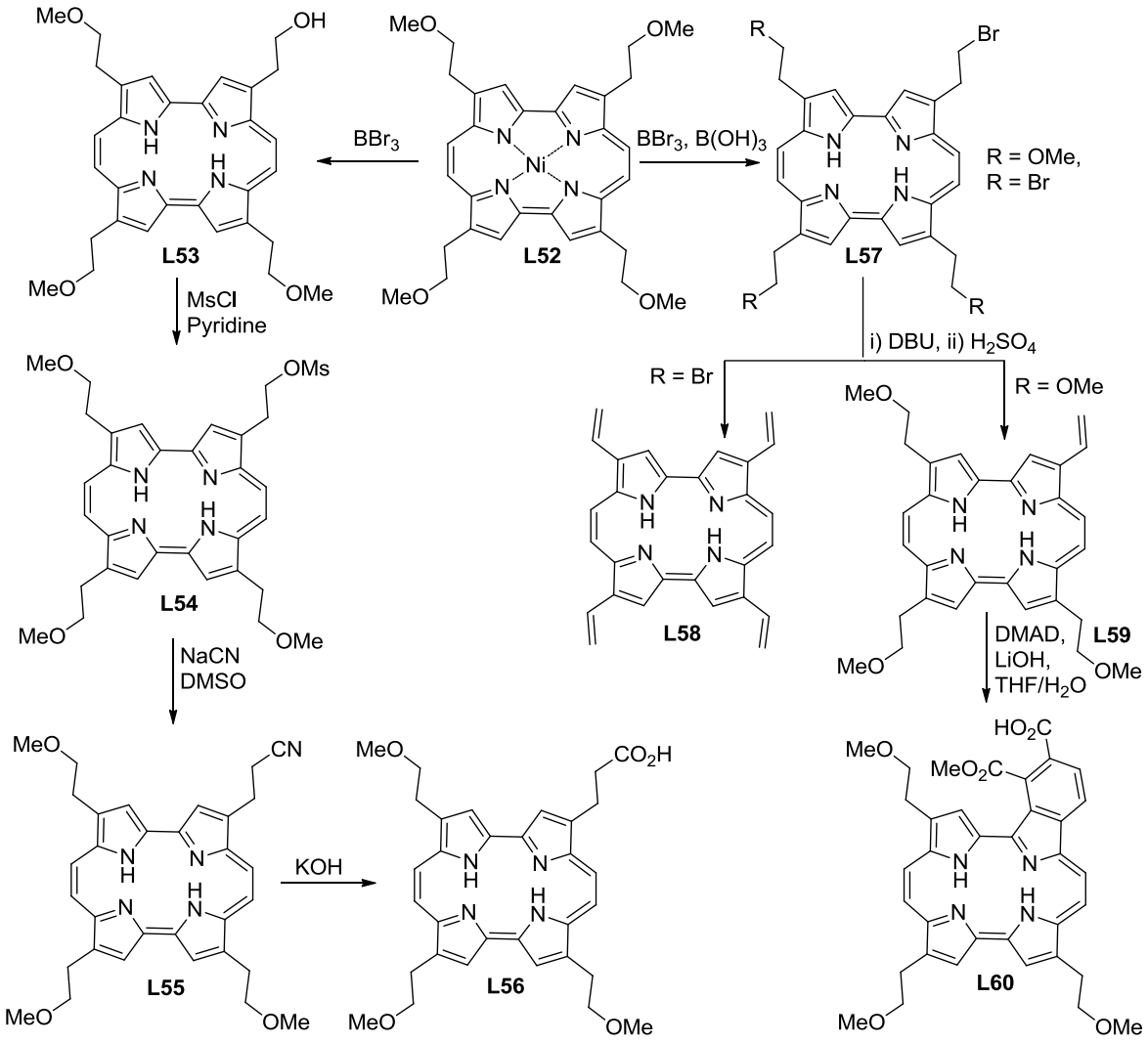

Scheme 3.8 Functional group interconversion in porphycenes.

3.1.5 Porphycene containing hetero atoms

Heteroatom substitution in porphycene involves replacement of pyrrolic nitrogen with hetero atoms such as S and O or via introduction of heteroatom at the periphery. Introduction of hetero atom often results in red shift in absorption spectra. Hence could be useful in PDT application. First of this kind reported by Vogel in 1988, was tetraoxaporphycene dication **L61**, which shows aromatic nature.[35] Porphycene having two nitrogen and two oxygen atoms (**L62**) was also prepared by Vogel, although not reported in public domain.[36] The sulfur analogue of **L61** (i.e. **L63**) could not be isolated in aromatized form.[37] However, dithiaporphycene **L64** was isolated as aromatic macrocycle, resembling property similar with parent porphycene in many respects.[38] Mixed furan-thiophene porphycenes (**L65-67**) were reported by Dai et al. could not be aromatized.[39] First porphycene containing heteroatom in its periphery was reported by Neidlein et al. using formylated pyrrolyl thiazole.[40] Resulting

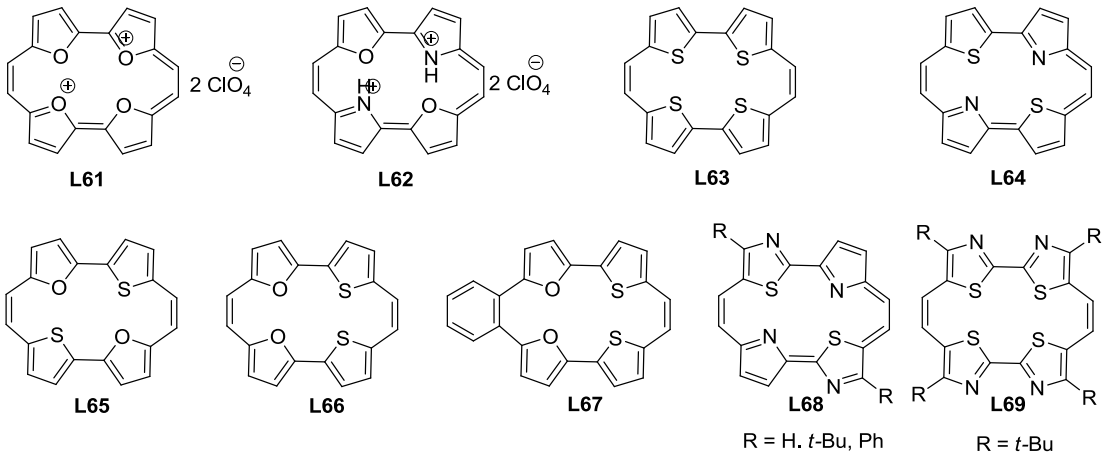

Figure 3.4 Porphycenes containing hetero atom.

macrocycle (**L68**) was aromatic and shows bathochromic shift in absorption compared to **L64**. However the tetrathia analogue (**L69**) could not be aromatized.[41] In 2003, Sessler and Nonell group independently reported synthesis of tetraazaporphycene containing biimidazole referred to as imidacene **L70** (Scheme 3.9).[42] While Sessler[42a] reported tetraalkyl derivative, on the other hand, Nonell [42b] synthesized the tetraaryl counterpart. Immediate effect of introduction of nitrogen at the periphery was seen in its absorption property. For instance, Q-bands of tetraarylimidacene shows 100 nm bathochromic shift compared to tetraphenyl-porphycene, which stimulated interest in their photophysical properties.

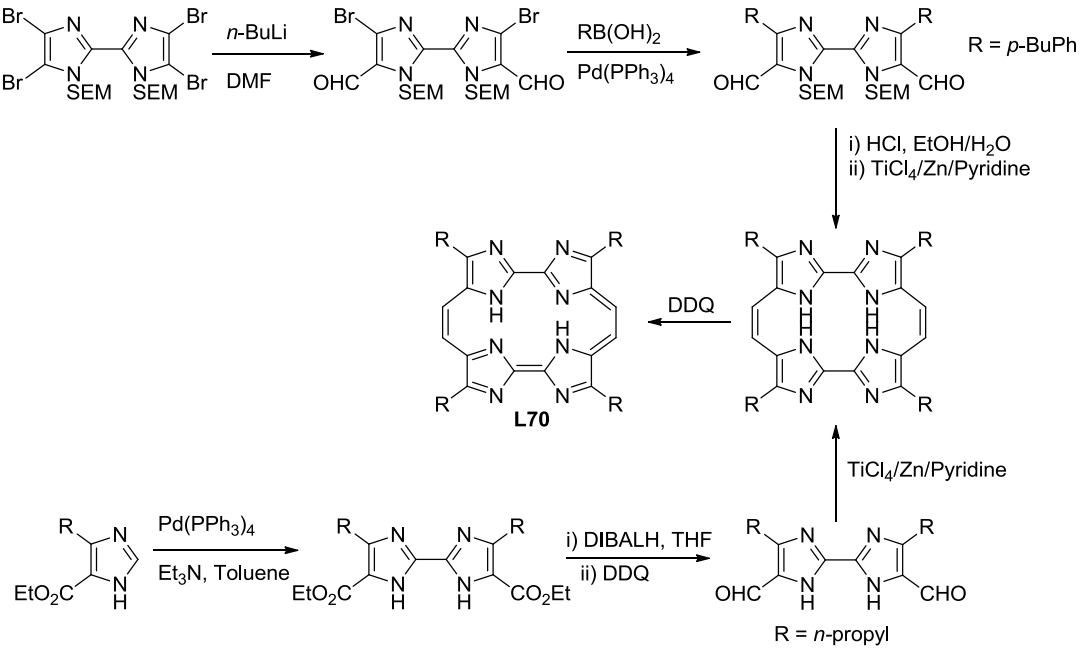

Scheme 3.9 Synthetic scheme of aryl and alkyl imidacenes.

3.1.6 π-Extended porphycenes through ring fusion

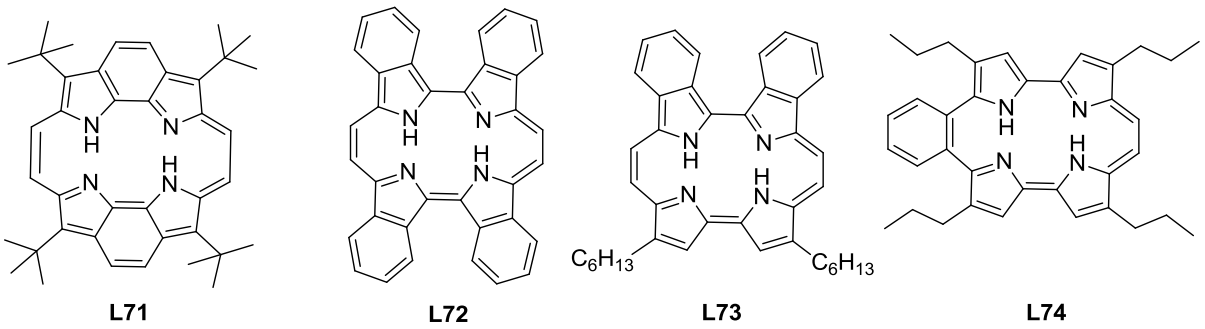

Figure 3.5 Examples of π-extended porphycenes.

Examples of porphycene having extended π-conjugation are very rare. Except the di- and tetrabenzoporphycene (β-fusion) reported by Yamada group,[25] detailed synthetic methodology as well as photophysical properties are not available in public domain for other systems such as Vogel's dibenzoporphycene **L71** (β,β'-fusion).[43] This is also true for 9,10-benzotetrapropylporphycene **L74**.[44] Synthesis of benzo-fused porphycene **L72** involves use of BCOD fused bipyrrole dialdehyde **L75**. McMurry coupling of BCOD fused bipyrrole provides the corresponding BCOD fused porphycene **L76**, which was subsequently converted to benzo-fused porphycene **L72** under thermal condition as shown in scheme 3.10.[25] Mixed McMurry coupling of BCOD-fused pyrrole dialdehyde and alkylated bipyrrole dialdehyde generates dibenzo porphycene **L73**, along with other two possible derivatives. As a result of

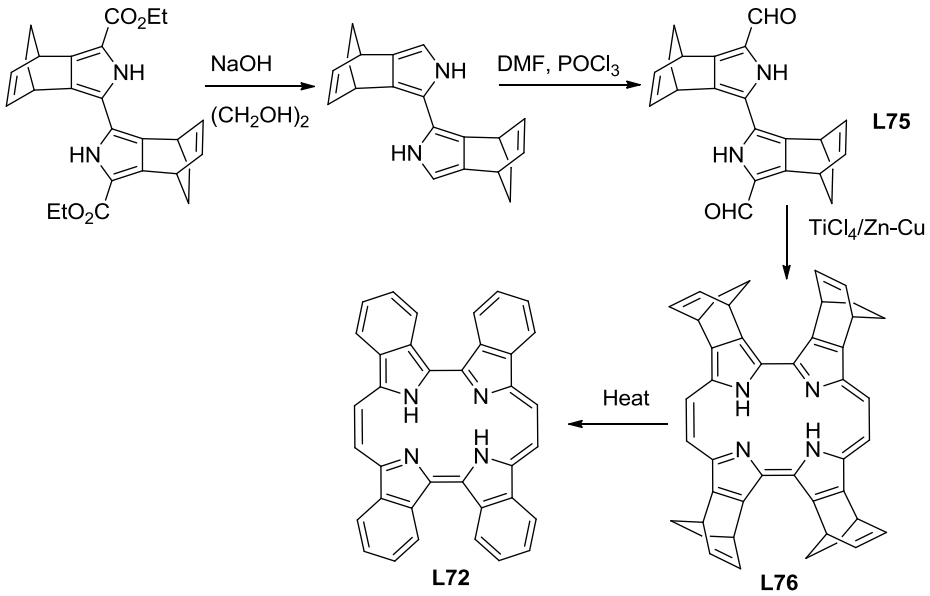

Scheme 3.10 Synthetic scheme for tetrabenzoporphycene.

π-extension, absorption spectrum of tetrabenzoporphycene **L72** undergoes substantial red shift compared to β-alkylated porphycenes. For example B-band was observed at 434 nm and lowest energy Q-type band was observed at 670 nm. Further, the *meso*-tetraalkylated analogue of **L72** (dodecasubstituted porphycene) is reported recently by the same group.[24] This macrocycle displays further red shift in absorption spectrum (B-band at ~ 450 nm, Q-band ~ 740 nm) compared to **L72**. 9,10-Benzotetrapropylporphycene **L74** was formed in the McMurry coupling of monovinylogous bipyrrole dialdehyde **L77**. This reaction gives **L79** as a predominant product while **L80** was obtained as a side product. This latter species could not be isolated but electrocyclization and spontaneous dehydrogenation produced **L74** in 0.7 % yield.[44]

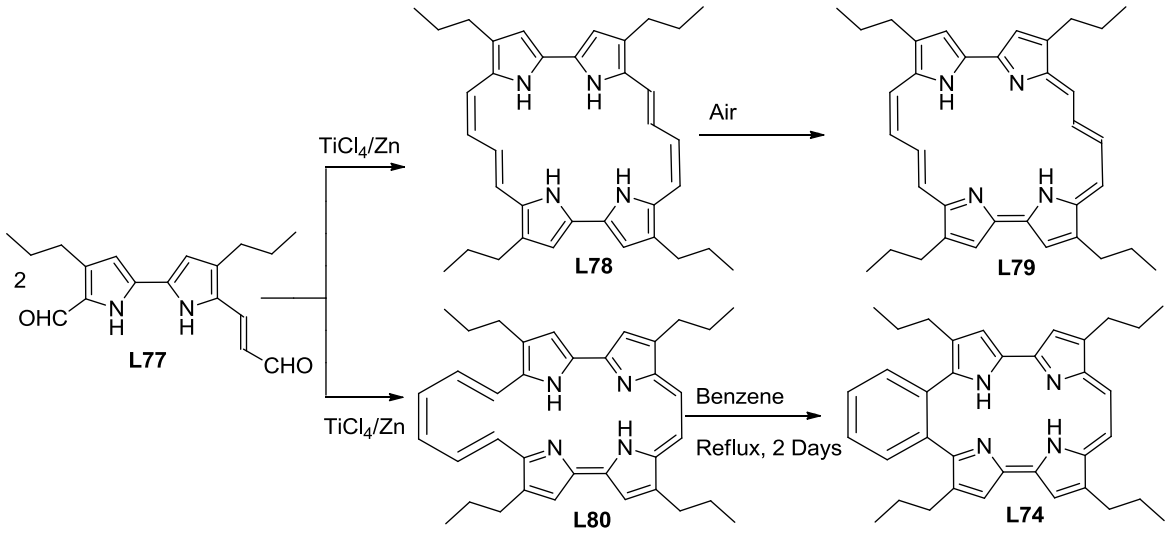

Scheme 3.11 Synthetic scheme for 9,10-benzotetrapropylporphycene **L74**.[44]

3.2 Research goal

Keeping in view the above perspective, we wish to investigate a porphycene system where two fused bipyrrolic units are involved in macrocycle formation. The fusion of these bipyrrolic entities with aromatic rings is expected to impart structural rigidity and further extend the aromatic conjugation, thereby display interesting structural as well as photophysical properties. In this context, we choose to synthesize naphthobipyrrole bearing alkyl substitution in the 3 and 8 positions (for numbering see figure 3.6), which can be further formylated in 2 and 9 positions thereby making them suitable for the McMurry coupling, introduced by Vogel for the porphycene synthesis. On the other hand acylation or benzoylation in 2 and 9 positions of naphthobipyrrole, followed by McMurry coupling would result in tetra-*meso*-substituted dinaphthoporphycenes. The designed dinaphthoporphycenes[45]

supposed to exhibit good solubility (in common organic solvents owing to alkyl chains at the periphery) and crystallinity.

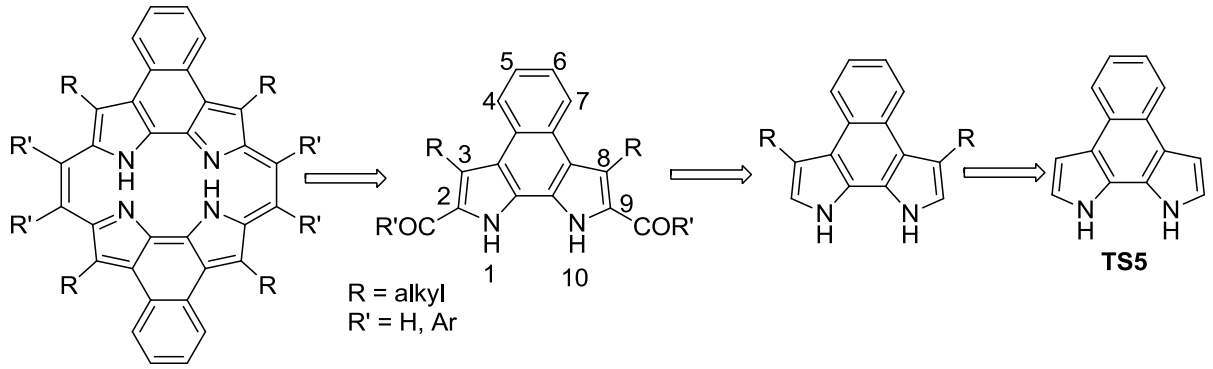

Figure 3.6 Retrosynthetic analysis for the synthesis of proposed dinaphthoporphycenes.

3.3 Results and discussion

3.3.1 Synthesis of alkylated naphthobipyrroles and its corresponding dinaphthoporphycenes

Unsubstituted naphthobipyrrole **TS5** was reported in literature in 1985.[46] Looking at its interesting structural feature, i.e. a bipyrrole fused with an aromatic ring, we anticipated this could be an interesting building block for the synthesis of π-extended porphyrinoids, since bipyrrole served to be a versatile precursor for the synthesis of numerous porphyrinoids. However, owing to its poor solubility in common organic solvents, this potential building block remained unexplored. Further, the Vilsmeier-Haack formylation of naphthobipyrrole is reported to yield the corresponding 3,8-diformyl derivative.[47] The origin of such claim was based on quantum-chemical calculation performed on unsubstituted naphthobipyrrole, which shows highest electron density distribution in 3 and 8 positions.[47] In order to modify its solubility, we deliberate to introduce alkyl chains at its periphery, particularly in the β-pyrrolic positions. Therefore, we proposed acylation reaction of **TS5** under Vilsmeier condition, followed by reduction under alkaline condition to yield the desired 3,8-dialkyl naphthobipyrrole. Unsubstituted naphthobipyrrole **TS5** was synthesized following literature method as described in chapter 2 of the thesis.[46] Vilsmeier acylation of **TS5** were carried out with *N*,*N*-dimethylpropanamide and *N*,*N*-dimethylisobutyramide. ^{1}H NMR analysis of the resultant products in DMSO-d_6 showed a symmetrical spectra indicating presence of C_2 axis in the molecule (unsymmetrical product such as 2,8-diacylated derivative is also possible at least in theory). Presence of alkyl signals also confirms incorporations of acyl groups. However, positions of acyl groups could not be confirmed unequivocally from the NMR

spectrum because acylation at both 3,8- or 2,9-positions supposed to display similar spectral

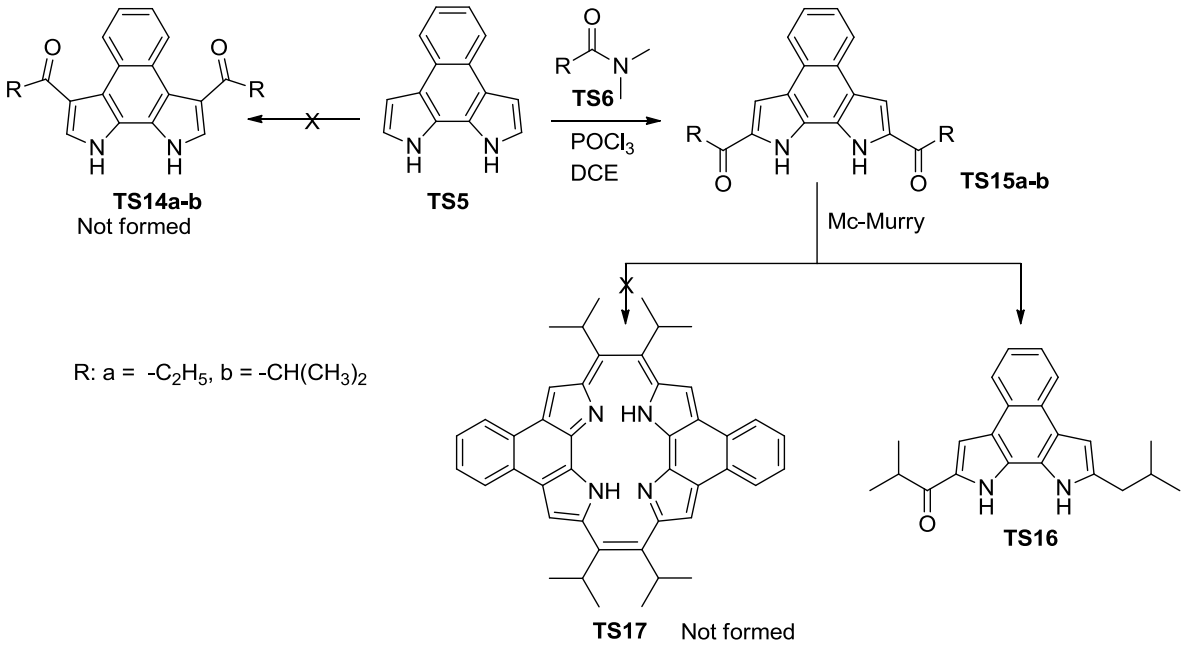

Scheme 3.12 Proposed synthesis of *meso*-alkylated dinaphthoporphycenes.

pattern. Therefore, our assumption regarding formation of **TS14** was mostly based on previous report of formylation.[47] Fortunately, we were able to grow single crystal for isobutyl derivative of naphthobipyrrole. Contrary to our assumption, X-ray structure revealed occurrence of acylation at 2,9-positions (**TS15b**), rather than at 3,8-positions (**TS14b**), resulting in the formation of 2,9-diketone derivatives (**TS15**) exclusively (Figure 3.7) . These diketones when subjected to McMurry type coupling did not yield any macrocycle. Interestingly we could able to isolate the one side reduced derivative (**TS16**) confirmed via single crystal X-ray diffraction analysis (Figure 3.7). The probable reason of this failure

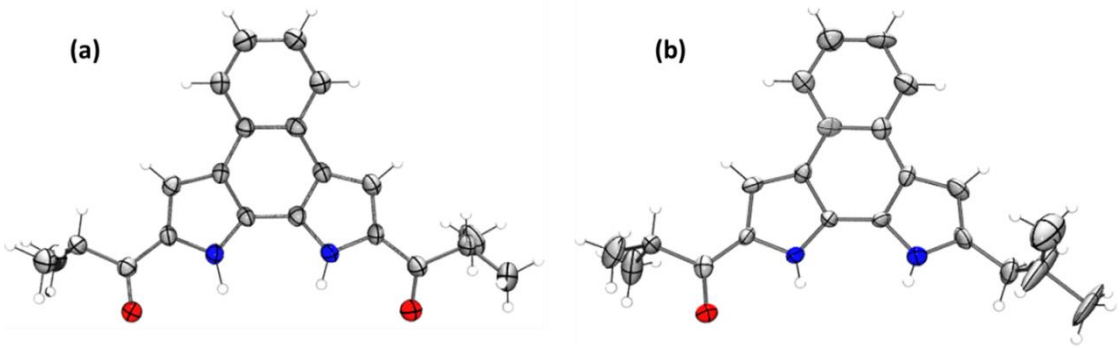

Figure 3.7 ORTEP of (a) isobutyl derivative **TS15b** and (b) its partially reduced counterpart **TS16**. Thermal ellipsoids are scaled to 35 % probability level.

could be insufficient solubility of **TS15b** along with steric congestions between the neighboring *i*-Pr groups. Acylation of the naphthobipyrrole diester (**TS4** chapter 2) and direct alkylation under Friedel-Crafts condition were also proved to be futile.

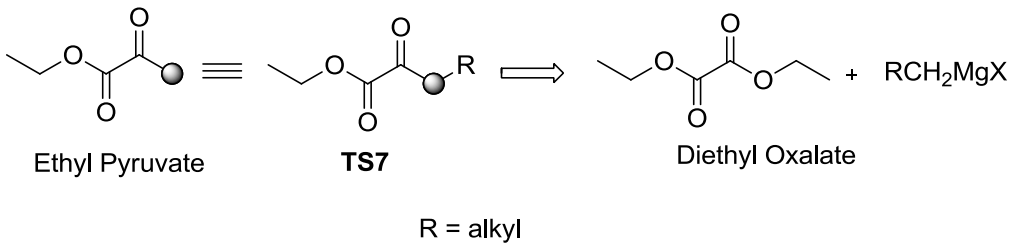

Scheme 3.13 General retro-synthetic strategy for synthesis of α-keto esters.

After being unsuccessful with these attempts, we closely looked at the reaction scheme for the synthesis of naphthobipyrrole and designed a new strategy for synthesis of 3,8-dialkylated naphthobipyrrole. Ethyl pyruvate contains one α-methyl group which is involved in cyclization during the PPE mediated cyclization of hydrazone **TS3** to its corresponding indole. If this methyl group is replaced with other alkyl chain of choice such that the resulting α-keto ester (**TS7**) contains at least a methylene unit α to the carbonyl in order to affect cyclization. The resultant naphthobipyrrole after acid mediated cyclization of the bis-hydrazone is expected to contain alkyl group at 3 and 8 positions. The desired α-keto esters of type **TS7** could be synthesized from selective Grignard reaction with diethyl oxalate, so as to react at only one ester carbonyl atom. The required Grignard reagent in turn could be prepared easily from corresponding alkyl bromide (chapter 2). These reactions were proved to be quite general in nature and well explored in literature.[48] We could able to make a range of α-keto esters, just by changing the R group (chapter 2, Scheme 2.4). After having the requisite α-keto esters in hand, we followed the similar methodology used for synthesis of unsubstituted naphthobipyrrole **TS5** (chapter 2, Scheme 2.2). The reaction of 2,3-naphthalene bishydrazine **TS2** with prepared α-keto esters **TS7** formed the corresponding bishydrazones **TS18** in nearly quantitative yield, which upon polyphosphate ester (PPE) mediated cyclization, led to easy introduction of β-alkyl groups in the resultant naphthobipyrrole diesters **TS19** (Scheme 3.14) in 26-67 % yield, from combined two steps. Subsequent base mediated hydrolysis and decarboxylation resulted α-free bipyrrole derivatives **TS20** in almost quantitative yield, which upon Vilsmeier-Haack formylation resulted in the formation of desired dialdehydes **TS21** in good yields (88-91 %). All the above steps are quite straightforward and could be carried out in gram scales. The bishydrazones were supposed to

form three geometrical isomers as the result of the two C=N double bonds in the product moiety, but their separation is not warranted, as the subsequent product is not at all affected

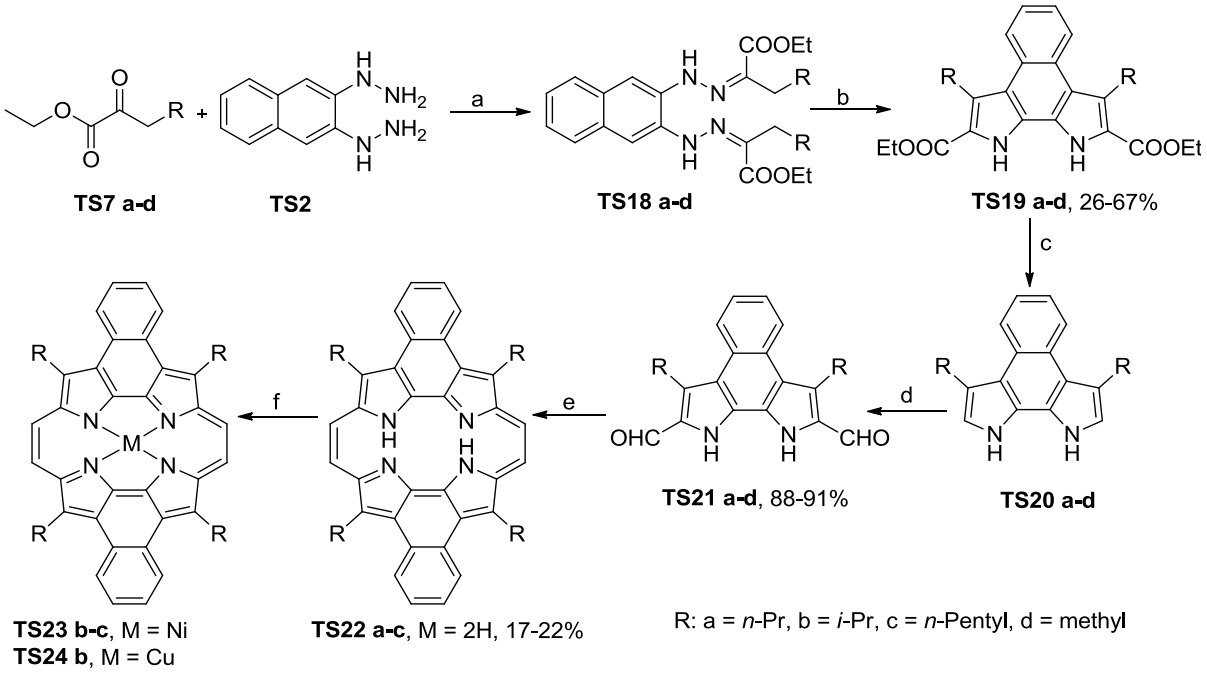

Scheme 3.14 Synthesis of dinaphthoporphycenes. (a) EtOH, reflux. (b) PPE 100 °C. (c) NaOH, $(CH_2OH)_2$, reflux. (d) DMF, $POCl_3$, NaOAc/H_2O. (e) $TiCl_4$/Zn-Cu, THF. (f) $Ni(acac)_2$, *o*-dichlorobenzene, reflux; $Cu(OAc)_2.H_2O$, $CHCl_3$/MeOH, Et_3N, reflux; $Pd(OAc)_2$, acetic acid, NaOAc reflux.

by this isomerism. However, for analytical purpose, the fastest moving isomer was separated in small quantity. With the required dialdehydes in hand, McMurry coupling reactions were performed to obtain the desired porphycenes. Unlike, in the case of dibenzoporphycene **L71**,[43] where unoxidized product was isolated after McMurry coupling and oxidised further to obtain the dibenzoporphycene, we obtained **TS22** directly in 17-22 % yields. This may be attributed to the easy reorientation of ring current for naphthalene moieties, while oxidation of the McMurry coupled product was not possible in case of the fused benzenoid ring leading to **L71**. However, methyl derivative of the dialdehyde **TS21d**, could not be converted to its corresponding porphycene probably due to its poor solubility in organic solvent. These porphycenes as well as their precursors were characterized by ^{1}H NMR, ^{13}C NMR spectroscopy, mass and elemental analysis. Isopropyl derivative of porphycene **TS22b** and its corresponding Ni and Cu complexes were also characterized by single crystal X-ray diffraction analysis, structural features of these molecules will be discussed later in this

section. Diesters **TS19b** and **TS19d** were also characterized by X-ray diffraction analysis, for which ORTEPs are shown in figure 3.8.

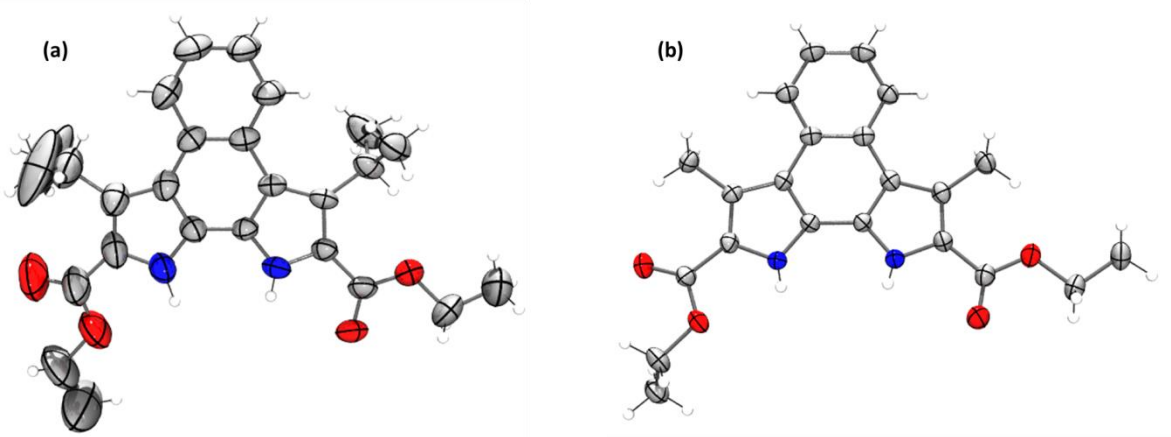

Figure 3.8 ORTEP of (a) *β*-di-*i*-propylnaphthobipyrrole diester **TS19b** and (b) *β*-di-methylnaphthobipyrrole diester **TS19d**. Thermal ellipsoids are scaled to 35 % probability level.

The proton NMR spectra of **TS22a-c** reveal highly deshielded NH protons appearing around 9 ppm that could be unequivocally assigned after deuterium exchange experiments. This may be attributed to strong intramolecular N-H...N hydrogen bonding in a rigid macrocyclic framework (due to the fused naphthalene rings).

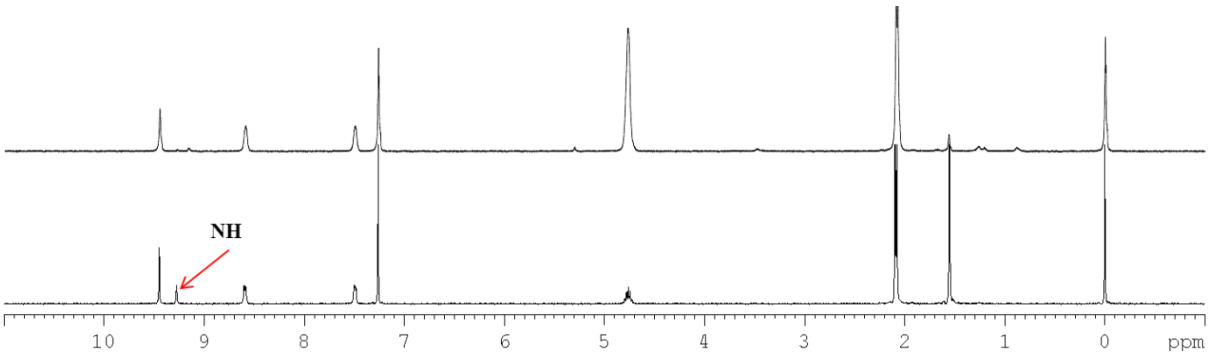

Figure 3.9 Bottom: ^{1}H NMR spectrum of **TS22b** in $CDCl_3$, Top: spectrum after deuterium exchange.

3.3.2 Optical studies of dinaphthoporphycenes

The absorption spectra of **TS22a-c** has large red shifted absorption bands compared to parent unsubstituted porphycene **L2**, where the lowest energy band appear about 715 nm.[1] These porphycenes show well-defined Soret bands, near 400 nm unlike **L71** and the lowest energy

Q-band is relatively more intense compared to Soret-band (~0.49), than other porphycenes.[49] In comparison to tetrabenzoporphycene **L72**[25] Soret band is relatively blue shifted by 13 nm, however, lowest energy Q band is red shifted by at least 45 nm. The intensity ratio between lowest energy band and Soret band of dinaphthoporphycene is also higher than **L72 (**0.49 vs. 0.13). Further, there are few UV bands with maxima at 265 nm, which can be attributed to the fused-naphthalene moieties in the macrocycle. Like dibenzoporphycene **L71**, porphycenes **TS22a-c** did not show any fluorescence at room temperature (< 10^{-4}).[50]

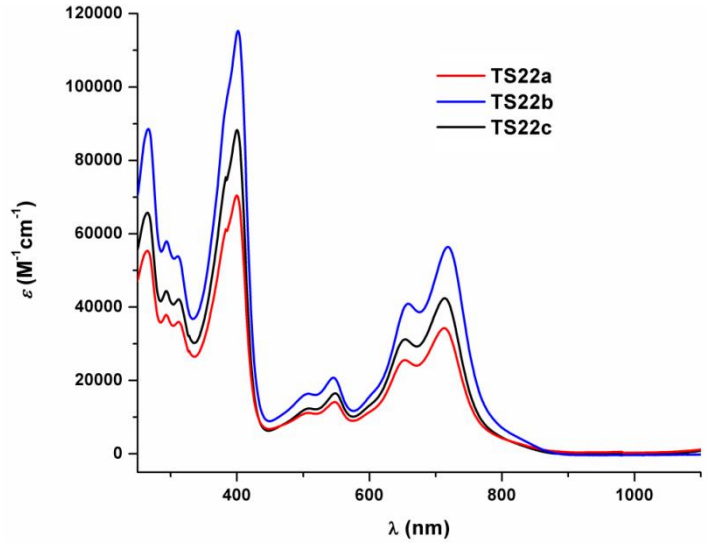

Figure 3.10 UV-Vis spectra of **TS22a-c** in $CHCl_3$.

3.3.3 Solid state structural analysis of dinaphthoporphycene

Solid state structure of **TS22b** could be derived explicitly from the single crystals obtained via slow evaporation of chloroform/hexane mixture, by X-ray diffraction (XRD) analysis, revealing a near planar geometry (Figure 3.11). Average deviation of nitrogen atoms from the mean porphycene plane (excluding the isopropyl substituents) is ±0.15 Å. The shortest N-N distance (N1…N2′) in **TS22b** is 2.49 Å much shorter compared to that of **L2**,[1] while the long (N1…N2) one being 2.95 Å. This short N1…N2′ distance thus accounts for the highly deshielded NH in ^{1}H NMR spectra, due to strong NH…N hydrogen bonding. Consequently, unlike other octaalkylporphycenes where core of the macrocycle is almost square (e.g. octaethylporphycene N1…N2′ distance 2.79 Å, N1…N2 distance 2.73 Å)[21a] dinaphthoporphycene has a rectangular core, which is a general characteristic of tetra-*meso* substituted porphycenes.[20] In fact it is having the most distinct rectangular core among all porphycene free base reported to date. The closest being 2,7,12,17-tetrahexyl-9,10,19,20-tetraethylporphycene, where N1…N2′ is 2.52 Å and N1…N2 distance is 2.96 Å.[24]

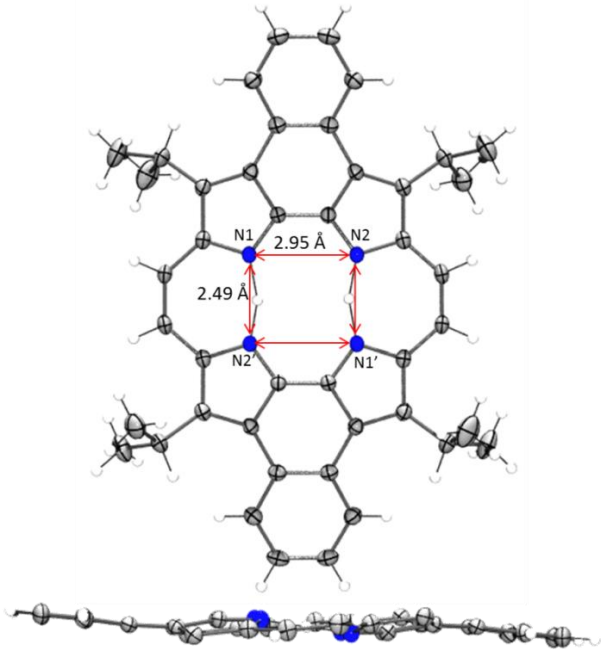

Figure 3.11 ORTEP of porphycene **TS22b**. Top: Front view. Bottom: Side view. Thermal ellipsoids are scaled to 35 % probability level. For clarity *i*-Pr group have been omitted from side view.

3.3.4 Metal complexation of dinaphthoporphycenes

The metal insertion reactions were investigated for **TS22a-c** with several metal ions, viz. Zn(II), Cu(II), Ru(II), Sn(II), Ni(II), Pd(II) etc. However, only Cu(II), Pd(II), and Ni(II) could be inserted successfully (**TS24b, TS25b** and **TS23b-c)**. **TS23a** could not be characterized due to lack of solubility. The absorption spectra of Ni(II)-complexes **TS23b-c** show a general trend of red shifted Soret band and blue shifted Q-bands for porphycenes (Figure 3.12).

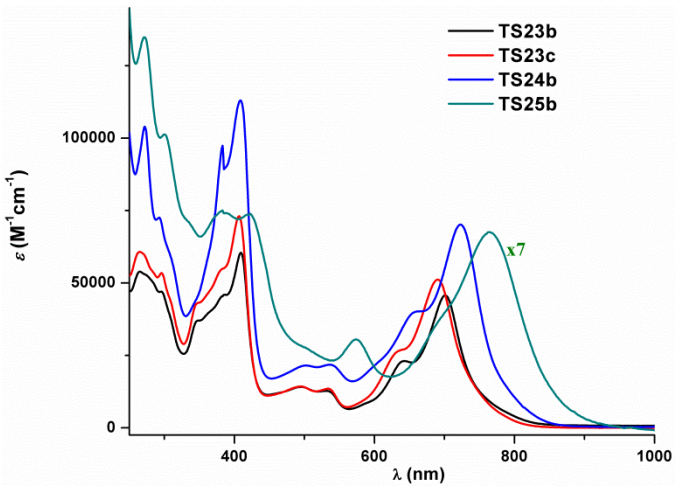

Figure 3.12 UV-Vis spectra of metal complexes of dinaphthoporphycenes in $CHCl_3$.

However, 4-banded Q-bands were observed, where relative intensity of Q_{III} and Q_{IV} interchanged upon metallation and the relatively broad Soret bands resolved with the appearance of clear shoulders on the higher energy side. Unlike Ni(II)-complexes **TS23b-c**, Cu(II)-complex **TS24b** shows red shifted Q-band (lowest energy band 718 vs. 723 nm) compared to its freebase counterpart. Further, Cu(II)-complex **TS24b** also displays higher extinction coefficient compared to Ni(II)-complexes **TS23b-c**, which is comparable with freebase dinaphthoporphycene **TS22b.** The ratio between lowest energy Q-band and Soret band also increases upon metallation (~0.49 vs. ~0.70). On the other hand, Pd(II)-complex **TS25b** shows drastically reduced absorption intensity of the Soret band compared to Ni(II)- and Cu(II)- complexes. Lowest energy Q-band and Soret band in turn becomes almost equal in intensity (ratio ~0.90). Unlike other complexes, Soret band no longer exist as sharp one and instead split into two broad signals. The lowest energy Q-band now shifted to 764 nm (46 nm red shifted compared to freebase). The abnormal absorption property of Pd-complex probably arises from substantial deviation of the macrocycle from planarity owing to bigger size of palladium compared to other metal ions studied. Although we were not able to grow single crystal to confirm the structural distortion (due to very poor solubility), ^{1}H NMR of Pd(II)-complex gives us a hint about the induced asymmetry in the complex (Figure 3.13). For instance, four methyl groups of isopropyl side chain appear as two sets of doublet at 2.31 and 1.16 ppm. For Ni(II)-complex, these signals appear as a single doublet at 1.99 ppm. The crystal structure of **TS23b** and **TS24b** were derived via XRD analysis (Figure 3.14). **TS23b** showed a much planar core with Ni sitting in the same plane of the porphycene and the

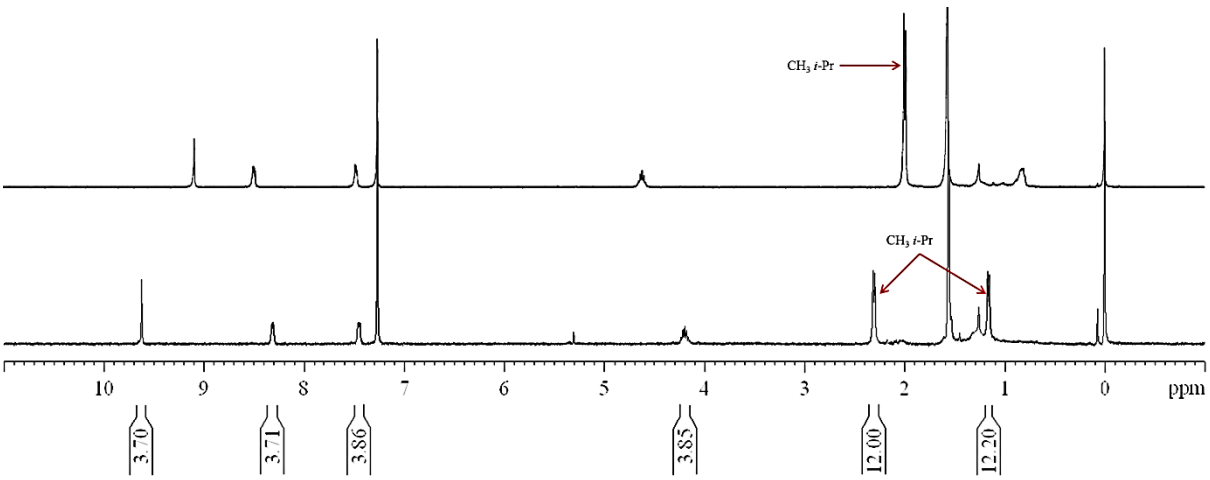

Figure 3.13 Comparison of ^{1}H NMR spectra of Pd-complex **TS25b** (bottom) and Ni-complex **TS23b** (top).

nitrogen atoms are slightly less deviated (±0.12 Å) from the mean porphycene plane than **TS22b** (Figure 3.14a)**.** However, the N4-core shows much dramatic change compared to the other metallated porphycenes reported so far. Here the N1-N2 distance decreases from 2.95 to 2.64 Å upon metallation, whereas the N1-N2' undergoes a concomitant increase from 2.49 Å to 2.67 Å, thereby resulting in an almost square type core. This is unprecedented in porph-

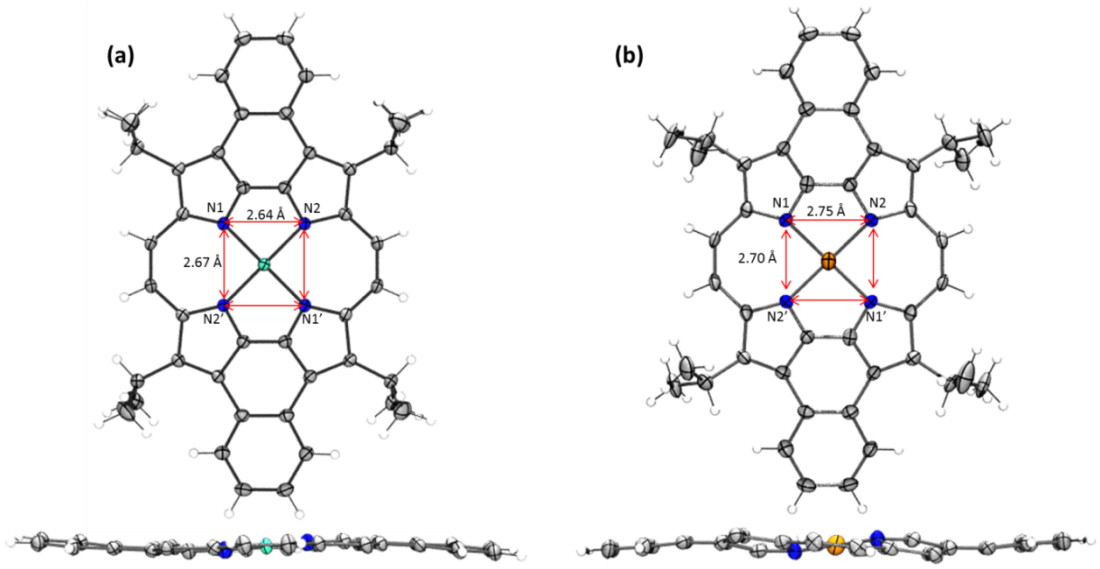

Figure 3.14 ORTEP of (a) Ni-porphycene **TS23b**: top - front view, bottom - side view. (b) Cu-porphycene **TS24b**: top - front view, bottom - side view. Thermal ellipsoids are scaled to 35 % probability level. For clarity *i*-Pr group have been omitted from side views.

ycene chemistry, because all porphycenes exhibit rectangular core upon metallation, irrespective of the geometry of free base porphycene whether square or rectangular. Crystal structure of Cu(II)-complex (**TS24b**) further confirms that this is a general phenomenon for dinaphthoporphycene as similar square type N4-core was observed. However, in case of copper complex expansion of porphycene core was observed probably owing to larger covalent radius of copper in comparison to nickel. ORTEP of Cu(II)-complex **TS24b** indicating the N**…**N distance is shown in figure 3.14 (b). **TS24b** shows slight deviation from planarity compared to **TS22b** and **TS23b**, as average deviation of nitrogen atoms from the mean porphycene plane (excluding the isopropyl substituents) is ±0.20 Å, where the Cu(II) ion resides in the plane of the porphycene. Probably this deviation from planarity induces the red shift observed in the absorption spectrum. As expected **TS24b** containing a d^9 metal ion is paramagnetic in nature and is EPR active showing line broadening in ^{1}H NMR spectra. EPR spectrum of the solid sample measured at room temperature is shown in figure 3.15.

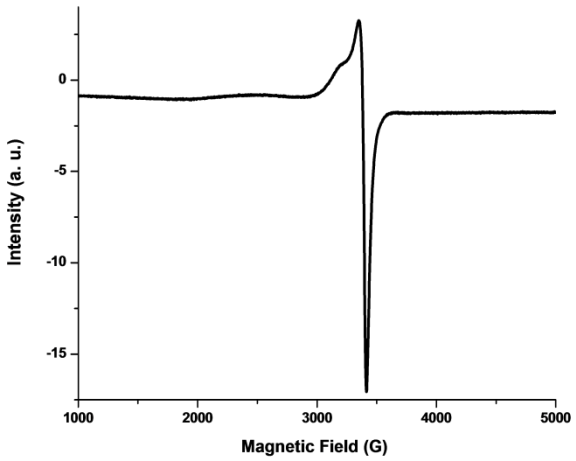

Figure 3.15 Solid state EPR spectrum of **TS24b** at room temperature.

3.3.5 Attempted synthesis of *meso*-tetraphenyldinaphthoporphycene

After synthesis and characterization of dinaphthoporphycenes, we also attempted synthesis of *meso*-tetraphenyl-dinaphthoporphycene **TS28**. The required precursor **TS26** can be synthesized from dibenzoylation of alkylated naphthobipyrrole (Scheme 3.15). Dibenzoylation of **TS20a** under modified Vilsmeier condition led us to isolate **TS26** in 45 % yield. **TS26** was characterized via single crystal X-ray diffraction analysis along with other spectroscopic means (Figure 3.16). Subjecting this to McMurry coupling did not yield the desired dodeca-substituted porphycene **TS28**, rather we obtained partially reduced derivative of **TS26**, as noticed earlier (Scheme 3.12) in the McMurry coupling of 2,9-diacyl derivative

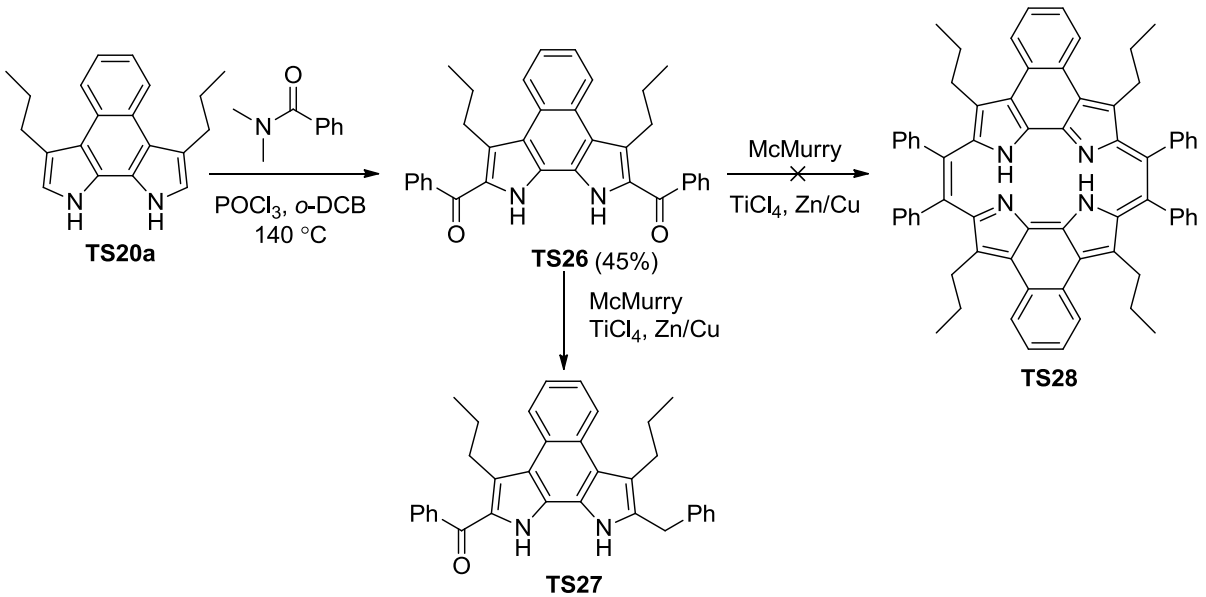

Scheme 3.15 Synthesis of 2,9-dibenzoyl naphthobipyrrole and its partially reduced analogue.

of naphthobipyrrole (**TS15b**). However, unlike previous case solubility of the starting material was better this time. Therefore, the failure of cyclization can be attributed to steric hindrance between the *meso*- and *β*-alkyl substituents. As it is evident that *meso* substitutions in porphycenes lead to shortening of N1…N2′ distance (2.53 Å for *meso*-tetrapropylporphycene),[20b] dinaphthoporphycene already having very short N1…N2′ distances (2.49 Å), probably could not accommodate further *meso* substituents.

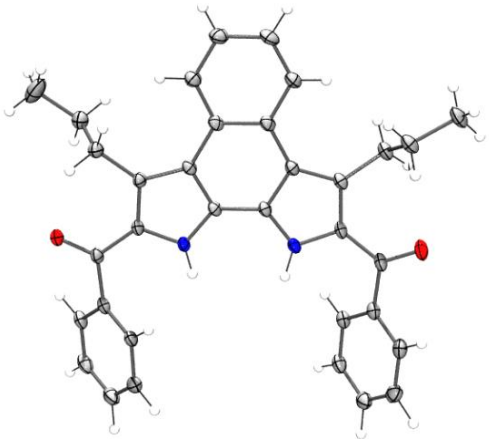

Figure 3.16 ORTEP of **TS26**. Thermal ellipsoids are scaled to 35 % probability level.

3.3.6 Nonlinear optical studies of dinaphthoporphycenes and its metal complexes

Third-order nonlinear optical (NLO) materials possess tremendous potential in applications such as two-photon PDT, optical limiting, 3D-optical memory.[51] Recently large enhancement of two photon absorption (2PA) cross section $\sigma^{(2)}$ was observed in case of conjugated porphyrin dimers, directly linked fused porphyrin dimers and expanded porphyrins.[52a-c] Particularly, aromatic core-modified porphyrins display very large values of $\sigma^{(2)}$.[52d-e] However, reports on three photon absorption (3PA) are scarce, in spite of its advantages in deep-site PDT, optical limiting, and 3D nano-fabrication leading to terabyte-level data storage.[53] Moreover, NLO studies on isomeric porphyrins are rare. To our knowledge, there is only one report on 2PA studies of porphycene.[54]

Nonlinear absorption (NLA) of **TS22a-c** and **TS23b-c** were measured by the open aperture Z-scan method using the chirped pulse amplified Ti:sapphire laser system delivering nearly transform-limited (~2 ps, 1 kHz repetition rate) pulses at 800 nm as an excitation source.[55] All the measurements were performed with 10^{-4} M solutions in chloroform and the solvent did not show any 2PA/3PA absorption. Table 3.1 shows the summary of NLO coefficients

Table 3.1 Summary of NLO coefficients extracted from data

sample	I_{oo} (GW/cm^2)	$\sigma^{(2)}$ (GM)	$\sigma^{(3)}$ (cm^{6}s^2/photon^2)
TS22a	78	8260	-
	118	-	1.44×10^{-75}
TS22b	98	11600	-
	132	-	3.69×10^{-75}
TS22c	74	14500	-
	117	-	1.03×10^{-74}
TS23b	74	21500	-
	120	-	8.01×10^{-75}
TS23c	120	7930	-
	407	-	4.52×10^{-75}

extracted from data. Our intensity dependent studies reveal that they exhibit two photon absorption (2PA) at low peak intensities and three photon absorption (3PA) at higher peak intensities (Figure 3.17).[45,56] This can be explained by the presence of two resonances in the absorption spectra of these porphycene molecules, one near 400 nm (Soret band) and another

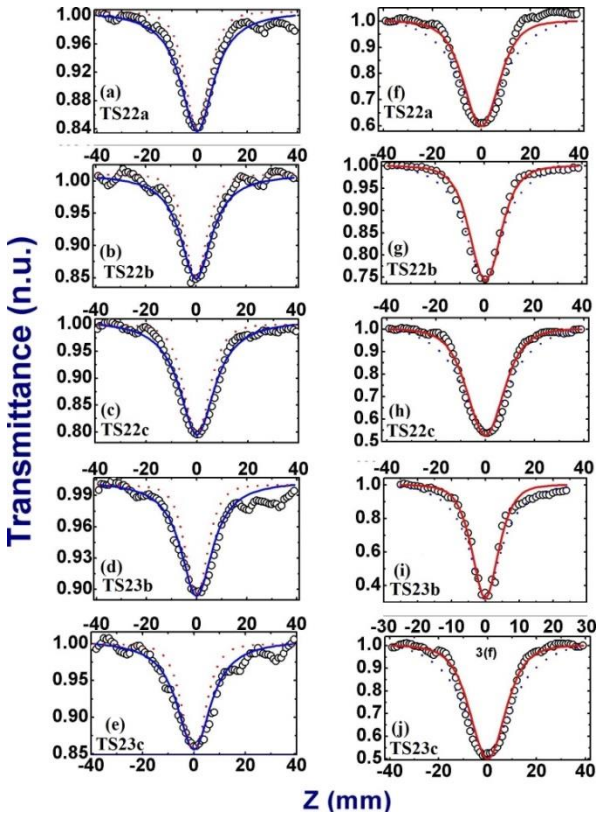

Figure 3.17 Open aperture Z-scans of porphycenes **TS22a-c** and **TS23b-c** at different peak intensities (see Table 1). For low peak intensities the 2PA has the best fit [blue solid lines are for 2PA and red dotted lines are for 3PA, (a–e)], while for high peak intensities 3PA has the best fit [red solid lines are for 3PA and blue dotted lines are for 2PA (f–j)

near 265 nm (naphthalene moiety), that may be responsible for the two possible excitation mechanisms. For the 800 nm photon these two resonances can act as two-photon (2P) and three-photon (3P) states, respectively. Figure 3.18 clearly illustrates the possible excitation mechanism for the porphycene derivatives causing the singular nonlinear absorption behavior of the molecules. At lower peak intensities the 2PA could be due to simultaneous absorption from S_0 to S_2 states (23250–28500 cm^{-1}, with single photon corresponds to 12500 cm^{-1}) via a virtual energy level of porphycene molecule while the 3PA is a result of 2PA and excited state absorption from S_2 state to the S_n states (33300–40000 cm^{-1}) of the porphycene molecule which occurs at higher laser intensity. Therefore 3PA observed in dinaphnaphthoporphycenes can be termed as *effective* 3PA rather than *instantaneous* 3PA. The difference between the *instantaneous* 3PA and *effective* 3PA is that in the former case three photons are simultaneously absorbed, whereas in the latter case at first two photons are absorbed simultaneously to an exited state (real state) of the molecule, which then undergo another one photon absorption to an higher excited state.[57]

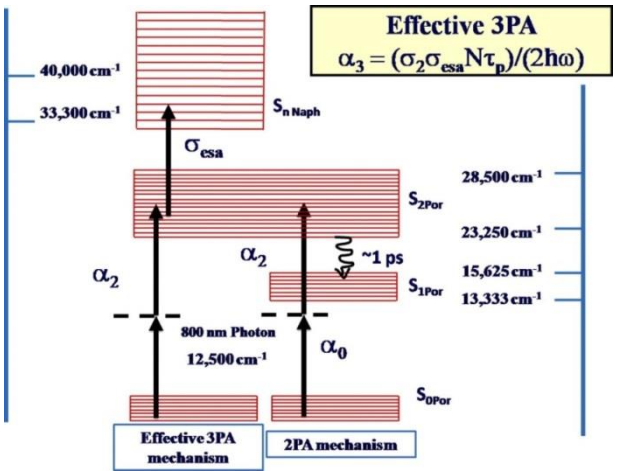

Figure 3.18 Schematic energy level diagram illustrating 2PA and 3PA resonances in dinaphthoporphycenes.

3.3.7 Excited state life time study of dinaphthoporphycenes and their metal complexes

Ultrafast excited state dynamics of dinaphthoporphycenes were investigated using femtosecond and picosecond degenerate pump-probe techniques at 600 and 800 nm, respectively.[58] Pump probe (p-p) results of dinaphthoporphycenes were obtained at 800 and 600 nm using ~2 ps and ~70 fs pulses respectively. Depending on the energy levels of these molecules, one would expect multi-exponential decay following different excitation mechanisms. Figure 3.19 illustrates the data obtained with ps pulses at 800 nm. The peak

intensities (~150 GW/cm^2) used in ps experiments were sufficient to access the three-photon states.[56] We observed photo-bleaching for all the porphycenes studied. The data were fitted with a double exponential decay, and two lifetimes were retrieved from the fits. We tried to fit the data for a single exponential, but the overall fit was poor. Fast decay retrieved was in the range of 1.8 –3.1 ps, while the slow component varied from 7 to 8.5 ps for different samples. The fast component is attributed to the internal conversion (IC) in these molecules (S_2 to S_1 states), whereas the slower one to the non-radiative decay back to the ground state (S_1 to S_0 states).[59]

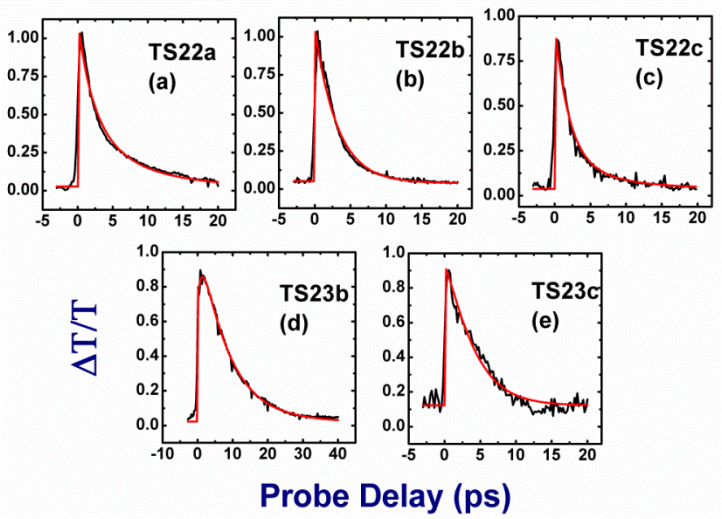

Figure 3.19 Excited state dynamics data of porphycenes **TS22a-c** and **TS23b-c** obtained using ps pulses at 800 nm. Noisy lines (black lines) represent the experimental data, while the smooth solid lines (red lines) are fits to the data.

To resolve further the dynamics below 2 ps, we performed the experiments with ~70 fs pulses at 600 nm. Photo-induced absorption was observed in the 600 nm fs pump-probe data for all the porphycenes. The negative transmission observed at 600 nm is depicted in figure 3.20 for all the porphycene derivatives (**TS22a-c** and **TS23b-c)**. The data were obtained with focused pump and probe pulses with pump peak intensities sufficient to excite the molecules to S_2 states. Probe is absorbed from these states to higher states (S_n), thereby reducing the transmission. Fits obtained using single/double exponential did not provide perfect match to the experimental data, and therefore, triple exponential equation was utilized and three different lifetimes were retrieved from the fits (Table 3.2). The fastest lifetime observed was in the 100 – 135 fs, which is attributed to the intramolecular vibrational relaxation (IVR)

within S2 states, while the slower component of 0.8–1.5 ps could be due to the IC and the slowest one in the 7.3 –10.0 ps range again due to non-radiative decay.

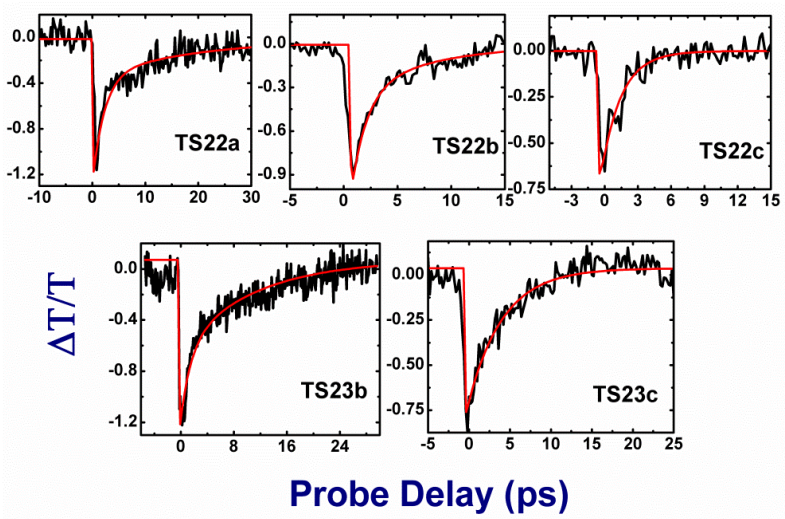

Figure 3.20 Excited state dynamics of porphycenes **TS22a-c** and **TS23b-c** using ~70 fs (estimated at the sample) pulses at 600 nm. The data was obtained using focused pump/probe beams. Noisy lines (black lines) represent the experimental data, while the smooth solid lines (red lines) are fits to the data.

Table 3.2 Lifetimes of porphycenes obtained using ps and fs pump-probe studies.

Samples	τ_2 (ps) 800 nm (ps p-p)	τ_1 (ps) 800 nm (ps p-p)	τ_3 (fs) 600 nm (fs p-p)	τ_2 (ps) 600 nm (fs p-p)	τ_1 (ps) 600 nm (fs p-p)
TS22a	2.0	7.2	120	0.8	8.0
TS22b	3.1	7.6	105	1.4	7.3
TS22c	2.0	7.2	102	1.2	8.2
TS23b	1.8	8.5	100	1.5	10.0
TS23c	1.8	7.0	135	1.2	8.1

3.4 Conclusion

In this chapter we demonstrated a generalized route towards synthesis of alkylated naphthobipyrroles bearing alkyl chain at their *β*-pyrrolic positions. This modification not only improves their solubility but also increase their selectivity towards further functionalization. Corresponding naphthobipyrrole dialdehydes were converted to novel *π*-extended porphycenes, namely dinaphthoporphycene following the classic McMurry coupling. As a result of extended *π*-conjugation dinaphthoporphycenes display dramatic improvement in

linear as well as nonlinear optical properties compared to other porphycenes (*β*-*β* non fused analogues). Metal coordination properties of dinaphthoporphycenes have been studied with several metal ions, where Cu(II), Pd(II) and Ni(II) complexes could be inserted successfully. These metal complexes showed a hitherto unknown square type N4-core upon metallation as inferred from solid state structure analyses. Nonlinear optical studies reveal that these simple systems show intensity dependent multi-photon absorbance possessing very high $\sigma^{(3)}$ and $\sigma^{(2)}$values. Ultrafast excited state dynamics of dinaphthoporphycenes were also investigated using femtosecond and picosecond degenerate pump-probe techniques. Attempt to synthesize *meso*-substituted dinaphthoporphycenes were not successful, presumably owing to increase steric hindrance.

3.5 Experimental details

Commercially available solvents were distilled before use. Reagents were used as received. Unsubstituted naphthobipyrrole **TS5** was synthesized using literature method.[46] *N*,*N*-dimethylpropionamide, *N*,*N*-dimethylisobutyramide and *N*,*N*-dimethylbenzamide were synthesized following literature methods. *α*-Keto esters **TS7a-d** were prepared following reported procedure[48] and the necessary Grignard reagents were made in situ. Synthetic details of these compounds have already been discussed in chapter 2 of the thesis. Details regarding 2PA and 3PA measurements and excited state life time study have also been discussed in chapter 2.

Synthesis of 2,9-dipropionyl naphthobipyrrole TS15a: *N*,*N*-dimethylpropionamide (0.80 mL, 7.26 mmol) was taken in a two neck round bottomed flask under N_2 atmosphere, cooled to 0^oC and freshly distilled $POCl_3$ (0.66 mL, 7.26 mmol) was added slowly to it with continuous stirring. After addition is completed, the reaction mixture was again stirred at room temperature for 2 h. Naphthobipyrrole **TS5** (300 mg, 1.45 mmol) was then dissolved in minimum volume of dry DCE, added to the Vilsmeier adduct at room temperature. The setup was then placed in a preheated oil bath (80°C), refluxed for 3 h, cooled to room temperature and sat. NaOAc solution was then added slowly and again heated to reflux for 2 h. The yellow precipitate thus formed was filtered under suction, washed with water and dried. Yield 390 mg (84 %).

^{1}H NMR (DMSO-d_6, 400MHz, δ in ppm): 11.85 (s, 2H, NH), 8.32 (m, 2H, CH-naph), 8.06 (s, 2H, CH-naph), 7.51 (m, 2H, CH-naph), 3.04 (q, 4H, J = 7.2 Hz, CH_2 ethyl), 1.19 (t, 6H, J = 7.2 Hz, CH_3 ethyl); ^{13}C NMR (in DMSO-d_6, 100MHz, δ in ppm): 191.93, 132.92, 125.71,

124.85, 124.32, 123.60, 122.14, 110.04, 30.78, 8.87; LCMS: m/z calculated for $C_{20}H_{18}N_2O_2$ (M+H) 319 found 319; Elemental analysis for $C_{20}H_{18}N_2O_2$ calcd. (found); C 75.45 (75.37), H 5.70 (5.68), N 8.80 (8.86); IR (KBr): ν (cm^{-1}) 3287, 1658, 1614, 1385, 914, 760.

Synthesis of 2,9-diisobutyl naphthobipyrrole TS15b: *N*,*N*-dimethylisobutyramide (0.64 mL, 5.06 mmol) was taken in a 50 mL two neck round bottomed flask under N_2 atmosphere, cooled to 0^oC and freshly distilled $POCl_3$ (0.46 mL, 5.06 mmol) was added slowly to it with continuous stirring. After complete addition, the reaction mixture was stirred at room temperature for 2 h. Naphthobipyrrole **TS5** (200 mg, 1.00 mmol) was then dissolved in minimum *N*,*N*-dimethylisobutyramide and added to the Vilsmeier adduct at room temperature. The setup was then placed in a preheated oil bath (80°C) and refluxed for 3 h, cooled to room temperature and saturated NaOAc solution was added slowly to it and again heated to reflux for 2 h, the yellow-green precipitate thus formed was filtered under suction, washed with water and dried. Yield 264 mg (79 %).

^{1}H NMR (DMSO-d_6, 400MHz, δ in ppm): 11.87 (s, 2H, NH), 8.34 (m, 2H, CH-naph), 8.12 (2H, CH-naph), 7.51 (m, 2H, CH-naph), 3.62 (m, 2H, CH *i*-Pr), 1.22 (d, 12H, J = 6.8 Hz, CH_3 *i*-Pr); ^{13}C NMR (DMSO-d_6, 100MHz, δ in ppm): 195.39, 132.14, 125.75, 124.88, 124.63, 123.66, 122.30, 110.14, 35.19, 19.67; LCMS: m/z calculated for $C_{22}H_{12}N_2O_2$ (M+H) 347 found 347; Elemental analysis for $C_{22}H_{12}N_2O_2$ calcd. (found); C 76.28 (76.12), H 6.40 (6.45), N 8.09 (8.15); IR (KBr): ν (cm^{-1}) 3281, 1641, 1604, 1467, 1263, 1059, 935, 744. This compound was also characterized by single crystal X-ray diffraction analysis.

Synthesis of TS16 (Proposed method for the synthesis of Porphycene TS17): To a slurry of low-valent titanium agent, generated by reduction of titanium tetrachloride (0.6 mL, 5.77 mmol) in dry THF (60 mL) with activated zinc (1 g) and CuCl (0.14 g), was added a solution of **TS15b** (125 mg, 0.87 mmol) in boiling THF (30 mL). The reaction mixture was heated under reflux for 20 min and then hydrolyzed by slow addition of 10 % aqueous solution of potassium carbonate (16 mL). Subsequently, the reaction mixture was filtered through celite to remove the excess metal, washed with dichloromethane and the washings were combined with the organic layer of the filtrate and dried over anhyd. Na_2SO_4 and solvent was removed in vacuum. TLC of the crude product shows no indication of product formation, even after treating with DDQ. The residue upon purification by silica column (eluent: $CHCl_3$) yielded one yellow color compound, which produced a diffraction grade crystal and its characterization revealed the formation of a partially reduced derivative **TS10**. This type of

product formation in McMurry reaction is not seen in literature to our knowledge. Further, this reaction did not yield any other non-polymeric product.

^{1}H NMR (in $CDCl_3$, 400 MHz): 1.02 (d, 6H, *J* = 6.8 Hz, -CH_3 *i*-Bu), 1.42 (d, 6H, *J* = 6.8 Hz, -CH_3 *i*-Pr), 1.90 (s, 2H, -CH_2 *i*-Bu), 3.12 (m, 1H, -CH *i*-Bu), 3.81 (m, 1H, -CH *i*-Pr), 6.75 (s, 1H, -CH naph), 7.51 (m, 2H, -CH naph), 8.04 (s, 1H, -CH naph), 8.26 (m, 2H, -CH naph), 10.50 (s, 1H, NH), 12.06(s, 1H, NH). HR-MS (ESI): m/z calcd for $C_{22}H_{25}N_2O$: 333.1967; found $[M+H]^+$ 333.1964.

General method for the synthesis of 2,3-naphthalene bishydrazones (TS18a-d):

TS18a: To a suspension of 2,3-naphthalene bishydrazine **TS2** (2g, 10.6 mmol) in ethanol (74 mL), α-keto ester[48] **TS7a** (5.7 g, 36 mmol) was added with continuous stirring. The mixture was then refluxed under nitrogen for 24 h. The resulting solution was concentrated in a rotary evaporator. Excess **TS7a** was distilled out in a Kugelrorh distillation apparatus (can be re-used). The red dense liquid thus obtained was extracted with hexane to obtain the product as a mixture of isomers and used in the next step without further purification. As the crude mass showed clear mass spectra, for analysis purpose only a small amount was purified by column to isolate the fastest moving isomer (10 % ethyl acetate-hexane).

^{1}H NMR ($CDCl_3$, 400MHz, δ in ppm): 12.55 (s, 2H, NH), 7.71 (s, 2H, CH naph), 7.68 (m, 2H, CH naph), 7.27 (m, 2H, CH naph), 4.31 (q, 4H, *J* = 6.8 Hz, CH_2 ester), 2.63 (t, 4H, *J* = 7.6 Hz, CH_2 *n*-Bu), 1.65 (m, 4H, CH_2 *n*-Bu), 1.44 (m, 4H, CH_2 *n*-Bu), 1.37 (t, 6H, *J* = 7.2 Hz, CH_3 ester), 0.97 (t, 6H, *J* = 7.2 Hz, CH_3 *n*-Bu); ^{13}C NMR ($CDCl_3$, 100MHz, δ in ppm): 163.61, 132.37, 131.46, 130.31, 126.73, 124.31, 111.86, 60.62, 32.77, 30.47, 22.59, 14.29, 14.12; LCMS: m/z calculated for $C_{26}H_{36}N_4O_4$ $[M+H]^+$ 469 found 469; Elemental analysis for $C_{26}H_{36}N_4O_4$ calcd. (found); C 64.64 (66.85), 7.74 (7.65), 11.96 (11.88); IR (neat): ν (cm^{-1}) 3224.2, 2957.5, 2932.06, 1683.0, 1550.2, 1520.7, 1471.8, 1367.4, 1274.8, 1232.3, 1154.5, 1096.6, 1025.8, 862.4, 739.6, 740.2, 687.8, 621.1.

TS18b: ^{1}H NMR ($CDCl_3$, 400MHz, δ in ppm): 12.63 (s, 2H, NH), 7.12 (s, 2H, CH naph), 7.68 (m, 2H, CH naph), 7.27 (m, 2H, CH naph), 4.31 (q , 4H, *J* = 7.2 Hz, CH_2 ester), 2.53 (d, 4H, *J* = 7.2 Hz, CH_2 *i*-Bu), 2.05 (m, 2H, CH *i*-Bu), 1.37 (t, 6H, *J* = 7.2 Hz, CH_3 ester), 0.98 (d, 12H, *J* = 6.4 Hz, CH_3 *i*-Bu); ^{13}C NMR ($CDCl_3$, 100MHz, δ in ppm): 163.83, 132.39, 130.89, 130.36, 126.80, 124.39, 111.98, 60.69, 41.52, 27.78, 22.60, 14.35; LCMS: m/z calculated for $C_{26}H_{36}N_4O_4$ (M+H) 469 found 469; Elemental analysis for $C_{26}H_{36}N_4O_4$ calcd.

(found); C 64.64 (66.51), 7.74 (7.69), 11.96 (12.07); IR (neat): *v* (cm^{-1}) 3201.5, 2956.1, 1676.4, 1552.8, 1528.0, 1468.9, 1366.6, 1209.5, 1229.0, 1154.7, 1027.2, 876.2, 743.6.

TS18c: ^{1}H NMR ($CDCl_3$, 400MHz, δ in ppm): 12.55 (s, 2H, NH), 7.71 (s, 2H, CH naph), 7.66 (m, 2H, CH naph), 7.25 (m, 2H, CH naph), 4.30 (q ,4H, *J* = 7.2 Hz, CH_2 ester), 2.62 (t, 4H, *J* = 7.6 Hz, CH_2 *n*-Hex), 1.65 (m, 4H, CH_2 *n*-Hex), 1.42 (m, 4H, CH_2 *n*-Hex), 1.35 (t, 6H, *J* = 7.2 Hz, CH_3 ester), 1.35 (8H, CH_2 *n*-Hex), 0.91 (t, 6H, *J* = 7.2 Hz, CH_3 *n*-Hex); ^{13}C NMR ($CDCl_3$, 100MHz, δ in ppm): 163.65, 132.41, 131.53, 130.35, 126.75, 124.34, 111.91, 60.63, 33.07, 31.87, 29.21, 28.27, 22.80, 14.31, 14.25; LCMS: m/z calculated for $C_{30}H_{44}N_4O_4$ (M+H) 525, found 525; Elemental analysis for $C_{30}H_{44}N_4O_4$ calcd. (found); C 68.55 (68.67), H 8.51 (8.45), N 10.77 (10.68); IR (KBr): *v* (cm^{-1}) 3209.84, 3051.66, 2928.21, 2856.83, 1680.15, 1550.91, 1525.83, 1440.96.

TS18d: ^{1}H NMR ($CDCl_3$, 400MHz, δ in ppm): 12.51 (s, 2H, NH), 7.23 (s, 2H, CH naph), 7.68 (m, 2H , CH naph), 7.28 (m, 2H, CH naph), 4.32 (q, 4H, *J* = 7.2 Hz, CH_2 ester), 2.66 (q, 4H, *J* = 7.2 Hz, CH_2 Et), 1.37 (t, 6H, *J* = 7.2 Hz, CH_3 ester), 1.23 (t, 6H, *J* = 7.2 Hz, CH_3 Et). ^{13}C NMR spectrum ($CDCl_3$, 100MHz, δ in ppm): 163.64, 132.51, 132.46, 130.37, 126.80, 124.38, 111.90, 60.73, 26.59, 14.34, 12.65. LCMS: m/z calculated for $C_{22}H_{28}N_4O_4$ (M-H) 411, found 411. Elemental analysis for $C_{22}H_{28}N_4O_4$ calcd. (found); C 64.06 (64.21), H 6.84 (6.75), N 13.58 (13.65). IR (KBr): *v* (cm^{-1}) 3232.99, 3045.87, 2986.08, 2932.06, 1682.08, 1568.27, 1437.10, 1365.72, 1307.85, 1248.06, 1149.68. M. P.: 100-103°C.

General method for the synthesis of naphthobipyrrole diesters (TS19a-d)

TS19a: 2,3-naphthalene bishydrazone **TS18a** (1 equiv.) obtained from the previous reaction, was directly taken and polyphosphate ester (6 equiv.) was added to it, the resulting mixture was heated at 100°C for 2 h with continuous stirring, cooled to room temperature and poured into ice-water. The yellowish white solid thus obtained was filtered under suction, washed several times with distilled water, dried and washed with hexane to get the pure product. Combined yield for the two steps 3.1 g (67 %).

^{1}H NMR ($CDCl_3$, 400MHz, δ in ppm): 10.79 (s, 2H, NH), 8.09 (2H, CH naph), 7.43 (2H, CH naph), 4.27 (4H, CH_2 ester), 3.10 (4H, CH_2 *n*-Pr), 1.53 (4H, CH_2 *n*-Pr), 1.15 (6H, CH_3 ester), 1.00 (6H, CH_3 *n*-Pr); ^{13}C NMR ($CDCl_3$, 100MHz, δ in ppm): 163.88, 129.84, 127.80, 124.22, 123.97, 120.52, 120.23, 61.06, 28.21, 23.13, 14.38, 13.95; LCMS: m/z calculated for $C_{26}H_{30}N_2O_4$ (M+H) 436 found 436; Elemental analysis for $C_{26}H_{30}N_2O_4$ calcd. (found); C

71.87 (71.92), H 6.96 (6.91), N 6.45 (6.39); IR (neat): ν (cm^{-1}) 3412.0, 3302.2, 1694.8, 1654.2, 1457.8, 1403.9, 1372.7, 1286.5. 1218.3. 1162.6, 1133.8, 1100.3, 1033.6, 780.2, 747.6, 707.6; M. P. 230-232°C.

TS19b: Two-step yield 26 %, ^{1}H NMR ($CDCl_3$, 400MHz, δ in ppm): 10.63 (brs, 2H, NH), 8.49 (2H, CH naph), 7.51 (m, 2H, CH naph), 4.43 (4H, CH_2 ester), 4.43 (2H, CH *i*-Pr), 1.55 (12H, CH_3 *i*-Pr), 1.34 (6H, CH_3 ester); ^{13}C NMR ($CDCl_3$, 100MHz, δ in ppm): 163.44, 135.63, 127.89, 126.08, 124.27, 123.89, 120.60, 61.40, 25.67, 20.90, 14.11; LCMS: m/z calculated for $C_{26}H_{30}N_2O_4$ (M+H) 435 found 435; Elemental analysis for $C_{26}H_{30}N_2O_4$ calcd. (found); C 71.87 (71.68), H 6.96 (6.91), N 6.45 (6.38); IR (neat): ν (cm^{-1}) 3357.4, 2359.2, 1709.6, 1659.5, 1622.6, 1556.1, 1519.7, 1460.4, 1395.5, 1287.8, 1194.7, 1144.6, 1098.1, 1035.4, 936.8, 717.6, 642.7; M. P. 250-251°C. This compound was also characterized by single crystal X-ray diffraction analysis.

TS19c: Two-step yield 48 %, ^{1}H NMR (DMSO-d_6, 400MHz, δ in ppm): 11.88 (2H, NH), 8.34 (2H, CH-naph), 7.51 (2H, CH-naph), 4.39 (4H, CH_2-ester), 3.44 (4H, CH_2 *n*-pentyl), 1.70 (4H, CH_2 *n*-pentyl), 1.46 (4H, CH_2 *n*-pentyl), 1.39 (4H, CH_2 *n*-pentyl), 1.38 (6H, CH_3-ester), 0.89 (6H, CH_3 *n*-pentyl); ^{13}C NMR ($CDCl_3$, 100MHz, δ in ppm): 164.17, 130.19, 127.84, 124.21, 124.09, 120.34, 120.15, 61.18, 32.34, 29.50, 26.28, 22.43, 14.32, 13.91; LCMS: m/z calculated for $C_{30}H_{38}N_2O_4$ (M+H) 491, found 490; Elemental analysis for $C_{30}H_{38}N_2O_4$ calcd. (found); C 73.44 (73.28), H 7.81 (7.84), N 5.71 (5.85); IR (KBr): ν (cm^{-1}) 3350.65, 2957.14, 2928.21, 2860.69, 1772.74, 1738.02, 1699.44, 1635.78, 1556.7, 1465.39, 1375.37, 1209.48; M.P. 210-212°C.

TS19d: Two-step yield 66 %. ^{1}H NMR (DMSO-d_6, 400MHz, δ in ppm): 11.81 (s, 2H, NH), 8.46 (m, 2H, CH naph), 7.51 (m, 2H, CH naph), 4.40 (q, 4H, J = 7.2 Hz, CH_2 ester), 2.96 (s, 6H, CH_3 Me), 1.40 (t, 6H, J = 7.2 Hz CH_3 ester). ^{13}C NMR (DMSO-d_6, 100MHz, δ in ppm): 161.54, 127.32, 124.06, 123.75, 123.16, 122.68, 120.62, 119.51, 60.10, 14.53, 13.11. LCMS: m/z calculated for $C_{22}H_{22}N_2O_4$ (M+H) 379 found 379. Elemental analysis for $C_{22}H_{22}N_2O_4$ calcd. (found); C 69.83 (69.72), H 5.86 (5.81), N 7.40 (7.56). IR (KBr): ν (cm^{-1}) 3350.65, 1672.43, 1558.62, 1475.68, 1400.45, 1383.09, 1284.71, 1228.77, 1132.32, 1086.02, 1018.51, 773.52. M. P. $^{\circ}$C 230 (decomposed).

General method for the synthesis of α-free naphthobipyrroles (TS20a-d)

TS20a: Naphthobipyrrole diesters **19a** (2 g, 4.6 mmol), ethylene glycol (40 mL), and NaOH

(1.2 g, 30.4 mmol) were taken in a round bottomed flask, kept under high vacuum for 1h. The mixture was then heated at reflux for 3 h under Ar atmosphere and cooled to 100°C and degassed water was (90 mL) added and stirred for another 5 min and then cooled to r.t. and the green colored precipitate thus formed was filtered under suction. The precipitate was washed thoroughly with water to remove the excess ethylene glycol, dried and finally washed with hexanes to obtain greenish white solid. The colored impurities were removed by filter column using silica gel with dichloromethane as the eluent. Yield 1.3 g (97 %).

^{1}H NMR ($CDCl_3$, 400MHz, δ in ppm): 8.45 (m, 2H, CH naph), 8.19 (s, 2H, NH), 7.47 (m, 2H, CH naph), 6.87(s, 2H, CH Py), 3.10 (t, 4H, J =7.6 Hz, CH_2 *n*-Pr), 1.86 (m, 4H, CH_2 *n*-Pr), 1.10 (t, 6H, J = 7.2 Hz CH_3 *n*-Pr); ^{1}H NMR ($CDCl_3$ + D_2O, 400MHz, δ in ppm): 8.45 (m, 2H, CH naph), 7.47 (m, 2H, CH naph), 6.87(s, 2H, CH Py), 3.10 (t, 4H, J = 7.6 Hz, CH_2 *n*-Pr), 1.86 (m, 4H, CH_2 *n*-Pr), 1.10 (t, 6H, J = 7.2 Hz CH_3 *n*-Pr); ^{13}C NMR (DMSO-d_6, 100MHz, δ in ppm): 126.49, 123.31, 122.06, 118.41, 118.36, 115.76, 30.21, 22.70, 14.17; LCMS: m/z calculated for $C_{20}H_{22}N_2$ (M+H) 291 found 291; Elemental analysis for $C_{20}H_{22}N_2$ calcd. (found); C 82.72 (82.58), H 7.64 (7.59), N 9.65 (9.71); M. P. 250 °C (decomposed).

TS20b: Yield: 90 %. ^{1}H NMR ($CDCl_3$, 400MHz, δ in ppm): 8.51 (2H, CH naph), 7.88 (s, 2H, NH), 7.49 (2H, CH naph), 6.85 (s, 2H, CH Py), 3.76 (m, 2H, CH *i*-Pr), 1.47 (d, 12H, J = 6.4 Hz, CH_3 *i*-Pr); ^{1}H NMR ($CDCl_3$, 400MHz, D_2O added, δ in ppm): 8.50 (m, 2H, CH naph), 7.47 (m, 2H, CH naph), 6.87 (s, 2H, CH Py), 3.76 (m, 2H, CH *i*-Pr), 1.47 (d, 12H, J = 6.4 Hz, CH_3 *i*-Pr); ^{13}C NMR ($CDCl_3$, 100MHz, δ in ppm): 127.94, 126.65, 124.50, 123.14, 122.75, 116.50, 116.33, 26.89, 23.80; LCMS: m/z calculated for $C_{20}H_{22}N_2$ (M+H) 291 found 291; Elemental analysis for $C_{20}H_{22}N_2$ calcd. (found); C 82.72 (82.65), H 7.64 (7.59), N 9.65 (9.56); M. P. 220°C.

TS20c: Yield: 96 %. ^{1}H NMR ($CDCl_3$, 400MHz, δ in ppm): 8.47 (2H, CH naph), 8.16 (2H , NH), 7.48 (2H , CH naph), 6.87 (s, 2H, CH Py), 3.13 (t, 4H, J = 7.2 Hz, CH_2 *n*-pentyl), 1.86 (m, 4H, CH_2 *n*-pentyl), 1.47 (m, 4H, CH_2 *n*-pentyl), 1.44 (m, 4H, CH_2 n-pentyl), 0.95 (t, 6H, J = 6.8 Hz CH_3 n-pentyl); ^{1}H NMR ($CDCl_3$, D_2O, 400MHz, δ in ppm): 8.46 (m, 2H, CH naph), 7.50 (m, 2H , CH naph), 6.88(s, 2H, CH Py), 3.12 (t, 4H, J = 7.2 Hz, CH_2 *n*-pentyl), 1.86 (m, 4H, CH_2 *n*-pentyl), 1.51 (m, 4H, CH_2 *n*-pentyl), 1.42 (m, 4H, CH_2 *n*-pentyl), 0.94 (t, 6H, CH_3 *n*-pentyl). ^{13}C NMR ($CDCl_3$, 100MHz, δ in ppm): 126.84, 124.20, 123.11, 122.69, 120.79, 118.22, 117.25, 32.24, 29.61, 28.57, 22.82, 14.33. LCMS: m/z calculated for

$C_{24}H_{30}N_2$ (M+H) 347, found 347; Elemental analysis for $C_{24}H_{30}N_2$ calcd. (found); C 83.19 (83.36), H 8.73 (8.65), 8.08 (8.15); M. P. 185°C (decomposed).

TS20d: Yield: 93.6 %. ^{1}H NMR ($CDCl_3$, 400 MHz, δ in ppm): 8.54 (m, 2H, CH naph), 7.853 (s, 2H, NH), 7.47 (m, 2H, CH naph), 6.82 (s, 2H, CH Py), 2.74 (s, 6H, CH_3 Me). ^{1}H NMR ($CDCl_3$, 400 MHz, D_2O added, δ in ppm): 8.54 (m, 2H, CH naph), 7.47 (m, 2H, CH naph), 6.80 (s, 2H, CH naph), 2.73 (s, 6H, CH_3 Me). ^{13}C NMR spectrum (in $CDCl_3$, 100MHz, δ in ppm): 127.04, 123.89, 123.10, 122.61, 119.00, 117.96, 115.32, 14.43. LCMS: m/z calculated for $C_{16}H_{14}N_2$ (M+H) 235 found 235. Elemental analysis for $C_{16}H_{14}N_2$ calcd. (found); C 82.02 (82.12), H 6.02 (6.10), N 11.96 (11.66). IR (KBr): ν (cm^{-1}) 3393.09, 2924.35, 2856.83, 1628.07, 1541.26, 1419.74, 754.23, 686.72. M. P. $^{\circ}$C: 230-240 (decomposed).

General method for the synthesis of naphthobipyrrole dialdehyde (TS21a-d)

TS21a: Dry DMF (2.6 ml, 33.5 mmol) was taken in a two necked round bottomed flask under N_2 atmosphere and cooled to 0°C; freshly distilled $POCl_3$ (3 ml, 32.9 mmol) was then added slowly to it with continuous stirring. After complete addition, the reaction mixture was stirred at room temperature for 1 h. Naphthobipyrrole **TS20a** (1.9 g, 6.6 mmol) was then dissolved in minimum volume of dry DCE and added to the Vilsmeier adduct at room temperature. The setup was then placed in a preheated oil bath (80°C) and refluxed for 3 h, cooled to room temperature and sat. NaOAc solution was then added slowly and again refluxed for 2 h. The yellow precipitate thus formed was filtered under suction, washed with water and dried. Finally, the product was washed with DCM to obtain the pure dialdehyde. Yield 2.1 g (91 %).

^{1}H NMR (DMSO-d_6, 400MHz, δ in ppm): 11.94 (s, 2H, NH), 10.02 (s, 2H, aldehyde), 8.31 (m, 2H, CH naph), 7.56 (m, 2H, CH naph), 1.78 (m, 4H, CH_2 *n*-Pr), 1.02 (t, 6H, J = 7.2 Hz, CH_3 *n*-Pr). ^{13}C NMR (DMSO-d_6, 100MHz, δ in ppm): 180.22, 131.73, 131.01, 127.14, 125.55, 124.86, 124.11, 119.65, 26.34, 23.31, 13.63. LCMS: m/z calculated for $C_{22}H_{22}N_2O_2$ (M-H) 345 found 345; Elemental analysis for $C_{22}H_{22}N_2O_2$ calcd. (found): C 76.28 (76.12), H 6.40 (6.51), N 8.09 (8.17); IR (neat): ν (cm^{-1}) 3270.1, 2966.3, 1655.5, 1608.6, 1466.9, 1412.9, 1380.9, 1352.2, 1282.5, 1115.6, 813.4, 758.4, 699.2, 657.0, 632.5; M. P. >290°C.

TS21b: Yield: 88 %. ^{1}H NMR ($CDCl_3$, 400MHz, δ in ppm): 12.30 (s, 2H, NH), 10.36 (s, 2H, aldehyde), 8.51 (2H, CH naph), 7.55 (m, 2H, CH naph), 4.26 (m, 2H, CH *i*-Pr), 1.74 (d, 12H, J = 6.8 Hz, CH_3 *i*-Pr). ^{13}C NMR (DMSO-d_6, 100MHz, δ in ppm): 181.28, 137.18, 131.54,

127.41, 125.10, 124.72, 124.56, 119.10, 26.50, 24.44. LCMS: m/z calculated for $C_{22}H_{22}N_2O_2$ (M+H) 347 found 347; Elemental analysis for $C_{22}H_{22}N_2O_2$ calcd. (found): C 76.28 (76.12), H 6.40 (6.51), N 8.09 (8.15); IR (neat): ν (cm^{-1}) 3316.6, 1631.1, 1592.7, 1461.3, 1429.4, 1386.3, 1352.4, 1272.2, 1134.0, 1019.5, 799.5, 750.3, 721.9; M. P. 290°C.

TS21c: Yield: 91 %. ^{1}H NMR (DMSO-d_6 , 400MHz, δ in ppm): 11.93 (s, 2H, NH), 9.99 (s, 2H, aldehyde), 8.29 (m, 2H, CH naph), 7.55 (m, 2H, CH naph), 1.74 (m, 4H, CH_2 *n*-pentyl), 1.41 (m, 4H, CH_2 *n*-pentyl), 1.32-1.42 (m, 8H, CH_2 *n*-pentyl), 0.86 (t, 6H, J = 7.2 Hz, CH_3 *n*-pentyl). ^{13}C NMR ($CDCl_3$, 100MHz, δ in ppm): 180.13, 131.58, 131.38, 127.13, 125.58, 124.86, 124.15, 119.64, 30.99, 29.86, 24.51, 22.01, 13.99. LCMS: m/z calculated for $C_{26}H_{30}N_2O_2$ (M+H) 403, found 402. Elemental analysis for $C_{26}H_{30}N_2O_2$ calcd. (found); C 77.58 (77.62), H 7.51 (7.55), N 6.96 (6.85); M. P. 274 °C.

TS21d: Yield: 73 %. ^{1}H NMR (DMSO-d_6, 400MHz, δ in ppm): 11.85 (s, 2H, NH), 10.03 (s, 2H, aldehyde), 8.41 (m, 2H, CH naph), 7.53 (m, 2H, CH naph), 2.92 (s, 6H, CH_3 Me). ^{13}C NMR (DMSO-d_6, 100MHz): 180.03, 131.52, 127.44, 126.50, 125.16, 124.66, 124.22, 120.58, 11.91. LCMS: m/z calculated for $C_{18}H_{14}N_2O_2$ (M+H) 291 found 291. Elemental analysis for $C_{18}H_{14}N_2O_2$ calcd. (found); C 74.47 (74.65), H 4.86 (4.88), N 9.65 (9.51). IR (KBr): ν (cm^{-1}) 3287.00, 3225.27, 1647.36, 1597.20, 1473.75, 1415.88, 1350.29, 1280.85, 1020.44, 999.22, 864.19, 806.32, 754.23. M. P. $^{\circ}$C 280 (decomposed).

General method for the synthesis of Dinaphthoporphycenes (TS22a-c)

TS22a: To a slurry of low-valent titanium agent, generated by reduction of (1.90 mL, 17.40 mmol) of titanium tetrachloride in dry THF (90 mL) with activated zinc (2.27 g) and CuCl (0.34 g), was added a solution of naphthobipyrrole dialdehyde **15a** (300 mg, 0.87 mmol) in boiling THF (230 mL). The reaction mixture was heated under reflux for 20 min and then hydrolyzed by slow addition of 10 % aqueous potassium carbonate (47 mL). The reaction mixture was filtered through celite to remove the excess metal, washed with dichloromethane and the washings were combined with the organic layer of the filtrate and dried over anhyd. Na_2SO_4 and freed from solvent by rotary evaporator and the solid residue was subjected to chromatography on a neutral alumina column using dichloromethane-hexane (1:1). The blue fraction thus obtained was evaporated to yield the dinaphthoporphycene as a blue solid and recrystallized from chloroform–hexane mixture. Yield 53 mg (20 %).

^{1}H NMR ($CDCl_3$, 400MHz, δ in ppm): 9.12 (s, 4H, *meso*-CH), 9.08 (s, 2H , NH), 8.38 (m, 4H, CH naph), 7.48 (m, 4H, CH naph), 3.91 (t, 8H, J = 7.6Hz, CH_2 *n*-Pr), 2.19 (m, 8H, CH_2 *n*-Pr), 1.26 (t, 12H, J = 7.2 Hz, CH_3 *n*-Pr); ^{1}H NMR ($CDCl_3$, 400MHz, D_2O added, δ in ppm): 9.15 (s, 4H, *meso*-CH), 8.40 (m, 4H, CH naph), 7.49 (m, 4H, CH naph), 3.92 (t, 8H, J = 7.2 Hz, CH_2 *n*-Pr), 2.17 (m, 8H, CH_2 *n*-Pr), 1.26 (t, 12H, J = 7.2 Hz, CH_3 *n*-Pr); LCMS: m/z calculated for $C_{44}H_{42}N_4$ (M+H) 628 found 628; Elemental analysis for $C_{44}H_{42}N_4$ calcd. (found); C 84.31 (84.51), H 6.75 (6.82), N 8.94 (9.12); UV/VIS (Chloroform): λ_{max} in nm (ε) 265 (55346), 293 (37885), 312(35983), 383 (61252), 400 (70461), 508 (11175), 548 (14135), 653 (25559), 713 (34262); M. P. > 290 °C. * ^{13}C NMR could not be obtained due to poor solubility.

TS22b: Yield 22 %. ^{1}H NMR ($CDCl_3$, 400MHz, δ in ppm): 9.45 (s, 4H, *meso*-CH), 9.27 (s, 2H, NH), 8.59 (m, 4H, CH naph), 7.49 (m, 4H, CH naph), 4.76 (m, 4H, CH *i*-Pr), 2.08 (d, 24H, J = 7.2 Hz, CH_3 *i*-Pr); ^{1}H NMR ($CDCl_3$, 400MHz, D_2O added, δ in ppm): 9.45 (s, 4H, *meso*-CH), 8.59 (4H, CH naph), 7.49 (m, 4H, CH naph), 4.76 (m, 4H, CH *i*-Pr), 2.08 (d, 24H, J = 6.4 Hz, CH_3 *i*-Pr). ^{13}C NMR ($CDCl_3$, 100MHz, δ in ppm): 146.7, 143.91, 133.91, 131.71, 131.47, 128.45, 127.42, 116.44, 28.52, 25.11; LCMS: m/z calculated for $C_{44}H_{42}N_4$ (M+H) 628 found 628; Elemental analysis for $C_{44}H_{42}N_4$ calcd. (found); C 84.31(84.22), H 6.75 (6.81), N 8.94 (8.86). UV/VIS (Chloroform): λ_{max} in nm (ε) 266 (88552), 294 (57940), 311 (53872), 388 (99947), 402 (115281), 508 (16393), 546 (20760), 658 (40926), 718 (56419); M. P. > 294 °C. This compound was also characterized by single crystal X-ray diffraction analysis.

TS22c: Yield 18 %. ^{1}H NMR ($CDCl_3$, 400MHz, δ in ppm): 9.13 (s, 4H, *meso*-CH), 9.09 (s, 2H , NH), 8.39 (m, 4H, CH naph), 7.49 (m, 4H, CH naph), 3.92 (t, 8H, J = 7.6Hz, CH_2 *n*-pentyl), 2.16 (m, 8H, CH_2 *n*-pentyl), 1.70 (m, 8H, CH_2 *n*-pentyl), 1.50 (m, 8H, CH_2 *n*-pentyl), 0.96 (t, 12H, J = 7.2 Hz CH_3 *n*-pentyl), ^{1}H NMR ($CDCl_3$, 400MHz, D_2O added, δ in ppm): 9.05 (s, 4H, *meso*-CH), 8.36 (m, 4H , CH naph), 7.47(m, 4H, CH naph), 3.87 (t, 8H, J = 8Hz, CH_2 *n*-pentyl), 2.12 (m, 8H, CH_2 *n*-pentyl), 1.70 (m, 8H, CH_2 *n*-pentyl), 1.49 (m, 8H, CH_2 *n*-pentyl), 0.95 (t, 12H, J = 7.2 Hz, CH_3 *n*-pentyl); ^{13}C NMR ($CDCl_3$, 100MHz, δ in ppm): 148.17, 137.27, 133.49, 132.04, 131.12, 127.43, 114.73, 32.56, 31.75, 27.72, 22.88, 14.29; LCMS: m/z calculated for $C_{52}H_{58}N_4$ (M-H) 738, found 738; Elemental analysis for $C_{52}H_{58}N_4$ calcd. (found); C 84.51 (84.45), H 7.91 (7.86), N 7.58 (7.71); UV/VIS (Chloroform): λ_{max} in

nm (ε) 265 (65742), 293 (44379), 312 (42125), 383 (75407), 400 (88276), 509 (12383), 548 (16524), 654 (31215), 714 (42406); M. P. 294°C (decomposed).

General method for the synthesis of Ni-complex of Dinaphthoporphycenes (TS23b-c)

TS23b: To a solution of **TS22b** (20 mg, 0.032 mmol) in *o*-dichlorobenzene (20 mL), $Ni(acac)_2$ (160 mg, 0.62 mmol) was added, followed by pyridine (0.6 ml, 7.2 mmol). The reaction mixture was refluxed for 12 h under N_2 atmosphere. Solvent was evaporated under reduced pressure. The resultant product was purified by neutral alumina column with chloroform-hexanes (1:1). The green band thus obtained was collected and the organic solvent was evaporated to obtain the complex as green solid. Yield: 19 mg (87 %).

^{1}H NMR ($CDCl_3$, 400MHz, δ in ppm): 9.09 (s, 4H, *meso*-CH), 8.49 (m, 4H, CH naph), 7.47 (m, 4H, CH naph), 4.62 (m, 4H, CH- *i*-Pr), 1.99 (d, 24H, J = 7.2 Hz, CH_3 *i*-Pr); ^{13}C NMR ($CDCl_3$, 100MHz, δ in ppm): 150.63, 149.34, 145.14, 134.53, 129.84, 127.87, 127.18, 112.27, 28.55, 24.22; LCMS: m/z calculated for $C_{44}H_{40}N_4Ni$ (M+H) 684 found 683; Elemental analysis for $C_{44}H_{40}N_4Ni$ calcd. (found); C 77.32 (77.15), H 5.90 (5.95), N 8.20 (8.32); UV/VIS (Chloroform): λ_{max} in nm (ε) 265 (53920), 295 (47038), 349 (37069), 386 (45941), 409 (60447), 496 (14168), 531 (12781), 643 (23088), 701 (45768); M. P. > 294°C. This complex was also characterized by single crystal X-ray diffraction analysis.

TS23c: Yield: Quantitative. ^{1}H NMR ($CDCl_3$, 400MHz, δ in ppm): 8.43 (s, 4H, *meso*-CH), 8.12 (m, 4H , CH naph), 7.42 (m, 4H, CH naph), 3.59 (t, 8H, CH_2 *n*-pentyl), 2.01 (m, 8H, CH_2 *n*-pentyl), 1.63 (m, 8H, CH_2 *n*-pentyl), 1.47 (m, 8H, CH_2 *n*-pentyl), 0.945 (t, 12H, J = 7.2 Hz, CH_3 *n*-pentyl); LCMS: m/z calculated for $C_{52}H_{56}N_4Ni$ (M-H) 794, found 794; Elemental analysis for $C_{52}H_{56}N_4Ni$ calcd. (found); C 78.49 (78.56), H 7.09 (7.16), N 7.04 (7.15); UV/VIS (Chloroform): λ_{max} in nm (ε) 265 (60719), 296 (53432), 347 (43022), 383 (54940), 407 (73040), 495 (14292), 534 (13543), 641 (27046), 690 (51195); M. P. 294°C (decomposed). * ^{13}C NMR could not be obtained due to poor solubility.

Synthesis of Cu-complex of Dinaphthoporphycene (TS24b)

To a solution of **TS22b** (20 mg, 0.032 mmol) in chloroform (30 mL), $Cu(OAc)_2.H_2O$ (160 mg, 0.8 mmol) in methanol (1 mL) was added, followed by triethylamine (1 ml, 7.2 mmol). The reaction mixture was then refluxed for 12 h under N_2 atmosphere. Solvent was evaporated under reduced pressure and the residue was washed with methanol to remove the

excess metal salt. The resultant product was recrystallized from chloroform-hexane (1:5), to get the complex as green solid. Yield: 16 mg (72 %).

UV/Vis (Chloroform): λ_{max} in nm (ε) 272 (103997), 293 (72563), 383 (97380), 386 (45941), 409 (112990), 502 (21535), 536 (21824), 657 (39954), 723 (70167). HR-MS (ESI): m/z calcd for $C_{44}H_{41}CuN_4$: 688.2627; found $[M+H]^+$ 688.2627. This complex was also characterized by single crystal X-ray diffraction analysis.

Synthesis of Pd-complex of Dinaphthoporphycene (TS25b)

To a solution of **TS22b** (15 mg, 0.024 mmol) in acetic acid (15 mL), $Pd(OAc)_2$ (52 mg, 0.23 mmol) was added, followed by addition of NaOAc (3 mg, 0.038 mmol). The reaction mixture was then refluxed for 12 h under N_2 atmosphere and the solvent was evaporated under reduced pressure. The residue was dissolved in dichloromethane and washed with water to remove the traces of acetic acid. Organic layer was evaporated and the resultant residue was purified on a basic alumina column to obtain the complex as green solid. Yield: 6 mg (34 %).

^{1}H NMR ($CDCl_3$, 400MHz, δ in ppm): 9.62 (s, 4H, *meso*-CH), 8.31 (m, 4H, CH naph), 7.45 (m, 4H, CH naph), 4.20 (m, 4H, CH- *i*-Pr), 2.31 (d, 12H, J = 7.2 Hz, CH_3 *i*-Pr), 1.16 (d, 12H, J = 7.2 Hz, CH_3 *i*-Pr). UV/Vis (Chloroform): λ_{max} in nm 271, 300, 383, 420, 574, 695, 764. HR-MS (ESI): m/z calcd for $C_{44}H_{40}PdN_4$: 730.2288; found $[M]^+$ 730.2167; Quantitative evaluation of absorption spectrum and recording of ^{13}C NMR were not possible due to poor solubility and probably the reason for not getting a good quality HR-MS spectrum.

Synthesis of 2,9-dibenzoyl naphthobipyrrole TS26

A mixture of $POCl_3$ (2.24 mL, 24.3 mmol) and N,N-dimethylbenzamide (2.46 g, 16.5 mmol) were stirred at 40 °C for 24 h under N_2 atmosphere. To this mixture, a solution of di-*n*-propylnaphthobipyrrole **TS20a** (200 mg, 0.69 mmol) in *o*-dichlorobenzene was added and heated at 140 °C for 16 h, cooled to room temperature and the reaction was quenched with sat. NaOAc (2.34 g, 149 mmol). The reaction mixture was further heated at 100 °C for 2h, cooled and the organic layer was separated, washed with water twice. Solvent was evaporated under reduced pressure and the residue was subjected to column chromatography on silica gel (5 % EtOAc/hexane). Yield: 150 mg (44 %).

^{1}H NMR ($CDCl_3$, 400 MHz, δ in ppm): 0.83 (t, 6H, J = 7.2Hz, CH_3 *n*-Pr), 1.71 (m, 4H, CH_2 *n*-Pr), 2.94 (m, 4H, CH_2 *n*-Pr), 7.40 (m, 4H, CH Ph), 7.52 (m, 4H, CH Ph), 7.65 (m, 4H, CH naph and Ph), 8.34 (m, 2H, CH naph), 11.43 (s, 2H, NH). ^{13}C NMR ($CDCl_3$, 100 MHz, δ in

ppm): 14.17, 23.38, 28.89, 121.43, 124.49, 124.68, 125.96, 127.99, 128.56, 128.74, 130.96, 131.19, 131.84, 139.74, 189.44. HR-MS (ESI): m/z calcd for $C_{34}H_{31}N_2O_2$: 499.2386; found 499.2385. This compound was also characterized by single crystal X-ray diffraction analysis.

Synthesis of TS27 (Proposed method for the synthesis of *meso*-tetraphenyl porphycene TS28): To a slurry of low-valent titanium agent, generated by reduction of titanium tetrachloride (0.44 mL, 4 mmol) in dry THF (30 mL) with activated zinc (523 mg, 8 mmol) and CuCl (79 mg, 0.80 mmol), was added a solution of **TS20** (100 mg, 0.20 mmol) in boiling THF (15 mL). The reaction mixture was heated under reflux for 20 min and then hydrolyzed by slow addition of 10 % aqueous solution of potassium carbonate (10 mL) and filtered through celite to remove the excess metal, washed with dichloromethane and the washings were combined with the organic layer of the filtrate. The organic component was washed and dried (anhyd. Na_2SO_4) and the solvent were removed under reduced pressure. TLC of the crude product shows no indication of product formation, even after treating with DDQ. Purification of the residue by silica gel column (eluent: 30 % ethyl acetate in hexane) yielded the partially reduced **TS22** as a yellow color compound.

^{1}H NMR (in $CDCl_3$, 400 MHz, δ in ppm): 0.69 (t, 3H, J = 7.2 Hz, CH_3 *n*-Pr), 0.95 (t, 3H, J = 7.2 Hz, CH_3 *n*-Pr), 1.68 (brs, 2H, CH_2 *n*-Pr), 2.04 (brs, 2H, CH_2 *n*-Pr), 2.64 (brs, 2H, CH_2 *n*-Pr), 2.86 (t, J = 7.6 Hz, 2H, CH_2 *n*-Pr), 3.58 (s, 2H, CH_2 Bn), 6.94 (m, 2H, CH Ph), 7.21 (m, 2H, CH Ph), 7.37 (m, 2H, CH Ph), 7.47 (m, 4H, CH Ph), 7.59 (m, 2H, CH naph), 8.24 (m, 1H, CH naph), 8.31 (m, 2H, CH naph), 11.03 (s, 1H, NH), 12.10 (s, 1H, NH). HR-MS (ESI): m/z calcd for $C_{34}H_{33}N_2O$: 485.2593; found 485.2591.

3.6 Crystallographic details

Crystallographic data for **TS15b**, **TS16, TS19d** and **TS26** were collected on BRUKER SMART-APEX CCD diffractometer. Crystallographic data for **TS19b, TS22b**, **TS23b** and **TS24b** were collected on Oxford Gemini A Ultra diffractometer with dual source.

Pertinent crystallographic data collection and refinement parameter are shown in the following tables:

Table 3.3 Crystallographic parameters of crystals of **TS15b**, **TS16**, **TS19d** and **TS26**

Crystal data	**TS15b**	**TS16**	**TS19d**	**TS26**
Formula unit	$C_{22}H_{22}N_2O_2$	$C_{22}H_{24}N_2O$	$C_{22}H_{22}N_2O_4$	$C_{34}H_{32}N_2O_3$
Formula wt.	346.42	332.43	378.42	516.62
Crystal system	Monoclinic	Monoclinic	Monoclinic	Monoclinic
T [K]	298 (2)	298 (2)	298 (2)	298 (2)
a [Å]	17.960 (6)	9.090 (7)	9.296 (7)	12.292 (3)
b [Å]	9.378 (3)	12.707 (10)	21.340 (16)	8.117 (2)
c [Å]	21.670 (8)	15.975 (13)	11.388 (8)	29.322 (8)
α [°]	90	90	90	90
β [°]	93.541 (7)	94.831 (14)	99.368 (12)	96.319 (4)
γ [°]	90	90	90	90
volume [$Å^3$]	3641 (2)	1839 (3)	2229 (3)	2907.8 (14)
Space group	P2(1)/n	P2(1)/c	P2(1)/c	P2(1)/n
Z′	2	1	1	1
Z	8	4	4	4
D_{calc} [$g.cm^{-3}$]	1.264	1.201	1.128	1.180
μ/mm^{-1}	0.082	0.074	0.078	0.075
Reflns collected	36867	16931	22338	23647
Unique reflns	7161	3237	4400	5103
Obs. reflns	2827	1476	3583	3868
R(int)	0.1411	0.2318	0.0431	0.0651
R_1 [$I > 2\sigma(I)$],	0.0675 (2827)	0.1600 (1476)	0.0726 (3583)	0.0608 (3868)
wR_2	0.1637 (7161)	0.3207 (3237)	0.1973 (4400)	0.1719 (5103)
GOF	0.956	1.099	1.103	1.114

Table 3.4 Crystallographic parameters of crystals of **TS19b**, **TS22b**, **TS23b** and **TS24b**

Crystal data	**TS19b**	**TS22b**	**TS23b**	**TS24b**
Formula unit	$C_{26}H_{30}N_2O_4$	$C_{44}H_{42}N_4$	$C_{44}H_{40}N_4Ni$	$C_{44}H_{40}N_4Cu$
Formula wt.	434.52	626.82	683.49	688.34
Crystal system	Monoclinic	Monoclinic	Orthorhombic	Monoclinic
T [K]	298 (2)	298 (2)	298 (2)	298 (2)
a [Å]	24.668 (2)	15.429 (2)	15.338 (3)	15.4483 (15)
b [Å]	17.4685 (9)	6.4378 (9)	13.793 (2)	6.4601 (5)
c [Å]	25.941 (2)	16.994 (3)	15.4883 (17)	19.949 (3)
α [°]	90	90	90	90
β [°]	107.172 (10)	105.454 (14)	90	124.174 (7)
γ [°]	90	90	90	90
volume [$Å^3$]	10680.0 (13)	1626.9 (2)	3276.6 (10)	1647.1 (3)
Space group	C 2/c	P2(1)/n	Pbca	P21/c
Z´	2	0.5	0.5	0.5
Z	16	2	4	2
D_{calc} [$g.cm^{-3}$]	1.075	1.280	1.385	1.388
μ/mm^{-1}	0.073	0.075	0.632	0.703
Reflns collected	5587	6269	8987	6974
Unique reflns	5587	3321	3351	3784
Obs. Reflns	2788	2113	2172	1234
R(int)	0.000	0.0200	0.0338	0.0732
R_1 [$I > 2\sigma(I)$],	0.0712	0.0416 (2113)	0.0377 (2172)	0.0763
wR_2	0.2237	0.0974 (3321)	0.1105 (3351)	0.2343
GOF	0.920	0.912	0.786	0.857

3.7 References

1. Vogel, E.; Köcher, M.; Schmickler, H.; Lex, J. *Angew. Chem., Int. Ed. Engl.* **1986**, *25*, 257.
2. (a) Sessler, J. L.; Weghorn, S. J. in *Expanded, Contracted and Isomeric Porphyrins*, Elsevier, Oxford, **1997**. (b) Sessler, J. L.; Gebauer, A.; Vogel, E. in *The Porphyrin Handbook* **2000**, *2*, 3. (c) Jasat, A.; Dolphin, D. *Chem. Rev*. **1997**, *97*, 2267. (d) Vogel, E. *Pure Appl. Chem.* **1996**, *68*, 1355.
3. (a) Fowler, C. J.; Sessler, J. L.; Lynch, V. M.; Waluk, J.; Gebauer, A.; Lex, J.; Heger, A.; Zuniga-y-Rivero, F.; Vogel, E. *Chem. Eur. J.* **2002**, *8*, 3485. (b) Baba, T.; Shimakoshi, H.; Aritome, I.; Hisaeda, Y. *Chem. Lett*. **2004**, *33*, 906. (c) Rachlewicz, K.; Latos-Grazynski, L.; Vogel, E.; Ciunik, Z.; Jerzykiewicz, L. B. *Inorg. Chem*. **2002**, *41*, 1979.
4. (a) Hayashi, T.; Okazaki, K.; Urakawa, N.; Shimakoshi, H.; Sessler, J. L.; Vogel, E.; Hisaeda, Y. *Organometallics* **2001**, *20*, 3074. (b) Lo, W.-Ch.; Che, Ch.-M.; Cheng, K.-F.; Mak, T. C. W. *Chem. Commun*. **1997**, 1205.
5. (a) Saoiabi, A.; Maroufi, N.; Laghzizil, A.; Barbe, J. M.; Guilard, R. *J. Maro. Chim. Heterocycl.* **2005**, *4*, 65. (b) Albrecht, V.; Wiehe, A.; Roeder B.; Neuberger, W. *WO Pat*. 2006007261, **2005**. (c) Barbe, J. M.; Richard, P.; Aukauloo, M. A.; Lecomte, C.; Petit, P.; Guilard, R. *J. Chem. Soc., Chem. Commun*. **1994**, 2757.
6. (a) Hayashi, T.; Dejima, H.; Matsuo, T.; Sato, H.; Murata D.; Hisaeda, Y. *J. Am. Chem. Soc.* **2002**, *124*, 11226. (b) Hayashi, T.; Murata, D.; Makino, M.; Sugimoto, H.; Matsuo, T.; Sato, H.; Shiro, Y.; Hisaeda, Y. *Inorg. Chem*. **2006**, *45*, 10530. (c) Matsuo, T.; Dejima, H.; Hirota, S.; Murata, D.; Sato, H.; Ikegami, T.; Hori, H.; Hisaeda, Y.; Hayashi, T. *J. Am. Chem. Soc*. **2004**, *126*, 16007. (d) Nakashima, H.; Hasegawa, J.-Y.; Nakatsuji, H. *J. Comput. Chem.* **2006**, *27*, 1363. (e) Matsuo, T.; Ikegami, T.; Sato, H.; Hisaeda, Y.; Hayashi, T. *J. Inorg. Biochem*. **2006**, *100*, 1265. (f) Matsuo, T.; Tsuruta, T.; Maehara, K.; Sato, H.; Hisaeda, Y.; Hayashi, T. *Inorg. Chem.* **2005**, *44*, 9391.
7. In order to describe porphyrinoid structures, a systematic nomenclature system has been proposed; it consists of the number of π-electrons in brackets, the general name of the compound, and the numbers of C atoms between the pyrrole units for each of the bridges set off by commas and in parentheses. See: Gosmann, M.; Franck, B. *Angew. Chem., Int. Ed. Engl.* **1986**, *25*, 1100.

8. (a) MacDonald, I. J.; Dougherty, T. J. *J. Porphyrins Phthalocyanines* **2001**, *5*, 105. (b) Sternberg, E. D.; Dolphin, D. *Tetrahedron* **1998**, *54*, 4151. (c) Dougherty, T. J.; Gomer, C. J.; Henderson, B. W.; Jori, G.; Kessel, D.; Korbelik, M.; Moan, J.; Peng, Q. *J. Natl. Cancer Inst.* **1998**, *90*, 889. (d) Aramendia, P. F.; Redmond, R. W.; Nonell, S.; Schuster, W.; Braslavsky, S. E.; Schaffner, K.; Vogel, E. *Photochem. Photobiol*. **1986**, *44*, 555. (e) Guardiano, M.; Biolo, R.; Jori, G.; Schaffner, K. *Cancer Lett*. **1989**, *44*, 1. (f) Milanesi, C.; Biolo, R.; Jori, G.; Schaffner, K. *Laser Med. Sci*., **1991**, *6*, 437. (g) Aicher, A.; Miller, K.; Reich, E.; Hautmann, R. *Urol. Res*., **1994**, *22*, 25. (h) Villanueva, A.; Cañete, M.; Nonell, S.; Borrell, J. I.; Teixidó, J.; Juarranz, A. *Anti-Cancer Drug Des*. **1996**, *11*, 89. i) Cañete, M.; Lapeña, M.; Juarranz, A.; Vendrell, V.; Borrell, J. I.; Teixidó, J.; Nonell, S.; Villanueva, A. *Anti-Cancer Drug Des*. **1997**, *12*, 543. (j) Karrer, S.; Abels, C.; Szeimies, R.-M.; Baumler, W.; Dellian, M.; Hohenleutner, U.; Goetz, A. E.; Landthaler, M. *Arch. Dermatol. Res*. **1997**, *289*, 132. (k) Karrer, S.; Szeimies, R.-M.; Ebert, A.; Fickweiler, S.; Abels, C.; Bäumler, W.; Landthaler, M. *Laser Med. Sci*. **1997**, *12*, 307. (l) Cañete, M.; Ortega, C.; Gavaldá, A.; Cristóbal, J.; Juarranz, A.; Nonell, S.; Teixidó, J.; Borrell, J. I.; Villanueva, A.; Rello, S.; Stockert, J. C. *Int. J. Oncol*. **2004**, *24*, 1221. (m) Kessel, D.; Conley, M.; Vicente, M. C. H.; Reiners, J. J. *Photochem. Photobiol*. **2005**, *81*, 569. (n) Arad, O.; Gavaldá, A.; Rey, O.; Rubio, N.; Sánchez-García, D.; Borrell, J. I.; Teixidó, J.; Nonell, S.; Cañete, M.; Juarranz, A.; Villanueva, A.; Stockert, J. C.; Jiménez, P. J. D. *Afinidad* **2002**, *500*, 343. (o) Stockert, J. C.; Cañete, M.; Juarranz, A.; Villanueva, A.; Horobin, R. W.; Borrell, J. I.; Teixidó, J.; Nonell, S. *Curr. Med. Chem*. **2007**, *14*, 997.
9. (a) Lauro, F. M.; Pretto, P.; Covolo, L.; Jori, G.; Bertoloni, G. *Photochem. Photobiol. Sci*. **2002**, *1*, 468.
10. (a) Mukaiyama, T.; Sato, T.; Hanna, J. *Chem. Lett*. **1973**, 1041. (b) McMurry, J. E.; Fleming, M. P. *J. Am. Chem. Soc.* **1974**, *96*, 4708. (c) McMurry, J. E. *Acc. Chem. Res.* **1983**, *16*, 405. (d) Lenoir, D. *Synthesis* **1977**, 553.
11. Anju, K. S.; Ramakrishnan, S.; Thomas, A. P.; Suresh, E.; Srinivasan, A. *Org. Lett*. **2008**, *10*, 5545.
12. (a) Grigg, R.; Johnson, A. W.; Wasley, J. W. F. *J. Chem. Soc*. **1963**, 359. (b) Crigg, R.; Johnson, A. W. *J. Chem. Soc*. **1964**, 3315. (c) Sessler, J. L.; Cyr, M.; Burrell, A. K. *Tetrahedron* **1992**, *48*, 9661. (d) Hinz, W.; Jones, R. A.; Patel, S. U.; Karatza, M.-H. *Tetrahedron* **1986**, *42*, 3753. (e) Rapoport, H.; Bordner, J. *J. Org. Chem*. **1964**, *29*,

2727. (f) Bordner, J.; Rapoport, H. *J. Org. Chem.* **1965**, *30*, 3824. (g) Bauer, H. *Chem. Ber*. **1968**, *101*, 1286. (h) Boger, D. L.; Patel, M.; *J. Org. Chem.* **1988**, *53*, 1405. (i) Falk, H.; Flödl, H. *Monatsh. Chem*. **1988**, *119*, 247. (j) Benincori, T.; Brenna, E.; Sannicolò, F.; Zotti, G.; Zecchin, S.; Schiavon, G.; Gatti, C.; Frigerio, G. *Chem. Mater*. **2000**, *12*, 1480.

13. Fanta, P. E. *Chem. Rev*. **1964**, *64*, 613.
14. Vogel, E.; Balci, M.; Pramod, K.; Koch, P.; Lex J.; Ermer, O. *Angew. Chem., Int. Ed. Engl.* **1987**, *26*, 928.
15. (a) Nonell, S.; Bou, N.; Borrell, J. I.; Teixidó, J.; Villanueva, A.; Juarranz, A.; Cañete, M. *Tetrahedron Lett*. **1995**, *36*, 3405. (b) Ikeda, H.; Sessler, J. L. *J. Org. Chem*. **1993**, *58*, 2340.
16. Gavaldá, A.; Borrell, J. I.; Teixidó, J.; Nonell, S.; Arad, O.; Grau, R.; Cañete, M.; Juarranz, A.; Villanueva, A.; Stockert, J. C. *J. Porphyrins Phthalocyanines* **2001**, *5*, 846.
17. (a) Arad, O.; Morros, J.; Batllori, X.; Teixidó, J.; Nonell, S.; Borrell, J. I. *Org. Lett*. **2006**, *8*, 847. (b) Farnier, M.; Soth, S.; Fournari, P. *Can. J. Chem*. **1976**, *54*, 1074. c) Farnier, M.; Soth, S.; Fournari, P. *Can. J. Chem*. **1976**, *54*, 1083.
18. a) Cañete, M.; Ortiz, A.; Juarranz, A.; Villanueva, A.; Nonell, S.; Borrell, J. I.; Teixidó, J.; Stockert, J. C. *Anti-Cancer Drug Des*. **2000**, *15*, 143.
19. (a) Vogel, E. *Pure Appl. Chem*. **1990**, *62*, 557. (b) Steiner, E.; Fowler, P. W. *Org. Biomol. Chem.* **2003**, *1*, 1785. (c) Vogel, E.; *J. Heterocycl. Chem*. **1996**, *33*, 1461.
20. (a) Vogel, E.; Grigat, I.; Köcher, M.; Lex, J. *Angew. Chem., Int. Ed. Engl.* **1989**, *28*, 1655. (b) Vogel, E.; Köcher, M.; Lex, J.; Enmer, O. *Isr. J. Chem*. **1989**, *29*, 257.
21. (a) Vogel, E.; Koch, P.; Hou, X.-L.; Lex, J.; Lausmann, M.; Kisters, M.; Aukauloo, A. M.; Richard, P.; Guilard, R. *Angew. Chem., Int. Ed. Engl.* **1993**, *32*, 1600. (b) Guilard, R.; Aukaloo, M. A.; Tardieux, C.; Vogel, E. *Synthesis* **1995**, *12*, 1480.
22. Sessler, J. L.; Aguilar, A.; Sánchez-García, D.; Seidel, D.; Köhler, T.; Arp, F.; Lynch, V. M. *Org. Lett*. **2005**, *7*, 1887.
23. (a) Barton, D. H. R.; Zard, S. Z. *J. Chem. Soc., Chem. Commun*. **1985**, 1098. (b) Barton, D. H. R.; Kervagoret, J.; Zard, S. Z. *Tetrahedron* **1990**, *46*, 7587.
24. Kuzuhara, D.; Yamada, H.; Yano, K.; Okujima, T.; Mori, S.; Uno, H. *Chem.-Eur. J.* **2011**, *17*, 3376.

25. Kuzuhara, D.; Mack, J.; Yamada, H.; Okujima, T.; Ono, N.; Kobayashi, N. *Chem.-Eur. J.* **2009**, *15*, 10060.
26. (a) Hayashi, T.; Nakashima, Y.; Ito, K.; Ikegami, T.; Aritome, I.; Suzuki, A.; Hisaeda, Y. *Org. Lett*. **2003**, *16*, 2845. (b) Hayashi, T.; Nakashima, Y.; Ito, K.; Ikegami, T.; Aritome, I.; Aoyagi, K.; Ando, T.; Hisaeda, Y. *Inorg. Chem*. **2003**, *42*, 7345.
27. (a) Will, S.; Rahbar, A.; Schmickler, H.; Lex, J.; Vogel, E. *Angew. Chem., Int. Ed. Engl.* **1990**, *29*, 1390. (b) Aritome, I.; Shimakoshi, H.; Hisaeda, Y. *Acta Crystallogr., Sect. C: Cryst. Struct. Commun.* **2002**, *58*, o563. c) Vogel, E.; Koch, P. A.; Rahbar, A.; Cross, A. D. *US Pat*. 5 244 671, **1993**.
28. Baba, T.; Shimakoshi, H.; Hisaeda, Y. *Tetrahedron Lett*. **2004**, *45*, 5973.
29. Mak, N.-K.; Kok, T.-W.; Wong, R. N.-S.; Lam, S.-W.; Lau, Y.-K.; Leung, W.-N.; Cheung, N.-H.; Huang, D. P.; Yeung, L.-L.; Chang, C. K. *J. Biomed. Sci*. **2003**, *10*, 418.
30. Vogel, E.; Mueller, M.; Halpern. O.; Cross, A. D. *US Pat.* 5 637 608, **1997**.
31. Porter, H. K. *Org. React*. **1973**, *20*, 455.
32. Vogel, E.; Richert, C.; Benninghaus, T.; Muller, M.; Cross, A. D. *US Pat.* 5 179 120, **1993**.
33. Richert, C.; Wessels, J. M.; Müller, M.; Kisters, M.; Benninghaus, T.; Goetz, A. E.; *J. Med. Chem.* **1994**, *37*, 2797.
34. Pandey, R. K. *J. Porphyrins Phthalocyanines* **2000**, *4*, 368.
35. (a) Vogel, E.; Sicken, M.; Röhrig, P.; Schmickler, H.; Lex, J.; Ermer, O. *Angew. Chem., Int. Ed. Engl.* **1988**, *27*, 411. (b) Bachmann, R.; Gerson, F.; Gescheidt, G.; Vogel, E. *J. Am. Chem. Soc*. **1993**, *115*, 10286.
36. Cöln, D. *PhD Thesis*, University of Cologne, **1991**.
37. (a) Ellinger, F.; Gieren, A.; Hübner, T.; Lex, J.; Lucchesini, F.; Merz, A.; Neidlein, R.; Salbeck, J. *Monatsh. Chem*. **1993**, *124*, 931. (b) Hu, Z.; Atwood, J. L.; Cava, M. P. *J. Org. Chem*. **1994**, *59*, 8071.
38. DeMunno, G.; Lucchesini, F.; Neidlein, R. *Tetrahedron* **1993**, *49*, 6863.
39. Dai, W.-M.; Mak, W. L. *Tetrahedron Lett*. **2000**, *41*, 10277.
40. Nüssbaumer, T.; Krieger, C.; Neidlein, R. *Eur. J. Org. Chem.* **2000**, *13*, 2449.
41. Nüssbaumer, T.; Neidlein, R. *Helv. Chim. Acta* **2000**, *83*, 1161.

42. (a) Sargent, A. L.; Hawkins, I. C.; Allen, W. E.; Liu, H. Sessler, J. L.; Fowler, C. J. *Chem. Eur. J.* **2003**, *9*, 3065. (b) Nonell, S.; Borrell, J. I.; Borrós, S.; Colominas, C.; Rey, O.; Rubio, N.; Sánchez-García, D.; Teixidó, J. *Eur. J. Org. Chem*. **2003**, *9*, 1635.
43. Vogel, E. *Pure Appl. Chem.* **1993**, *65*, 143.
44. Dietrich, H.-J. *PhD Thesis*, University of Cologne, **1994**.
45. (a) Sarma, T.; Panda, P. K.; Anusha, P. T.; Rao, S. V. *Org. Lett.* **2011**, *13*, 188. (b) During the preparation of this manuscript Sessler's group published a communication: Roznyatovskiy, V.; Lynch, V.; Sessler, J. L. *Org. Lett.* **2010**, *12*, 4424.
46. Samsoniya, Sh. A.; Trapaidze, M. V.; Kuprashvili, N. A.; Kolesnikov, A. M.; Suvorov, N. N. *Khim. Geterotsikl. Soedin.* **1985**, 1222.
47. Trapaidze, M. V.; Samsoniya, Sh. A.; Kuprashvili, N. A.; Mamaladze, L. M.; Suvorov, N. N. *Khim. Geterotsikl. Soedin.* **1988**, 603.
48. (a) Weinstock, L. M.; Currie, R. B.; Lovell, A. V. *Synth. Commun.* **1981**, *11*, 943. (b) Kelly, N. M.; Reid, R. G.; Willis, C. L.; Winton, P. L. *Tetrahedron Letters*, **1995**, *36*, 8315.
49. Sanchez-Garcia, D.; Sessler, J. L. *Chem. Soc. Rev.* **2008**, *37*, 215.
50. Dobkowski, J.; Galievsky, V.; Starukhin, A.; Vogel, E.; Waluk, J. *J. Phys. Chem. A* **1998**, *102*, 4966.
51. (a) Köhler, R. H.; Cao, J.; Zipfel, W. R.; Webb, W. W.; Hanson, M. R. *Science* **1997**, *276*, 2039. (b) Kawata, S.; Sun, H.-B.; Tanaka, T.; Takada, K. *Nature* **2001**, *412*, 697. (c) Torre, G.; Vazquez, P.; Agullo-Lopez, F.; Torres, T. *Chem. Rev.* **2004**, *104*, 3723. (d) Kumar, R. S. S.; Rao, S. V.; Giribabu, L.; Rao, D. N. *Chem. Phys. Lett.* **2007**, *447*, 274. (e) Dy, J.; Ogawa, K.; Kamada, K.; Ohta, K.; Kobuke, Y. *Chem. Commun.* **2008**, 3411. (f) He, G. S.; Tan, L.-S.; Zheng, Q.; Prasad, P. N. *Chem. Rev.* **2008**, *108*, 1245. (g) Pawlicki, M.; Collins, H. A.; Denning, R. G.; Anderson, H. L. *Angew. Chem., Int. Ed.* **2009**, *48*, 3244.
52. (a) Ogawa, K.; Ohashi, A.; Yoshihara, K.; Kobuke, Y.; Kamada, K.; Ohta, K. *J. Am. Chem. Soc.* **2003**, *125*, 13356. (b) Drobizhev, M.; Stepanenko, Y.; Dzenis, Y.; Karotki, A.; Rebane, A.; Taylor, P. N.; Anderson, H. L. *J. Phys. Chem. B* **2005**, *109*, 7223. (c) Kim, D. Y.; Ahn, T. K.; Kwon, J. H.; Kim, D.; Ikeue, T.; Aratani, N.; Osuka, A.; Shigeiwa, M.; Maeda, S. *J. Phys. Chem. A* **2005**, *109*, 2996. (d) Rath, H.; Sankar, J.; PrabhuRaja, V.; Chandrashekar, T. K.; Nag, A.; Goswami, D. *J. Am.*

Chem. Soc. **2005**, *127*, 11608. (e) Rath, H.; PrabhuRaja, V.; Chandrashekar, T. K.; Nag, A.; Goswami, D.; Joshi, B. S. *Org. Lett.* **2006**, *8*, 2325.

53. (a) He, G. S.; Markowicz, P. P.; Lin, T.-C.; Prasad, P. N. *Nature* **2002**, *415*, 767. (b) Drobizhev, M.; Karotki, A.; Kruk, M.; Dzenis, Y.; Rebane, A.; Suo, Z.; Spangler, C. W. *J. Phys. Chem. B* **2004**, *108*, 4221. (c) Suo, Z.; Drobizhev, M.; Spangler, C. W.; Christensson, N.; Rebane, A. *Org. Lett.* **2005**, *7*, 4807. (d) Samoc, M.; Morrall, J. P.; Dalton, G. T.; Cifuentes, M. P.; Humphrey, M. G. *Angew. Chem., Int. Ed.* **2007**, *46*, 731. (e) Wu, P. L.; Feng, Z. J.; Tam, H. L.; Wong, M. S.; Cheah, K. W. *J. Am. Chem. Soc.* **2009**, *131*, 886. (f) Morisue, M.; Ogawa, K.; Kamada, K.; Ohta, K.; Kobuke, Y. *Chem. Commun.* **2010**, 2121.
54. Arnbjerg, J.; Ana, J.-B.; Martin, J. P.; Nonell, S.; Borrell, J. I.; Christiansen, O.; Ogilby, P. R. *J. Am. Chem. Soc.* **2007**, *129*, 5188.
55. Sheik-Bahae, M.; Said, A. A.; Wei, T.-H.; Hagan, D. J.; Van Stryland, E. W. *IEEE J. Quantum Electron.* **1990**, *26*, 760.
56. Rao, S. V.; Prashant, T. S.; Swain, D.; Sarma, T.; Panda, P. K.; Tewari, S. P. *Chem. Phys. Lett.* **2011**, *514*, 96.
57. (a) Fakis, M.; Tsigaridas, G.; Polyzos, I.; Giannetas, V.; Persphonis, P.; Spiliopoulos, I.; Mikroyannidis, J. *Chem. Phys. Lett.* **2001**, *342*, 155. (b) Sutherland, R. L.; Brant, M. C.; Heinrichs, J.; Slagle, J. E.; McLean, D. G.; Fleitz, P. A. *J. Opt. Soc. Am. B* **2005**, *22*, 1939. (c) Anémian, R.; Morel, Y.; Baldeck, P. L.; Paci, B.; Kretsch, K.; Nunzi, J.–M.; Andraud, C. *J. Mater. Chem.* **2003**, *13*, 2157.
58. Swain, D.; Anusha, P. T.; Prashant, T. S.; Tewari, S. P.; Sarma, T.; Panda, P. K.; Rao, S. V. *Appl. Phys. Lett*. **2012**, *100*, 141109.
59. Fita, P.; Radzewicz, C.; Waluk J.; *J. Phys. Chem. A* **2008**, *112*, 10753.

CHAPTER 4

Cyclo[4]naphthobipyrroles

4.1 Introduction

4.1.1 Background

One of the primary goals in synthesizing expanded porphyrin was to get absorption spectra that are bathochromically shifted compared to porphyrin due to its extended π-conjugation. However, larger expanded porphyrin containing 6 or more pyrrole rings often adopts non-planar or figure eight structure thereby disrupting the effective conjugation pathway, hence proved to be non-aromatic or weakly aromatic in nature as discussed in chapter 1. Albeit, many of these non-planar systems exhibit interesting properties such as isolation of synthetically challenging stable Möbius aromatic and antiaromatic system, the initial goal remained unsatisfied without a planar aromatic larger expanded porphyrins that possess 'all-NH-in' conformation just like as porphyrin that would display the classic disk-like structure of simple porphyrins.

This elusive goal could be achieved by reducing the number of *meso* carbon atoms thereby inducing structural rigidity within the macrocycle. This target can be derived, formally, by replacing all four *meso*-carbon bridges of porphyrin **L1** with four additional pyrrolic rings. Thus in 2002, Sessler and coworkers reported cyclo[8]pyrrole or [30]octaphyrin(0.0.0.0.0.0.0.0), where all the eight pyrrole units are directly linked through their α-carbon atoms to each other resulting in a 30π aromatic system, which adopts a planar conformation.[1a] However, the difficulty associated with the synthesis of appropriate building block led to synthesis of very few cyclo[8]pyrroles following a biphasic, acid mediated (H_2SO_4), $FeCl_3$ catalyzed oxidative coupling of alkylated bipyrroles.[1] The cyclo[8]pyrroles,

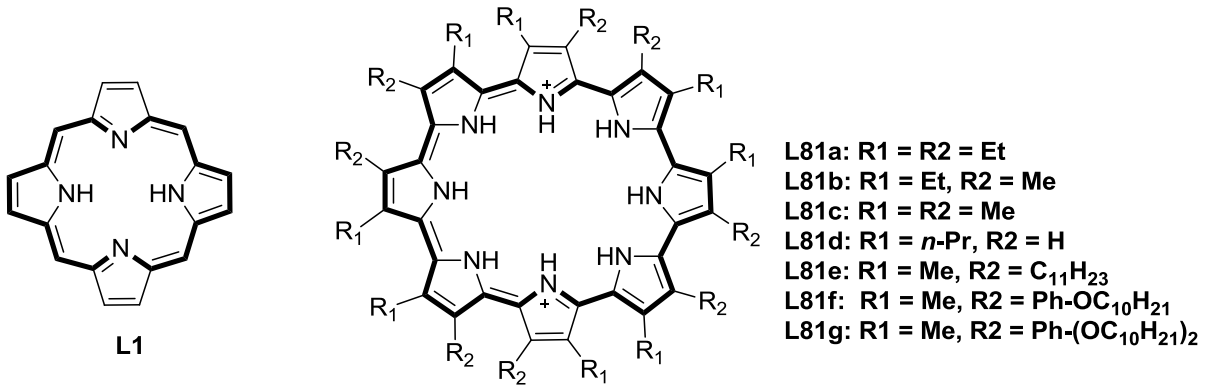

Figure 4.1 Cyclo[8]pyrroles.

were isolated in the form of their dihydrogen sulfate salts, where in sulphate ion coordinates strongly with the pyrrolic NH's at the core of the macrocycle that persists in both solid and

solution state. Yields of the macrocycles were found to be remarkably good (> 70%).[1a] It is noteworthy to mention that sulfate played a very important role in the formation of cyclo[8]pyrrole. Use of other acids (HNO_3) either leads to decomposition of the starting material or leads to formation of its smaller congeners (HCl).[2] Later on electrochemical synthesis of cyclo[8]pyrrole was reported by Christophe Bucher's group in association with J. L. Sessler.[3]

4.1.2 Basic properties of cyclo[8]pyrroles

The most striking feature about this macrocycle is that it possesses a very strong near infrared (NIR)[4] absorption band at ~1100 nm (also designated as L band) compared to a weaker Soret type near UV-band at ~430 nm (B band), unlike the other porphyrinoids where the lower energy bands are of feeble intensity (Figure 4.2). In literature, there are very few examples of dyes possessing intense absorption band beyond 1000 nm.[5] This attribute, make this cyclo[8]pyrrole also a promising material for optical storage and signalling devices.[6] Further,

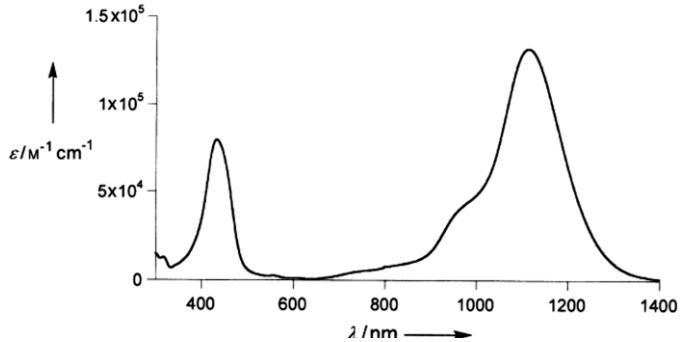

Figure 4.2 Typical absorption profile of cyclo[8]pyrrole. In figure absorption spectrum of **L81b** measured in dichloromethane.[1a]

cyclo[8]pyrroles display a great affinity towards sulfate ion, The diprotonated form of an organic-solubilized cyclo[8]pyrrole derivative **L81e**,[1d] bearing eight undecyl chains on the *β*-pyrrolic positions, was found to extract sulfate anion effectively from neutral aqueous media into a toluene organic phase in the presence of phase-transfer catalyst, Aliquat 336-nitrate (A336N).

Another interesting attribute of cyclo[8]pyrrole derivatives is their formation of supramolecular liquid crystalline adduct with nitroaromatic compounds.[1c] Exposure of dihydrogen sulfate salts of appropriately substituted cyclo[8]pyrroles **L81e-f** to electron-deficient acceptor molecules gives discotic liquid crystals stabilized via electron-donor/electr-

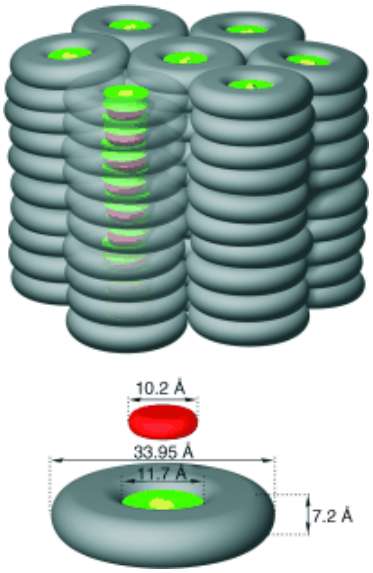

Figure 4.3 An idealized model of the hexagonal columnar (Col_h) mesophase, derived for **L81c**· **TNB** adduct.[1c] TNB (trinitrobenzene) molecules (red) intercalate into stacks of cyclo[8]pyrrole cores (green) coordinated to the sulfate ions (yellow). The volume occupied by the substituents, including molten aliphatic chains, is shown schematically in gray.

on-acceptor interactions (Figure 4.3),[1c] making them promising for explosive sensing.[7] Dihydrochloride salts of hexadecaethylcyclo[8]pyrrole (**C8**) in presence of a pyrene carboxylate anion produces a supramolecular ensemble, **C8**-**Py** (**Py**: pyrene) which, upon photoexcitation, results in charge transfer from cyclo[8]pyrrole to pyrene moiety thereby forming $\mathbf{C8}^{\bullet+}$-$\mathbf{Py}^{\bullet-}$ (Figure 4.4). This electron transfer is particularly interesting despite the fact that pyrene typically acts as a good electron donor. Another interesting feature of this ensemble is that, after initial photoinduced charge separation, it decays to the triplet excited state of cyclo[8]pyrrole ^{3}**C8***, which then returns to the ground state extremely slowly, in a time exceeding 200 ms.[1e]

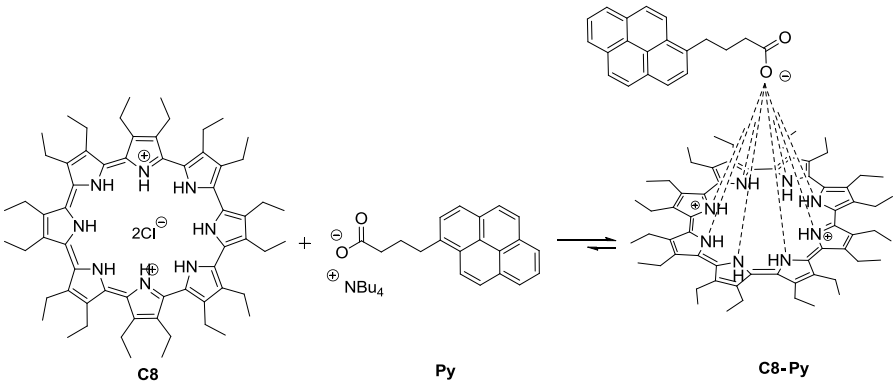

Figure 4.4 Proposed complex formation of cyclo[8]pyrrole and pyrene.[1e]

Cyclo[8]pyrrole bears structural resemblance with natural product telomestatin[8] (Figure 4.5) that acts as a telomerase inhibitor via stabilizing G-quadruplexes. This system contains seven oxazole and one thiazoline subunits even though not fully conjugated. Telomerase is a ribonucleoprotein enzyme active in 85-90% of all human tumor cells.[9] Interactions between telomerase and the specialized ends of linear chromosomes or telomeres have shown to be a key step in the immortalization of tumor cells. Given the structural similarity of cyclo[n]pyrroles with telomestatin, Bowers and coworkers in collaboration with Sessler group studied interaction of diprotonated cyclo[n]pyrroles (where n = 6-8) and the human telomere G-quadruplex sequence T4. They proposed that modulations in macrocycle structure and soluble forms of these systems or their analogues may have a role to play as telomerase inhibitors.[10]

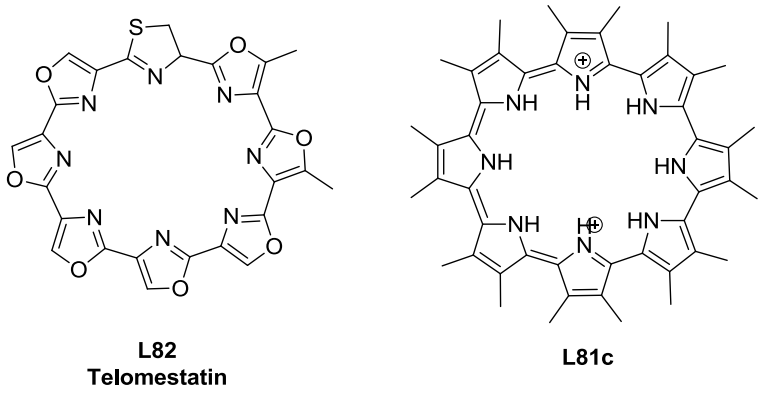

Figure 4.5 Structure of telomestatin and a proposed model cyclo[8]pyrrole studied as its inihibitor.

Cyclo[8]pyrroles (**L81a,c**) undergoes reductive N-alkylations upon treatment with NaH and an alkyl halide to produce an 32-π octa-N-alkylated product.[11] However, these N-alkylated products show highly distorted structure in solid state and exhibit non-aromatic nature as judged by their NMR spectra. These systems could be oxidized electrochemically leading to 30-π electron aromatic species, however, their chemical oxidation is yet to be achieved.

4.1.3 Cyclo[6]pyrrole, cyclo[7]pyrrole and related macrocycles

4.1.3.1 Cyclo[6]pyrrole and cyclo[7]pyrrole

Smaller congeners of cyclo[8]pyrrole namely cyclo[6]pyrrole and cyclo[7]pyrrole were made possible by similar methodology i.e. $FeCl_3$ mediated biphasic oxidative coupling, used to prepare cyclo[8]pyrroles. However, HCl (acid with smaller anion) is required instead of

H_2SO_4.[2] Nonetheless this leads to formation of cyclo[6]pyrrole and cyclo[7]pyrrole along with cyclo[8]pyrrole. These cyclo[n]pyrroles (n = 6-7) prepared from tetraethylbipyrrole were found to be aromatic in nature, possessing 22 and 26 π-electrons respectively. Solid state structure of cyclo[6]pyrrole shows a near planar structure, whereas that of cyclo[7]pyrrole displays distorted bowl like structure (Figure 4.6). Analogous to those of cyclo[8]pyrrole **L81a**, the UV-Vis spectra of both cyclo[6]pyrrole **L83** and cyclo[7]pyrrole **L84** display weak Soret (B band) and very strong L-bands (Figure 4.7). Cyclo[6]pyrrole **L83** upon treatment with $UO_2[N(SiMe_3)_2]_2{\cdot}2THF$ produces the novel uranyl complex of cyclo[6]pyrrole, which was observed to be highly planar. Upon complexation, the formally 22-π aromatic **L83** oxidized to 20-π antiaromatic, yet stable species.[12]

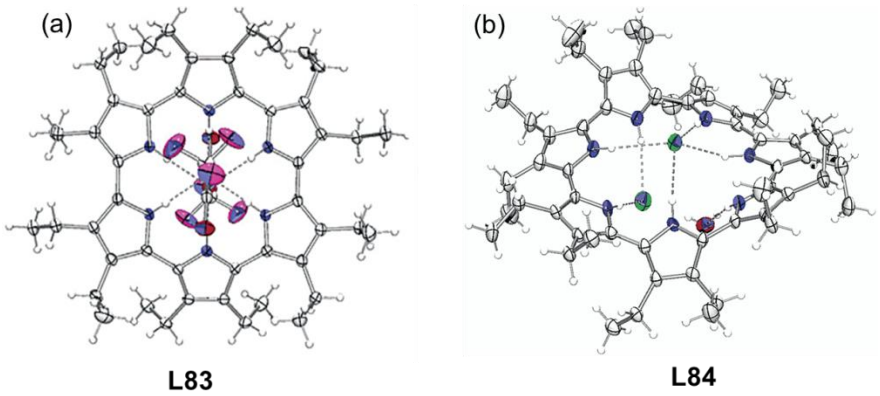

Figure 4.6 Solid state structure of (a) cyclo[6]pyrrole **L83** and (b) cyclo[7]pyrrole **L84** as bis-TFA and bis-HCl salt respectively.[2]

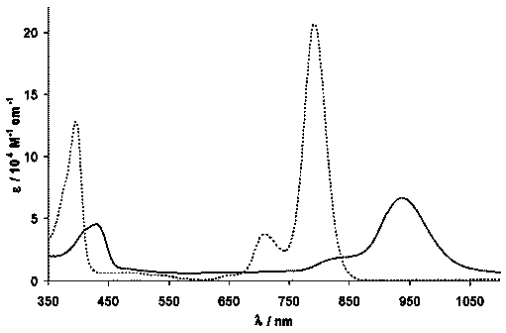

Figure 4.7 UV-Vis-NIR spectra of cyclo[6]pyrrole **L83** (···) and cyclo[7]pyrrole **L84** (—).[2]

4.1.3.2 Cyclo[m]pyridine[n]pyrroles

Very recently Sessler and coworkers reported synthesis and electronic properties of hybrid cyclo[m]pyridine[n]pyrroles (Figure 4.8).[13] Like cyclo[6]pyridine **L85**,[14] these macrocycles are best described as locally aromatic compounds lacking long-range inter-subunit conjugation. However, upon protonation an extension of the π-conjugation in the

macrocycles could be noticed. Thus protonated **L86** and **L87** exhibits electronically delocalized 24 π-electron antiaromatic characters.

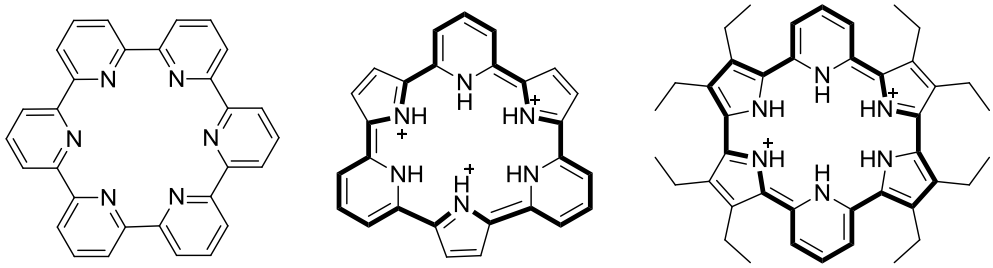

L85 **L86** **L87**

Figure 4.8 Structures of cyclo[6]pyridine **L85**, cyclo[3]pyridine[3]pyrrole **L86** and cyclo[2]pyridine[4]pyrrole **L87**.

4.1.4 Cyclo[n]thiophenes

In 2000, Bäuerle and coworkers reported the synthesis of very large thiophene based macrocycles.[15] Reaction of cyclooligothiophenediacetylene **L88** (obtained from thiophenediynes under modified Eglington-Glaser conditions), with $Na_2S•9H_2O$, gave rise to cyclo[12]thiophene **L89** in 23% yield (Scheme 4.1**)**. Analogous reactions led to the isolation

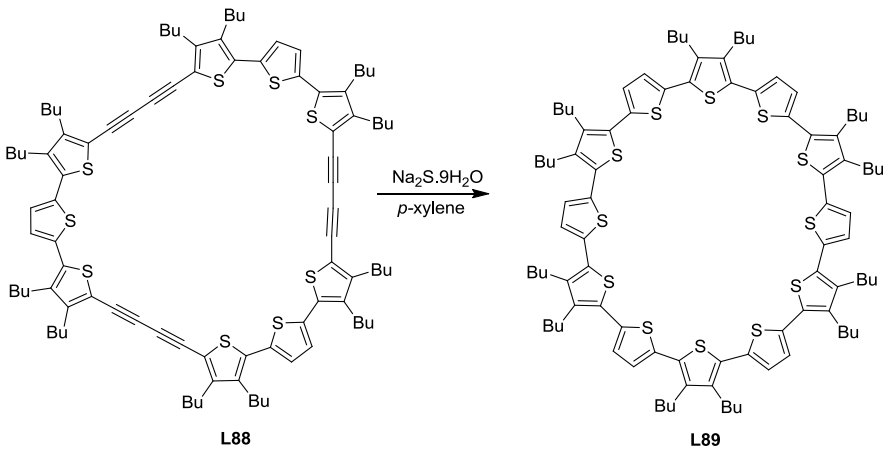

L88 **L89**

Scheme 4.1 Synthesis of cyclo[12]thiophene.

of cyclo[16]thiophene and cyclo[18]thiophene in yields of 7 and 27%, respectively. Interestingly, despite of their (4n) π-electron conjugation pathways, these molecules did not show ring current effects. Very recently Christophe Bucher and coworkers in collaboration with Sessler group reported electrochemical oxidation of a terpyrrole, 2,5-bis(3,4-diethyl-2-pyrrolyl)thiophene leading to the synthesis of thiophene containing cyclo[9]pyrrole **L90**.[16] This macrocycle possess 34-π electron and thus shows aromatic nature as evident from ^{1}H

NMR as well as UV-Vis spectrum. Unlike the case of **L81**, UV-Vis spectrum of bis-TFA salts of **L90** reveals a Soret-like signal centered at 549 nm (ε = 91500 $M^{-1}cm^{-1}$), is stronger than the L-band centered at 1201 nm (ε = 75500 $M^{-1}cm^{-1}$). However, synthesis of all aza cyclo[9]pyrrole is not reported so far.

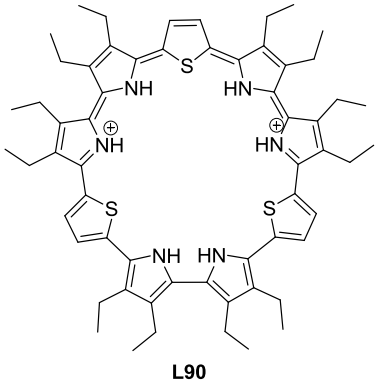

L90

Figure 4.9 Thiophene containing cyclo[9]pyrrole.

4.1.5 π-Extended cyclo[8]pyrroles

Recently Okujima et al. reported synthesis of cyclo[8]isoindoles, the first example of π-extended cyclo[8]pyrrole **L92**, based on the retro-Diels–Alder reaction of a BCOD-fused cyclo[8]pyrrole **L91**.[17a] BCOD-fused cyclo[8]pyrrole in turn was synthesized from BCOD-fused bipyrrole. These authors have explored different oxidizing agent such as CAN, $NaNO_2$, and $Ce(SO_4)_2$ in addition to $FeCl_3$, used for synthesis of **L81**. X-ray structure of **L91** has a near-planar structure like β-alkyl substituted cyclo[8]pyrroles, however, there is a marked

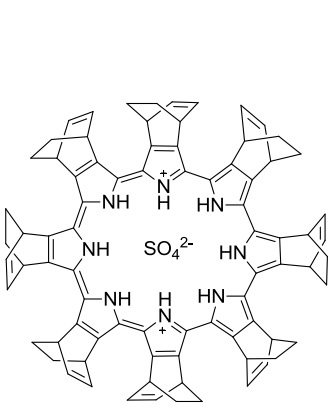

L91

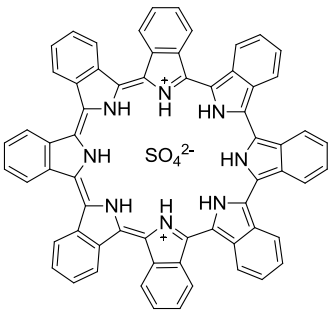

L92

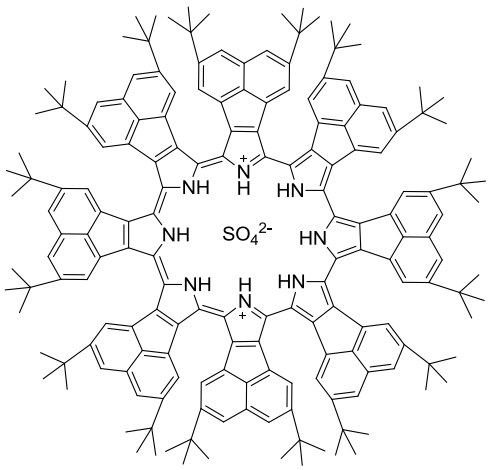

L93

Figure 4.10 Structure of BCOD fused cyclo[8]pyrrole **L91**, cyclo[8]isoindole **L92** and cyclo[8]acenaphthopyrrole **L93**.

saddling of the π-system of **L92**. Unlike β-alkyl substituted cyclo[8]pyrroles, absorption spectrum of **L92** shows a markedly red shifted and intensified Soret band (627 nm) along with a less intense L-band centered at 1078 nm. In continuation to their effort directed towards synthesis of annulated porphyrinoids, very recently Okujima et al. reported acenaphthylene-fused cyclo[8]pyrrole, namely cyclo[8]acenaphthopyrrole **L93** that exhibit significantly red shifted absorption spectrum.[17b] Interestingly, unlike cyclo[8]isoindole **L92**, Soret band of **L93** (at 512 nm) is less intense compared to the near-IR L-band (at 1482 nm), thereby displaying a trend similar of that observed in case of cyclo[8]pyrroles.[1]

4.2 Research goal

Recently, it was observed that fusion of aromatic systems onto a bipyrrolic unit, imparts a dramatic effect on the spectroscopic properties of the benzodipyrrole derived sapphyrin[18] and very recently, in dinaphthoporphycenes, we observed the fusion of naphthalene moieties onto a porphycene core led to a remarkable effect on both the linear and the nonlinear absorption of the porphycene system, along with interesting coordination chemistry.[19] Inspired by the interesting photophysical properties of cyclo[8]pyrroles, we were interested to explore the effect of fusion of alternate bipyrroles, using fused bipyrrole as a precursor namely alkylated naphthobipyrrole, on the photophysical and structural attributes of the resultant cyclo[8]pyrrole. The cyclo[8]pyrrole thus obtained possessing rigid and extended π-conjugation framework, would be expected to display interesting photophysical properties. Moreover, the presence of the alkyl groups at the remaining β-pyrrole positions will impart desired solubility to the resultant macrocycles in organic media and thereby may enhance their utility for various application oriented studies.

4.3 Results and discussion

4.3.1 Synthesis of cyclo[4]naphthobipyrroles

The precursors, β-dialkylnaphthobipyrroles, reported recently by us and Sessler's group independently, were synthesized following our strategy as described in chapter 2.[19b] Subjecting these bipyrroles to Sessler's method,[1a] i.e. addition of bipyrrole solution in dichloromethane via syringe pump to a biphasic mixture of dichloromethane and ferric chloride in 1M sulfuric acid (over 9 h) and subsequent stirring of the resultant reaction mixture for 5 h led to very little formation of the desired cyclo[4]naphthobipyrroles.[20] Therefore, we tried to modulate the conditions to optimize the formation of the desired products (Table 4.1). For example, by simple extension of the reaction time from 5 h to 15 h,

in case of **TS20b** resulted in substantial increase in the yield of **TS29b** (11 %, entry 1) and further increase of reaction time did not have any bearing on the overall yield of the reaction.

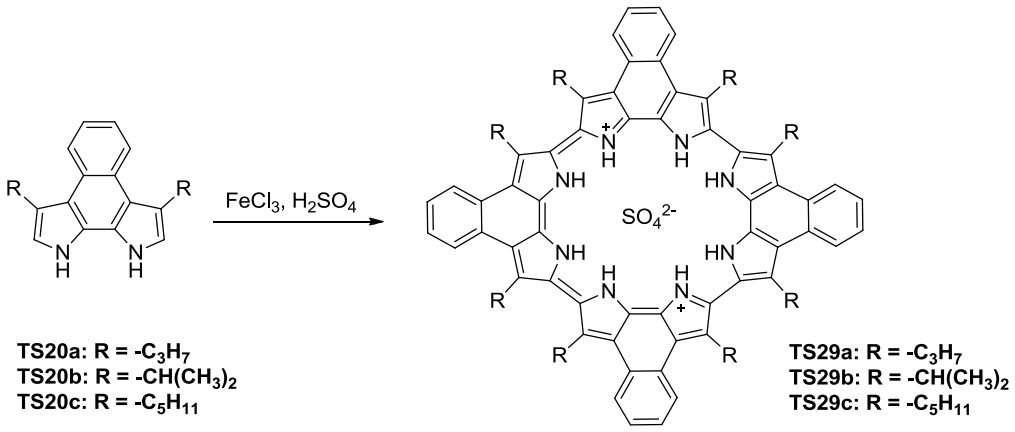

Scheme 4.2 Oxidative coupling of naphthobipyrroles.

Table 4.1 Synthesis of cyclo[4]naphthobipyrroles **TS29a-c**.

Entry	Substrate	Oxidant	Equiv.	Acid	Yield (%)
1	**TS20b**	$FeCl_3$	10.0	H_2SO_4	11
2	**TS20b**	$FeCl_3$	16.7	H_2SO_4	13
3	**TS20b**	$FeCl_3$	6.6	H_2SO_4	6
4	**TS20b**	$Ce(SO_4)_2.H_2O$[a]	1.8	H_2SO_4	0
5	**TS20a**	$FeCl_3$	16.7	H_2SO_4	1
6	**TS20a**	$FeCl_3$	6.6	H_2SO_4	11
7	**TS20a**	$FeCl_3$	2.0	H_2SO_4	0.6
8	**TS20a**	$Ce(SO_4)_2.H_2O$[a]	1.8	H_2SO_4	3
9	**TS20c**	$FeCl_3$	16.7	H_2SO_4	1
10	**TS20c**	$FeCl_3$	6.6	H_2SO_4	8

[a]: For procedure see reference 17a.

Under this condition, increasing the oxidizing agent $FeCl_3$ content (16.7 equiv.) led to a marginal increase in the yield (13 %, entry 2), whereas, decreasing the $FeCl_3$ content (6.6 equiv.) led to a drop in the yield (6 %). However, when we employed the optimal conditions for **TS29b** towards the synthesis of **TS29a**, the yield reduced drastically (1 %, entry 5). Reduced quantity of $FeCl_3$ (6.6 equiv.) on the other hand resulted in an increase in the yield (11 %, entry 6). But further reducing the content of $FeCl_3$ (2.0 equiv.) only resulted in minimal formation of **TS29a** (0.6 %, entry 7). The opposite behaviour of **TS20a** and **TS20b** towards varying quantities of $FeCl_3$ may be attributed to the lesser nonbonding interaction between the adjacent isopropyl groups of the two neighboring naphthobipyrrole units in

TS20b (one hydrogen on the first carbon atom of the alkyl chain) than that between the two adjacent *n*-propyl groups in **TS20a** (two Hs on the first carbon atom). The lesser nonbonding interaction may help in cyclization of **TS20b** to **TS29b** than polymerization under relatively strong oxidizing condition, whereas, in case of **TS20a**, greater nonbonding interaction promotes the polymerization process compared to cyclization to form **TS29a**. Therefore, cyclization becomes more facile under relatively milder oxidizing condition. The above trend is again confirmed in case of the *n*-pentyl substituted naphthobipyrrole **TS20c** (entries 9 and 10).

During the preparation of our manuscript, the first example of π-extended cyclo[8]pyrrole, cyclo[8]isoindole **L92** was reported by Okujima et al. via oxidative coupling of bicyclo[2.2.2]octadiene (BCOD)-fused 2,2´-bipyrrole, followed by the retro-Diels–Alder reaction of the resultant cyclo[8]BCODpyrrole **L91**.[17a] Therefore, we explored their optimal reaction conditions for our synthetic purpose. Use of optimized condition of Okujima et al. i.e. cerium sulphate in presence of 6M sulfuric acid and sodium sulfate and tetra(*n*-butyl)ammonium bisulfate as additives could led to no formation of **TS29b** (even by extending the reaction time from 2 days to 5 days, entry 4), whereas **TS29a** could be obtained in much lesser yield (3 % after 2 days and did not increase further even after 5 days, entry 8). All the macrocycles were characterized using ^{1}H and ^{13}C NMR spectroscopy, MALDI-TOF mass, UV-Vis-NIR absorption study and elemental analysis.[20a]

4.3.2. ^{1}H NMR analysis of cyclo[4]naphthobipyrroles

^{1}H NMR spectra lend further credence to the above assumption regarding the effect on the non-bonding interaction in these cyclo[4]naphthobipyrroles **TS29a-c**. For example, the spectrum of **TS29b** displays a multiplet at 5.66 ppm (-CH) and two sets of clearly resolved doublets for the methyl signals (1.68 and 2.86 ppm), whereas, in case of **TS29a** the methylene protons adjacent to the macrocycle appear as a broad singlet (4.95 ppm) and the neighboring methylene protons appear as two sets of broad singlets (2.35 and 2.54 ppm); in **TS29c** the methylene signals adjacent to the macrocycle itself appear as a broad doublet(4.88–5.00 ppm) along with two more broad singlets (2.17 and 2.53 ppm) for the neighbouring methylene protons (Figure 4.11). Variable-temperature ^{1}H NMR measurements in toluene-d_8 for **TS29b** at 100 °C display little change in the resonances of the methyl signals of the isopropyl substituents, except broadening above 80 °C (Figure 4.12). However, in case of **TS29c**, at high temperature (100 °C) a more symmetric structure could be observed (Figure 4.13). The above pattern indicates that in **TS29c**, at high temperature, both the excha-

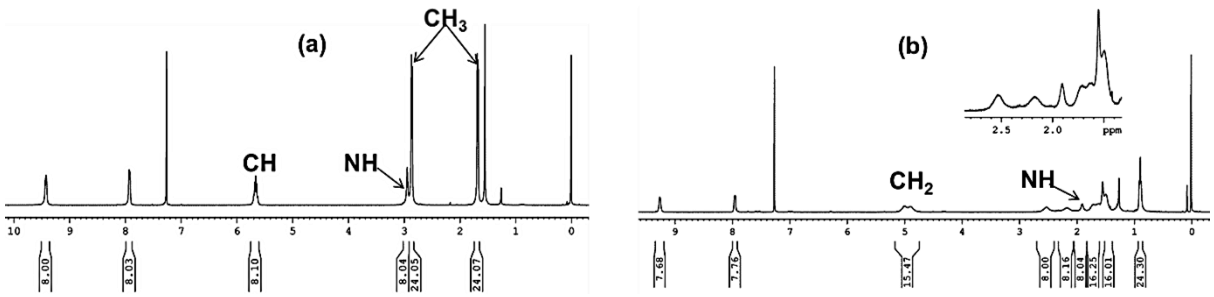

Figure 4.11 ^{1}H NMR spectra of : (a) **TS29b** and (b) **TS29c** in $CDCl_3$.

nge of methylene protons and the anion exchange between both sides of the macrocycle is fast and in case of **TS29b** this phenomenon is still slow or non-existent. Although not a

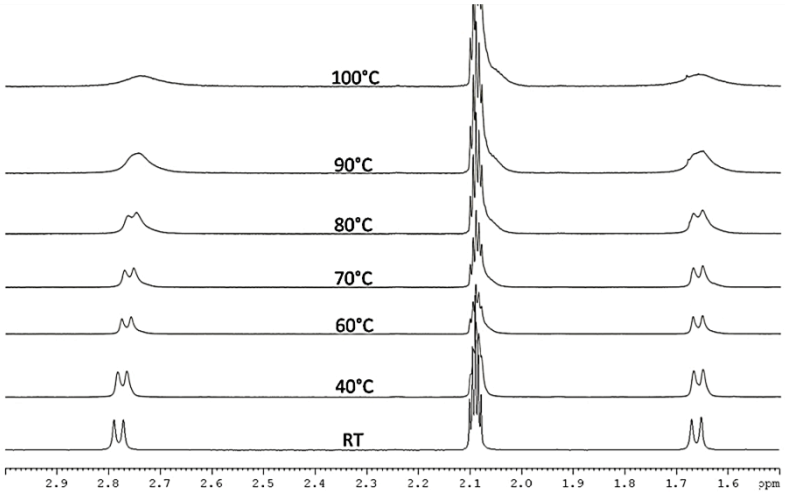

Figure 4.12 Selected region of variable-temperature ^{1}H NMR spectra of **TS29b** in toluene-d_8.

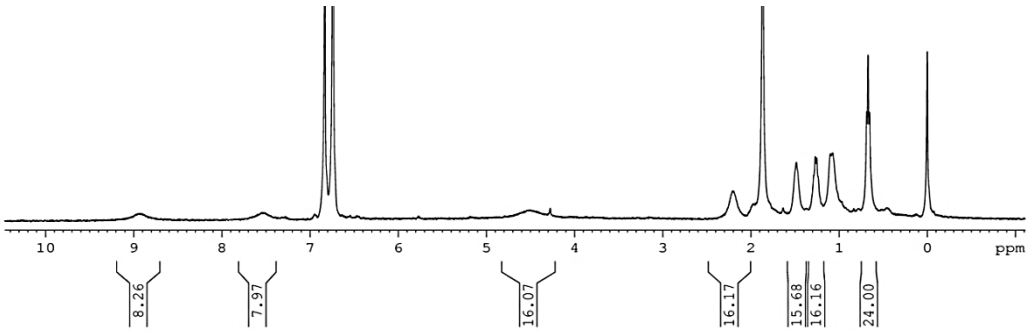

Figure 4.13 ^{1}H NMR spectrum of **TS29c** in toluene-d_8 at 100 °C.

conclusive evidence, it is worth noting from the above facts that the anion exchange between the two sides of cyclo[4]naphthobipyrroles is aided by the faster exchange between the protons of the substituent alkyl chains with nonbonding interactions and thereby causing a diastereotopic effect. Further, we can also conclude that in the case of **TS29b**, this slow or

lack of anion exchange results from the hindered exchange of the methyl groups of the isopropyl substituents. However, more detailed studies are needed to confirm the above hypothesis. This type of molecular asymmetry owing to rigid anion binding is not observed in the case of cyclo[8]pyrroles reported so far. The inner imino protons however appear as a singlet in all the three new cyclo[8]pyrroles at 1.96, 2.95 and 1.90 ppm for **TS29a, TS29b** and **TS29c** respectively, which is quite down field shifted compared to **L81c** (-0.84 ppm),[1a] indicating a greater distortion of the macrocycles from planarity in case of **TS29**.

4.3.3 Solid state structural analysis of cyclo[4]naphthobipyrrole

The solid state structure of **TS29b** could be unequivocally elucidated via single crystal diffraction analysis of the crystal obtained from the slow evaporation of a mixture of chloroform and methanol solution. As expected, **TS29b** was obtained as its dihydrogen sulfate salt (Figure 4.14). The crystal structure is similar to those of **L81b** and **L91**,[1a,17a] containing a monoclinic cell and *P21/c* space group with Z = 4. However, unlike the so far reported cyclo[8]pyrroles where alternate pyrrole units tilt above and below the plane formed

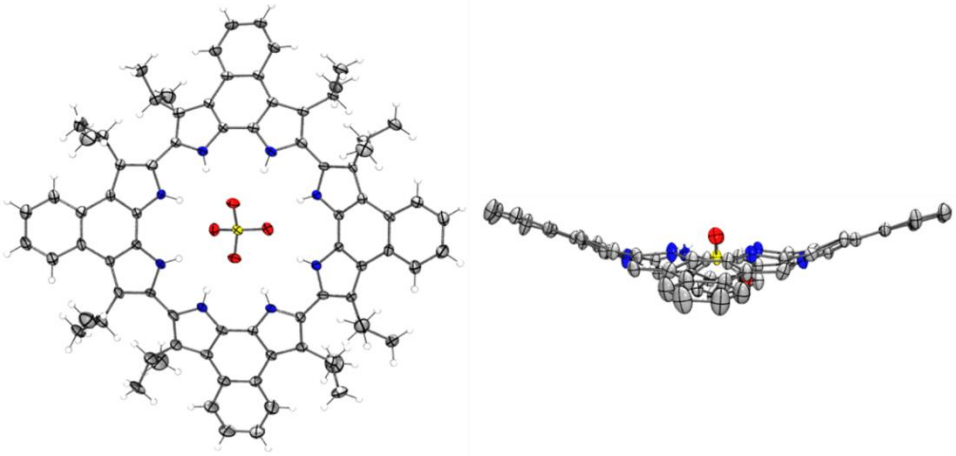

Figure 4.14 ORTEP of **TS29b**. The thermal ellipsoids are scaled to 35% probability level (Solvent chloroform molecule removed for clarity). Left: front view; right: side view (H atoms and alkyl side chains were omitted for clarity).

by the 16 α-carbon atoms, in this case owing to the fusion of the naphthalene moieties onto the periphery of the cyclo[8]pyrrole macrocycle, alternate bipyrrolic entities tilt above and below the above said mean plane, with large dihedral angles between the adjacent naphthobipyrrole units (44.60-47.12°). In comparison, the dihedral angles between adjacent pyrrole units in **L81b** are found to be lesser (31.17-42.68°). Further, the pyrrole nitrogens in **TS29b** are relatively more distorted from the above mentioned mean plane ranging from 0.06

to 0.25 Å compared to **L81b** (0.06 to 0.185 Å).[1a] The greater distortion observed in case of **TS29b** could be explained from the fact that there are only four bonds to accommodate the steric strain of the cyclo[8]pyrrole macrocycle, owing to the imposed structural rigidification, compared to **L81b** and **L91**, where it is distributed over eight bonds. The sulfate ion at the core is bound through eight hydrogen bonds to the cyclo[4]naphthobipyrrole moiety, where its each oxygen atom is H-bonded to the two pyrrolic NHs of one naphthobipyrrole unit with N…O distance (D Å) ranging from 2.775 to 2.853 Å (2.751-3.327 Å, for compound **L81b**; 2.774-2.996 Å and 2.820-2.917 Å for compound **L91** and **L92** respectively). This indicates the sulphate ion is more symmetrically placed in the core in case of **TS29b**.

4.3.4 Optical studies of cyclo[4]naphthobipyrroles

The UV-Vis-NIR absorption spectra of **TS29a-c** are shown in figure 4.15. Fusion of four naphthalene moieties onto the cyclo[8]pyrrole periphery led to marginal red shift (3 – 11 nm)

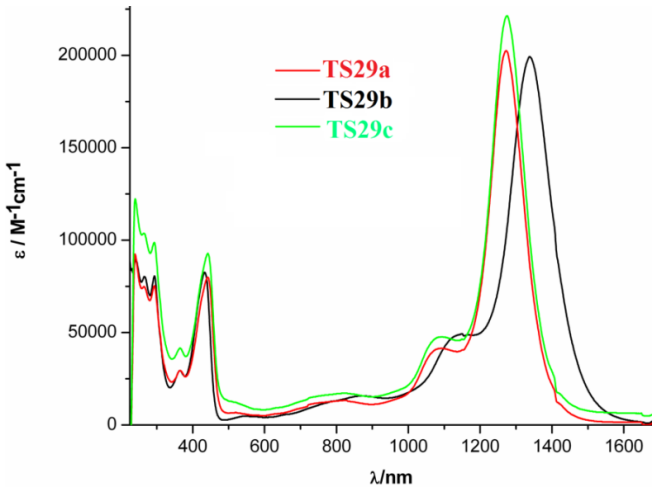

Figure 4.15 UV-Vis-NIR absorption spectra of cyclo[4]naphthobipyrroles **TS29a-c** in chloroform.

of the Soret type B-bands compared to **L81b**,[1a] however very large red shifted near infrared (NIR) L-bands were observed (161 – 228 nm), with **TS29b** displaying the most intense band at 1339 nm. Further, the relative intensity ratio of the L-band to B-band[1b] increased quite significantly (2.384 – 2.533) compared to *β*-alkylated cyclo[8]pyrrole **L81b** (1.657), and the BCOD fused analogue **L91** (1.514). We found the L-bands are very sensitive to the nature of the substituents than the B-bands. For example, even changing the substituents from branched to normal alkyl group resulted in a large blue shift in the absorption of the L band (**TS23b** – 1339 vs. **TS23a** – 1273 and **TS23c** – 1276 nm), whereas the B-band undergoes a relatively

small red shift (**TS23b** – 434 vs. **TS23a** and **TS23c** – 442 nm). This attribute is again reflected on the higher energy bands associated with both the L (**TS23b** – 1151, 884; **TS23a** – 1095, 829 and **TS23c** – 1097, 830 nm) and B bands (**TS23a-c**: 367-365nm). Further, the absorption bands in the UV-region remain unchanged and are ascribed to the naphthalene moieties, which indicates that while the naphthalene moiety remains largely unaffected, however its fusion imposes great structural and electronic effects on the resultant cyclo[8]pyrrole macrocycles. It is of great significance to note that while fusion of aromatic rings to the *β*-pyrrole units individually (*β*-pyrrole fusion), has a slight blue shift in the absorption of the lowest energy band and sometimes reversal of intensity of the B and L bands (conversion of **L91** to **L92** led to significant decrease in the intensity of L band), that onto the bipyrrolic units (*β*-bipyrrole fusion) led to very large red shift in the absorption of the L-band while retaining the typical pattern of cyclo[8]pyrroles (a very strong L-band).

4.3.5 Solvent dependent absorption properties of cyclo[4]naphthobipyrroles

Ground state absorption spectra of cyclo[4]naphthobipyrroles changes drastically upon going from non-polar to highly polar solvent. Specifically the characteristic intense band of the cyclo[8]pyrrole observed in the NIR region either disappear or appear as a very weak, broad band (Figure 4.16) depending upon concentration and molecule under study. For instance, absorption spectra of *i*-propyl derivative **TS29b** measured in DMSO (2×10^{-6} M) reveals disa-

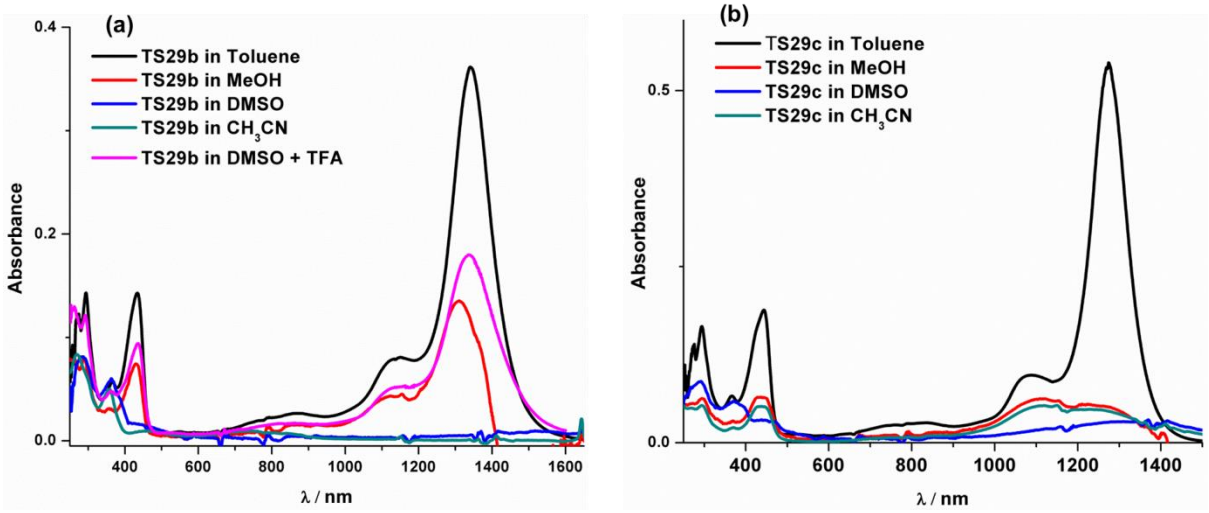

Figure 4.16 UV-Vis-NIR absorption spectra of cyclo[4]naphthobipyrrole (a) **TS29b** and (b) **TS29c**, in different solvents. To ensure solubility in MeOH, acetonitrile and DMSO, 2% dichloromethane was used. (Concentration of all solutions measured for **TS29b** and **TS29c** are 2×10^{-6} M and 1.8×10^{-6} M respectively).

ppearance of the strong absorption band in the NIR region, whereas solution of **TS29b** in toluene having same molar concentration exhibits well defined typical spectral features of cyclo[8]pyrroles. A closer inspection (Figure 4.16a) reveals that two weak bands in the higher energy region, namely around 387 and 282 nm are common in both polar and nonpolar solvents. Interestingly, addition of acid to the solution in polar solvent, for instance DMSO results in the recovery of the spectrum that was observed in nonpolar solvents such as toluene (Figure 4.16a). Similar spectral features were also observed for **TS29c** (Figure 4.16b). These observations suggest strong change in geometry of the macrocycle, such as deviation from planarity, which is probably possible only upon decomplexation of the anion. To get further insight about the spectral properties of cyclo[4]naphthobipyrrole in absence of sulfate ion, free-base form was generated by washing a solution of cyclo[4]naphthobipyrrole in toluene with aqueous NaOH. Upon conversion of **TS29b** to its free-base, intensity of the NIR band at 1339 nm drastically reduces and appearance of a broad peak, whose absorption maxima shifted to 1522 nm (Figure 4.17a). Similar peak broadening and reduced intensity of the NIR band was also observed in case of *n*-pentyl derivative **TS29c** (Figure 4.17b). However, unlike **TS29b**, absorption maxima of free-base **TS29c** in the NIR region do not undergo much shift.

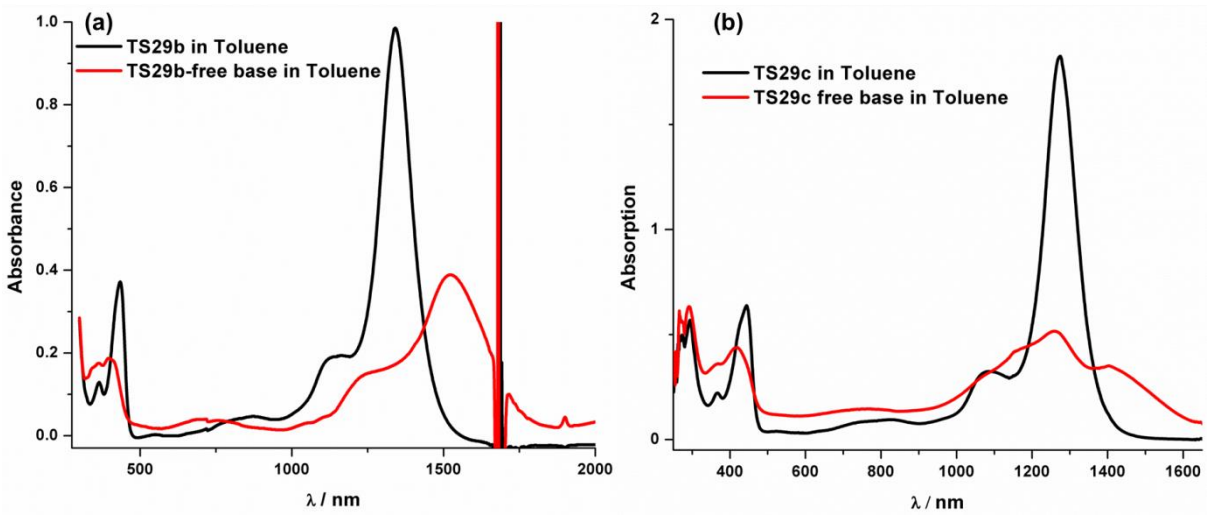

Figure 4.17 Comparison of UV-Vis-NIR absorption spectra of cyclo[4]naphthobipyrrole and its free-base form in toluene, (a) **TS29b** (concentration ~ 5.4×10^{-6} M) and (b) **TS29c** (concentration ~ 6.1×10^{-6} M) .

Above studies reveal that absorption spectra of cyclo[4]naphthobipyrroles largely depends on the geometry of the macrocycle. On the other hand, geometry of the macrocycle is governed by the coordination of the anion at the core of the macrocycle. In highly polar solvent such as

DMSO, the macrocycle undergo conformational changes, leading to a featureless absorption profile owing to distorted geometry, possibly as a result of decomplexation of anion from the cavity and the resultant HSO_4^- (as SO_4^{2-} does not exist under milder condition) could be stabilized by the solvent molecules. Therefore, it can be concluded that the spectra observed in $CHCl_3$ and toluene correspond to the species containing the sulfate ion in the cavity.

During our attempt to understand if the sulfate ion exchanges or not in presence of other acids, interesting spectral signature was obtained. Upon addition of TFA to a solution of **TS29b**, intensity of L band slowly decreases with gradual appearance of several new bands at 985, 853, 735, 620, 542 and 468 nm (Figure 4.18a), whereas the decrease in the intensity of B band is relatively less pronounced. The new species generated upon addition of TFA is assigned as the one electron oxidized form of **TS29b** i.e. **TS29b**$^{\bullet+}$. Similar spectral changes were also observed by Sessler and coworkers, upon one-electron electrochemical oxidation of hexadecaethylcyclo[8]pyrrole.[1e] Further, this oxidized form **TS29b**$^{\bullet+}$ can be reduced to get back **TS29b** by addition of DBU (Figure 4.18b). These observations indicate existence of a

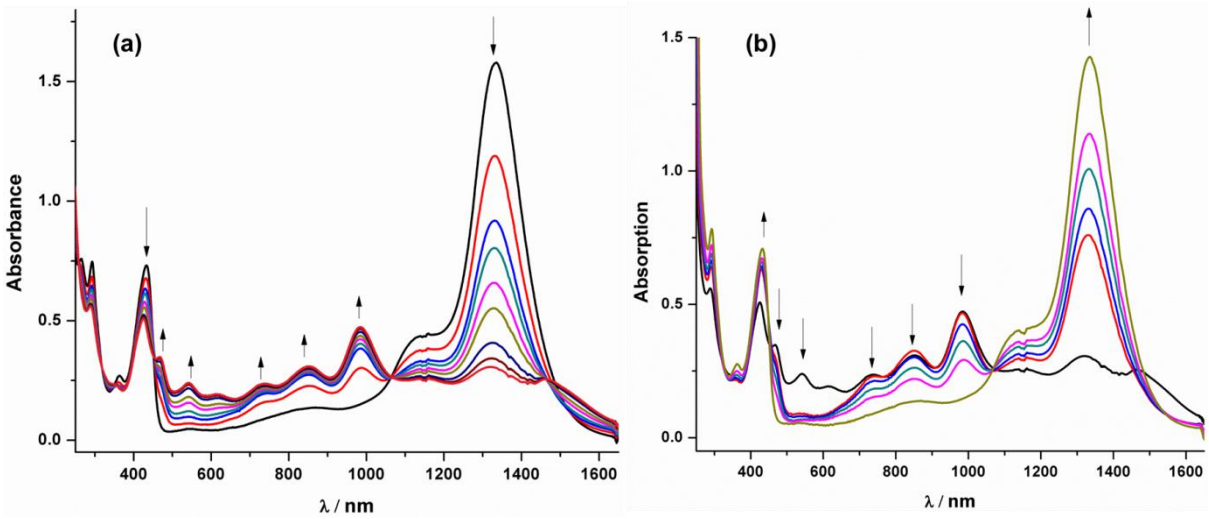

Figure 4.18 Spectrophotometric titration of **TS29b** (a) with TFA and then (b) with DBU (same solution titrated with TFA) in dichloromethane. Direction of arrows indicates increase and decrease in peak intensity upon addition of TFA and DBU.

proton coupled electron transfer (PCET) reduction of dioxygen in presence of TFA by **TS29b** thereby producing **TS29b**$^{\bullet+}$ and H_2O_2. The reverse process may occur in the presence of DBU, which can deprotonate H_2O_2 to reduce **TS29b**$^{\bullet+}$ back to **TS29b**, whereby deprotonated H_2O_2 is oxidized to O_2. Very recently Yamada and coworkers reported η^5-cyclopentadienyliron(II)–[14]triphyrin(2.1.1) that undergoes similar one electron oxidation

upon titrating with TFA producing Fe(III)-complex, which can be converted to its original state by treating with DBU.[21] Proton-coupled electron transfer plays pivotal role in biological electron-transfer systems such as photosynthesis and respiration.[22] A number of synthetic models have been reported by using metal complexes of porphyrins and its analogues for reduction of dioxygen, which is not only of immense biological interest, but also of great technological importance as fundamentals of fuel cells.[23]

4.3.6 Electron paramagnetic study of cyclo[4]naphthobipyrroles

To test the radical nature of **TS29b**$^{\bullet+}$ generated in presence of TFA, we checked electron paramagnetic resonance (EPR) spectrum of **TS29b** in presence and absence of TFA. According to our expectation EPR spectrum of **TS29b** in presence of TFA revealed a broad signal with g value of 2.0032, typical of a mono radical (S = 1/2) character (Figure 4.19a). To our surprise, however the parent compound **TS29b** also appeared to be EPR active (Figure 4.19a). **TS29b** possessing 30 π-electrons is expected to be EPR-inactive provided all electrons are paired. To get further information regarding this, EPR spectra of **TS29b** and **TS29c** and their corresponding free-base forms were recorded both in solid and solution state. Surprisingly in all cases we observed EPR signal. Although not a confirmation, however these findings suggest the possible existence of a low lying triplet state close to the highest occupied molecular orbitals (HOMO) in cyclo[4]naphthobipyrroles, which make them stable biradicals at room temperature.[24] Detailed computation study in this direction is still underway at present.

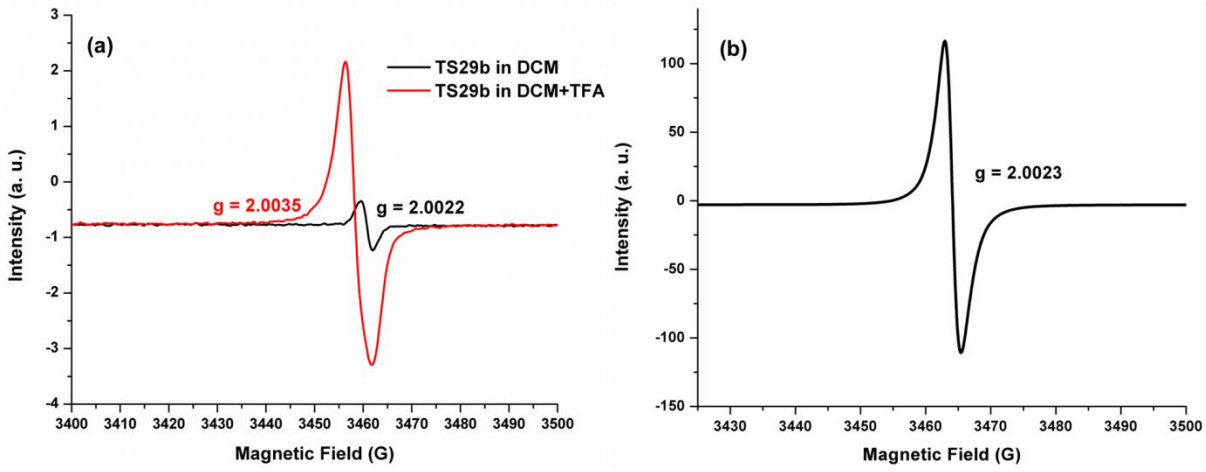

Figure 4.19 (a) EPR spectra of dichloromethane solution of **TS29b** in presence and absence of TFA measured in glass capillary and (b) solid state EPR spectrum of free-base **TS29b** measured at room temperature.

4.3.7 Nonlinear optical studies of cyclo[4]naphthobipyrroles

In recent time, there has been continuous effort for synthesis of new nonlinear optical (NLO) materials with large two photon absorption (2PA) cross-sections ($\sigma^{(2)}$) owing to their various potential applications.[25] Although porphyrins with 18 π-electrons are quite promising, simple porphyrin monomer often exhibit low 2PA value (<100 GM). In this regard, expanded porphyrins possessing greater number of π-electrons proved to be good candidates as new NLO materials with large $\sigma^{(2)}$ values.[26] Therefore, in order to assess the effect of this naphthalene fusion (by both rigidification and π-extension), we chose to explore the NLO response of cyclo[4]naphthobipyrroles.

Nonlinear absorptions (NLA) of **TS29a-c** were measured by the open aperture Z-scan[27] method at wavelengths of 600, 640, 680 and 800 nm. Figure 4.20 shows typical open aperture Z-scan data of **TS29a-c** obtained at the above mentioned wavelengths. All the data exhibited a valley near Z = 0. The data was fitted by conventional Z-scan analysis in which the propagation equation was solved. Summary of NLO coefficients obtained from the fits are provided in Table 4.2.[28]

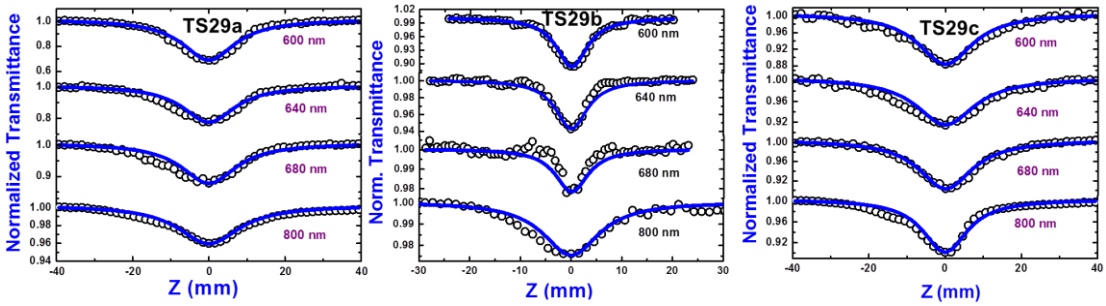

Figure 4.20 Open aperture Z-scan data of **TS29a-c** at different wavelengths. Open circles are the experimental data while the solid lines are theoretical fits.

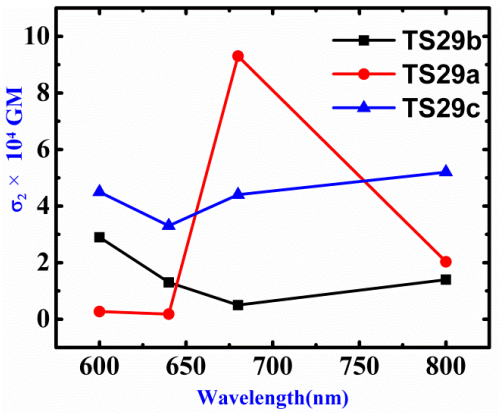

Figure 4.21 Spectral dependence of σ_2 in **TS29a-c**. The solid line is only a guide to the eye.

Table 4.2 Summary of nonlinear optical coefficients and 2PA cross sections of **TS29a-c**. The values in parenthesis are peak intensities in GW/cm^2.

	TS29a		TS29b		TS29c	
λ (nm)	β (cm/W) $\times 10^{-11}$	σ_2 ($\times 10^4$ GM)	β (cm/W) $\times 10^{-11}$	σ_2 ($\times 10^4$ GM)	β (cm/W) $\times 10^{-11}$	σ_2 ($\times 10^4$ GM)
600	0.15 (133)	0.40	3.20 (122)	2.90	3.35 (133)	4.50
640	0.11 (117)	0.22	1.50 (129)	1.30	2.65 (117)	3.30
680	5.80 (103)	9.70	0.62 (114)	0.50	3.65 (103)	4.40
800	2.15 (62)	5.00	1.50 (58)	1.50	5.60 (62)	5.20

The values of σ_2 evaluated for **TS29a-c** were in the range of 0.40-9.70 × 10^{-4} GM. The 2PA coefficients are plotted against wavelength and the data is presented in Figure 4.21. The two photon resonance corresponding to 600 nm excitation is ~33,333 cm^{-1}, whereas for an 800 nm photon it is 25,000 cm^{-1}. Except for the molecule **TS29a**, variation in β with wavelength was minimal. **TS29a** exhibited strongest β at 680 nm. However, **TS29c** exhibited highest β at 600, 640 and 800 nm compared to **TS29b** and **TS29a** probably owing to increased planarity of *n*-alkyl substituted cyclo[4]naphthobipyrrole than the *i*-propyl substituted cyclo[4]naphthobipyrrole.

4.3.8 Excited state life time study of cyclo[4]naphthobipyrroles

Excited state dynamics of cyclo[4]naphthobipyrroles **TS29a-c** were studied using fs pump-probe technique.[28] Figure 4.22 shows the degenerate pump-probe data of **TS29a-c** obtained at

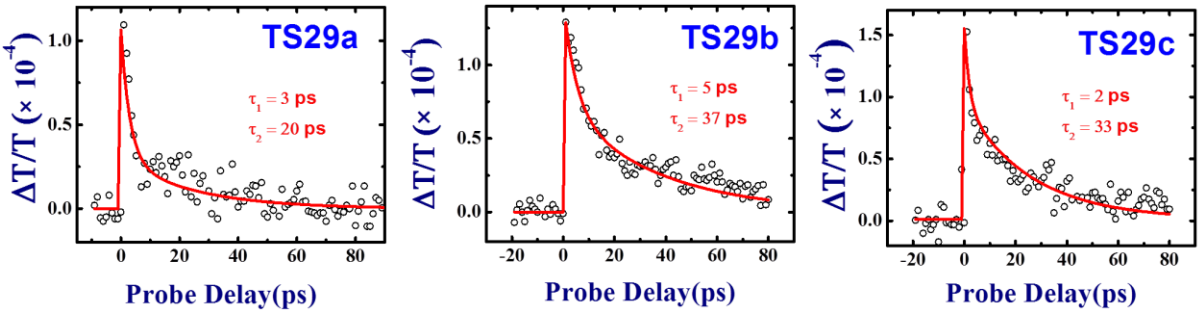

Figure 4.22 Femtosecond degenerate pump probe data of **TS29a-c** recorded at 600 nm indicating two lifetimes. Open circles are the experimental data, while the solid (red) lines are double exponential fits.

600 nm using ~70 fs pulses with typical pump energies of ~10 μJ. The data was fitted for a double exponential[29] and two lifetimes (τ_1 and τ_2) were retrieved from each of the fits. The

Table 4.3 Excited state lifetimes of cyclo[4]naphthobipyrroles **TS29a-c** obtained using fs pump-probe studies.

Samples	τ_1 in ps 600 nm (fs p-p)	τ_2 in ps 600 nm (fs p-p)
TS29a	3	20
TS29b	5	37
TS29c	2	33

values of τ_1 and τ_2 were 3 and 20 ps for **TS29a**; 5 and 37 ps for **TS29b**; and 2 and 33 ps for **TS29c**, respectively. Figure 4.23 shows a simplified energy level diagram indicating the excitations and decay profiles for these macrocycles. Excitation with focused 600 nm photons, enables two photo absorption (2PA) resulting in populating the S_2 states. The de-excitation mechanism broadly could be consisting of two processes. At first the molecules from the lowest vibrational state of S_2 manifold relax to highest vibrational states of S_1 manifold (internal conversion, IC) followed by intra-molecular vibrational relaxation (IVR) from highest states of S_1 to lowest states of S_1. These are typically fast processes (<1 ps for IC, ~1-3 ps for IVR) and therefore, the shorter lifetimes observed in pump-probe data (3-5 ps) could be attributed to this relaxation. Secondly, from the lowest vibrational states of S_1 manifold the molecules relax to ground state (S_0) via non-radiative mechanism by releasing the energy to solvent (also called as vibrational cooling). This process typically occurs in few tens of ps in such molecules. The longer lifetime can be associated with such a process in

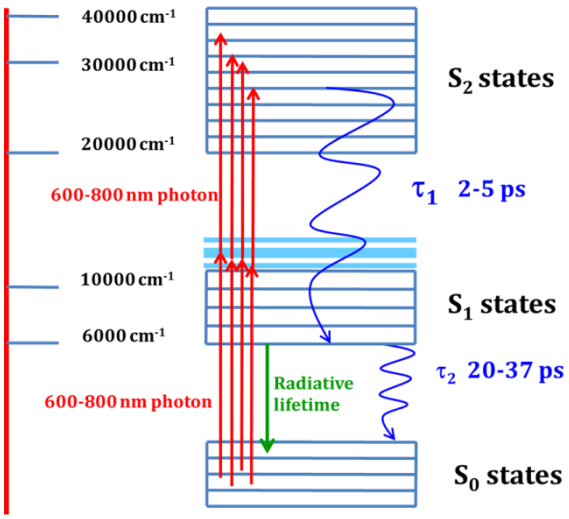

Figure 4.23 Schematic energy level diagram of **TS29a-c** explaining the double exponential behavior (τ_1 and τ_2) observed in pump-probe data.

TS29a-c. No aggregation behaviour was observed under the concentration (10^{-4}-10^{-5} M) used for the measurement (confirmed from absorption spectral studies), therefore we can neglect the inter-molecular contributions to the lifetimes observed. Our initial EPR studies discussed above suggest that the triplet ground state could be much closer to the singlet ground state and there could be a possible contribution of this to the longer decay times observed. However, further detailed studies (such as non-degenerate pump-probe and transient absorption) are essential to exactly identify the complicated decay dynamics in these molecules.

4.4 Conclusion

In conclusion, we have successfully synthesized cyclo[4]naphthobipyrroles. We observed that the cyclo[8]pyrrole moiety is very sensitive to the nature of the substituents at its periphery owing to the involvement of large number of nonbonding interactions. This is reflected not only in their photophysical properties but also in their synthesis from the corresponding bipyrroles. For example, Sessler and coworkers observed drastic reduction in yield in case of **L81d**, where one β-pyrrole position of each pyrrole units remain unsubstituted, whereas in the present case the type of alkyl substituents (branched vs. normal) decides their reactivity towards oxidizing agent. These macrocycles display large red shifted NIR absorption owing to the enforced structural rigidity and extended π-conjugation compared to other cyclo[8]pyrroles, with **TS29b** showing the most intense band at 1339 nm.

Absorption spectra of cyclo[4]naphthobipyrroles in polar solvents, such as DMSO undergo a drastic change compared to their corresponding spectra in $CHCl_3$ or toluene. In particular, intensity of NIR bands reduces dramatically and appears as a very weak and broad band. This seems to be caused by two effects: (i) dissociation of the anion from the sulfate-stabilized complex, possibly stabilized by specific interaction with the solvent and (ii) concomitant changes in geometry. Noticeable decrement in intensity of the NIR band was also observed for free-base cyclo[4]naphthobipyrrole indicating the assumed geometrical change in absence of counter anion. Solvent sensitivity of the electronic spectra in combination with the absorption in the near IR range make cyclo[4]naphthobipyrroles promising objects for studying molecular recognition and ion transfer phenomenon.

Further, in presence of acid, cyclo[4]naphthobipyrrole undergoes one electron oxidation thereby producing radical cation as evident from EPR measurement. This radical cation can be reduced back to its original state by treating with DBU. Perhaps this oxidation of

cyclo[4]naphthobipyrrole in presence of acid is accompanied by reduction of dioxygen thereby producing H_2O_2. This type of proton-coupled electron transfer (PCET) is not only of biological interest but also of technological importance as fundamentals of fuel cells.

Another very interesting feature observed in case of cyclo[4]naphthobipyrrole is that both the free-base and sulfate salts are found to be EPR active in solution as well as in solid state. This in turn indicates possible existence of close lying triplet state to HOMO in cyclo[4]naphthobipyrrole, making it exist as a stable biradical. Detail theoretical and experimental investigation is underway at present to prove this hypothesis.

The NLO properties of cyclo[4]naphthobipyrroles, are explored using Z-scan method. Large two-photon absorption cross sections in the range of 0.2–5.2 × 10^4 GM were observed in the 600–800 nm spectral range from the data recorded with ~1.5 ps pulses. Excited state dynamics studied using fs pump-probe technique revealed the presence of two lifetimes. The shorter lifetime was assigned to the non-radiative relaxation from lowest S_n vibrational states to lowest S_1 vibrational states, while the longer lifetime was assigned to the internal conversion from lowest S_1 vibrational states to the ground state (S_0). These cyclo[4]naphthobipyrroles, in particular **TS29b** (owing to its good solubility) can be of great importance for practical application as NIR dyes and possess potential for various photonic applications, apart from their potential utility in light harvesting, dye-sensitized solar cells and bio imaging.

4.5 Experimental details

General procedure for oxidative coupling of naphthobipyrroles:

TS29b. A 1-L round bottom flask was charged with a stirring bar and dichloromethane (500 mL). A solution of $FeCl_3$ (2.7 g, 17 mmol) in aq. 1M H_2SO_4 (100 mL) was then added. The resulting biphasic mixture was stirred at around 300 rpm, while a solution of alkylated naphthobipyrrole (0.3 g, 1 mmol) in dichloromethane (60 mL) was added via a syringe pump over a period of 9 h with the needle submerged into the organic phase. After complete addition the reaction mixture was stirred for 15 h at room temperature. Organic layer was separated and dried over anhyd. sodium sulfate; solvent was evaporated to obtain the crude compound. The crude product was purified by column chromatography on silica gel using dichloromethane as the eluent. The greenish-yellow band was collected. The solid residue obtained after removal of the solvent was recrystallized from $CHCl_3$/methanol to yield **TS29b** as a dark green powder.

TS29a and **TS29c**. The amount of $FeCl_3$ used was 6.6 equiv. compared to naphthobipyrrole, whereas, the remaining procedure is same as described above for **TS29b**.

TS29a: Yield 11%, ^{1}H NMR (400 MHz, $CDCl_3$, δ in ppm): 1.23 (t, 24H, -CH_3 *n*-Pr), 1.96 (s, 8H, NH), 2.35 (brs, 8H, CH_2 *n*-Pr), 2.54 (brs, 8H, CH_2 *n*-Pr), 4.95 (brs, 16H, CH_2 *n*-Pr), 7.97 (brs, 8H, CH naph), 9.27 (brs, 8H, CH naph); ^{13}C NMR (100 MHz, $CDCl_3$, δ in ppm): 15.01, 24.66, 29.85, 125.21, 125.36, 126.13, 127.03, 127.41, 129.59, 131.88; MS (MALDI-TOF): *m*/*z* calcd for $C_{80}H_{81}N_8O_4S$ [M+H^+] 1249.610; found 1249.600; elemental analysis calcd (%) for $C_{80}H_{80}N_8O_4S$: C 76.89, H 6.45, N 8.97; found: C 76.93, H 6.51, N 8.85; UV/Vis ($CHCl_3$) λ_{max} [nm] (log ε): 265 (4.87), 294 (4.88), 366 (4.47), 442 (4.90), 829 (4.12), 1095 (4.62), 1273 (5.31).

TS29b: Yield 13%, ^{1}H NMR (400 MHz, $CDCl_3$, δ in ppm): 1.68 (d, J = 7.2 Hz, 24H, -CH_3 *i*-Pr), 2.86 (d, J = 7.2 Hz, 24H, -CH_3 *i*-Pr), 2.95 (s, 8H, NH), 5.66 (m, 8H, -CH *i*-Pr), 7.92 (m, 8H, CH naph), 9.42 (brs, 8H, CH naph); ^{13}C NMR (100 MHz, $CDCl_3$, δ in ppm): 21.81, 24.46, 29.84, 126.23, 126.56, 128.15, 130.39, 130.60, 131.46; MS (MALDI-TOF): *m*/*z* calcd for $C_{80}H_{80}N_8O_4S$ [M^+] 1248.524; found 1248.602; elemental analysis calcd (%) for $C_{80}H_{80}N_8O_4S$: C 76.89, H 6.45, N 8.97; found: C 76.91, H 6.49, N 8.85; UV/Vis ($CHCl_3$) λ_{max} [nm] (log ε): 266 (4.90), 294 (4.91), 367 (4.47), 434 (4.92), 884 (4.20), 1151 (4.69), 1339 (5.30).

TS29c: Yield 8%, ^{1}H NMR (400 MHz, $CDCl_3$, δ in ppm): 0.89 (t, 24H, -CH_3 *n*-pentyl), 1.49 (brs, 16H, CH_2 *n*-pentyl), 1.69 (brs, 16H, CH_2 *n*-pentyl), 1.90 (brs, 8H, NH), 2.17 (brs, 8H, CH_2 *n*-pentyl), 2.53 (brs, 8H, CH_2 *n*-pentyl), 4.88-5.00 (brd, 16H, CH_2 *n*-pentyl), 7.95 (brs, 8H, CH naph), 9.26 (brs, 8H, CH naph); ^{13}C NMR (100 MHz, $CDCl_3$, δ in ppm): 14.25, 22.72, 30.65, 31.09, 32.86, 125.10, 125.47, 125.93, 126.79, 127.27, 129.25, 131.71; MS (MALDI-TOF): *m*/*z* calcd for $C_{96}H_{112}N_8O_4S$ [M^+] 1473.858; found 1473.856; elemental analysis calcd (%) for $C_{96}H_{112}N_8O_4S$: C 78.22, H 7.66, N 7.60; found: C 78.32, H 7.59, N 7.51; UV/Vis ($CHCl_3$) λ_{max} [nm] (log ε): 265 (5.02), 293 (4.99), 365 (4.62), 442 (4.97), 830 (4.24), 1097 (4.68), 1276 (5.34).

4.6 Crystallographic details

Crystallographic data for **TS29b** was collected on Oxford Gemini A Ultra diffractometer with dual source. Pertinent crystallographic data collection and refinement parameter are shown in the following table:

Table 4.4 Crystallographic parameters of crystals of **TS29b.**

Crystal data	**TS29b**
Formula unit	$C_{80}H_{80}N_8.SO_4.CHCl_3$
Formula wt.	1368.95
Crystal system	Monoclinic
T [K]	298 (2)
a [Å]	9.318 (6)
b [Å]	25.547 (11)
c [Å]	39.251 (2)
α [°]	90
β [°]	93.058 (5)
γ [°]	90
volume [$Å^3$]	8965.5 (8)
Space group	P1 21/c1
Z´	1
Z	4
D_{calc} [$g.cm^{-3}$]	1.014
μ/mm^{-1}	0.171
Reflns collected	39214
Unique reflns	15230
Observed reflns	5862
R(int)	0.0861
R_1 [$I > 2\sigma(I)$],	0.0825
wR_2	0.2303
GOF	0.906

4.7 References

1. (a) Seidel, D.; Sessler, J. L.; Lynch, V. *Angew. Chem. Int. Ed.* **2002**, *41*, 1422. (b) Gorski, A.; Köhler, T.; Seidel, D.; Lee, J. T.; Orzanowska, G.; Sessler, J. L.; Waluk, J. *Chem. Eur. J.* **2005**, *11*, 4179. (c) Stępień, M.; Donnio, B.; Sessler, J. L. *Angew. Chem. Int. Ed.* **2007**, *46*, 1431. (d) Eller, L. R.; Stępień, M.; Fowler, C. J.; Lee, J. T.; Sessler, J. L.; Moyer, B. A. *J. Am. Chem. Soc.* **2007**, *129*, 11020. (e) Sessler, J. L.; Karnas, E.; Kim, S. K.; Ou, Z.; Zhang, M.; Kadish, K. M.; Ohkubo, K.; Fukuzumi, S. *J. Am. Chem. Soc*. **2008**, *130*, 15256. (f) Karnas, E.; Kim, S. K.; Johnson, K. A.; Sessler, J. L.; Ohkubo, K.; Fukuzumi, S. *J. Am. Chem. Soc.* **2010**, *132*, 16617.
2. Köhler, T.; Seidel, D.; Lynch, V.; Arp, F. O.; Ou, Z.; Kadish, K. M.; Sessler, J. L. *J. Am. Chem. Soc*. **2003**, *125*, 6872.
3. Bucher, C.; Devillers, C. H.; Moutet, J.–C.; Pécaut , J.; Sessler, J. L. *Chem. Commun.* **2006**, 3891.
4. Fabian, J. *Chem. Rev*. **1992**, *92*, 1197.
5. (a) Blake, I. M.; Rees, L. H.; Claridge, T. D. W.; Anderson, H. L. *Angew. Chem. Int. Ed.* **2000**, *39*, 1818. (b) Tsuda, A.; Osuka, A. *Science* **2001**, *293*, 79. (c) Kurotobi, K.; Kim, K. S.; Noh, S. B.; Kim, D.; Osuka, A. *Angew. Chem. Int. Ed*. **2006**, *45*, 3944. (d) Pschirer, N. G.; Kohl, C.; Nolde, F.; Qu, J.; Müllen, K. *Angew. Chem. Int. Ed*. **2006**, *45*, 1401. (e) Davis, N. K. S.; Thompson, A. L.; Anderson, H. L. *J. Am. Chem. Soc.* **2011**, *133*, 30.
6. (a) Brédas, J. L.; Adant, C.; Tackx, P.; Persoons, A.; Pierce, B. M. *Chem. Rev.* **1994**, *94*, 243. (b) Peng, Z.; Geise, H. J. *Bull. Soc. Chim. Belg*. **1996**, *105*, 739.
7. Yinon, J. *Anal. Chem*. **2003**, *75*, 99 A-105A.
8. Shin-ya, K.; Wierzba, K.; Matsuo, K. -i.; Ohtani, T.; Yamada, Y.; Furihata, K.; Hayakawa, Y.; Seto, H. *J. Am. Chem. Soc*. **2001**, *123*, 1262.
9. Greider, C. W.; Blackburn, E. H. *Cell* **1985**, *43*, 405.
10. Baker, E. S.; Lee, J. T.; Sessler, J. L.; Bowers, M. T. *J. Am. Chem. Soc.* **2006**, *128*, 2641.
11. Köhler, T.; Ou, Z.; Lee, J. T.; Seidel, D.; Lynch, V.; Kadish, K. M.; Sessler, J. L. *Angew. Chem. Int. Ed.* **2005**, *44*, 83.
12. Melfi, P. J.; Kim, S. K.; Lee, J. T.; Bolze, F.; Seidel, D.; Lynch, V. M.; Veauthier, J. M.; Gaunt, A. J.; Neu, M. P.; Ou, Z.; Kadish, K. M.; Fukuzumi, S.; Ohkubo, K.; Sessler, J. L. *Inorg. Chem*. **2007**, *46*, 5143.

13. Zhang, Z.; Lim, J. M.; Ishida, M.; Roznyatovskiy, V. V.; Lynch, V. M.; Gong, H. – Y.; Yang, X.; Kim, D.; Sessler, J. L. *J. Am. Chem. Soc*. **2012**, *134*, 4076.
14. (a) Newkome, G. R.; Lee, H.-W. *J. Am. Chem. Soc.* **1983**, *105*, 5956. (b) Toner, J. L. *Tetrahedron Lett*. **1983**, *24*, 2707. (c) Bell, T. W.; Firestone, A. *J. Am. Chem. Soc.* **1986**, *108*, 8109.
15. Krömer, J.; Rios-Carreas, I.; Fuhrmann, G.; Musch, C.; Wunderlin, M. *Angew. Chem. Int. Ed.* **2000**, *39*, 3481.
16. Bui, T. –T.; Iordache, A.; Chen, Z.; Roznyatovskiy, V. V.; Saint-Aman, E.; Lim, J. M.; Lee, B. S.; Ghosh, S.; Moutet, J. –C.; Sessler, J. L.; Kim, D.; Bucher, C. *Chem. Eur. J.* **2012**, *18*, 5853.
17. (a) Okujima, T.; Jin, G.; Matsumoto, N.; Mack, J.; Mori, S.; Ohara, K.; Kuzuhara, D.; Ando, C.; Ono, N.; Yamada, H.; Uno, H.; Kobayashi, N. *Angew. Chem. Int. Ed.* **2011**, *50*, 5699. (b) Okujima, T.; Ando, C.; Mack, J.; Mori, S.; Hisaki, I.; Nakae, T.; Yamada, H.; Ohara, K.; Kobayashi, N.; Uno, H. *Chem. Eur. J.* **2013**, doi: 10.1002/chem.201301294.
18. Panda, P. K.; Kang, Y.-J.; Lee, C.-H. *Angew. Chem. Int. Ed.* **2005**, *44*, 4053.
19. (a) Roznyatovskiy, V.; Lynch, V.; Sessler, J. L. *Org. Lett.* **2010**, *12*, 4424. (b) Sarma, T.; Panda, P. K.; Anusha, P. T.; Rao, S. V. *Org. Lett.* **2011**, *13*, 188.
20. (a) Sarma, T.; Panda, P. K. *Chem. Eur. J.* **2011**, *17*, 13987. (b) Roznyatovskiy, V. V.; Lim, J. M.; Lynch, V. M.; Lee, B. S.; Kim, D.; Sessler, J. L. *Org. Lett.* **2011**, *13*, 5620.
21. Xue, Z.; Kuzuhara, D.; Ikeda, S.; Sakakibara, Y.; Ohkubo, K.; Aratani, N.; Okujima, T.; Uno, H.; Fukuzumi, S.; Yamada, H. *Angew. Chem. Int. Ed.* **2013**, *52*, 7306.
22. (a) Takahashi, E.; Wraight, C. A. *Biochemistry* **1992**, *31*, 855. (b) Ferguson-Miller, S.; Babcock, G. T. *Chem. Rev*. **1996**, *96*, 2889. (c) Babcock, G. T.; Wikström, M. *Nature* **1992**, *356*, 301. (d) Babcock, G. T. *Proc. Natl. Acad. Sci. U.S.A.* **1999**, *96*, 12971. (e) Kaila, V. R. I.; Verkhovsky, M. I.; Wikström, M. *Chem. Rev*. **2010**, *110*, 7062. (f) Stowell, M. H. B.; McPhillips, T. M.; Rees, D. C.; Soltis, S. M.; Abresch, E.; Feher, G. *Science* **1997**, *276*, 812. (g) Rotello, V. M. In *Electron Transfer in Chemistry*; Balzani, V., Ed.; Wiley-VCH: Weinheim, Germany, **2001**.
23. (a) Chufán, E. E.; Puiu, S. C.; Karlin, K. D. *Acc. Chem. Res*. **2007**, *40*, 563. (b) Collman, J. P.; Devaraj, N. K.; Decréau, R. A; Yang, Y.; Yan, Y. -L.; Ebina, W.; Eberspacher, T. A; Chidsey, C. E. D. *Science* **2007**, *315*, 1565. (c) Rosenthal, J.;

Nocera, D. G. *Acc. Chem. Res*. **2007**, *40*, 543. (d) Savéant, J.-M. *Chem. Rev*. **2008**, *108*, 2348. (d) Halime, Z.; Kotani, H.; Li, Y.; Fukuzumi, S.; Karlin, K. D. *Proc. Natl. Acad. Sci. U.S.A.* **2011**, *108*, 13990. (e) Yamada, Y.; Fukunishi, Y.; Yamazaki, S.; Fukuzumi, S. *Chem. Commun*. **2010**, *46*, 7334. (f) Disselkamp, R. S. *Energy Fuels* **2008**, *22*, 2771. (g) Disselkamp, R. S. *Int. J. Hydrogen Energy* **2010**, *35*, 1049. (h) Lei, T.; Tian, Y. M.; Wang, G. L.; Yin, J. L.; Gao, Y. Y.; Wen, Q.; Cao, D. X. *Fuel Cell*s **2011**, *11*, 431.

24. (a) Koide, T.; Furukawa, K.; Shinokubo, H.; Shin, J. -Y.; Kim, K. S.; Kim, D.; Osuka, A. *J. Am. Chem. Soc.* **2010**, *132*, 7246. (b) Ishida, M.; Karasawa, S.; Uno, H.; Tani, F.; Naruta, Y. *Angew. Chem. Int. Ed.* **2010**, *49*, 5906.
25. (a) Mody, T. D.; Sessler, J. L. in *Perspectives in Supramolecular Chemistry*: *Supramolecular Materials and Technologies*, **1999**, *4*, 245. (b) Zhou, W. H.; Kuebler, S. M.; Braun, K. L.; Yu, T. Y.; Cammack, J. K.; Ober, C. K.; Perry, J. W.; Marder, S. R. *Science* **2002**, *296*, 1106. (c) Parthenopoulos, D. A.; Rentzepis, P. M. *Science* **1989**, *245*, 843. (d) Cumpston, B. H.; Ananthavel, S. P.; Barlow, S.; Dyer, D. L.; Ehrlich, J. E.; Erskine, L. L.; Heikal, A. A.; Kuebler, S. M.; Lee, I.-Y. S.; McCord-Maughon, D.; Qin, J.; Röckel, H.; Rumi, M.; Wu, X. -L.; Marder, S. R.; Perry, J. W. *Nature* **1999**, *398*, 51. (e) Torre, G.; Vázquez, P.; Agulló-López, F.; Torres, T. *Chem. Rev*. **2004**, *104*, 3723.
26. (a) Lim, J. M.; Yoon, Z. S.; Shin, J. –Y.; Kim, K. S.; Yoon, M. –C.; Kim, D. *Chem. Commun*. **2009**, 261. (b) Gokulnath, S.; Chandrashekar, T. K. *J. Chem. Sci*. **2008**, *120*, 137.
27. Sheik-Bahae, M.; Said, A. A.; Wei, T.-H.; Hagan, D. J.; Van Stryland, E. W. *IEEE J. Quantum Electron.* **1990**, *26*, 760.
28. Swain, D.; Anusha, P. T.; Sarma, T.; Panda, P. K.; Rao, S. V. *Chem. Phys. Lett.* **2013**, *580*, 73.
29. Anusha, P. T.; Swain, D.; Hamad, S.; Giribabu, L.; Prashant, T. S.; Tewari, S. P.; Rao, S. V. *J. Phys. Chem. C* **2012**, *116*, 17828.

CHAPTER 5

Naphthosapphyrins

5.1 Introduction

5.1.1Background

Sapphyrin is the first example of expanded porphyrin reported in literature. It also remains as one of the most widely studied expanded porphyrins so far. Sapphyrin can be formally derived from porphyrin by replacing one pyrrole unit with a bipyrrole moiety. Thus, like porphyrin, sapphyrin also contains four *meso*-carbon atoms. However, owing to increased number of pyrroles sapphyrin possess 22 π-electrons in its shortest conjugation pathway compared to 18 π-electrons of porphyrin and hence aromatic in nature, similar to that of porphyrin (Figure 5.1).

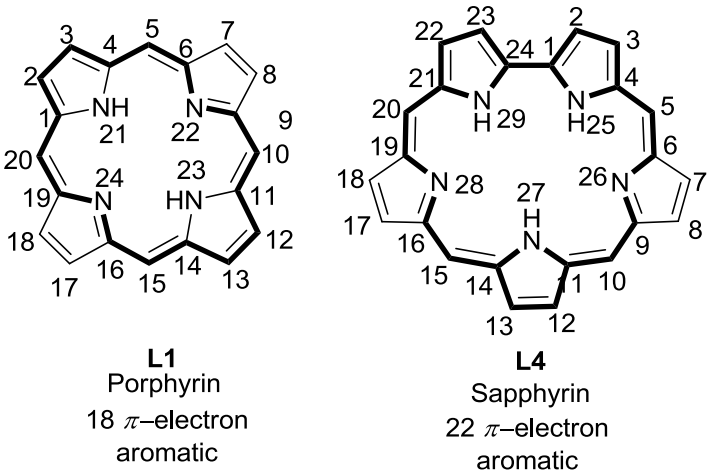

Figure 5.1 Core structures of porphyrin and sapphyrin.

The beginning of sapphyrin was an outcome of serendipity rather than rational synthesis. It was R. B. Woodward group who first noticed formation of a pentapyrrolic macrocycle during their study directed towards the synthesis of vitamin B_{12}. Treatment of a linear tetrapyrrole (**L94a**, Scheme 5.1) with formic acid and HBr, followed by oxidation with iodine gave rise to

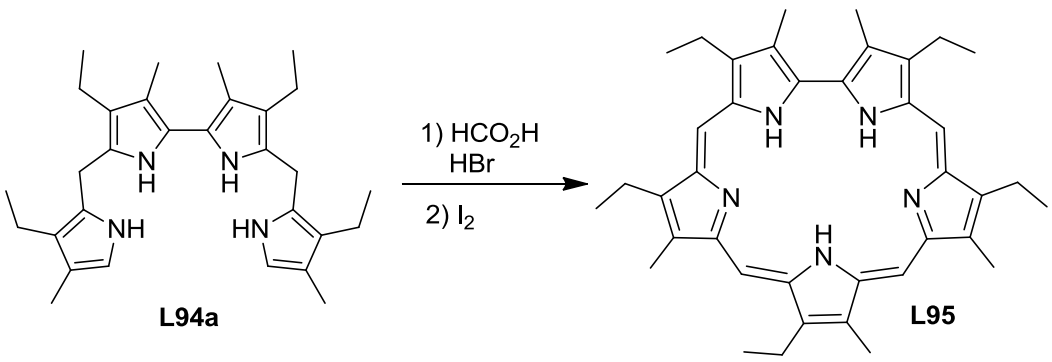

Scheme 5.1 First serendipitous synthesis of sapphyrin.

a pentapyrrolic byproduct instead of the desired corrole. Due to its brilliant blue color in solid state, they assigned the trivial name "sapphyrin" to this compound. Synthesis of sapphyrin was first mentioned at the aromaticity conference in Sheffield, UK, 1966, during the discussion period followed after the formal oral presentation of Woodward.[1] But in 1969 Johnson and coworkers first reported dioxasapphyrin as a byproduct during their effort towards the synthesis of heteroatom analogue of corrole (Scheme 5.2).[2,3] Formation of macr-

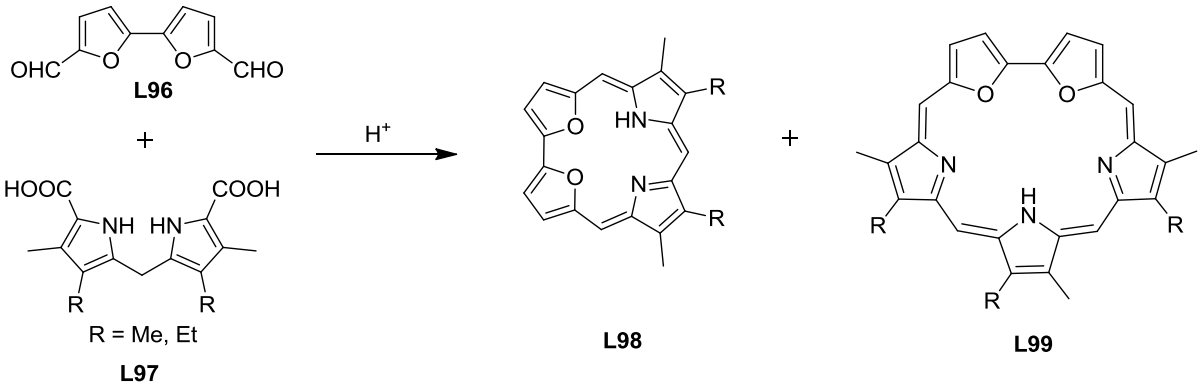

Scheme 5.2 First serendipitous synthesis of heterosapphyrin.

ocycle **L99** was further confirmed by the condensation of tripyrrane **L100** with bis-formyl bifuran **L96**, followed by oxidation, as shown in scheme 5.3.[2] This type of method later became popular as a MacDonald type [3 + 2] approach for the synthesis of sapphyrin because of the number of pyrrole-like units in each precursor.

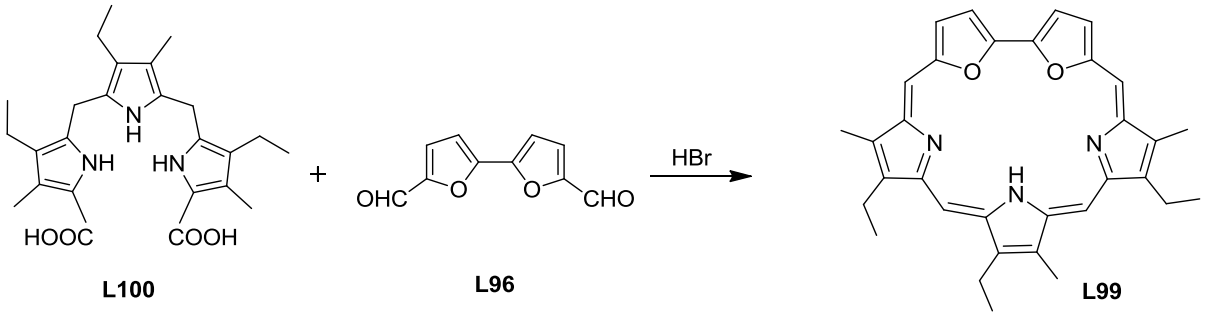

Scheme 5.3 First rational synthesis of heterosapphyrin.

5.1.2 Synthesis of *β*-alkylated sapphyrin

After the initial reports by Johnson and coworkers two independent publications appeared in literature, one from the Johnson group and the other from the Woodward group describing the systematic synthesis and study of sapphyrin.[4] In the full paper describing the synthesis of sapphyrin, Woodward group also used an analogous [3 + 2] approach, specifically reaction

between a diformylbipyrrole and a diacid tripyrrane to generate all azasapphyrins such as **L101a**. They have also shown that indeed sapphyrin could be synthesized by treating linear tetrapyrrole **L94a** with 2,5-diformyl-3,4-dimethylpyrrole in presence of formic acid confirming their earlier observations.[4a] However, [3 + 2] approach leading to sapphyrin proved to be more general and later used by several research groups for the synthesis of sapphyrins.[5] This was in turn made more feasible by Sessler and coworkers by introducing simple high-yielding route to both dicarboxyl-substituted tripyrranes and *β*-substituted bipyrroles.[6] The same report also revealed the anion recognition properties of sapphyrin in its diprotonated form, which stimulated greater interest to evaluate anion recognition properties of sapphyrin. As a result sapphyrin derivatives have been studied extensively for use in a variety of applications, including anion sensing, transport, chromatography-based purification of anions etc.[7]

In 1999, Richter and Lash reported an improved synthesis of sapphyrin by using $FeCl_3$ as an oxidant in the aromatization step of a [4 + 1] synthesis.[8] Condensation of the linear tetrapyrrole diacid **L94b** with pyrrole dialdehyde **L100b** in presence of TFA (Scheme 5.4)

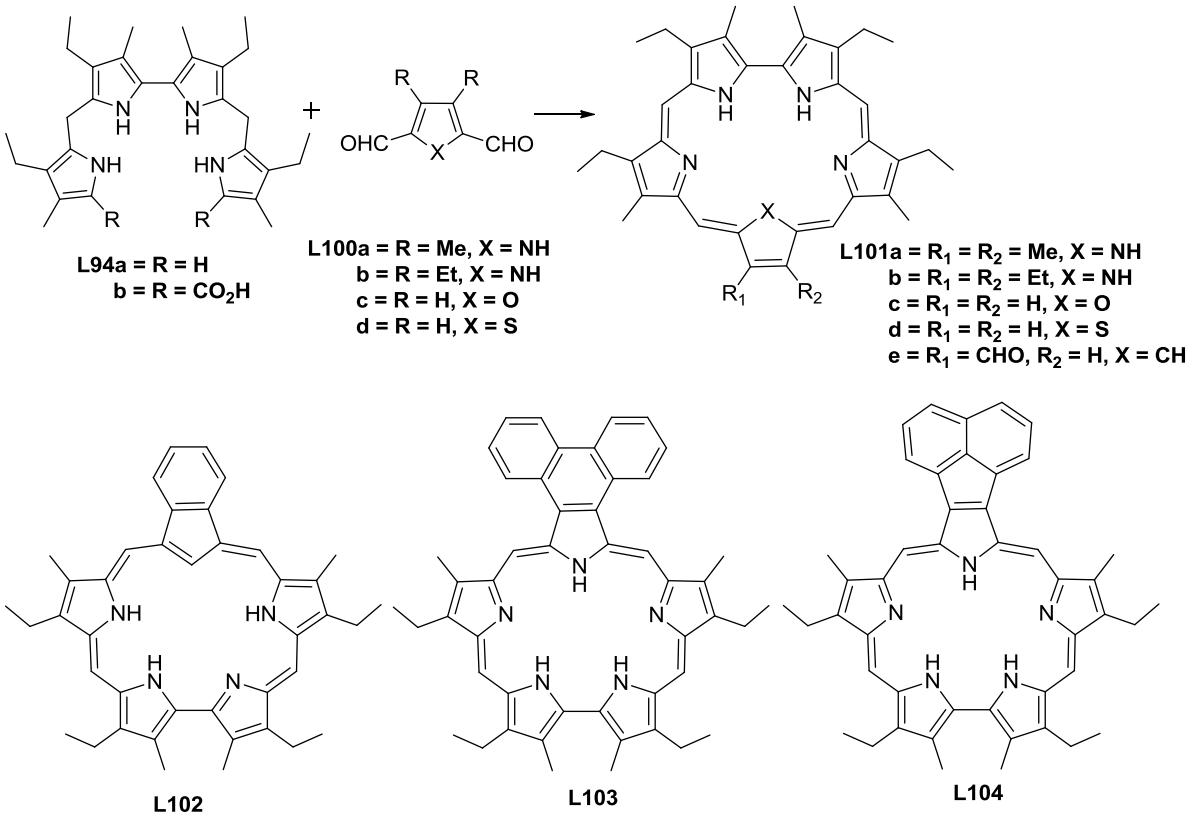

Scheme 5.4 Synthesis of sapphyrins using [4 + 1] methodology.

followed by oxidation with 0.1 M aqueous $FeCl_3$ gave rise to sapphyrin **L101b** in 50 % yield compared to 36 % using DDQ. They have also utilized this methodology to synthesize heterosapphyrins **L101c-d** along with carbasapphyrin (**L101e, L102)** and linearly annulated sapphyrin such as **L103** and **L104**.[8]

Another alternative [4 + 1] approach, shown in scheme 5.5, was reported by Paolesse and Smith, where an a,c-biladiene (**L105a-b**) was used as a tetrapyrrolic precursor and reacted with formylpyrrole **L106a-b** in acetic acid or acidic ethanol.[9]

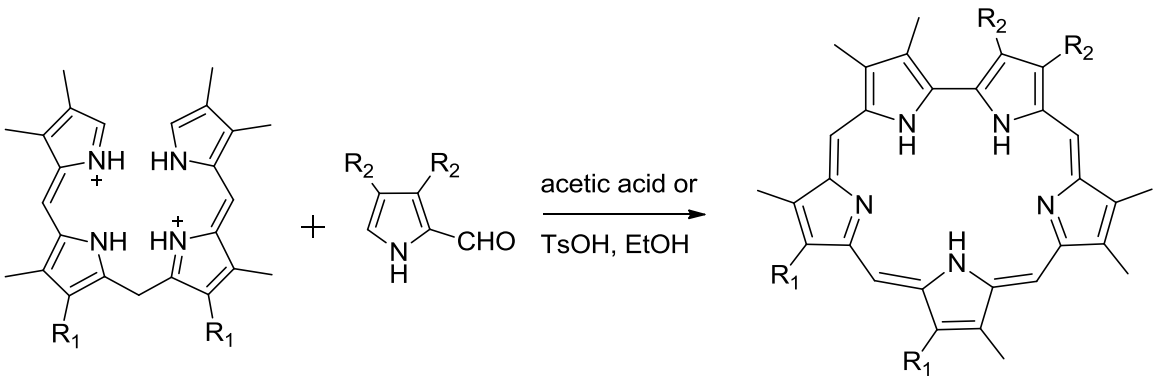

L105a = R_1 = Me
b = R_1 = Et

L106a = R_2 = Me
b = R_2 = Et

L107a = R_1 = R_2 = Me
b = R_1 = R_2
c = R_1 = Et, R_2 = Me

Scheme 5.5 Synthesis of sapphyrins using [4 + 1] methodology.

In 2001, Sessler and coworkers reported a [3 + 1 + 1] method for synthesis of sapphyrin that involves direct pyrrole-pyrrole bond formation during macrocyclization (Scheme 5.6). They

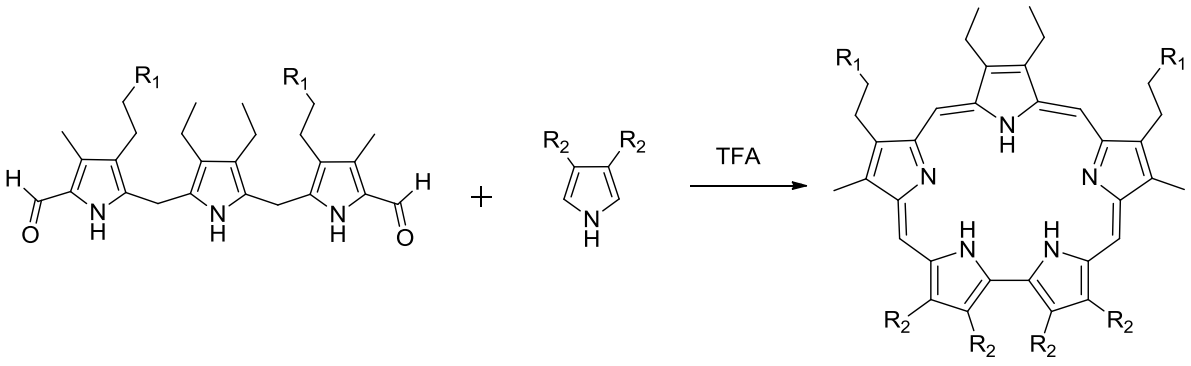

L108a = R_1 = CH_2OH
b = R_1 = H

L109a = R_2 = Me
b = R_2 = OMe
c = R_2 = Et

L110a = R_1 = CH_2OH, R_2 = Me
b = R_1 = CH_2OH, R_2 = OMe
c = R_1 = CH_2OH, R_2 = Et
d = R_1 = H, R_2 = Et

Scheme 5.6 Synthesis of sapphyrins using [3 + 1 + 1] methodology.

found this method more efficient for the synthesis of *β*-substituted sapphyrins, compared to the [3 + 2] MacDonald type condensation reaction owing to reduced number of steps, as no preformed bipyrrole is required in this strategy.[10]

5.1.3 *meso*-Aryl-substituted sapphyrins

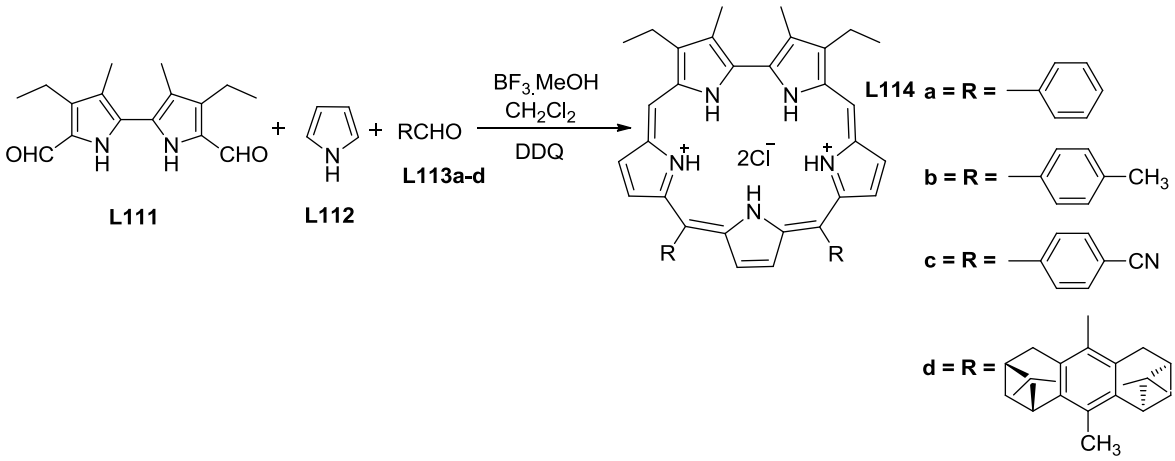

Scheme 5.7 Synthesis of *meso*-diarylsapphyrins using [2 + 1 + 1 + 1] methodology.

In 1995 Sessler and coworkers described the synthesis of *meso*-diarylsapphyrins following a [2 + 1 + 1 + 1] method involving one-pot condensation reaction between diformyl bipyrrole **L111**, pyrrole **L112** and aryl aldehydes **L113a-c** using BF_3.MeOH as Lewis acid catalyst allows preparation of 10,15-diphenylsapphyrins **L114a-c** in *ca.*10 % yield.[11] Use of a non-racemic aldehyde such as **L113d**, instead of simple benzaldehyde permits to isolate chiral sapphyrin such as **L114d**.[11]

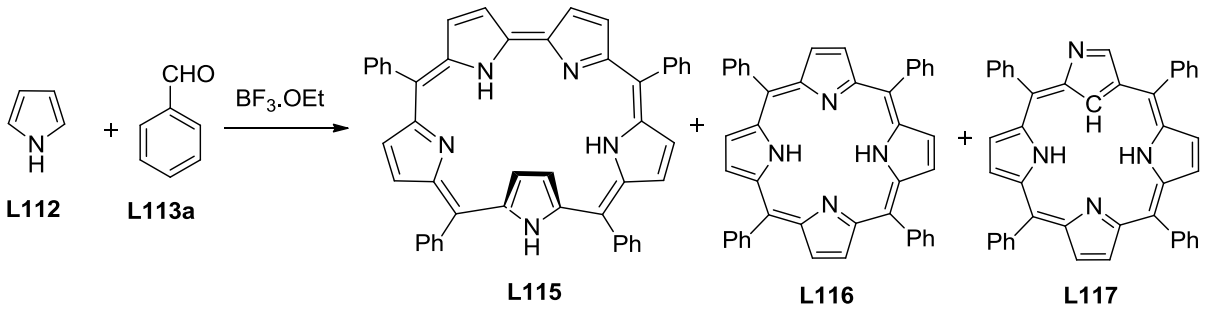

Scheme 5.8 One pot synthesis of *meso*-tetraphenylsapphyrin.

Grażyński and coworkers again in 1995 isolated *meso*-tetraarylsapphyrin in a Rothemund-type condensation of pyrrole and benzaldehyde in presence of BF_3-etherate (Scheme 5.8).[12] This reaction yields, 5,10,15,20-tetraphenylsapphyrin **L115** in low yield (*ca.* 1.1 %) apart

from 5,10,15,20-tetraphenylporphyrin **L116** and inverted tetraphenylporphyrin 2-aza-21-carba-5,10,15,20-tetraphenylporphyrin **L117**. Dolphin and coworkers have synthesized *meso*-di and tetraarylsapphyrin following a [3 + 2] strategy involving acid catalyzed condensation between 5,10-diphenyltripyrrane and with either bipyrrole dialdehyde or bipyrrole and benzaldehyde.[13]

Chandrashekar and coworkers have also reported synthesis of *meso*-tetraarylsapphyrins using dipyrromethanes as the single precursors.[14] Exposure of dipyrromethanes **L118** to one equivalent of TFA, followed by oxidation with chloranil, gives rise to sapphyrins **L119** as a major product in yields of up to 11 % (for Ar = phenyl, Scheme 5.9), along with other products, such as porphyrins. However, product distribution and yield were found to largely

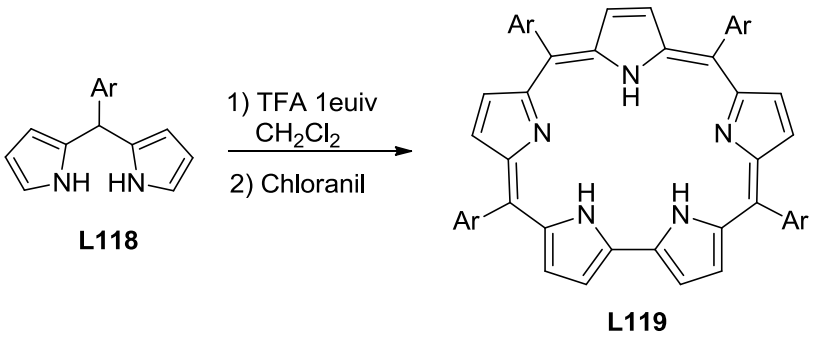

L118 **L119**

Scheme 5.9 Dipyrromethane based synthesis of *meso*-tetraarylsapphyrin.

dependent on the nature and concentration of the acid used, for instance use of *p*-TsOH instead of TFA resulted in formation of porphyrin along with N-confused porphyrins and no sapphyrins forms under this condition. Looking at the synthetic availability of dipyrromethanes such as **L118** this method could provide an attractive alternative means of producing all-azasapphyrins.

Very recently synthesis of *meso*-tetraarylsapphyrin have been reported starting from open chain pentapyrrole **L120** that was obtained as a byproduct in the synthesis of triarylcorrole (Scheme 5.10).[15] Previously, Ka and Lee describe an attempt to obtain all azasapphyrins by the oxidative coupling of pentapyrromethanes which led to synthesis of porphyrin via formation of phlorins.[16] In an another similar attempt Gross and coworkers were able to isolate the Rh-complex of *meso*-tetraarylsapphyrin, even though the crude sapphyrin (free-base) product proved to be unstable to chromatographic workup.[17]

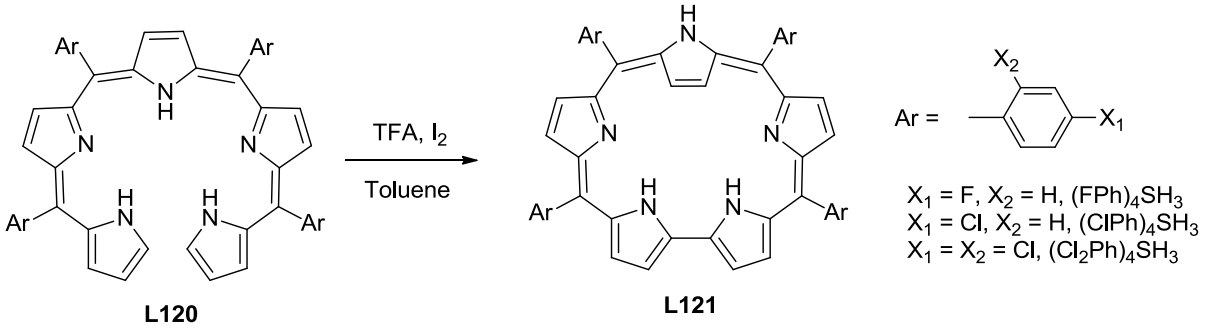

L120 L121

Scheme 5.10 Pentapyrrole based synthesis of *meso*-tetraarylsapphyrin.

5.1.4 π-Extension in sapphyrins

The first example of π-extension in sapphyrin was reported by Richter and Lash in 1999 during their effort related to improved synthesis of sapphyrin by use of $FeCl_3$ in the aromatization step of a [4 + 1] synthesis as described in scheme 5.4. The UV-Vis spectrum of free-base phenanthrosapphyrin **L103** exhibits a Soret band at 473 nm whereas acenaphthosapphyrin **L104** displays further red shifted Soret band at 500 nm. Nonetheless both the compounds exhibits substantial red shifted absorption spectra compared to the β-alkylated sapphyrins.[8]

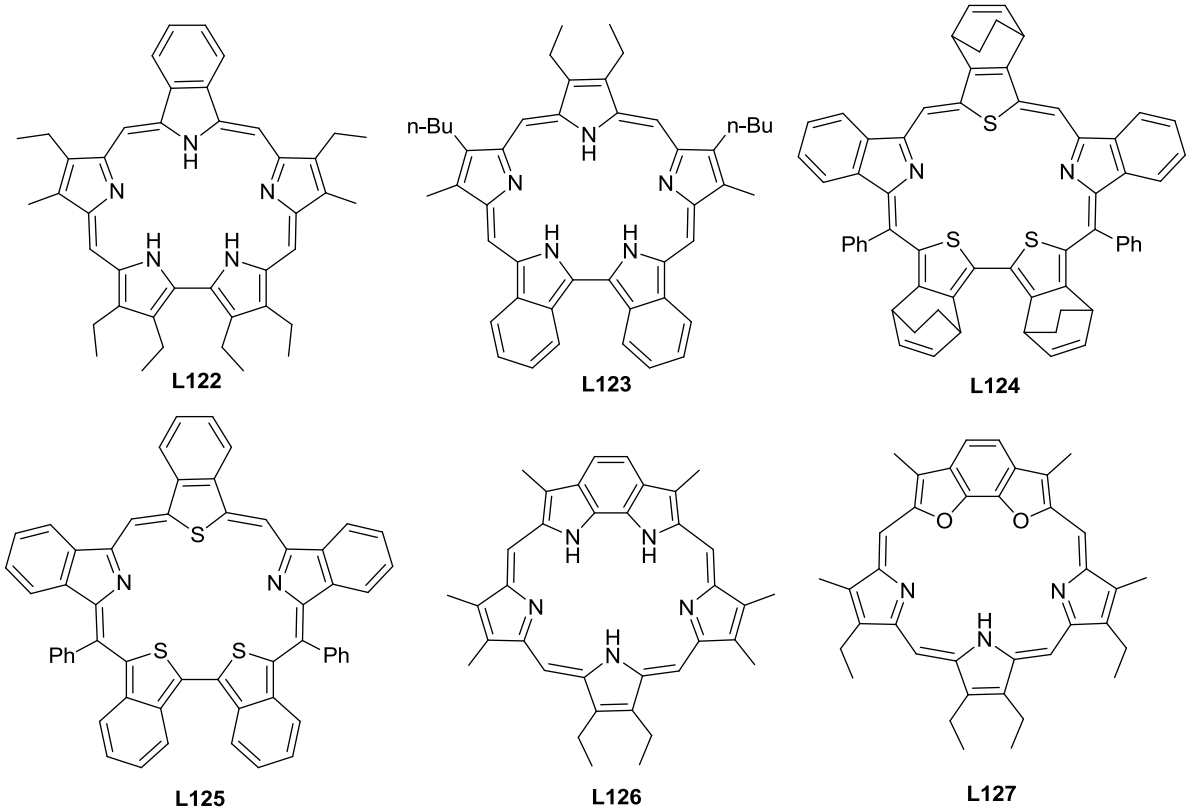

L122 L123 L124

L125 L126 L127

Figure 5.2 Annulated π-extended sapphyrins.

In 2004 Ono and coworkers reported benzo-fused sapphyrin **L122** that involves their retro Diels-Alder approach utilized for synthesizing various π-extended porphyrinoids. Condensation of bipyrrole dialdehyde with BCOD fused tripyrromethane diacid lead to synthesis of mono-BCOD fused sapphyrin which was subsequently converted to **L122** by heating at high temperature (200 °C). On the other hand, **L123** was synthesized from condensation of BCOD fused bipyrrole diacid with tripyrromethane dialdehyde, followed by retro Diels-Alder reaction of the resulting macrocycle. In comparison to their BCOD-fused analogues, **L122** and **L123** shows a red shift of 12 and 22 nm respectively in their corresponding absorption maxima.[18] In continuation to their work, Okujima and Ono reported BCOD-fused trithiasapphyrin following a [3 + 2] type approach, which can be selectively converted to trithiadibenzosapphyrin **L124** or trithiapentabenzosapphyrin **L125** depending upon temperature used during the thermal conversion process. Fusion of five benzene rings to the trithiasapphyrin causes substantial red shift and enhancement in absorption spectra. For instance an intense Soret band was observed at 551 nm and Q-bands appear at 710, 766, 810 and 915 nm.[19]

In 2005 Lee and coworkers reported a benzodipyrrole derived sapphyrin **L126**, wherein benzodipyrrole dialdehyde was condensed with a tripyrromethane diacid in a [3 + 2] MacDonald type approach.[20] Absorption spectrum of benzosapphyrin **L126** was found to be red shifted compared to decaalkylsapphyrin such as **L101b** as a result of its extended π-conjugation. The Soret type band appeared at 466 and 469 nm in its free-base and diprotonated form respectively.[20]

Dioxabenzosapphyrin **L127**, oxygen analogue of benzosapphyrin **L126** was also reported by Lee and Sessler following a similar approach employed in the synthesis of **L126**. The absorption spectrum of free-base **L127** was found to be very broad compared to **L126** or decaalkyl sapphyrin.[21] Absorption maxima lie below 400 nm along with very broad Q-bands centered at 650 and 750 nm. However, in diprotonated form an intense Soret type band appeared at 455 nm along with Q-band that is resolved to some extend compared to its free-base. These authors also tested the anion binding ability of dioxabenzosapphyrin as well as benzosaphyrin. This study reveals that **L127** in its diprotonated form binds only weakly with fluoride and chloride ions compared to diprotonated **L126**. However interaction of diprotonated **L127** with neutral Ar-OH species was found to be more compared to diprotonated **L126** and decaalkylsapphyrin.

Very recently Lee in collaboration with Sessler, Kim and our group reported synthesis of *meso*-tetraarylnaphthosapphyrin derived from naphthobipyrrole. Reaction of unsubstituted naphthobipyrrole with pentafluorobenzaldehyde and pyrrole in presence of TFA yields naphthosapphyrin **L129**, albeit in low yield, along with formation of naphthorubyrin **L130**.[22]

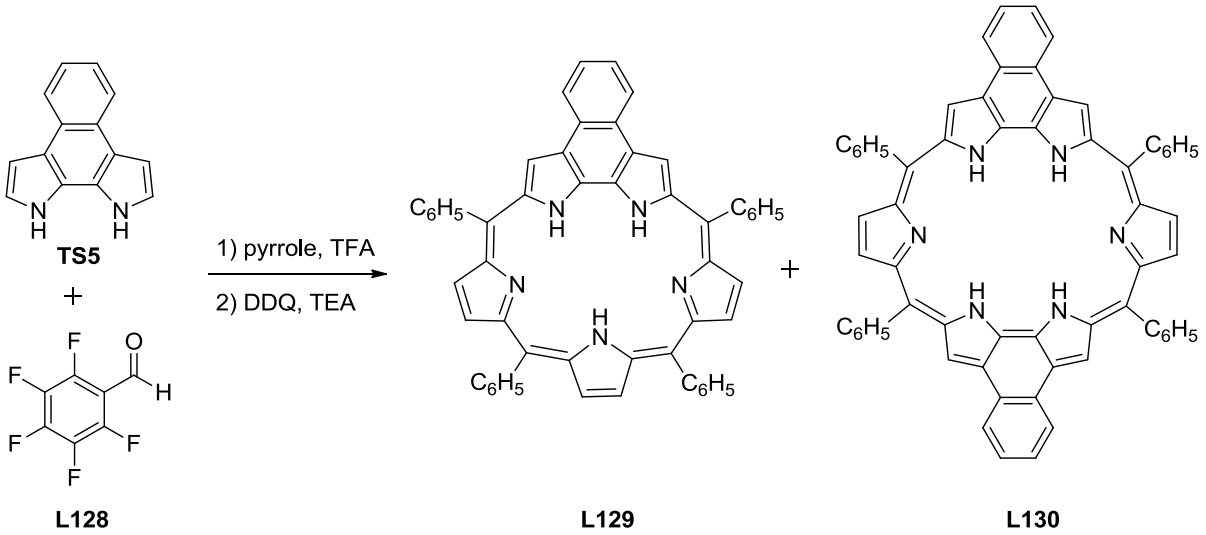

Scheme 5.11 Synthesis of naphthosapphyrin **L129**.

Optical spectra of free-base **L129** shows a split Soret like band at 508 and 533 nm along with three Q-type absorption bands at 643, 715 and 781 nm. These values are red shifted compared to *meso*-tetraarylsapphyrin **L115** (Soret: 484; Q: 648, 736, 771) and benzosapphyrin **L126** due to extended π-conjugation and structural rigidification.

5.1.5 Structural diversity in sapphyrins

In the very first report regarding the synthesis of *meso*-tetraarylsapphyrin Grażyński and coworkers determined that the free-base form of tetraphenyl sapphyrin **L115** exist in a conformation wherein pyrrole ring opposite to the bipyrrole unit undergoes a 180° ring flipping thereby producing an inverted sapphyrin.[12] This observation is in contrast to that observed for *meso*-free decaalkylsapphyrin such as **L131** that exhibits a planar structure where all pyrrole nitrogens point inwards. Interestingly, **L115** in its diprotonated form again exhibits a normal planar structure. This flexibility of **L115** leading to planar and inverted arrangement could be easily followed by ^{1}H NMR spectral analysis. For instance free-base form of **L115 ($TPSH_3$)** i.e. inverted structure exhibits a signal at 11.76 ppm corresponding pyrrolic NH at 27-position, whereas β-pyrrole CH at 12 and 13 position resonates at -1.28 ppm. Upon protonation NH resonance jump to upfield position (-2.74 ppm for bis-HCl salt)

along with a down field shift of *β*-pyrrole CH (8.86 ppm) indicating a planar structure similar to *β*-alkylated sapphyrin (Scheme 5.12).

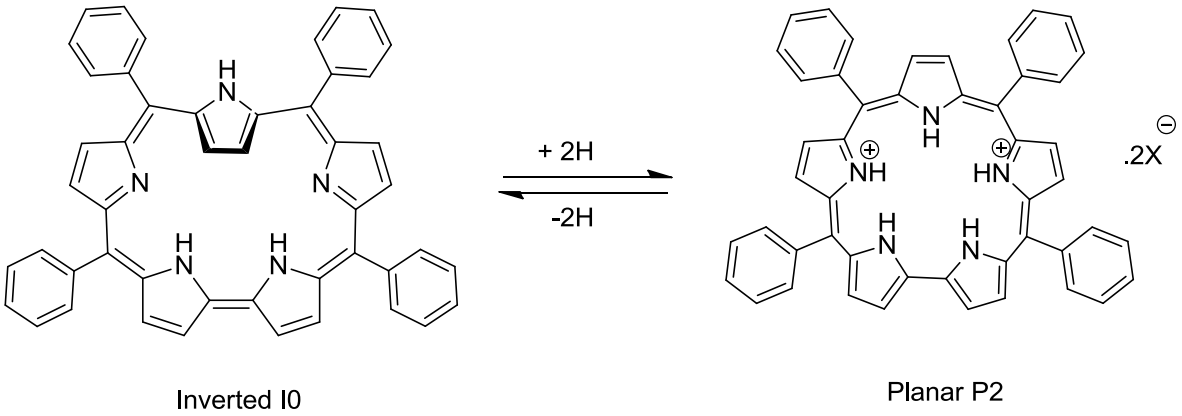

Scheme 5.12 Proton induced interconversion between inverted and planar form in tetraphenyl sapphyrin.

In another detailed study, Grażyński and coworkers showed that in fact two structurally different dicationic forms namely planar and inverted do exist in solution.[23] Their concentration depends simply on the counter anion concentration (Scheme 5.12). For example when $TPSH_3$: acid molar ratio is 1:2 planar structure is observed as explained above however, in presence of excess acid (*ca.* 50 equiv.) dicationic planar P2 conformation undergoes another ring flip thereby producing an inverted dicationic form. These conformational changes were reflected in their respective ^{1}H NMR spectra as well as in absorption spectra. For instance *β*-pyrrole CH at 12 and 13 position now resonates at -0.57 ppm whereas signal corresponding to 27-NH resonance shifted to 14.30 ppm. Similar inverted dicationic form in presence of excess acid was also observed for recently reported naphthosapphyrin **L129**.[22]

Sapphyrin containing one or more heterocyclic ring other than pyrrole (heterosapphyrin) also displays diverse structural variation.[24] For example, **L136** wherein two pyrrole nitrogens have been replaced with either S or Se exhibits normal planar structure unlike *meso*-tetraarylsapphyrin.[25] Interestingly, sapphyrins **L132**, **L133, L135** and **L137** again exhibit inverted arrangement.[26,13] ^{1}H NMR and X-ray structure analysis show that inverted structure is generally observed for larger core size and presence of smaller hetero atom (N or O) in the two flanking heterocyclic rings in the constituent tripyrromethane unit. Presence of heavy atom such as S or Se in these two rings leads to planar structure as observed for **L136** despite

having four *meso*-substituents. Crystal structure analysis of these molecules, carried out by Chandrashekar and coworker revealed presence of N-H…S and NH…Se hydrogen bonding interaction in the macrocyclic cavity.[27] Another notable feature, described by these authors is

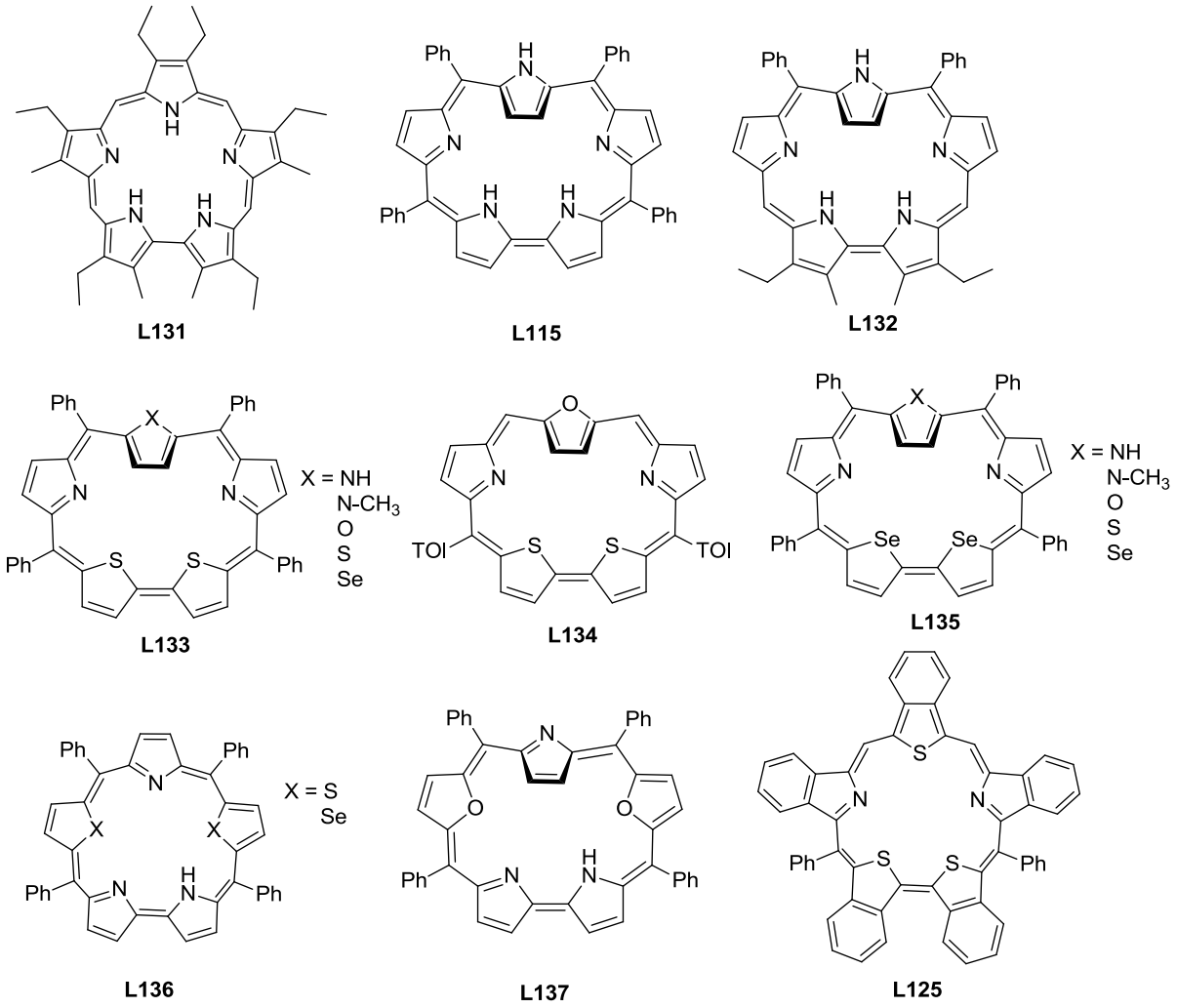

Figure 5.3 Structural diversity in sapphyrins.

the existence of rare supramolecular C-H…S and C-H…Se hydrogen bonds in these structures. Further, Lee and coworker postulated that inversion of thiophene ring in **L133** (X = S) is caused by the large ring strain arising from large C_{α}-$C_{\alpha'}$ distance of bithiophene, rather than the presence of *meso*-aryl substituents. To prove this hypothesis, they synthesized oxa-dithia-sapphyrin **L134**, wherein the two *meso*-aryl substituents flanking the heterocyclic ring that undergoes inversion has been removed. Interestingly, despite of removal of *meso*-substituents **L134** exhibits inverted arrangement as evidenced by X-ray crystallographic analysis, as well as by ^{1}H NMR spectroscopy, thereby confirming their assumption.[28] However, trithiapentabenzosapphyrin **L125** reported by Okujima et al. don′t show any ring

inversion owing to the presence of *β*-substituents despite of having similar expanded core as **L134** and **L133** (X = S).[19] Unlike the *meso*-aryl pentaazasapphyrin, core-modified sapphyrins do not exhibit proton triggered conformational changes and the inverted or normal planar structures remain intact.

5.2 Research goal

Broadly two types of sapphyrins are known in literature namely, *meso*-substituted and *β*-substituted sapphyrins. From the above discussion regarding structural diversity of sapphyrins, it can be inferred that heterocyclic ring inversion in sapphyrin may arise owing to a number of factors such as *meso*-aryl substitutions, steric strain and the presence of stabilizing hydrogen bonding interactions, may also play an important role in selection of appropriate geometry of the macrocycle. Whatsoever may be the case, conformational flexibility is possible if the heterocyclic ring undergoing inversion is unsubstituted. In this regard, we opt to synthesize *β*-alkylsapphyrin derived from alkylated naphthobipyrrole wherein pyrrole ring opposite to naphthobipyrrole is devoid of any substitution (**TS31**). We also choose to synthesize all *β*-substituted sapphyrin derived from alkylated naphthobipyrrole (**TS30**). The effect of ring fusion on structural as well as optical properties will be very interesting to study. For having better comparisons we also planned the synthesis of *β*-alkylated sapphyrin such as **TS32** derived from tetraethylbipyrrole.

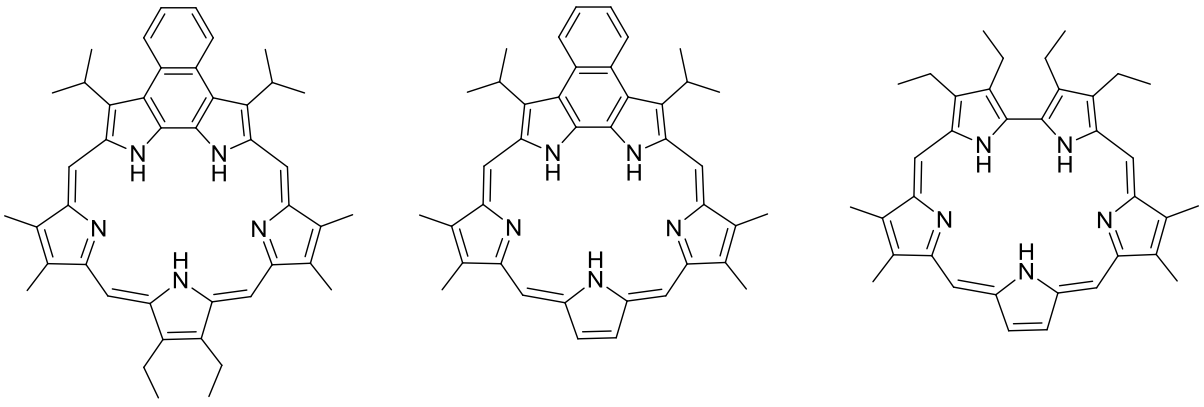

Figure 5.4 Proposed synthesis of sapphyrins.

5.3 Results and discussion

5.3.1 Synthesis of naphthosapphyrin TS30, TS31 and 2,3,22,23-tetraethyl-7,8,17,18-tetramethylsapphyrin TS32

Meso-tetraarylnaphthosapphyrin **L129** has been reported recently by Lee group in collaboration with Sessler, Kim and our group.[22] Naphthosapphyrin **L129** was synthesized following a [2 + 1 + 1 + 1] in presence of TFA in low yield (1 %). Taking the advantage of good solubility of alkylated naphthobipyrroles, we followed a rational MacDonald type [3 + 2] approach for the synthesis of alkylated naphthosapphyrins.[20] Condensation of naphthobipyrrole dialdehyde **TS21b** with tripyrrane diacid **TS11** or **TS34** in acidified (*p*-TsOH) ethanol, in presence of oxygen leads to the formation naphthosapphyrin **TS30** and **TS31** in 18 % and 26 % yield respectively. Synthesis of **TS11** is reported in literature and described in chapter 2 of the thesis. However, **TS34** is previously unknown and synthesized following a similar strategy used to synthesize **TS11** as shown in Scheme 5.14.

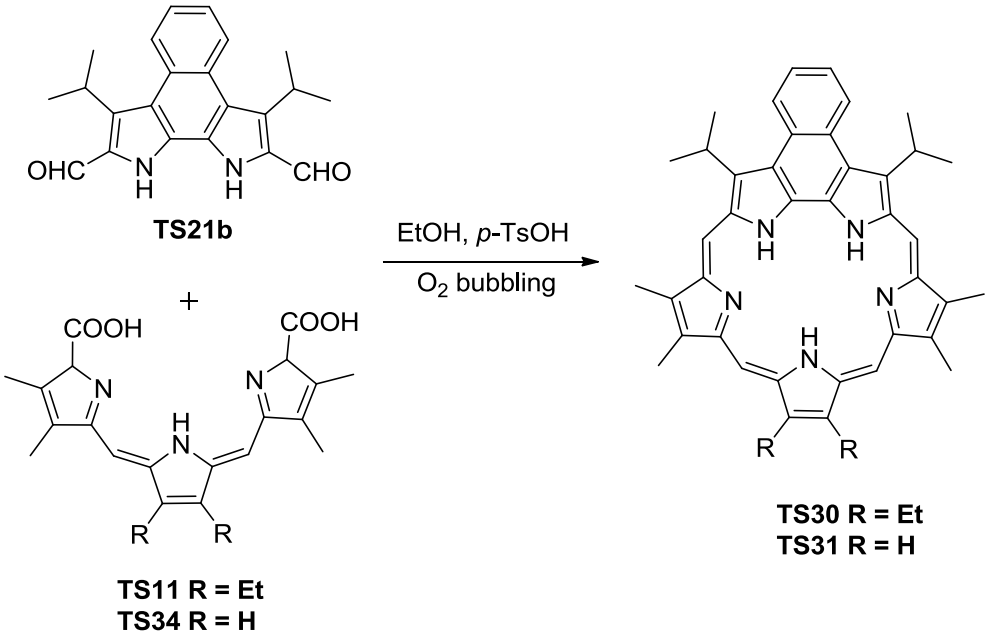

Scheme 5.13 Synthesis of naphthosapphyrins **TS30** and **TS31**.

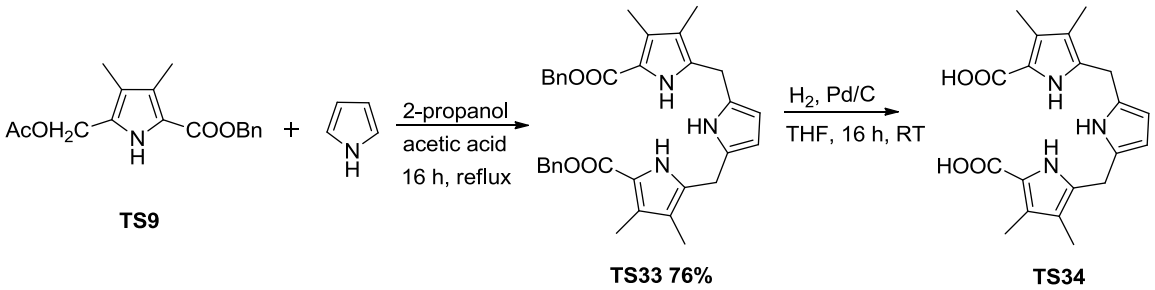

Scheme 5.14 Synthesis of tripyrrane diacid **TS34**.

Octaalkylsapphyrin **TS32** was also synthesized following a similar [3 + 2] strategy as

described in Scheme 5.13 for the synthesis of naphthosapphyrins. Namely, condensation of tetraethylbipyrrole dialdehyde **TS13** (details in chapter 2) with tripyrrane diacid **TS34** yield the desired sapphyrin **TS32** in 25 % yield. All the sapphyrins thus synthesized were characterized by NMR and UV-Vis spectroscopy, along with HR-MS analyses. Further, **TS30** was also characterized using single crystal X-ray diffraction analysis.

5.3.2 ^{1}H NMR analyses of naphthosapphyrins TS30, TS31 and 2,3,22,23-tetraethyl-7,8,17,18-tetramethylsapphyrin TS32

^{1}H NMR spectra of **TS30** measured in $CDCl_3$ at room temperature shows a very broad signal at -0.51 ppm corresponding to NH resonance (as revealed by D_2O exchange) along with signals corresponding to *meso*-protons at 11.27 and 10.92 ppm. Thus confirming a planar structure (all nitrogen in) as observed for decaalkylsapphyrins.[7] In comparison to benzosapphyrin **L126** where three sets of NH's were observed in free-base, tautomerization of NH protons seems to be more rapid in **TS30**. Upon protonation clear set of NHs in 2:1:2 ratios appeared. Position of NH signal varies with respect to presence of different counter anion as revealed from the ^{1}H NMR spectra of diprotonated **TS30** prepared by washing free-base with different protic acids. Table 5.1 shows the position of NH and *meso* signal with respect to different counter anion. It can be understood from the table that the *meso*-CH signals are not much affected by the change in counter anion. However, significant shift observed in case of NH-signal, probably owing to the different coordinating mode of the counter anion with pyrrolic NH and the resultant strength of the hydrogen bonds.

Table 5.1 NH and *meso*-CH chemical shift with respect to different counter anion.

Compounds	*meso*-CH shift (in ppm)	*β*-pyrrole CH	NH-shift (in ppm)
TS30-2·HCl	11.85 (s), 11.54 (s)	-	-3.17, -3.65, -4.34
TS30-·H_2SO_4	11.85 (brs), 11.54 (brs)	-	-3.16, -3.71, -4.34
TS30-2·p-TsOH	11.75 (s), 11.36 (s)	-	-4.05, -4.26, -4.87
TS30-2·$HClO_4$	11.94 (s), 11.63 (s)	-	-5.14, -5.51, -6.41
TS31-2·HCl	11.96 (s), 11.65 (s)	10.35	-3.54, -3.56, -4.81
TS31-2·*p*-TsOH	11.85 (s), 11.47 (s)	10.31	-4.19, -4.43, -5.26
TS31-2·TFA	11.99 (s), 11.65 (s)	10.43	-3.91, -3.99, -5.13

^{1}H NMR spectrum of free-base **TS31** measured in $CDCl_3$ shows similar trend like **TS30**. For example a broad signal at -0.95 ppm corresponding to NH resonance (as revealed by D_2O

exchange), signal corresponding to *meso*-CH and *β*-pyrrolic CH appeared at 10.73, 10.20 and 9.55 respectively, thereby confirming absence of any inverted conformation in the macrocycle at least at room temperature. In the free-base form of **TS31**, chemical shift and integration of NH signal were found to depend on the amount of residual water present in the NMR solvent and varies in the range from -3.56 to 0.44 ppm. Figure 5.5 shows change in NH-chemical shift of **TS31** with addition of water. Similar behavior was also observed for **TS30**. ^{1}H NMR spectra of diprotonated form of **TS31** shows a similar pattern to that of **TS30**,

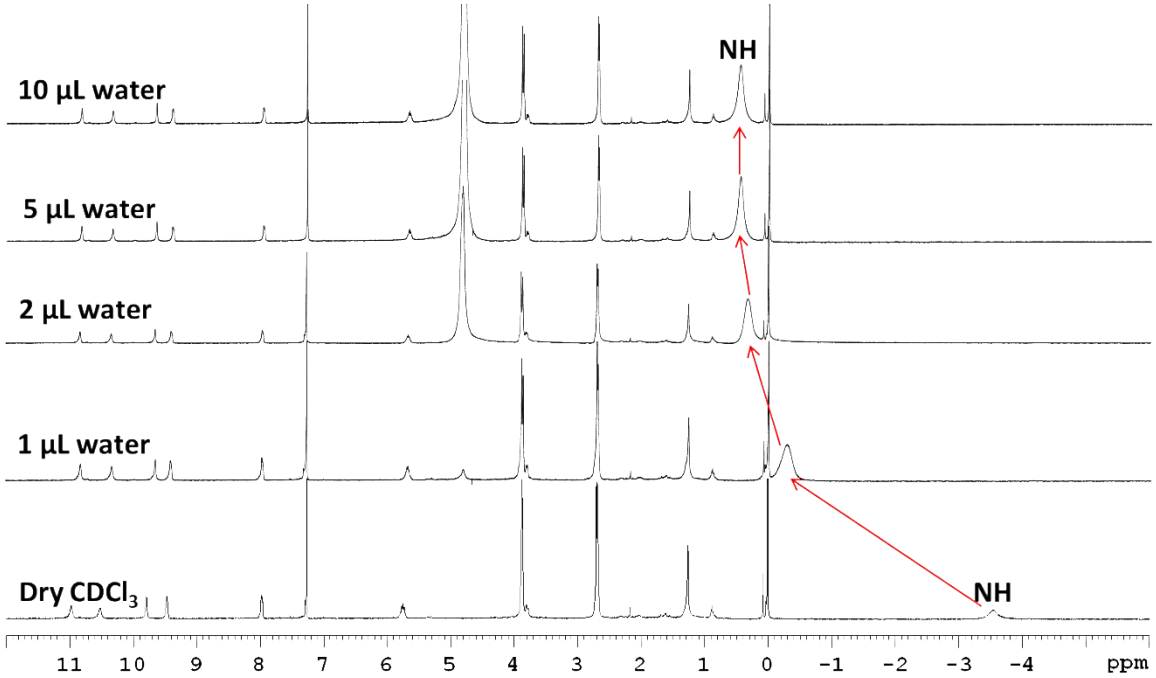

Figure 5.5 ^{1}H NMR spectra of free-base **TS31** recorded in $CDCl_3$ showing NH-chemical shift with added water.

however, relatively broad signal were observed corresponding to NH resonances. Given the fact that **TS31** possess one unsubstituted pyrrole opposite to the naphthobipyrrole unit we were interested to see if there is any inversion occurs in presence of excess anions. To check this, we titrated a $CDCl_3$ solutions of TS31 free-base against known amount of TFA (Figure 5.6). The result ruled out any kind of inversion, even in the presence of excess amount of TFA, as no significant change in the spectra could be detected, which could be attributed to the corresponding inverted structure. ^{1}H NMR spectral analysis of **TS32** measured in $CDCl_3$ at room temperature shows a broad NH signal at -1.71 ppm, a pair of *meso*-CH appeared at 11.08 and 10.69 ppm along with *β*-pyrrolic CH at 9.76 ppm which is found to be very broad in comparison to **TS31**. This broadening of *β*-pyrrolic CH probably indicates more flexible

nature of this pyrrole compared to that of relatively rigid **TS31**. However, ^{1}H NMR spectrum of **TS32** in presence of excess TFA shows rather drastic change in the spectrum accompanied

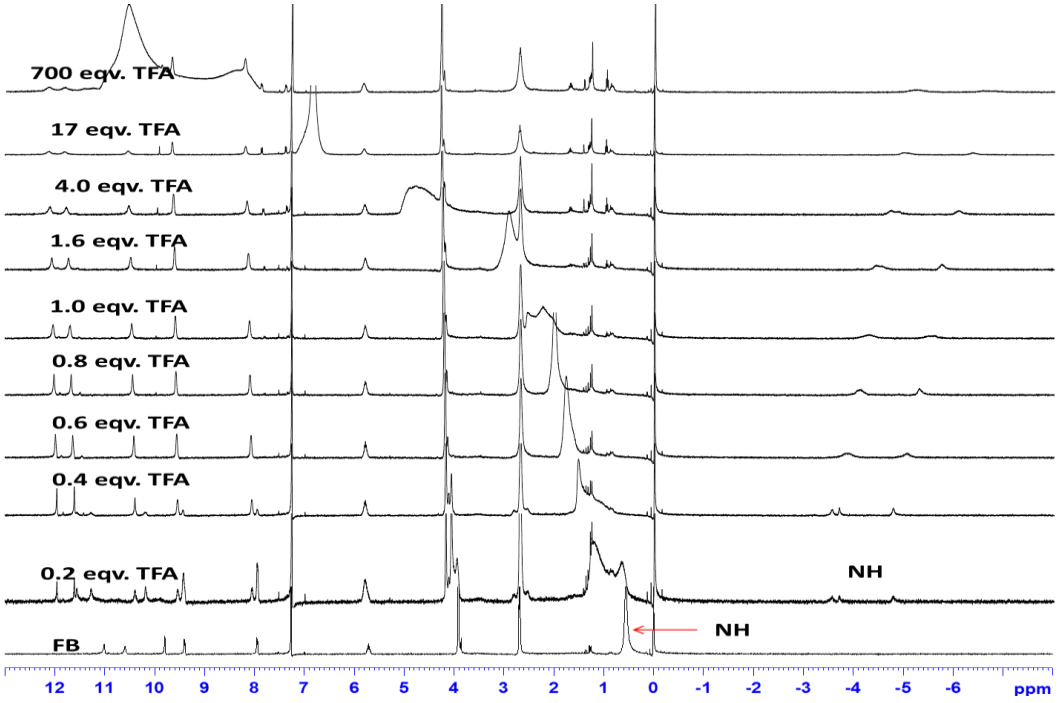

Figure 5.6 ^{1}H NMR titration of **TS31** free-base against TFA in $CDCl_3$.

with sharpening of the signals. For instance, four sets of triplets corresponding to ethyl CH_3 appears, instead of two observed in case free-base. All other CH protons also split into four sets along with six broad NH signals in the up field region, revealing an asymmetry in the structure (Figure 5.7). Further, the signals corresponding to *β*-pyrrole protons and *meso*-protons also undergo split, with one set of latter suffering larger split (10.50 and 11.47 ppm). This asymmetry persists even after removal of excess of acid present (by drying and again

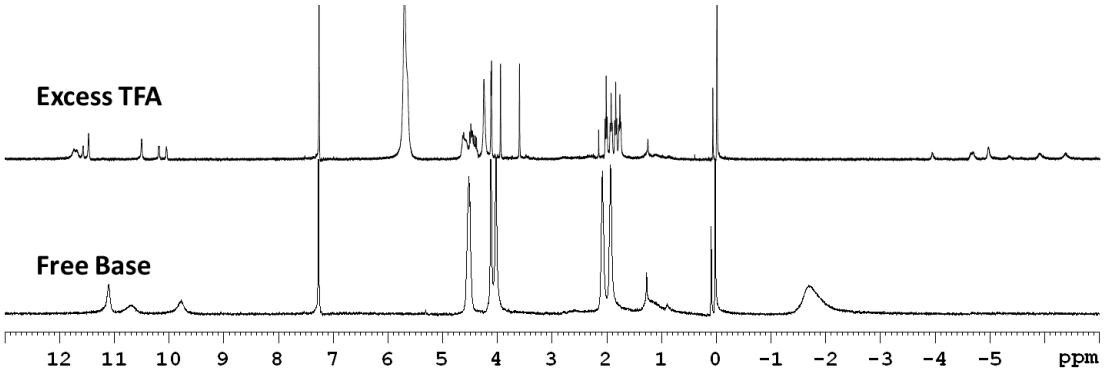

Figure 5.7 ^{1}H NMR spectra of **TS32** free-base in absence and in presence of excess of TFA in $CDCl_3$.

dissolving in $CDCl_3$ proton NMR was recorded). Although we don't have any clinching evidence, still from the above data we can speculate, owing to the greater steric repulsion between the two diethylpyrroles of the constituent bipyrrole entity, probably one of them gets distorted out of the sapphyrins mean plane upon protonation, thereby causing the resultant asymmetry. Further, the protonated species appears to possess a more rigid geometry than the corresponding free-base (sharper proton signals noticed in the former). However, elaborate study including variable temperature NMR study or X-ray crystal structure can reveal the actual picture.

5.3.3 Structural analysis of TS30

Solid state structure of **TS30** as its dihydrochloride salt (crystals obtained via slow evaporation of chloroform/hexane mixture) could be derived explicitly by X-ray diffraction (XRD) analysis. The structure of **TS30** reveals a near planar geometry. The two nitrogens of the bipyrrolic fragment N25, N29 distorted from the mean plane defined by the sapphyrin core (excluding alkyl substituents) by 0.33 and 0.27 Å respectively. These deviations are relatively more in comparison to the benzosapphyrin **L126** (0.19 and 0.09 Å). This reflects more strain in naphthobipyrrole moiety of **TS30** compared to its benzo counterpart. The other three nitrogens of tripyrrane fragment lies closer to the mean plane with a deviation in the

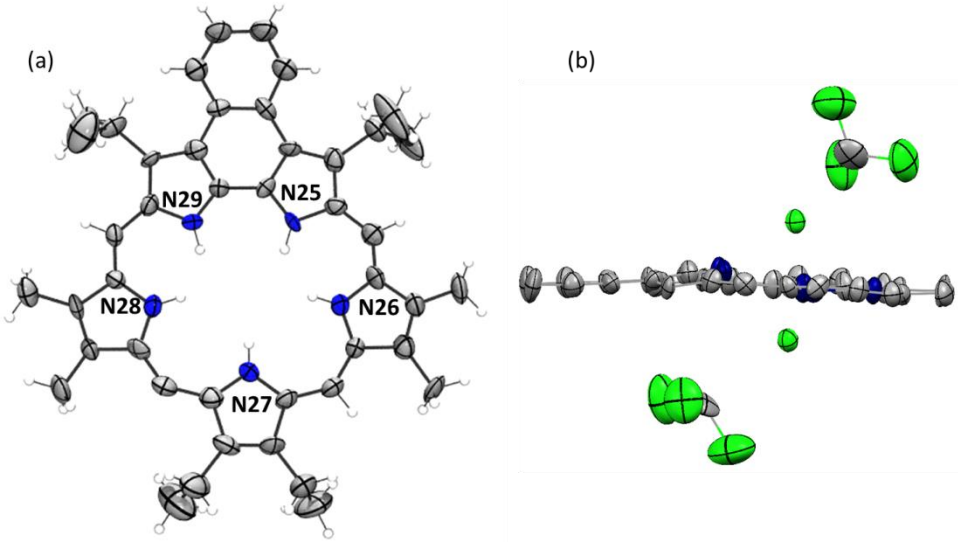

Figure 5.8 ORTEP of naphthosapphyrin **TS30·2HCl**. (a) Front view, two solvent ($CHCl_3$) molecules and chloride counter anions are omitted for clarity. (b) Side view, H-atoms and peripheral alkyl groups are omitted for clarity. Thermal ellipsoids are scaled to 35 % probability level.

range from 0.05 to 0.13 Å. Two chlorides ions were found above and below the macrocyclic core, wherein each of them were hydrogen bonded to three pyrrolic NH of the macrocycle with N…Cl distance (D Å) ranging from 3.08 to 3.26 Å. Distance of these two Cl^- from the mean plane were found to be 1.73 and 1.97 Å. The N-N distance between the N28-N26 is found to be 5.54 Å. This value is slightly greater than fluoride complex of decaalkylsapphyrin **L131**[6] (5.40 Å) and dihydrochloride salt of *meso*-diphenylsapphyrin **L132**[11] which is known to be inverted in its free-base form (5.33 Å). Sapphyrins containing bithiophene units are known to possess larger core size, with values generally found in the range of 6.23 - 6.39 Å.[28]

5.3.4 Optical properties of naphthosapphyrins TS30, TS31 and 2,3,22,23-tetraethyl-7,8,17,18-tetramethylsapphyrin TS32

The absorption spectra of free-base **TS30** shows a split Soret like band with absorption maxima at 488 nm and a shoulder at 468 nm whereas Q-like transitions appeared at 671, 692, 730 and 765 nm respectively (Figure 5.9). Thus Soret band is 22 nm and lowest energy Q-band is 37 nm red shifted in comparison to benzosapphyrin **L126**.[20] Similar split Soret band at 502 and 527 nm were also observed for analogous *meso*-tetraarylnaphthosapphyrin **L129**.[22] These bands are slightly red shifted compared to **TS30** owing to the *meso*-substituents in **L129**. Upon protonation, intensity of the Soret band increases depending upon the acid used for protonation (Figure 5.9). Maximum value of extinction coefficient obtained for bis-perchlorate salt of **TS30** (Table 5.2). Overall the extinction coefficients for both free-base and diprotonated form were found to be less compared to that of decaalkylsapphyrin. Similar trend was also observed for benzosapphyrin **L126**.[20] Diprotonated **TS30** displays a blue shifted Soret band (10 to 15 nm) compared to free-base. Upon protonation Q-bands also undergoes a blue shift with a relatively intense Q-like transition in the range of 696-699 nm, accompanied by a broad shoulder around 724-727 nm. The absorption pattern observed for different salts are more or less similar. All salts and free-base emit around 730 nm (Figure 5.9). However, quantum yield of free-base is found to be less compared to its diprotonated counterpart (Table 5.2).

Like **TS30** absorption spectrum of free-base **TS31** shows a well-defined split Soret band namely at 465 and 486 nm. Several Q-type absorption bands appeared at 670, 690, 733 and 771 nm revealing a similar pattern to that of **TS30** (Figure 5.10). Diprotonated form of **TS31** (obtained by washing with aqueous solution of different acids) show an increase in intensity

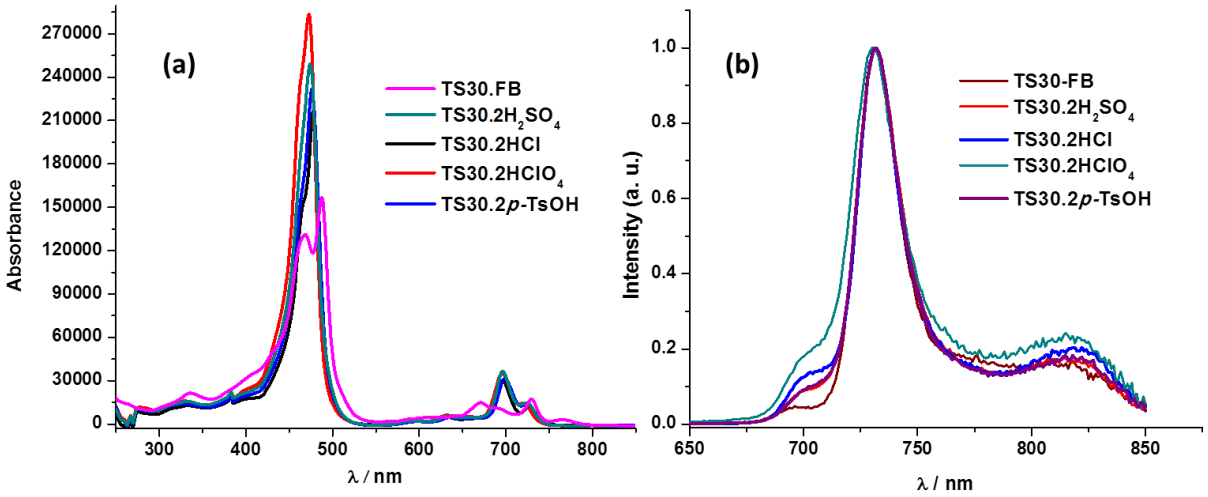

Figure 5.9 (a) UV-Vis and (b) normalized emission spectra of naphthosapphyrin **TS30** and its diprotonated salts measured in $CHCl_3$.

Table 5.2 Summary of absorption and emission properties of **TS30** and **TS31** in $CHCl_3$.

Compound	Solvent	Absorption		Emission		
		λ_{max} (nm)	ε ($M^{-1}cm^{-1}$)	λ_{exc} (nm)	λ_{max} (nm)	ϕ_f[a] (%)
TS30	$CHCl_3$	488	156000	502	732	1.3
TS30-2·HCl	$CHCl_3$	478	216000	440	731	3.8
TS30-2·HClO$_4$	$CHCl_3$	473	283000	498	730	2.1
TS30-2·H$_2$SO$_4$	$CHCl_3$	474	249000	497	731	5.3
TS30-2·PTSA	$CHCl_3$	476	231000	497	731	4.5
TS31	$CHCl_3$	486	109000	500	737	1.4
TS31-2·HCl	$CHCl_3$	475	199000	498	737	5.4
TS31-2·HClO$_4$	$CHCl_3$	459	200000	440	729	8.1
TS31-2·H$_2$SO$_4$	$CHCl_3$	470	122000	497	736	5.9
TS31-2·PTSA	$CHCl_3$	474	169000	500	736	4.3

[a]Florescence quantum yields were measured using tetraphenylporphyrin (TPP) as a reference.[29]

of Soret band with a marginal blue shift, accompanied by increased intensity and blue shift of the Q-bands compared to free-base form. Two well resolved Q-bands appeared around 699 (intense) and 731 nm revealing a similar pattern to that of diprotonated **TS30**. One notable difference between the two protonated sapphyrins is that splitting in the Soret band observed for free-base form remained in protonated **TS31**, which was not observed in case of protonat-

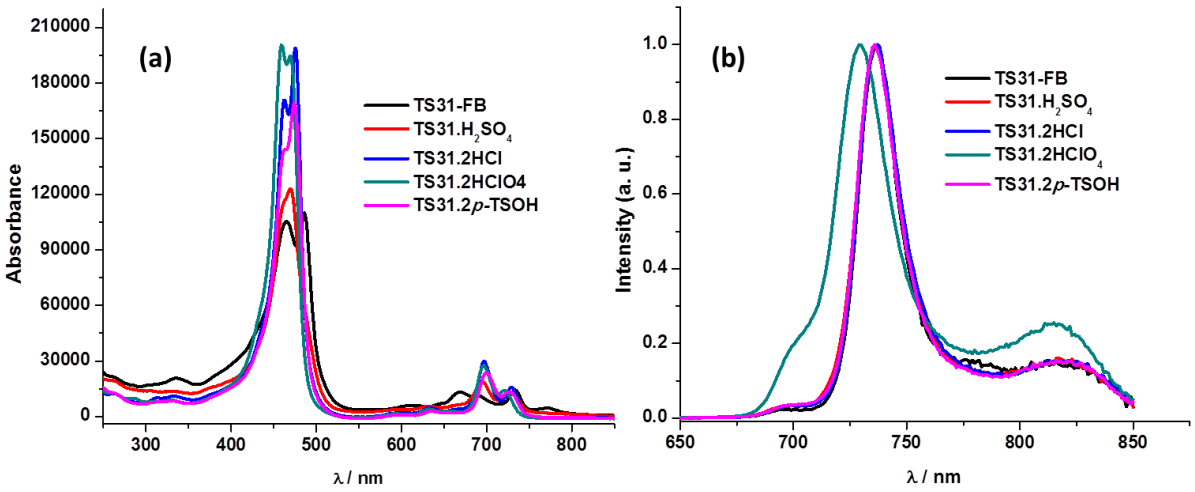

Figure 5.10 (a) UV-Vis and (b) normalized emission spectra of naphthosapphyrin **TS31** and its diprotonated salts measured in $CHCl_3$.

ed **TS30**. Emission spectra of free-base **TS31** as well as its different salts are shown in figure 5.10b. Except **TS31.2HClO$_4$** emission spectra of the rest of the compounds were found to be around 736 nm, which is slightly red shifted (5 nm) compared to **TS30** and its corresponding salts. To monitor if there is any structural change in presence of excess acid, a solution of **TS31** was titrated against a known amount of TFA (Figure 5.11a). No significant change was observed upon titrating with excess TFA, thereby excluding any structural change even in presence of excess acid. The spectra became almost saturated before addition of 2 equivalents of acids reflecting the fact that there is not much structural difference between mono and dicationic forms and moreover, the pK_{a1} and pK_{a2} values are very close. Similar titration with **TS30** free-base revealed analogous behavior (Figure 5.11b).

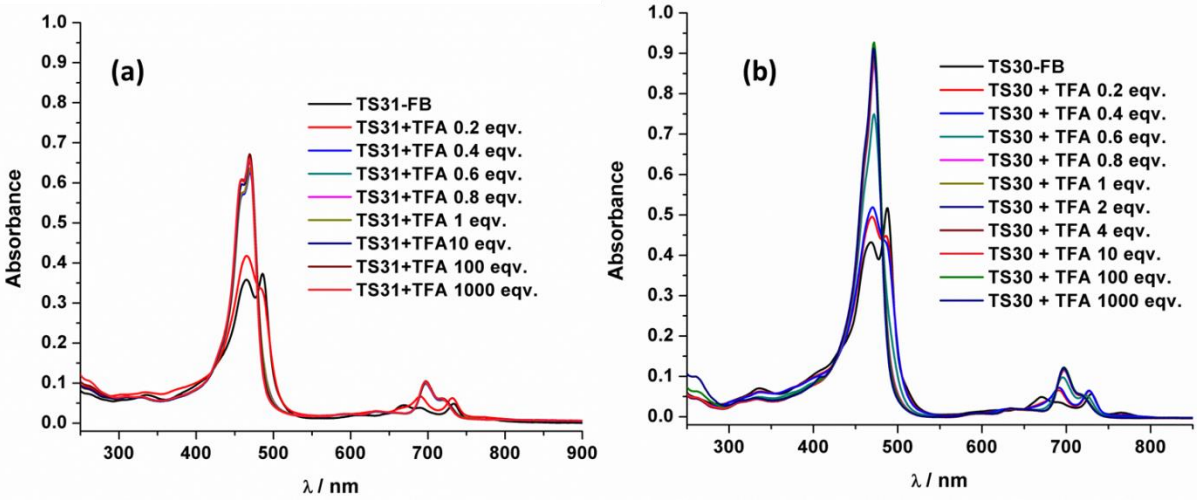

Figure 5.11 UV-Vis spectral titration of: (a) **TS31** and (b) **TS30** against TFA in $CHCl_3$.

UV-Vis absorption spectrum of free-base 2,3,22,23-tetraethyl-7,8,17,18-tetramethylsapphyrin **TS32** shows a Soret band at 454 nm along with three Q-type transitions at 648, 676 and 716 nm (Figure 5.12). Protonation caused a blue shift in Soret band (4 nm) as well as in the lowest energy Q-band (32 nm). Again titration of **TS32** with TFA does not result in any appreciable change in spectrum except increase in intensity, which confirms absence of any structural change, similar to that noticed in case of **TS31**.

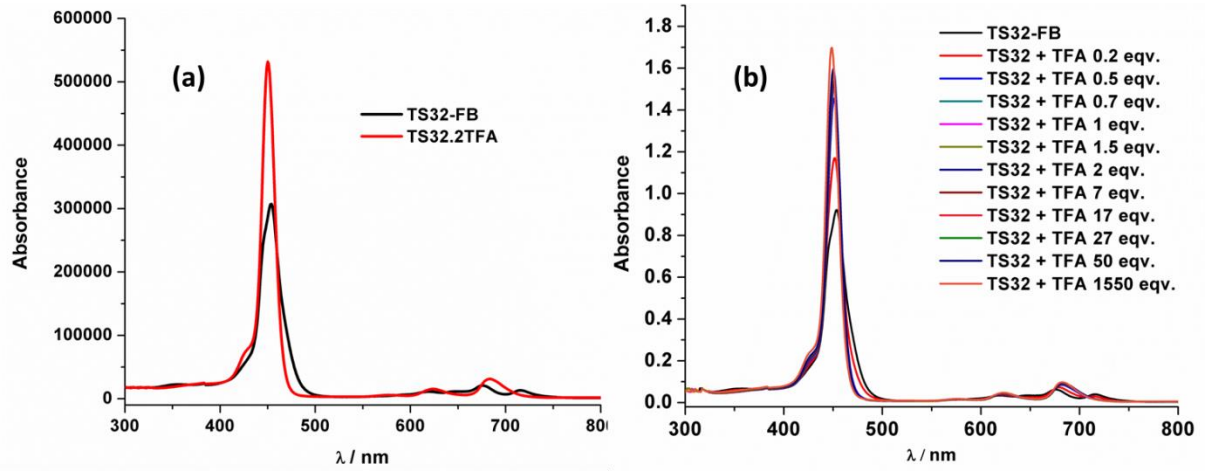

Figure 5.12 (a) UV-Vis spectra of **TS32** free-base and its TFA salt and (b) UV-Vis spectral titration of **TS32** with TFA in $CHCl_3$.

5.4 Conclusion

A rational synthesis of *meso*-unsubstituted alkylated naphthosapphyrins **TS30** and **TS31** has been demonstrated along with a previously unknown octaalkylsapphyrin **TS32**. Comparative photophysical properties of these molecules are presented. **TS31** and **TS32** were designed in such a way that pyrrole ring opposite to bipyrrolic fragment is unsubstituted in order to observe if there exist any conformational flexibility in this pyrrole ring even in the absence of *meso*-substituents. Our ^{1}H NMR and UV-visible spectroscopic studies rules out presence of any inverted structure in these macrocycle at least in room temperature. The steric strain imposed by ring fusion in **TS31** is not sufficient enough to cause an inversion in pyrrole ring opposite to it, as observed in case of *meso*-tetraaryl and hetero sapphyrins analogues. However, in case of **TS32** broadening of the *β*-pyrrolic protons in free-base form and complex nature of ^{1}H NMR spectrum in presence of TFA indicates that in comparison to **TS31** this system is more flexible, probably resulting in one of the bipyrrolic pyrrole moiety going out of the plane to relieve the steric strain. Therefore it may be possible to observe new ways of ring inversion in a system where bipyrrole is more sterically crowded.

5.5 Experimental

Synthesis of tetramethyltripyrromethane dibenzylester TS33

Benzyl 5-(acetoxymethyl)-3,4-dimethylpyrrole-2-carboxylate **TS9** (500 mg, 1.7 mmol) was dissolved in ethanol (20 mL). Acetic acid (0.49 mL, 8.5 mmol) was added followed by addition of pyrrole (0.059 mL, 0.85 mmol). The reaction mixture was heated to reflux for 24 h under nitrogen atmosphere with continuous stirring. After the completion of the reaction, (monitored by checking TLC) solvent was evaporated. Residue was again dissolved in dichloromethane and washed with water to remove the excess acetic acid. Organic layer was evaporated and purified in a silica column using a mixture of hexane and ethyl acetate (9 : 1) as eluent, to obtain the desired tetramethyltripyrromethane **TS33** as a white solid. Yield: 357 mg (76.6 %).

^{1}H NMR (400 MHz, $CDCl_3$, δ in ppm): 1.83 (s, 6H, -CH_3), 2.21 (s, 6H, -CH_3), 3.66 (s, 4H, -CH_2 *meso*), 4.31 (s, 4H, -CH_2 Bn), 5.90 (s, 2H, -CH Py), 7.05 (m, 4H, -CH Ph), 7.23 (m, 2H, -CH Ph), 7.27 (m, 4H, -CH Ph); ^{13}C NMR (100 MHz, $CDCl_3$, δ in ppm): 8.68, 11.40, 24.46, 65.34, 104.78, 116.76, 117.19, 126.46, 127.31, 127.92, 128.27, 133.13, 136.96, 163.02. HR-MS (ESI): *m/z* calcd for $C_{34}H_{36}N_3O_4$ $[M+H]^+$: 550.2706; found 550.2702.

Synthesis of tripyrrane diacid TS34

Tripyrrane dibenzylester **TS33** (350 mg, 0.64 mmol) was dissolved in freshly distilled dry THF (50 mL) and placed in a round bottom flask. The solution was diluted with methanol (17 mL). After that 5 % Pd/C (180 mg, 0.084 mmol) was added, air was flushed out from the vessel with H_2 and the reaction mixture was stirred under an atmosphere of H_2 for 16 h. After completion of the reaction, the catalyst was removed by suction filtration over celite pad and the solvent was evaporated under reduced pressure (below 30 °C), dried under high vacuum and used directly in the next step without further purification and characterization.

Synthesis of naphthosapphyrin TS30

β-Isopropyl naphthobipyrrole dialdehyde **TS21b** (170 mg, 0.49 mmol) was placed in a 500 mL round bottom flask containing absolute ethanol (360 mL), heated to reflux until any undissolved material remains. After cooling to room temperature, tripyrromethane dicarboxylic acid derivative **TS11** (210 mg, 0.49 mmol) was added followed by the addition of *p*-TsOH.H_2O (378 mg, 1.96 mmol). Reaction was protected from light and stirred for 24 h at room temperature with continuous oxygen bubbling through the reaction mixture. After the completion of the reaction, solvent was evaporated under reduced pressure, the residual dark

solid material was dissolved in $CHCl_3$ and washed thoroughly with water. Organic layer was evaporated and the resulting residue was purified over a silica column ($CHCl_3$ with increasing methanol content up to 10 % V/V). Green fraction thus obtained was collected and washed with 1 M aqueous NaOH solution to get the product in free-base form. Repeated column chromatography is necessary to obtain the pure product. Yield 57 mg, 18 %.

^{1}H NMR (400 MHz, $CDCl_3$, δ in ppm): -0.53 (brs, 3H, NH), 2.08 (brs, 6H, -CH_3 Et), 2.65 (brd, 12H, -CH_3 *i*-Pr), 3.96 (s, 12H, -CH_3 Me), 4.52 (brd, 4H, CH_2 Et), 5.74 (m, 2H, -CH *i*-Pr), 7.94 (m, 2H, -CH naph), 9.41 (m, 2H, -CH naph), 10.92 (s, 2H, CH *meso*), 11.26 (s, 2H, CH *meso*); HR-MS (ESI): *m/z* calcd for $C_{44}H_{48}N_5$ $[M+H]^+$: 646.3910; found 646.3909; UV-Vis ($CHCl_3$) λ_{max} (ε): 335 (21343), 468 (130921), 488 (156565), 624 (4724), 671 (14845), 689 (10942), 730 (17024), 765 (3065).

Diprotonated salts were obtained by washing a $CHCl_3$ solution of free-base with aqueous solution of various acids.

TS30.2HCl: ^{1}H NMR (400 MHz, $CDCl_3$, δ in ppm): -4.37 (s, 2H, NH), -3.64 (s, 1H, NH), -3.17 (s, 2H, NH), 2.30 (t, *J* = 7.2 Hz, 6H, -CH_3 Et,), 2.68 (d, *J* = 6.8Hz, 12H, -CH_3 *i*-Pr), 4.14 (s, 12H, -CH_3 Me), 4.65 (m, 4H, CH_2 Et), 5.79 (m, 2H, -CH *i*-Pr), 8.01 (m, 2H, -CH naph), 9.50 (m, 2H, -CH naph), 11.54 (s, 2H, CH *meso*), 11.85 (s, 2H, CH *meso*).

TS30.2HClO$_4$: ^{1}H NMR (400 MHz, $CDCl_3$, δ in ppm): -6.41 (s, 2H, NH), -5.51 (s, 1H, NH), -5.14 (s, 2H, NH), 2.29 (t, *J* = 7.6 Hz, 6H, -CH_3 Et), 2.66 (d, *J* = 7.2 Hz, 12H, -CH_3 *i*-Pr), 4.18 (s, 12H, -CH_3 Me), 4.67 (q, *J* = 7.2 Hz, 4H, CH_2 Et), 5.75 (m, 2H, -CH *i*-Pr), 8.08 (m, 2H, -CH naph), 9.63 (m, 2H, -CH naph), 11.63 (s, 2H, CH *meso*), 11.95 (s, 2H, CH *meso*).

TS30.2*p*-TsOH: ^{1}H NMR (400 MHz, $CDCl_3$, δ in ppm): -4.88 (s, 2H, NH), -4.26 (s, 1H, NH), -4.05 (s, 2H, NH), 2.36 (m, 6H, -CH_3 Et), 2.74 (d, *J* = 7.2 Hz, 12H, -CH_3 *i*-Pr), 4.10 (s, 12H, -CH_3 Me), 4.61 (q, *J* = 7.2 Hz, 4H, CH_2 Et), 5.41 (s, 4H, Ph *p*-TsOH), 5.73 (m, 2H, -CH *i*-Pr), 8.03 (m, 2H, -CH naph), 9.45 (m, 2H, -CH naph), 11.37 (s, 2H, CH *meso*), 11.75 (s, 2H, CH *meso*).

TS30.H$_2$SO$_4$: ^{1}H NMR (400 MHz, $CDCl_3$, δ in ppm): -4.34 (s, 2H, NH), -3.71(s, 1H, NH), -3.16 (s, 2H, NH), 2.27 (brs, 6H, -CH_3 Et), 2.69 (brs, 12H, -CH_3 *i*-Pr), 4.15 (brs, 12H, -CH_3 Me), 4.66 (brs, 4H, CH_2 Et), 5.79 (brs, 2H, -CH *i*-Pr), 8.03 (s, 2H, -CH naph), 9.52 (s, 2H, -CH naph), 11.54 (s, 2H, CH *meso*), 11.85 (brs, 2H, CH *meso*).

Synthesis of naphthosapphyrin TS31

β-Isopropyl naphthobipyrrole dialdehyde **TS21b** (125 mg, 0.36 mmol) was placed in a 500

mL round bottom flask containing absolute ethanol (350 mL), heated to reflux until any undisolved material remains. After cooling to room temperature tetramethyltripyrromethane dicarboxylic acid **TS34** (134 mg, 0.36 mmol) was added, followed by the addition of *p*-TsOH.H_2O (275 mg, 1.44 mmol). Reaction was protected from light and stirred for 24 h at room temperature with continuous oxygen bubbling through the reaction mixture. After the completion of the reaction, solvent was evaporated under reduced pressure, the residual dark solid material was dissolved in $CHCl_3$ and washed thoroughly with water. Organic layer was evaporated and the resulting residue was purified over a silica column ($CHCl_3$ with increasing methanol content up to 10 % V/V). Green fraction thus obtained was collected and washed with 1 M aqueous NaOH solution to get the product in free-base form. Repeated column chromatography is necessary to obtain the pure product. Yield 56 mg, 26 %.

^{1}H NMR (400 MHz, $CDCl_3$, δ in ppm): -0.95 (brs, 3H, NH), 2.68 (d, J = 7.2 Hz, 12 H, -CH_3 *i*-Pr), 3.83 (s, 6H, -CH_3 Me), 3.86 (s, 6H, -CH_3 Me), 5.65 (m, 2 H, -CH *i*-Pr), 7.96 (m, 2H, -CH naph), 9.38 (m, 2H, -CH naph), 9.55 (s, 2H, -CH Py), 10.20 (s, 2H, CH *meso*), 10.74 (s, 2H, CH *meso*); HR-MS (ESI): *m/z* calcd for $C_{40}H_{40}N_5$ $[M+H]^+$: 590.3284; found 590.3286; UV-Vis ($CHCl_3$) λ_{max} (ε): 335 (20735), 465 (105402), 486 (109862), 615 (5884), 670 (13220), 690 (11324), 733 (14325), 771 (4526).

Diprotonated salts were obtained by washing a $CHCl_3$ solution of free-base with aqueous solution of various acids.

TS31.2HCl: ^{1}H NMR (400 MHz, $CDCl_3$, δ in ppm): -4.81 (brs, 2H, NH), -3.56 (brs, 1H, NH), -3.54 (brs, 2H, NH), 2.71 (d, J = 7.2 Hz, 12 H, -CH_3 *i*-Pr), 4.19 (s, 12H, -CH_3 Me), 5.81 (m, 2 H, -CH *i*-Pr), 8.02 (m, 2H, -CH naph), 9.52 (m, 2H, -CH naph), 10.36 (s, 2H, -CH Py), 11.65 (s, 2H, CH *meso*), 11.96 (s, 2H, CH *meso*).

TS31.2TFA: ^{1}H NMR (400 MHz, $CDCl_3$, δ in ppm): -5.13 (brs, 2H, NH), -3.99 (brs, 1H, NH), -3.91 (brs, 2H, NH), 2.67 (brs, 12 H, -CH_3 *i*-Pr), 4.20 (s, 12H, -CH_3 Me), 5.79 (m, 2 H, -CH *i*-Pr), 8.07 (m, 2H, -CH naph), 9.56 (m, 2H, -CH naph), 10.43 (s, 2H, -CH Py), 11.65 (s, 2H, CH *meso*), 11.99 (s, 2H, CH *meso*).

TS31.2*p*-TsOH: ^{1}H NMR (400 MHz, $CDCl_3$, δ in ppm): -5.26 (brs, 2H, NH), -4.43 (brs, 2H, NH), -4.19 (brs, 1H, NH), 2.76 (brs, 12 H, -CH_3 *i*-Pr), 4.13 (s, 12H, -CH_3 Me), 5.33 (s, 4H, Ph *p*-TsOH), 5.77 (m, 2H, -CH *i*-Pr), 8.05 (m, 2H, -CH naph), 9.48 (m, 2H, -CH naph), 10.31 (s, 2H, -CH Py), 11.48 (s, 2H, CH *meso*), 11.83 (s, 2H, CH *meso*).

Synthesis of 2,3,22,23-tetraethyl-7,8,17,18-tetramethylsapphyrin TS32

Tetraethylbipyrrole dialdehyde **TS13** (70 mg, 0.24 mmol) was placed in a 500 mL round bottom flask containing absolute ethanol (200 mL). Tetramethyltripyrromethane dicarboxylic acid **TS34** (90 mg, 0.24 mmol) was added, followed by the addition of *p*-TsOH.H_2O (185 mg, 0.97 mmol). Reaction was protected from light and stirred for 24 h at room temperature with continuous oxygen bubbling through the reaction mixture. After the completion of the reaction, solvent was evaporated under reduced pressure, the residual dark solid material was dissolved in $CHCl_3$ and washed thoroughly with water. Organic layer was evaporated and the resulting residue was purified over a silica column ($CHCl_3$ with increasing methanol content up to 10 % V/V). Green fraction thus obtained was collected and washed with 1 M aqueous NaOH solution to get the product in free-base form. Repeated column chromatography is necessary to obtain the pure product. Yield 23 mg, 25 %.

^{1}H NMR (400 MHz, $CDCl_3$, δ in ppm): -1.69 (brs, 3H, NH), 1.94 (s, 6H, -CH_3 Et), 2.08 (s, 6H, -CH_3 Et), 4.03 (s, 6H, -CH_3 Me), 4.12 (s, 6H, -CH_3 Me), 4.50 (brs, 8H, -CH_2 Et), 9.80 (brs, 2H, -CH Py), 10.70 (brs, 2H, CH *meso*), 11.06 (brs, 2H, CH *meso*). HR-MS (ESI): *m/z* calcd for $C_{36}H_{42}N_5$ $[M+H]^+$: 544.3440; found 544.3439; UV-Vis ($CHCl_3$) λ_{max} (ε): 270 (170060), 454 (307256), 676 (20942), 716 (13363).

Spectrum of diprotonated salt was recorded by addition of excess TFA directly to a $CDCl_3$ solution of free-base in the NMR tube.

TS32.2TFA: ^{1}H NMR (400 MHz, $CDCl_3$, δ in ppm): -6.40 (brs, 1H, NH), -5.90 (brs, 1H, NH), -5.30 (brs, 1H, NH), -5.0 (brs, 1H, NH), -4.64 (brs, 1H, NH), -3.93 (brs, 1H, NH), 1.77 (t, *J* = 7.6 Hz, 3H, -CH_3 Et), 1.84 (t, *J* = 7.6 Hz, 3H, - CH_3 Et), 1.93 (t, *J* = 7.6 Hz, 3H, -CH_3 Et), 2.01 (t, *J* = 7.6 Hz, 3H, -CH_3 Et), 3.60 – 4.25 (s, 12H, -CH_3 Me), 4.38 – 5.70 (m, 8H, -CH_2 Et), 10.04 (brs, 1H, -CH Py), 10.17 (brs, 1H, -CH Py),10.49 (brs, 1H, CH *meso*), 11.46 (brs, 1H, CH *meso*), 11.57 (brs, 1H, CH *meso*), 11.70 (brs, 1H, CH *meso*). UV-Vis ($CHCl_3$) λ_{max} (ε): 270 (170060), 450 (531906), 624 (15412), 684 (31114).

5.6 Crystallographic details

Crystallographic data for **TS30.2HCl** was collected on Oxford Gemini A Ultra diffractometer with dual source. Pertinent crystallographic data collection and refinement parameters are shown in the following table:

Table 5.3 Crystallographic parameters of crystals of **TS30.2HCl**

Crystal data	**TS30.2HCl**
Formula unit	C_{44} H_{47} N_5.2HCl.2$CHCl_3$
Formula wt.	957.52
Crystal system	Triclinic
T [K]	293 (2)
a [Å]	11.7524 (18)
b [Å]	13.482 (2)
c [Å]	15.789 (2)
α [°]	73.411 (14)
β [°]	83.366 (13)
γ [°]	86.846 (13)
volume [$Å^3$]	2381.0 (6)
Space group	P -1
Z′	1
Z	2
D_{calc} [$g.cm^{-3}$]	1.336
μ/mm^{-1}	0.511
Reflns collected	18639
Unique reflns	10667
Observed reflns	1785
R(int)	0.2007
R_1 [I > 2σ(I)]	0.1159 (1785)
wR_2	0.3715 (10667)
GOF	0.916

5.7 References

1. First mentioned by Woodward, R. B. in Aromaticity: An International Symposium, Sheffield, U. K., **1966**.
2. Broadhurst, M. J.; Grigg, R.; Johnson, A. W. *J. Chem. Soc., Chem. Commun.* **1969**, 23.
3. Broadhurst, M. J.; Grigg, R.; Johnson, A. W. *J. Chem. Soc., Chem. Commun.* **1969**, 1480.
4. (a) Bauer, V. J.; Clive, D. L. J.; Dolphin, D.; Paine, J. B.; Harris, F. L.; King, M. M.; Loder, J.; Wang, S. W. C.; Woodward, R. B. *J. Am. Chem. Soc.* **1983**, *105*, 6429. (b) Broadhurst, M. J.; Grigg, R.; Johnson, A. W. *J. Chem. Soc., Perkin Trans. I.* **1972**, 1124.
5. (a) Johnson, A. W. In *Porphyrin and Metalloporphyrins*; Smith, K. M., Ed.; Elsevier: Amsterdam, **1976**, 750. (b) Grigg, R. In The Porphyrins, *Vol. 2*; Dolphin, D., Ed.; Academic Press: New York, **1978**, 327. (c) Sessler, J. L.; Weghorn, S. J. *Expanded, Contracted and Isomeric Porphyrins* Pergamon, New York, **1997**.
6. Sessler, J. L.; Cyr, M. J.; Lynch, V.; McGhee, E.; Ibers, J. A. *J. Am. Chem. Soc*. **1990**, *112*, 2810.
7. Sessler, J. L.; Davis, J. M. *Acc. Chem. Res.* **2001**, *34*, 989.
8. (a) Richter, D. T.; Lash, T. D. *Tetrahedron Lett.* **1999**, *40*, 6735. (b) Richter, D. T.; Lash, T. D. *J. Org. Chem.* **2004**, *69*, 8842.
9. Paolesse, R.; Licoccia, S.; Spagnoli, M.; Boschi, T.; Khoury, R. G.; Smith, K. M. *J. Org. Chem*. **1997**, *62*, 5133.
10. Sessler, J. L.; Shevchuk, S.; Davis, J. M. *Tetrahedron Lett.* **2001**, *42*, 2447.
11. Sessler, J. L.; Lisowski, J.; Boudreaux, K. A.; Lynch, V.; Barry, J.; Kodadek, T. J. *J. Org. Chem.* **1995**, *60*, 5975.
12. Chmielewski, P. J.; Latos-Grażyński, L.; Rachlewicz, K. *Chem. Eur. J.* **1995**, *1*, 68.
13. Bruckner, C.; Sternberg, E. D.; Boyle, R. W.; Dolphin, D. *Chem. Commun*. **1997**, 1689.
14. Narayanan, S. J.; Sridevi, B.; Srinivasan, A.; Chandrashekar, T. K.; Roy, R. *Tetrahedron Lett.* **1998**, *39*, 7389.
15. Yuan, M.; Ou, Z.; Fang, Y.; Huang, S.; Xue, Z.; Lu, G.; Kadish, K. M. *Inorg. Chem*. **2013**, *52*, 6664.
16. Ka, J. W.; Lee, C. H. *Tetrahedron Lett*. **2001**, *42*, 4527.

17. Simkhovich, L.; Rosenberg, S.; Gross, Z. *Tetrahedron Lett*. **2001**, *42*, 4929.
18. Ono, N.; Kuroki, K.; Watanabe, E.; Ochi, N.; Uno, H. *Heterocycles* **2004**, *62*, 365.
19. Okujima, T.; Kikkawa, T.; Kawakami, S.; Shimizu, Y.; Yamada, H.; Ono, N.; Uno. H. *Tetrahedron*, **2010**, *66*, 7213.
20. Panda, P. K.; Kang, Y.–J.; Lee, C.–H. *Angew. Chem., Int. Ed.* **2005**, *44*, 4053.
21. Cho, D.-G; Plitt, P.; Kim, S. K.; Lynch, V.; Hong, S.-J.; Lee, C.-H.; Sessler, J. L. *J. Am. Chem. Soc*. **2008**, *130*, 10502.
22. Kee, S.-Y.; Lim, J. M.; Kim, S.-J.; Yoo, J.; Park, J.-S.; Sarma, T.; Lynch, V. M.; Panda, P. K.; Sessler, J. L.; Kim, D.; Lee, C.-H. *Chem. Commun.* **2011**, *47*, 6813.
23. Rachlewicz, K.; Spurtta, N.; Latos-Grażyński, L.; Chmielewski, P. J.; Szterenberg, L. *J. Chem. Soc., Perkin Trans. 2* **1998**, 959.
24. Misra, R.; Chandrashekar, T. K. *Acc. Chem. Res.* **2008**, *41*, 265.
25. (a) Narayanan, S. J.; Sridevi, B.; Chandrashekar, T. K.; Vij, A.; Roy, R. *J. Am. Chem. Soc.* **1999**, *121*, 9053
26. (a) Srinivasan, A.; Anand, V. G.; Narayanan, S. J.; Pushpan, S. K.; Kumar, M. R.; Chandrashekar, T. K.; Sugiura, K.-I.; Sakata, Y. *J. Org. Chem.* **1999**, *64*, 8693. (b) Rachlewicz, K.; Sprutta, N.; Chmielewski, P. J.; Latos-Grazynski, L. *J. Chem. Soc., Perkin Trans. 2* **1998**, 969.
27. Narayanan, S. J.; Sridevi, B.; Chandrashekar, T. K.; Vij, A.; Roy, R. *Angew. Chem. Int. Ed.* **1998**, *37*, 3394.
28. Shin, K.; Lim, C.; Choi, C.; Kim, Y.; Lee, C.-H. *Chem. Lett.* **1999**, *28*, 1331.
29. Ohno, O.; Kaizu, Y.; Kobayashi, H. *J. Chem. Phys.* **1985**, *82*, 1779.

CHAPTER 6

Naphthobipyrrole derived BODIPY complexes

6.1 Introduction

Recently NIR dyes drew wide attention of researchers, owing to their potential in optical engineering, analytical chemistry, biology, and medicine as new revolutionary tools for noninvasive and simple in vivo optical imaging. NIR fluorescent dyes have been often spotlighted owing to the advantages of this region as significant reduction of the background signal due to the lowest auto-absorption and auto-fluorescence of biomolecules in the NIR region, low-light scattering and deep penetration of NIR light and the possibility to use as low-cost excitation light sources.[1] For instance water, melanin, proteins, and hemoglobin (Hb) absorbs between 200 and 650 nm, covering essentially the whole visible range. In addition to absorbing light, tissues can also reflect, refract and scatter incident photons thereby reducing their achievable sensitivity.[2]

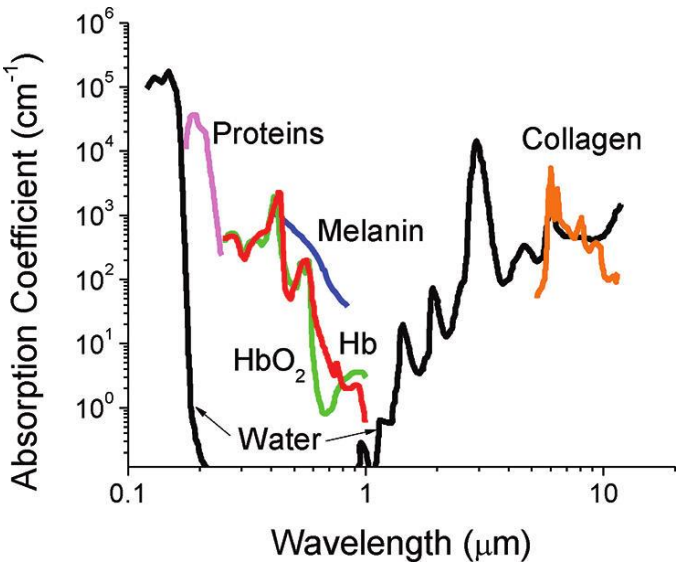

Figure 6.1 Absorbance of various tissues and blood components from 0.2 to 10 μm.[2d-f]

Therefore, much attention has been focused in recent years on the development of absorption imaging agents and fluorophores, whose absorbance or emission maxima falls in the region of minimal tissue absorbance/autofluorescence i.e. between 650-1450 nm, known as imaging window.

6.1.1 Desired characteristics of NIR dyes

For effective application of NIR dye in sensing, particularly for biological samples, demands good solubility in water.[3] Many of the NIR dyes are water insoluble owing to its extended π-conjugation. Another common problem associated with NIR dyes is aggregation, which often reduces fluorescence intensities and alter their absorption properties.[4] Moreover strong

absorption and emission with high fluorescence quantum yield and photostability are most desirable quality of an efficient NIR dye. Among the fluorescent organic NIR dyes cyanine and squaraine are the most well-known. Infact, indocyanine green **L141** (ICG) is the only FDA approved long wavelength dye for direct administration in medical diagnostics.[5] Recently, BODIPY dyes precisely conformationally restricted, show immense promise as a potential NIR dye. A very brief introduction of cyanine and squaraine dyes along with NIR absorbing and emitting BODIPY dyes are presented below.

6.1.2 Cyanine dyes

Cyanine dyes (Figure 6.2) are often employed as fluorescent probe for investigating biological processes such as enzyme activity[6], calcium and zinc[7], nitric oxide[8] and proton

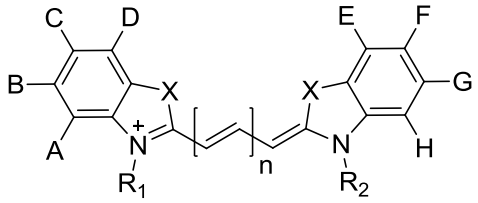

L138

Figure 6.2 General structure of a cyanine dye. A–H are hydrogens or functionalities including SO_3H or may be a labeling position. X = $C(CH_3)_2$, O, or S; R_1 and R_2 = alkyl groups and can include a labeling position; n = 1–3.

concentration[9] as well as *in vivo* imaging. General structure of cyanine dye (Cy) contains a polymethine chain connected with two heterocyclic units at its terminals (Figure 6.2). One of the nitrogen atoms is a positively charged iminium and the other is an amine. The spectral range of absorption and emission can be tuned by adjusting length of the polymethine chain, usually increasing one vinylene unit (CH = CH), causes red shift by about 100 nm. Thus this class of dye provides broad wavelength tunability. Particularly NIR absorption and emission with high extinction coefficient and moderate quantum yield make them appealing for varieties of applications. However, most cyanine dyes self-aggregate in aqueous solutions.[10] Substitution by sulfonate groups on the aromatic rings of the dyes reduces aggregation in water. For instance Cy5 (**L139** absorption/emission: 650/667 nm) and Cy7 (**L140** absorption/emission: 750/777 nm) are highly soluble in water and fluoresce brightly.[11] Another problem associated with Cy dyes is the presence of long polymethine chain (n > 3) often causes reduction of extinction coefficient and fluorescence quantum yield owing to its

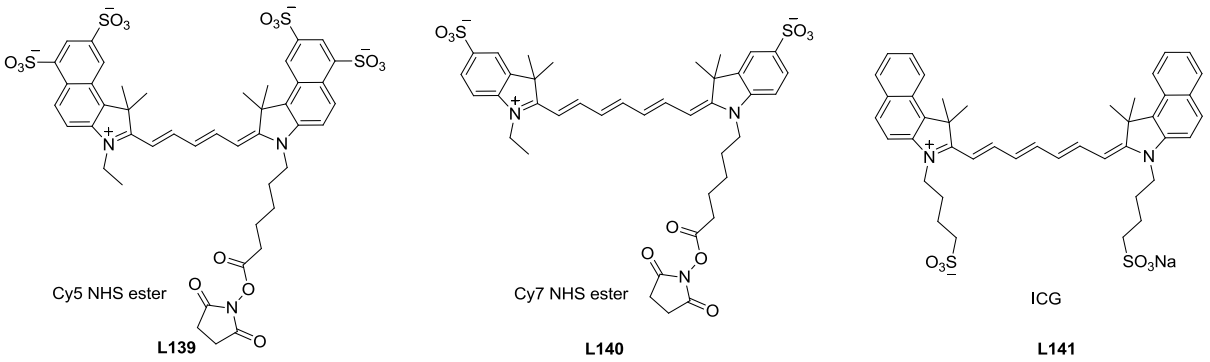

Figure 6.3 Representative examples of some cyanine dyes.

structural flexibility. However, replacing linear polymethine chain with a bridged polymethine chain makes the long link less flexible. Two examples of dyes with this feature are NIR 820 (**L142**) and IRDye 78 (**L143**) which has an absorption maximum at 790 nm and an emission maximum at 820 nm.[12]

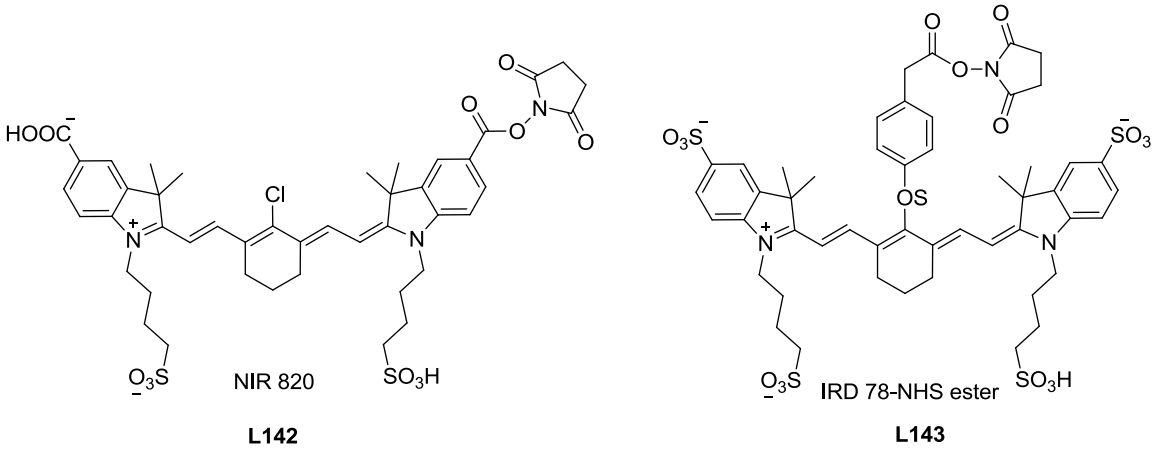

Figure 6.4 Structure of conformationally rigid NIR cyanine dye.

6.1.3 Squaraine dyes

Squaraines are a class of dye with resonance-stabilized zwitterionic structures that possess a cyclobutenediyliumdiolate core. General structure of squaraine contains an electron deficient four membered ring connected with two electron donating groups so as to form a donor-acceptor-donor (D-A-D) sequence. Typical examples of squaraine are shown in Figure 6.5. Squaraines in general possess high extinction coefficient, fluorescence quantum yield and photostability in the visible to near-IR region. These features made them useful for wide ranging applications such as imaging,[13] nonlinear optics,[14] photovoltaics,[15] photodynamic therapy[16] and ion sensing.[17] Squaraine dyes were first synthesized in 1965 by Triebs and

Jacob, by reacting pyrrole with 3,4-dihydroxy-3-cyclobutene-1,2-dione **L146** (squaric acid) as shown in scheme 6.1.[18] Later a plethora of squaraine dyes with tunable optical properties

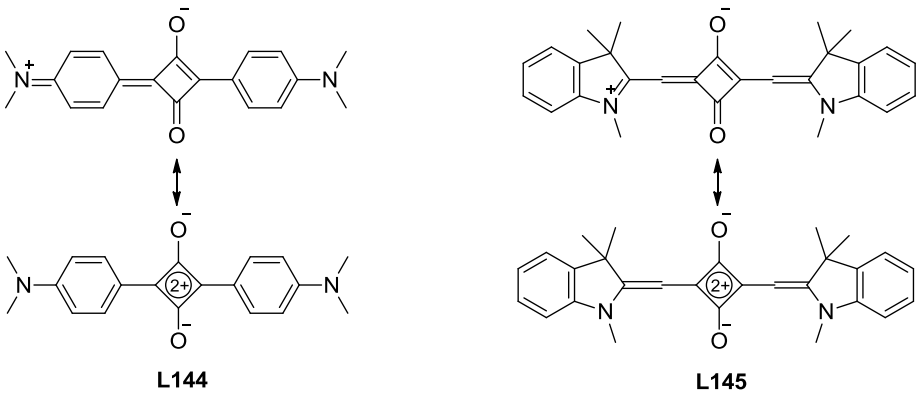

Figure 6.5 Resonance structures of squaraine dyes.

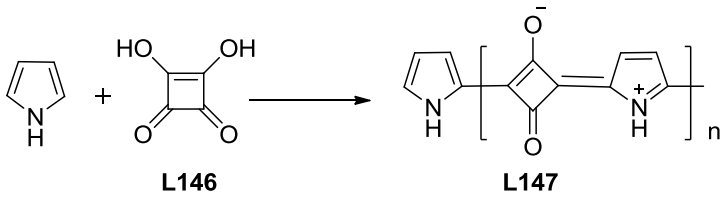

Scheme 6.1 General synthetic pathway to squaraine dye.

have been synthesized by coupling of electron-rich aromatic or heterocyclic compounds such as N,N-dialkylanilines, benzothiazoles, phenols, azulenes and pyrroles with squaric acid. Red shift in absorption and emission properties of squaraines can be achieved either by the use of strong electron donors or by the extension of conjugation. In recent times a large number of

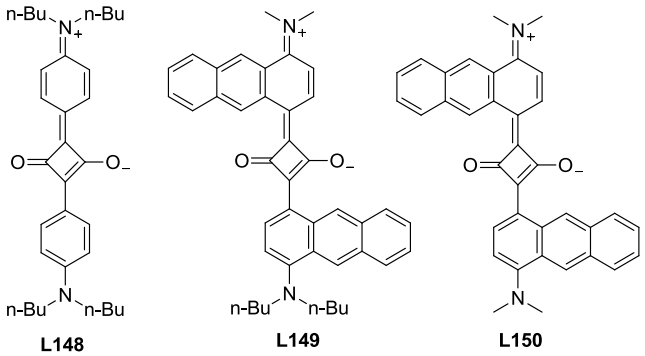

Figure 6.6 π-extension in squaraine dye.

squaraines with near-IR absorption and emission has been synthesized using this approach.[19] For example replacement of the dialkylaniline moiety of bis[4-(N,N-

dibutylamino)phenyl]squaraine DBAS (**L148**), with dialkylanthracene yields squaraine dyes **L149** and **L150**,[19a] with their absorption and emission spectra strongly shifted to the NIR region (Figure 6.7).

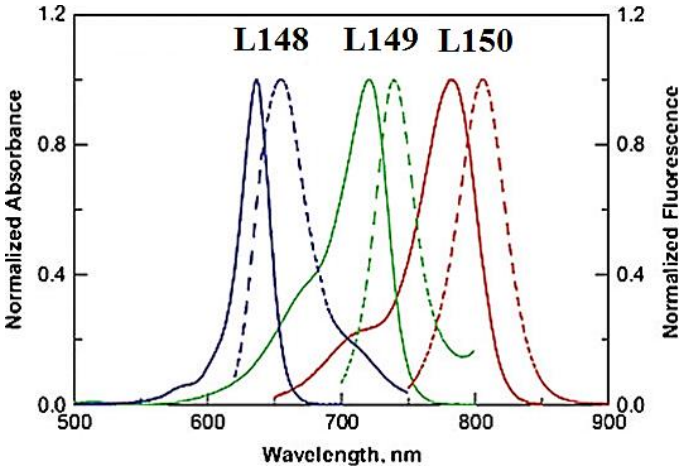

Figure 6.7 Normalized absorption (solid lines) and emission spectra (dashed lines) of **L148**, **L149**, and **L150** in toluene.[19a]

6.1.4 Boron dipyrromethene based NIR dyes

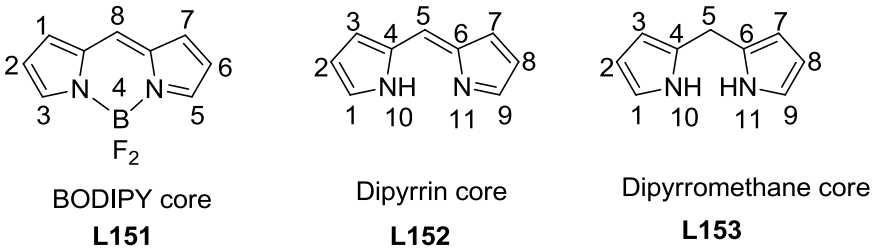

Figure 6.8 IUPAC numbering system of BODIPY and dipyrromethene.

Although various NIR fluorescent dyes have been emerged in recent times, many of them suffer from certain insufficient optical characteristics such as low fluorescence quantum yields or a lack of photostability.[20] Therefore, quest for new efficient NIR dyes, endowed with intense absorption and greater fluorescent quantum yield still continues. Difluoro-4-bora-3a,4a-diaza-*s*-indacene dye commonly known as BODIPY dyes were first discovered in 1968 by Treibs and Kreuzer.[21] Unsubstituted BODIPY **L151** has not been reported in the literature until very recently.[22] BODIPY has been recognized as one of the prospective alternative for NIR dyes as this represents an unique class of fluorophore, that displays strong absorption and sharp emission with high quantum yield,[23] photostability and chemostability.[20] These attributes made BODIPYs attractive for a variety of applications including laser dyes,

luminescent devices,[25] chemical sensors[26] and photovoltaic devices.[27] They are relatively insensitive to the polarity and pH of their environment and are reasonably stable at physiological conditions. Simple modifications to their structures enable tuning of their fluorescence characteristics; consequently, these dyes are widely used to label proteins and DNA.[28]

However, most of this potential class of fluorophore absorb and emit below 600 nm and have relatively low extinction coefficient (ε around 80000 $M^{-1}cm^{-1}$), which makes them undesirable for various applications in biotechnology and imaging. In order to overcome this deficiency, several synthetic modifications have been performed on the parent BODIPY moiety, which includes extension of π-conjugation,[29] introduction of intramolecular charge transfer (ICT) character[30] and replacement of carbon with nitrogen bridge-head in the BODIPY skeleton.[31] The extension of the π-conjugation has so far been achieved via introduction of ethynyl and vinyl groups or fusion of BODIPY with aryl groups at it periphery.

Towards this, BODIPYs with fused aromatic polycyclic or heteroaromatic rings have gained much attention.[32] Fused BODIPY systems are generally synthesized by oxidative fusion of BODIPY with aryl moiety at the periphery or by condensation of π-extended fused pyrrole with an aldehyde and subsequent conversion to the desired target. However, efforts in the latter direction are limited, owing to the associated synthetic challenges involved in making π-extended fused pyrroles.[32a-h] So far, fusion of aromatic ring resulted in significant red shift in absorption and emission properties of the BODIPY dyes, owing to the extended π-conjugation. However, an efficient dye in addition needs to possess sharp absorption and emission bands with high extinction coefficient and quantum yield simultaneously, in order to find practical application. Most of the NIR dyes synthesized so far lacked one or more attributes. For instance, very recently reported benzo-fused bis-BODIPY **L155** shows emission around 940 nm, which is very attractive, yet displays arguably very weak emission (ϕ_f < 1 %).[32g] Similarly, perylene-fused BODIPY **L156** shows aggregation dependent emission at 830 nm but possesses moderate extinction coefficient and very low quantum yield.[32h] On the other hand, bis-BODIPY **L158** with absorption and emission above 840 nm is highly labile under aerobic condition.[32i] Very few derivatives possess these qualities, especially beyond 700 nm.[32a-b,31c] Therefore, quest for new efficient NIR dyes, endowed with intense absorption and higher fluorescent quantum yield still continues. Among these Keio

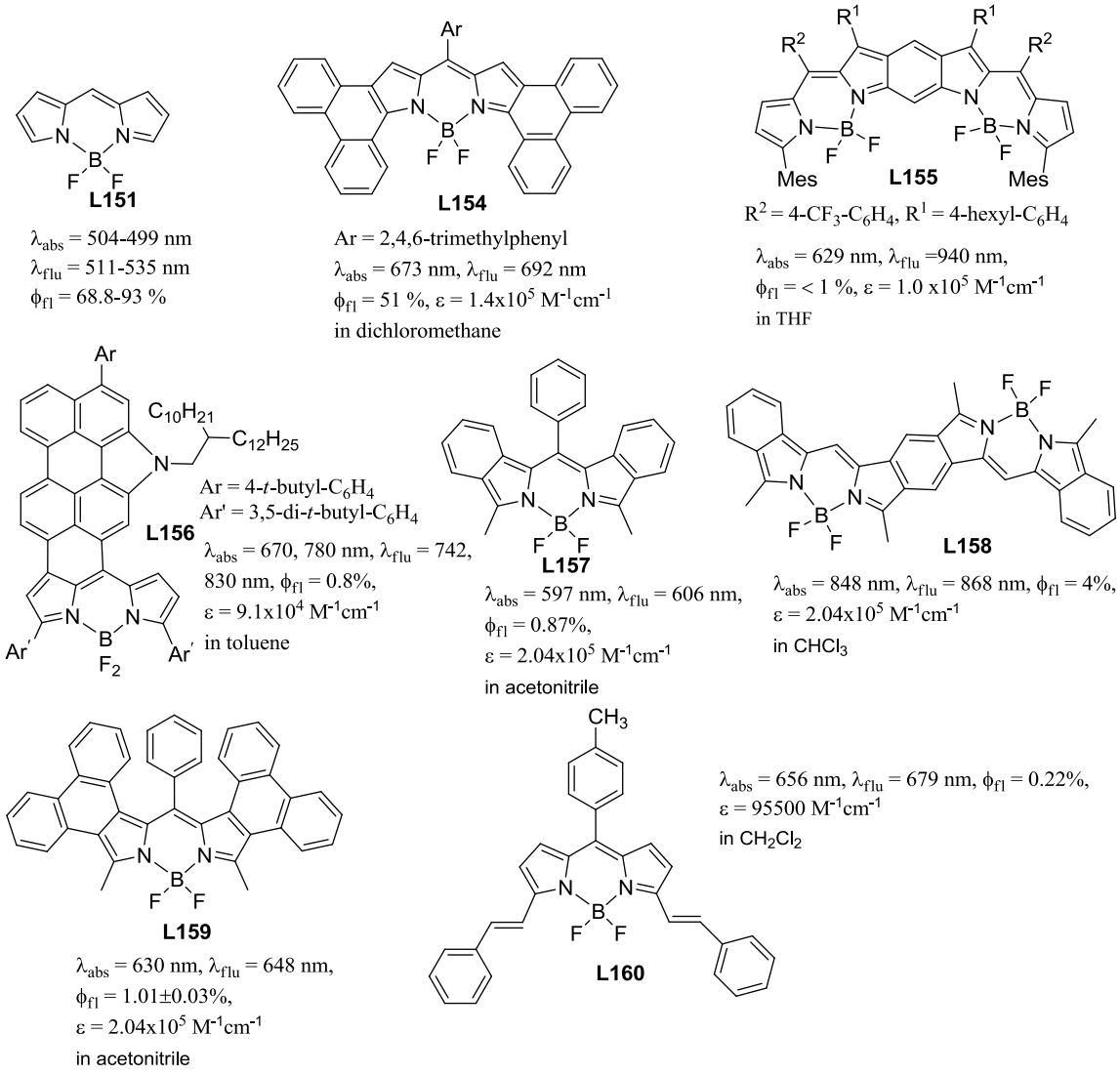

Figure 6.9 Structure of various π-extended BODIPYs along with their photophysical properties.

Fluors dye (KFL) and conformationally restricted aza BODIPY are worth mentioning (Figure 6.10). KFL dyes were first introduced by the Suzuki group in 2008. They have reported an array of heteroaryl fused BODIPY based monomers, whose absorption/emission properties can be tuned by introduction of appropriate functional groups at the BODIPY periphery.Thus, a range of BODIPYs possessing tuned emission wavelengths from 583 to 738 nm and greatly improved extinction coefficients as high as 316000 M^{-1} cm^{-1} could be achieved. Aza-BODIPY dyes are well known for their sharp red shifted absorption and emission with good extinction coefficient, quantum yield and insensitivity towards solvent polarity. Although precursor aza-dipyrromethene chromophore was synthesized in 1940,[33] synthesis of the first aza-BODIPY did not appear in literature until 1993.[34] However, resurgence of interest in aza-

BODIPY dyes occurred from 2002 onward, beginning with research largely from O'Shea′s group, and this has resulted in syntheses numerous aza-BODIPY dyes.[35,31e] Among the aza-BODIPY dyes conformationally restricted systems drew particular attention due to their enhanced photophysical properties in comparison to non-constrained systems (**L165** vs. **L166**).

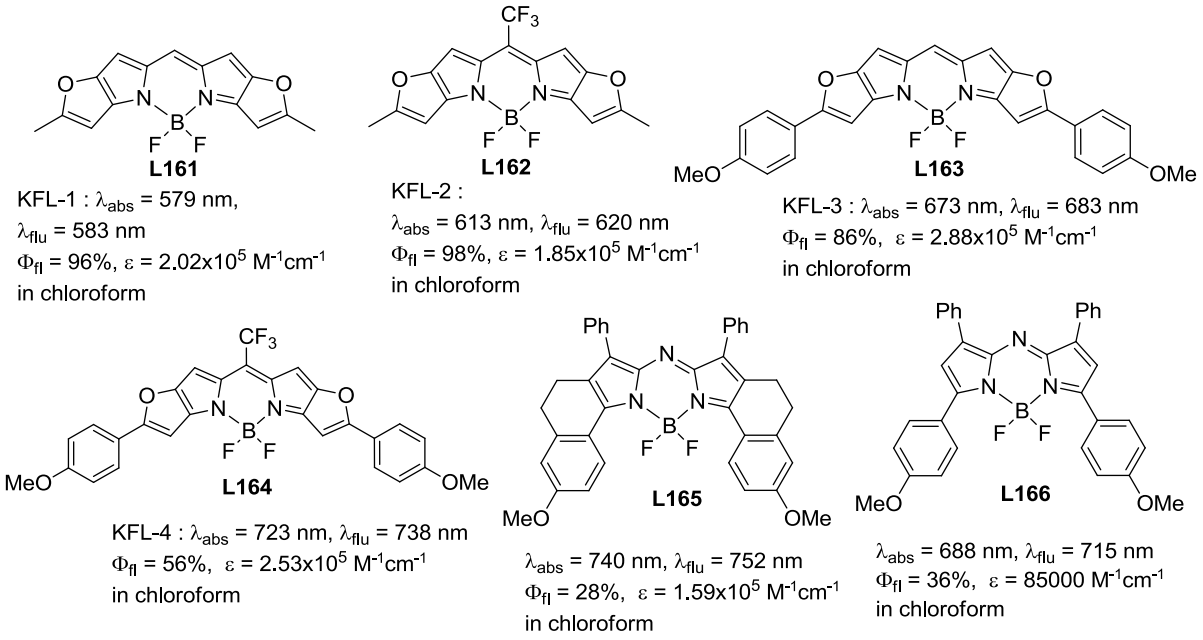

Figure 6.10 Selected examples of BODIPY based NIR dyes having intense absorption and emission with high extinction coefficient and quantum yield.

6.2 Research Goal

As described in the previous chapters we have utilized naphthobipyrrole for the synthesis of various π-extended porphyrinoids, which displays unprecedented optical and structural features. Inspired by those findings we were interested to explore naphthobipyrrole as a BODIPY precursor.[36] The resulting BODIPY supposed to possess unique spectral properties owing to the rigid framework of naphthobipyrrole as well as the extended π-conjugation.

6.3 Results and discussion

6.3.1 Synthesis of bis-naphthobipyrrolylmethene.HCl TS33 and its BODIPY complex TS35

Scheme 6.2 depicts the synthetic route to bis-naphthobipyrrolylmethene and its BODIPY complex **TS35**. Bis-naphthobipyrrolylmethene hydrochloride salt **TS33** was originally

obtained as an unexpected by-product in $FeCl_3$ mediated oxidative coupling reaction of naphthobipyrrole to yield cyclo[4]naphthobipyrrole.[36d] Initially, it was presumed to be a

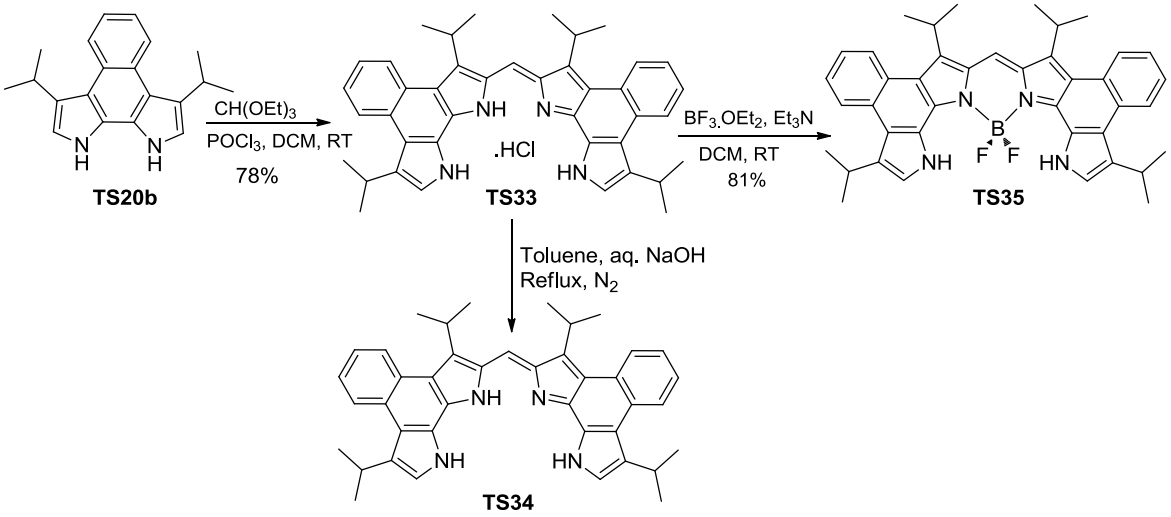

Scheme 6.2 Synthetic route to bis-naphthobipyrrolylmethene **TS33.HCl** and its BODIPY complex **TS35**.

higher analogue i.e. cyclo[n]naphthobipyrrole (n>4) and could not be characterized unequivocally owing to the very low yield (due to the presence of a *meso*-like proton signal at 8.16 ppm and absence of molecular ion peak in HR-MS). Interestingly, this compound was first characterized by single crystal X-ray diffraction analysis and found to be a hydrochloride salt of bis-naphthobipyrrolylmethene **TS33** and subsequently other spectroscopic data complied with. Since neither any formyl equivalent (as carbon source) nor HCl were used in the reaction, the source of *meso* carbon can be attributed to the solvent dichloromethane, which under the reaction condition, probably oxidized to a formic acid derivative liberating HCl. Compound **8** appeared to be an interesting building block for synthesis of novel π-extended porphyrinoids owing to its interesting structure, photophysical properties and stability. However, the yield of the product obtained in this route was very low (*ca.* 2 %). Subsequently, we adopted rational synthetic approach,[37] where reaction of naphthobipyrrole **TS20b** and triethylorthoformate in presence of $POCl_3$ led us to isolate **TS33** in 78 % yield, again as the mono hydrochloride salt (Scheme 6.2). Treating compound **TS33** with triethylamine and $BF_3.OEt_2$ furnished the desired BODIPY **TS35** in 81 % yield.[38] Compound **TS33** and its corresponding free-base **TS34** shows solvent dependent absorption and emission properties which will be discussed later in this section.

6.3.2 Structural analysis of TS33 and TS35

X-ray structure of compound **TS33** (Figure 6.11) displayed its almost planar nature owing to the *β*-*β* fusion of the constituent bipyrrolic moieties. Two outer pyrrolic nitrogens N1 and N4

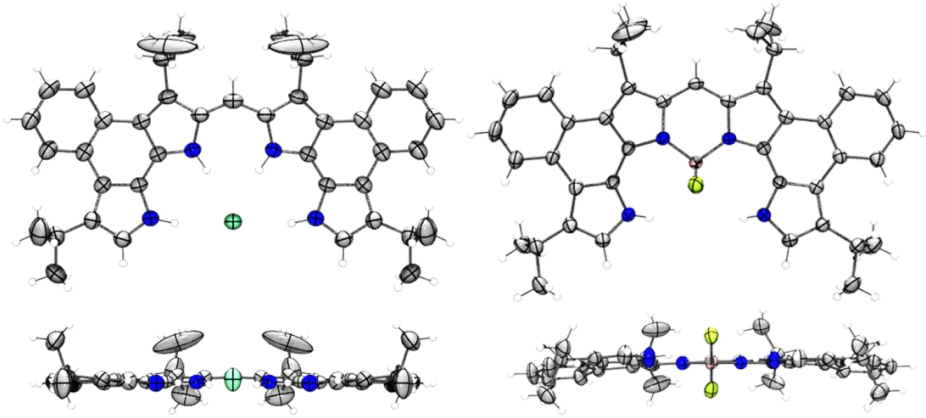

Figure 6.11 ORTEP of left: **TS33** and right: **TS35.** Thermal ellipsoids are scaled to 35 % probability level.

lies above the mean plane (0.22 Å) defined by the dipyrromethene unit. Outer fused *o*-phenylene moieties lie below the mean plane with a maximum distance of 0.30 Å. Chloride ion was found at 0.38 Å above the mean plane and hydrogen bonded to four pyrrolic NHs with an N-H…Cl distance in the range of 3.17-3.18 Å. On the other hand, X-ray structure of BODIPY **TS35** (Figure 6.11) shows comparatively more deviation from planarity than compound **TS33**, in an otherwise near planar structure. The two outer pyrrole nitrogens N1 and N4 were found to be above the mean plane defined by the BODIPY core by a distance of 0.37 and 0.14 Å respectively. Furthermore, the two fused *o*-phenylene moieties lies below the mean plane with a maximum deviation of 0.55 and 0.58 Å. Interestingly, we noticed good face to face *π*-*π* stacking interaction in compound **TS33** (interplanar distance of 3.94 Å), where the two molecules in adjacent plane face in the opposite direction (Figure 6.12). In case of its BODIPY derivative **TS35** *π*-*π* stacking interaction is reduced (interplanar distance of 4.29 Å), with ladder like arrangement of the molecules facing same direction (Figure 6.13).

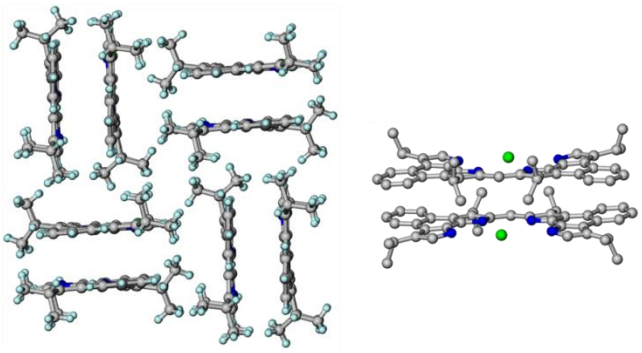

Figure 6.12 POV-Ray picture of packing pattern in crystal structure of compound **TS33**.

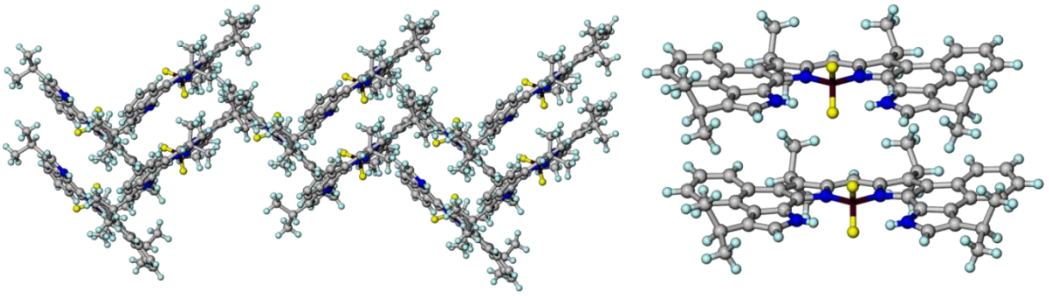

Figure 6.13 POV-Ray picture of packing pattern in crystal structure of compound **TS35**.

6.3.3 Photophysical properties of bis-naphthobipyrrolylmethene-BODIPY TS35

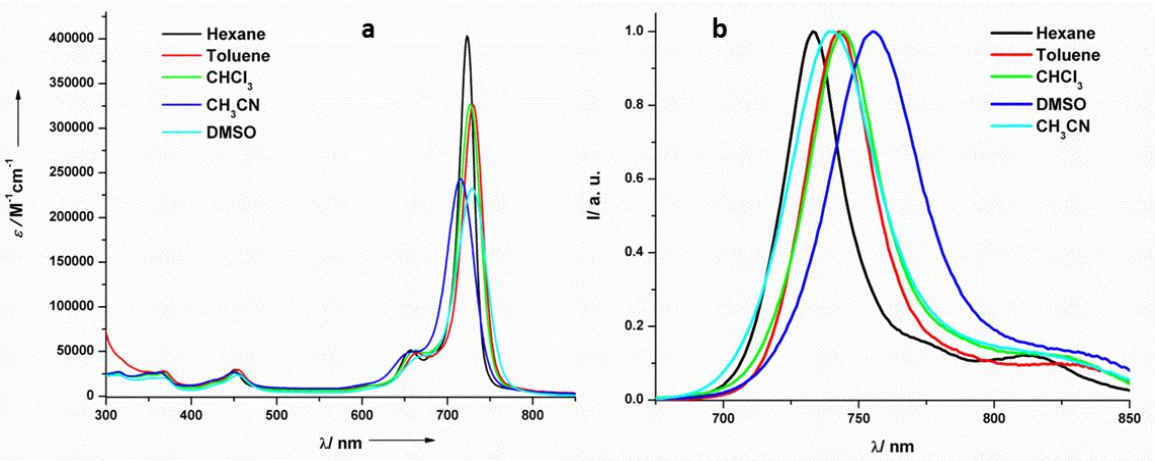

Figure 6.14 (a) UV-Vis-NIR absorption and **(**b) normalized emission spectra of **TS35** in different solvents.

Absorption and emission properties of compound **TS35** were studied in different solvents (Figure 6.14) and Table 6.1 summarizes the data. Compound **TS35** displayed substantially red shifted absorption (727 nm) and emission maxima (744 nm) in chloroform compared to recently reported biphenyl fused BODIPY **L154** (Figure 6.9).[32j] In addition, compound **TS35** exhibits very high extinction coefficient with ε of 327000 $M^{-1}cm^{-1}$ and reasonably high fluorescence quantum yield (0.63). To the best of our knowledge, BODIPY dyes having higher extinction coefficient than **TS35** is not known, the closest being KFL-7 dye [ε = 316000 $M^{-1}cm^{-1}$, λ_{max} (abs) = 662 nm, λ_{max}(flu) = 671 nm in $CHCl_3$].[32b] The absorption and emission properties of compound **TS35** were not much affected by the nature of the solvent. No aggregation was observed under the concentration range studied. The fluorescence excitation spectra of **TS35** (Figure 6.15) match the absorption spectra in all solvents studied,

moreover, λ_{abs} (max) = λ_{ex} (max). However, in polar solvents like DMSO and acetonitrile relatively more stokes shift observed accompanied with a decrease in their fluorescence

Table 6.1 Summary of optical properties of compound **TS35**.

Solvent	Absorption		Emission					
	λ_{max} in nm (log ε)	fwhm (cm^{-1})	λ_{exc} (nm)	λ_{max} (nm)	Stokes shift (cm^{-1})	fwhm (cm^{-1})	ϕ^a	τ_f (ns)
Hexane	723 (5.61)	402	655	733	189	487	0.65	4.70
Toluene	730 (5.51)	555	655	743	239	550	0.62	4.40
$CHCl_3$	727 (5.51)	577	660	744	315	583	0.63	4.45
CH_3CN	715 (5.39)	775	655	739	454	715	0.48	3.80
DMSO	729 (5.37)	798	660	755	472	704	0.44	3.39

[a] Fluorescence quantum yield were measured using DOTC iodide as reference.[39]

quantum yields, which is still quite high for this class of NIR dyes (ϕ_f > 0.4). The singlet state lifetime of **TS35** measured in different solvent shows decrease in life time as we increase the polarity of the solvent in analogy with the trends observed in quantum yield and extinction coefficient measurements (Figure 6.16). These values are better or comparable with KFL-4 dye **L164**, which is regarded to possess best optical properties amidst the BODIPY dyes [λ_{max}(abs) = 723 nm, log ε = 5.40, λ_{max}(flu) = 738 nm, fwhm = 31 nm and ϕ_f = 0.56 in $CHCl_3$].[32a] Absorption and emission properties of our BODIPY dye **TS35** also competes well with cyanine dye Cy7 [λ_{max}(abs) = 742 nm, log ε = 5.38, λ_{max}(flu) = 772 nm and ϕ_f = 0.28 in ethanol] which is one of the most widely used NIR dye.[40] Further, in spite of two additional unbound pyrrole derivatives with free α-positions, dye **TS35** shows quite good photostability [exposure to 365 nm (8 watt UV lamp) for 96 h shows absorption λ_{max} decrease by 31 %; only 1 % decrease per 3 h of average irradiation].

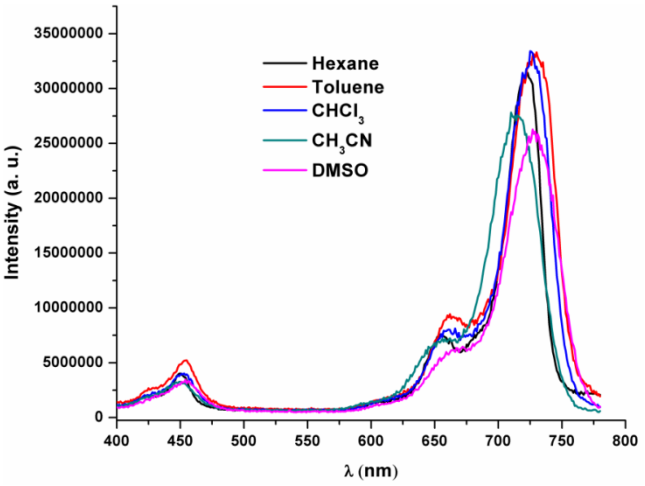

Figure 6.15 Excitation spectra of **TS35** in different solvents (emission at 790 nm).

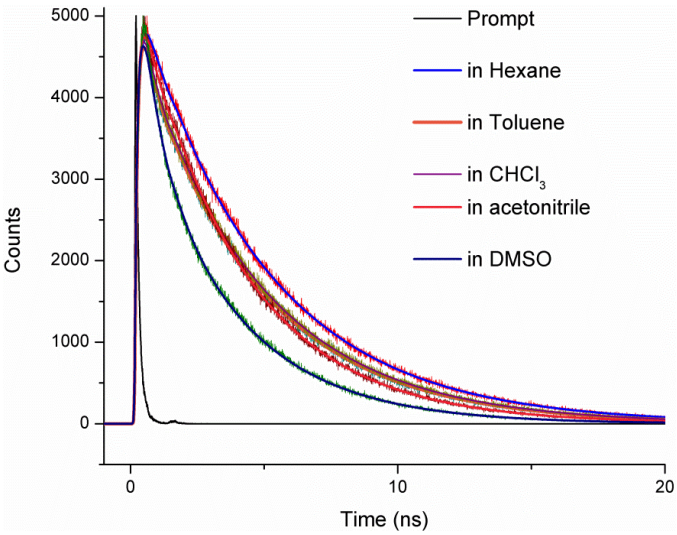

Figure 6.16 Fluorescence decay profile of **TS35** in different solvents**.**

6.3.4 Photophysical properties of bis-naphthobipyrrolylmethene hydrochloride salt TS33 and its free-base TS34

Solvent dependent absorption was observed for compounds bis-naphthobipyrrolylmethene hydrochloride salt **TS33** and and its free-base **TS34**. Free-base **TS34** was obtained by refluxing a solution of chloride salt **TS33** in toluene with aqueous NaOH under nitrogen atmosphere followed by washing with double distilled water. Organic layer was dried and stored under vacuum with a NaOH plug to avoid any acid contamination. Ground state absorption spectra of **TS33** and **TS34** differ dramatically upon changing polarity of solvent from less polar hexane, toluene and dichloromethane to more polar DMSO and methanol (Figure 6.17a, c). For example, absorption spectrum of chloride salt **TS33** measured in toluene shows an intense band at 724 nm with rather high extinction coefficient (log ε = 5.4),

whereas that recorded in methanol shows a hypsochromically shifted broad band at 635 nm with a much reduced ε value (log ε = 4.8). Comparatively large stokes shift were observed in polar solvent in their respective emission spectra (16 nm in hexane vs. 48 nm in DMSO). Similar phenomenon was also observed in case of free-base **TS34.** Table 6.2 summarizes the absorption and emission properties of compounds **TS33** and **TS34** studied in different solvents. The possible explanation for this solvent dependent behaviour may be attributed to the solvent induced deprotonation of compounds **TS33** and **TS34**. In nonpolar solvents compound **TS34** exist in its free-base form whereas in polar solvents the equilibrium is shifted towards the anionic form. Similar reasoning could be put forward for the chloride salt **TS33**. In non-polar solvents compound **TS33** exist as its chloride salt, whereas in case of polar solvents it exists predominantly in its anionic form owing to deprotonation and

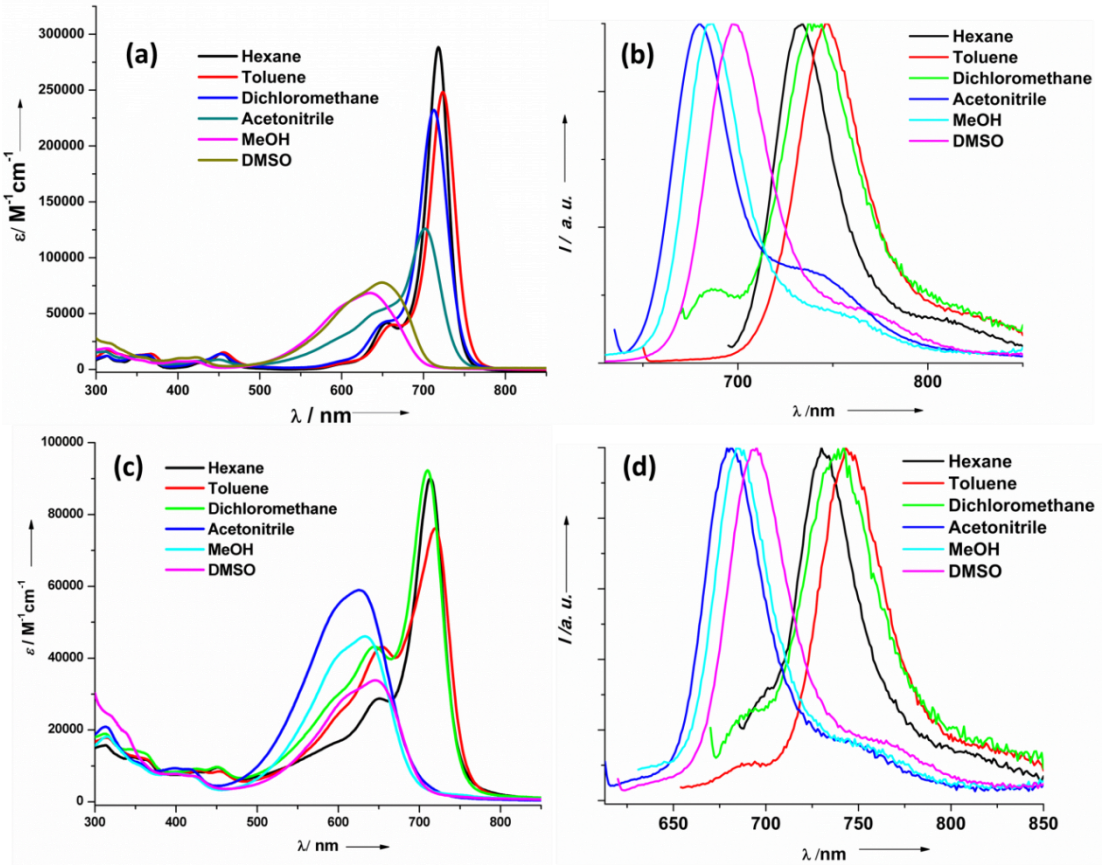

Figure 6.17 (a) UV-Vis-NIR absorption and (b) Emission spectra of **TS33**; (c) UV-Vis-NIR absorption and (d) Emission spectra of **TS34** studied in different solvents.

Table 6.2 Summary of absorption and emission properties of **TS33** and **TS34**.

Sl. No.	Compound	λ_{exc} (nm)	Solvent	λ_{max} (nm)	λ_{em} (nm)	Stokes shift (cm^{-1})	log ε	ϕ^a
1.	**TS34**	680	Hexane	713	730	326	4.95	

		645	Toluene	719	743	449	4.88	0.02
		665	CH_2Cl_2	710	742	607	4.96	
		608	CH_3CN	625	679	1272	4.77	0.01
		620	Methanol	633	684	1178	4.66	
		615	DMSO	645	695	1115	4.53	
2.	**TS33**	690	Hexane	718	734	304	5.46	
		645	Toluene	724	747	425	5.39	0.11
		665	CH_2Cl_2	713	737	457	5.37	
		630	CH_3CN	702	680		5.10	0.05
		620	Methanol	635	686	1171	4.84	
		615	DMSO	649	697	1061	4.89	

[a]Fluorescence quantum yield were measured using DOTC iodide as reference.[39]

subsequent decomplexation caused by the solvent molecules. To prove this hypothesis we performed mixed solvent titration of **TS33** and **TS34** in toluene and methanol (Figure 6.18). The reason behind choosing toluene and methanol is that both solvents are miscible at any proportions and both the compounds show good solubility in these solvents. Besides absorption spectra obtained in these solvents are completely different for both **TS33** and **TS34**. If the dissolved molecule adopts different structural forms, mixed solvent titration should show the changes in equilibrium between these forms. As a result distinct isosbestic

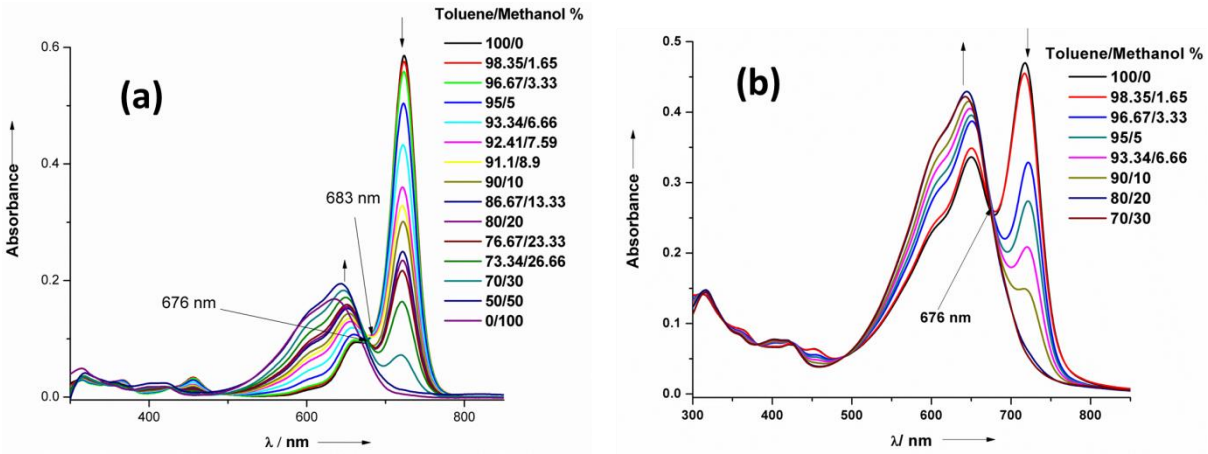

Figure 6.18 (a) Absorption spectra of **TS33** in toluene/methanol mixture (Conc. $2x10^{-6}$ M). **(b)** Absorption spectra of **TS34** in toluene/methanol mixture (Conc. $1x10^{-5}$ M). Arrows indicates the direction of spectral changes upon going from pure toluene to methanol.

points are seen in such cases. Whereas in case of solvatochromic effects mainly shift in absorption bands are observed with no isosbestic point.[41] In the present study, free-base **TS34** shows a distinct isosbestic point around 676 nm, where the intensity of the absorption band at 719 nm corresponding to free-base decreases with increasing methanol concentration, whereas a new peak emerges at 642 nm. The titration with the chloride salt **TS33** shows

similar behaviour. However, two isosbestic points were observed, indicating the presence of two equilibriums in case of **TS33**, namely between the salt and the free-base and again between the free-base and the anionic form. Increasing methanol percentage first leads to the formation of free-base **TS33**, which subsequently converts to its anionic form with further increase in methanol percentage. Upon addition of excess triethylamine or strong base such as KO^{t}Bu (potassium *tert*-butoxide) to a solution of chloride salt **TS33** and free-base **TS34** in toluene leads to spectral changes, which resemble to their corresponding spectra obtained in polar solvents (Figure 6.19a-d). Therefore, from the above observations, it could be inferred that spectral changes observed for compounds **TS33** and **TS34** in polar solvent are due to solvent induced deprotonation of the NH-hydrogen of both **TS33** and **TS34**. This in turn indicates the acidic nature of these hydrogens.

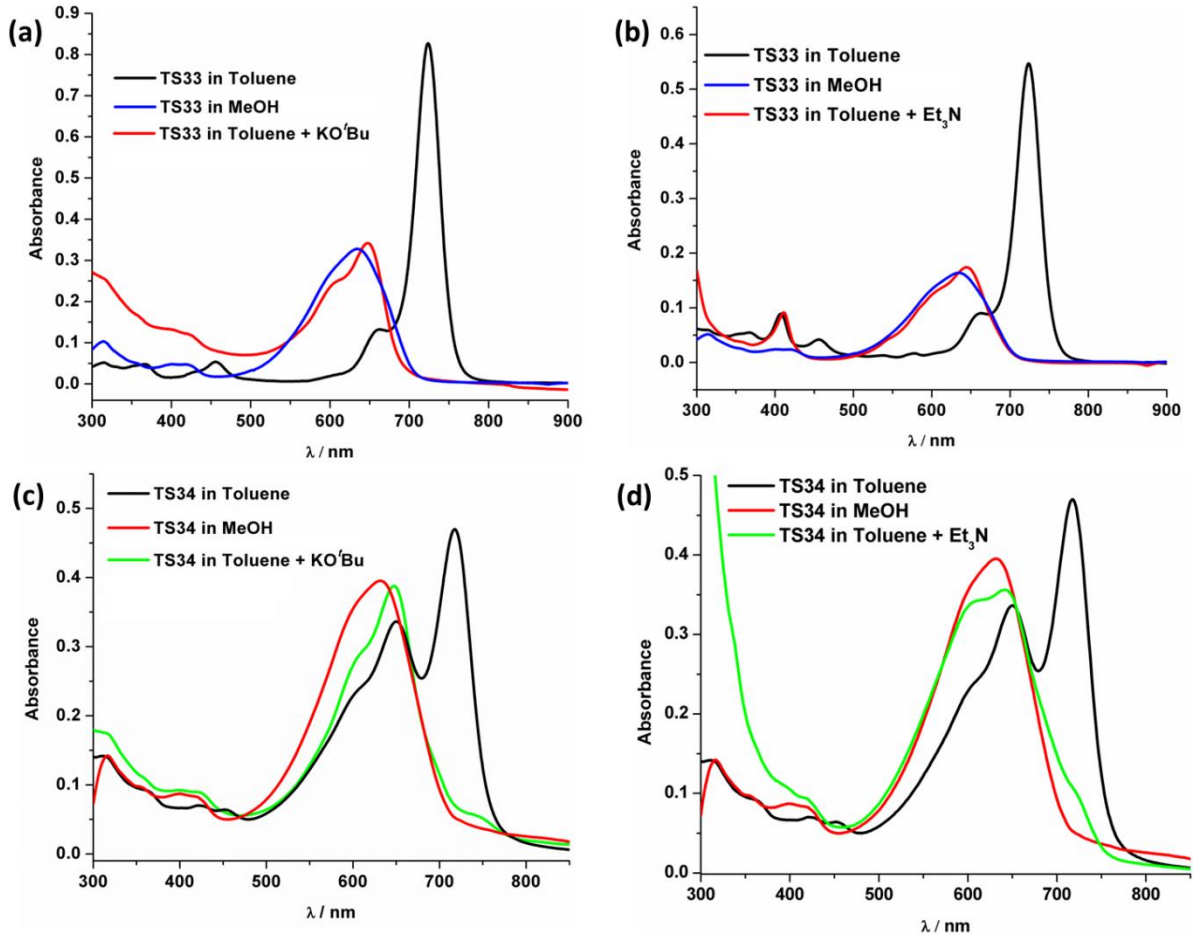

Figure 6.19 Changes in UV-Vis spectra of top**: TS33** in toluene upon addition of (a) excess KO^{t}Bu, (b) excess triethylamine; bottom: **TS34** in toluene upon addition of (c) excess KO^{t}Bu, (d) excess Et_3N. Spectra in methanol are also shown for comparison.

Room temperature ^{1}H NMR spectrum of chloride salt **TS33** in $CDCl_3$ shows two NH-signals at 12.59 ppm and 11.69 ppm. However, free-base **TS34** displays no distinct NHs signal at room temperature and only at low temperature (-50°C, $CDCl_3$) one signal clearly appears at 12.20 ppm along with two other broad signals at 11.57 and 9.91 ppm (Figure 6.20) probably owing to NH resonance. Free-base **TS34** upon titration with TBAF (in acetonitrile-d_3) shows a peak near 15.8 ppm, which may be assigned to formation of HF_2^- ion upon deprotonation of the pyrrolic NH (Figure 6.21). Absorption spectra of **TS33** and **TS34** in presence of TBAF also show similar pattern to that obtained in polar solvents (Figure 6.22). Very recently this type of solvent induced deprotonation was reported in literature for free-base corrole derivative.[41]

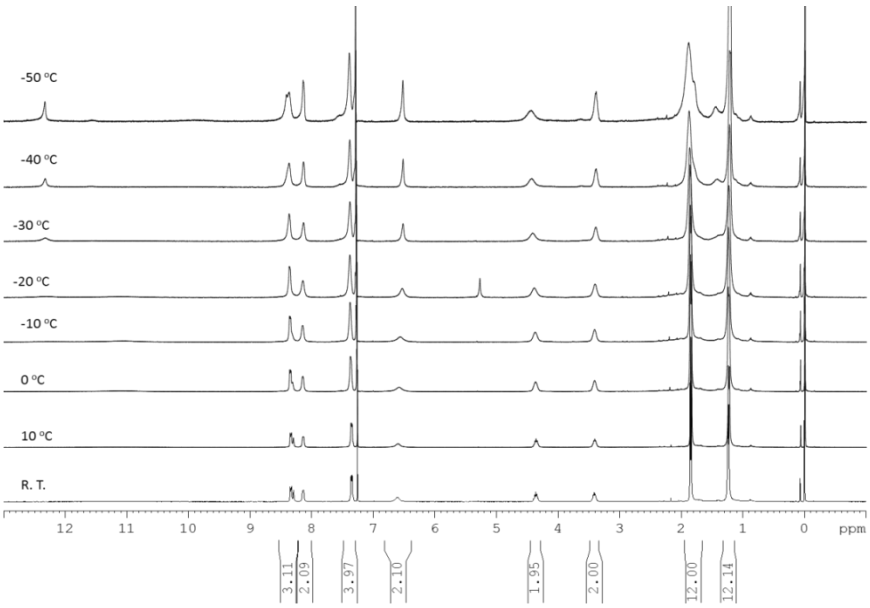

Figure 6.20 Variable temperature ^{1}H NMR spectra of **TS34** in $CDCl_3$.

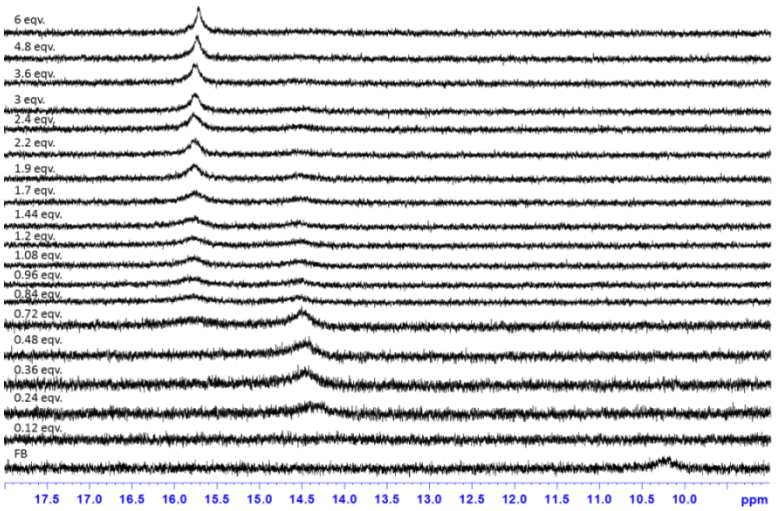

Figure 6.21 Selected spectral regions of ^{1}H NMR titration of **TS34** with TBAF in CD_3CN.

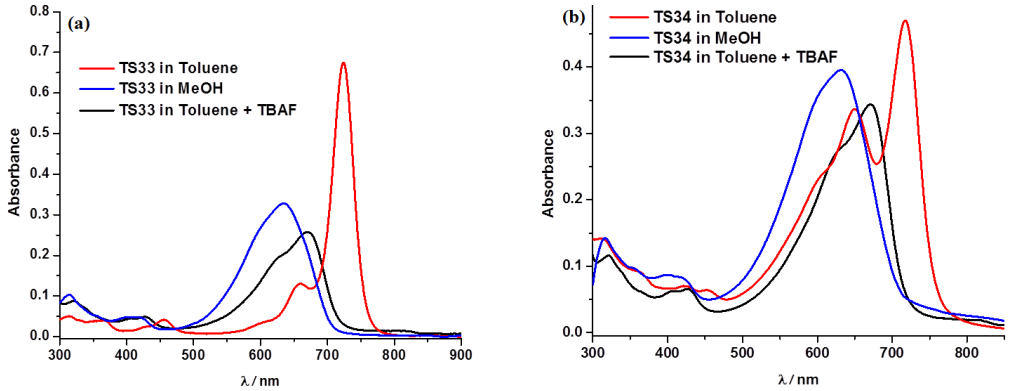

Figure 6.22 Changes in UV-Vis spectra of (a) **TS33** (salt), (b) **TS34** (free-base) in toluene upon addition of excess TBAF. Spectra in methanol are also shown for comparison.

6.3.5 Formylation of bis-naphthobipyrrolylmethene-BODIPY TS35

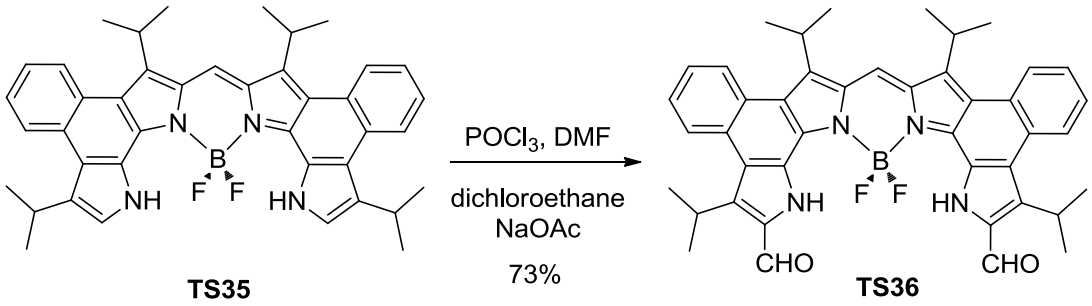

Scheme 6.3 Synthetic route to BODIPY-dialdehyde **TS36.**

The excellent yield of the bis-naphthobipyrrolylmethene BODIPY **TS35** allowed us to utilize this material for further functionalization. **TS35** possesses two terminal pyrroles with free α-positions which can be subjected to electrophilic aromatic substitution reactions. First choice was to introduce formyl groups; this is partly because of our earlier experience with naphthobipyrrole **TS20b** that undergoes easy formylation at α-pyrrolic positions. Moreover, formylated BODIPY not only allows preparing a variety of derivatives with improved photophysical properties but also shows immense potential as a sensor.[42,26g,29h] Thus, we were able to introduce formyl groups at the α-positions of the terminal pyrroles in 73 % yield, following Vilsmeier-Haack formylation condition. This is the first report regarding direct formylation of BODIPY at 3,5-positions.

6.3.6 Photophysical properties of TS36

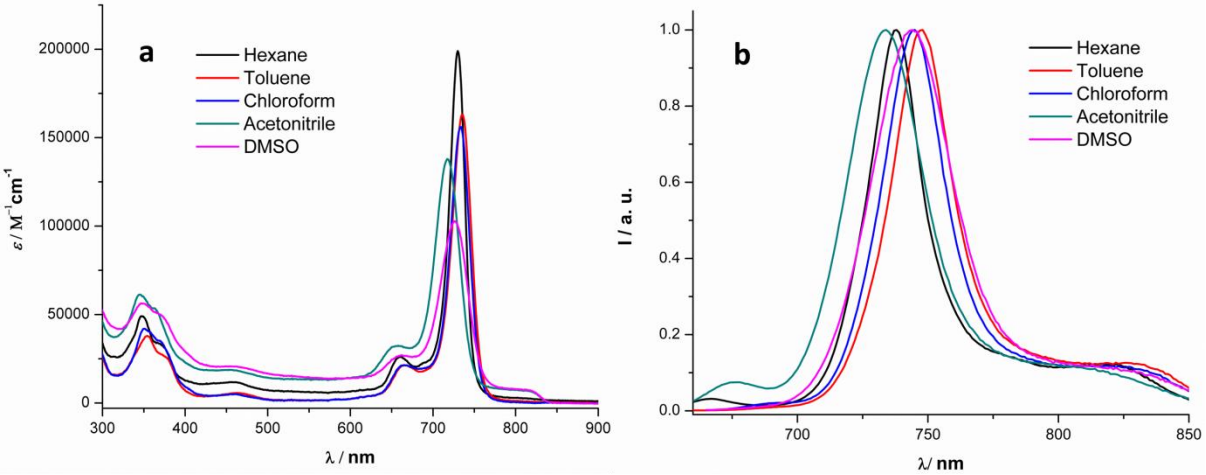

Figure 6.23 UV-Vis-NIR (**a**) absorption and **(b)** emission of **TS36** in different solvents.

Absorption and emission maxima of **TS36** did not show much change in comparison to **TS35**. However, we observed an enhancement in quantum yield and decrease in extinction coefficient upon formylation in comparison to **TS35**. Similar behavior was also reported for 3,5-diformyl BODIPY by Ravikanth and coworker.[42b] A summary of the photophysical properties of bis-naphthobipyrrolylmethene-BODIPY-dialdehyde **TS36** is presented in Table 6.3.

Table 6.3 Summary of optical properties of compound **TS36**.

Solvent	Absorption		Emission				
	λ_{max} in nm (log ε)	fwhm (cm^{-1})	λ_{exc} (nm)	λ_{max} (nm)	Stokes shift (cm^{-1})	fwhm (cm^{-1})	ϕ_f[a]
Hexane	730 (5.30)	413	655	738	148	351	0.99
Toluene	735 (5.21)	514	655	748	236	516	0.79
$CHCl_3$	734 (5.19)	507	660	745	201	523	0.74
CH_3CN	717 (5.14)	717	655	734	323	651	0.83
DMSO	726 (5.01)	819	660	744	333	687	0.66

[a] Fluorescence quantum yield were measured using DOTC iodide as reference.[39]

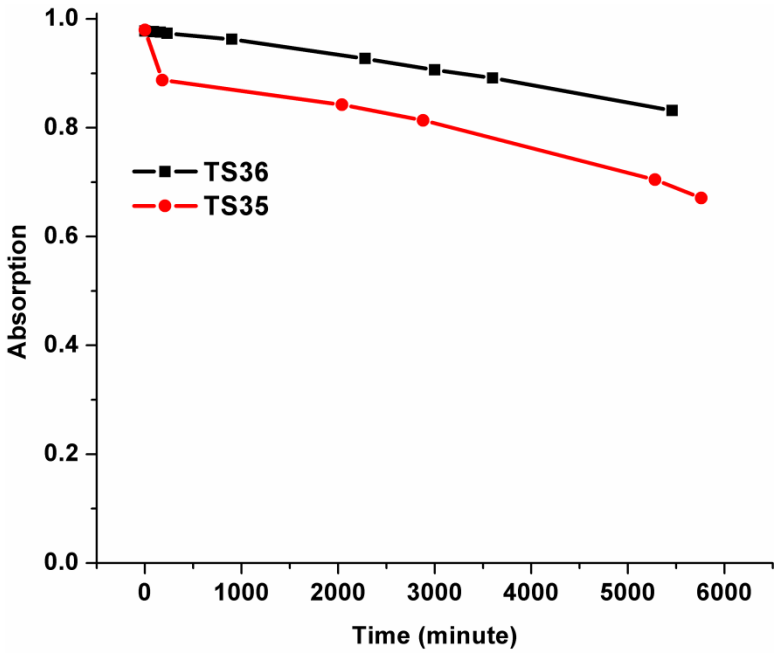

Figure 6.24 Change in optical density of **TS35** and **TS36** monitored at their corresponding absorption maxima with irradiation time of 8 watt UV lamp.

Dialdehyde **TS36** shows excellent photostability probably owing to absence of reactive free α-pyrrolic positions. Thus irradiation of an air saturated solution of **TS36** with 8 watt UV lamp for 91 h shows only 15 % decrease in initial intensity i.e. only 1 % decreases per 6 h of average irradiation.

6.3.7 Synthesis of BODIPY dimer derived from monomer TS35

Initially after the synthesis and characterization of bis-naphthobipyrrolylmethene **TS33** we planned to utilize this building block for synthesis of expanded porphyrinoids. However, in spite of several attempts we were not able to isolate any macrocycle. This compound seems to be less reactive and this attribute is further highlighted when we found it in unreacted condition in many cases. The successful synthesis of the BODIPY complex **TS35** led us to employ it as a precursor for expanded porphyrinoids. This is because of better reactivity of BODIPY complex compared to its precursor. For instance, Vilsmeier formylation of bis-naphthobipyrrolylmethene BODIPY complex smoothly furnishes the desired dialdehyde in good yield however; under identical condition bis-naphthobipyrrolylmethene hydrochloride salt **TS33** gives a mixture of mono and di-formylated products in low yield. We deliberate syntheses of octaphyrin(1.0.0.0.1.0.0.0) using bis-naphthobipyrrolylmethene BODIPY complex **TS35**. Octaphyrin(1.0.0.0.1.0.0.0) **L168** was reported by Sessler and coworkers following a Cr(VI) based oxidative coupling strategy starting from alkylated bis-

bipyrrolylmethene **L167** (Scheme 6.4a).[43] As evident from X-ray crystallographic analysis octaphyrin **L168**, substantially deviates from planarity and proved to be non-aromatic in nature. We adopted the similar methodology to construct the desired naphthobipyrrole appended octaphyrin(1.0.0.0.1.0.0.0) containing two BF_2 groups inside. The desired product is expected to adopt a planar structure owing to rigid framework of BODIPY **TS35**, hence expected to display interesting chemistry. However, in our case reaction did not proceed to furnish the corresponding macrocycle as observed for alkylated bis-bipyrrolylmethene **L167**, rather we were able to isolate linear dimer **TS37** of bis-naphthobipyrrolylmethene BODIPY complex **TS35**. Dimeric BODIPY complex **TS37** was characterized by X-ray crystallographic analysis as well as by other spectroscopic means. Detailed outline of the reaction methodology is shown in scheme 6.4 (b). Thus, reaction of **TS35** with 0.4 equivalent of $Na_2Cr_2O_7$ in TFA furnishes **TS37** in 20 % yield. So far no cyclic products could be isolated and characterized either by increasing or decreasing amount of oxidizing agent. For instance using 1 equivalent of $Na_2Cr_2O_7$ neither leads to formation of macrocycle nor the linear dimer **TS37**. BODIPY complex of type **TS37** is hitherto unknown and shows interesting photophysical and structural properties. Nevertheless BODIPY dimer **TS37** possessing extended π-conjugation appears to be very interesting and promising.

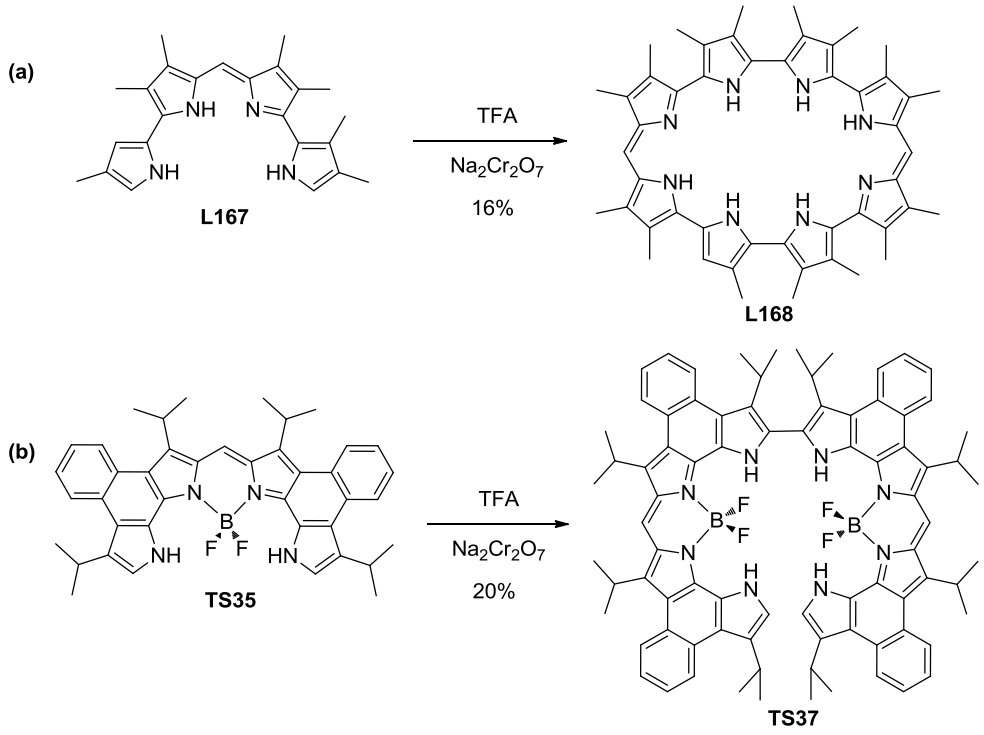

Scheme 6.4 (a) Synthesis of octaphyrin(1.0.0.0.1.0.0.0)[43]; (b) Synthesis of BODIPY dimer **TS37**.

6.3.8 Photophysical properties of BODIPY dimer TS37

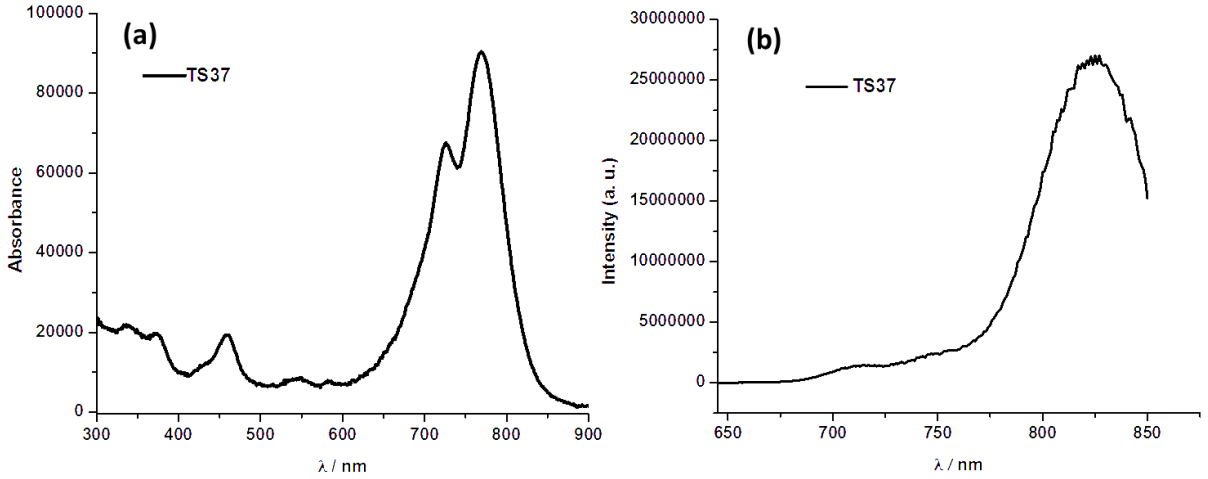

Figure 6.25 (a) UV-Vis-NIR and (b) emission spectra of BODIPY dimer **TS37** in $CHCl_3$ (excited at 635 nm).

UV-Vis-NIR spectrum of **TS37** recorded in chloroform shows two peaks in the NIR region at 726 nm and 769 nm. In comparison to its monomer **TS35** absorption maxima of dimer **TS37** is red shifted by 42 nm. However, extinction coefficient of **TS37** drastically reduced compared to its monomer (log ε 4.9 vs. 5.51 in $CHCl_3$). Emission spectrum of **TS37** recorded in $CHCl_3$ shows emission maxima at 825 nm, which is 79 nm red shifted compared to its corresponding monomer **TS35** (Full range emission spectrum could not be obtained due to lack of required instrumental facility). Large stokes shift was observed for BODIPY dimer **TS37** (56 nm vs. 17 nm for monomer). Thus BODIPY dimer **TS37** possessing absorption and emission in the NIR region may find application as a novel NIR dye for imaging study of biomolecules.

6.3.9 Structural analysis of BODIPY-dimer TS37

X-ray structure of compound **TS37** (Figure 6.26) shows an interesting helical arrangement of the two BODIPY units. The dihedral angle between the adjacent pyrrole (connecting the two BODIPY units) is found to be 120.4°. The distance between two B atoms was found to be

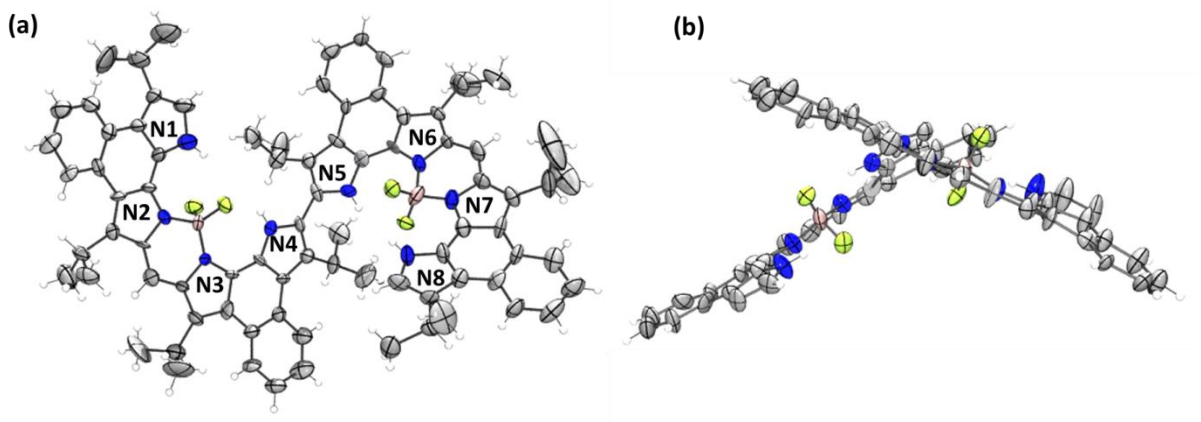

Figure 6.26 ORTEP of BODIPY-dimer **TS37**: (a) Top view and (b) side view. Thermal ellipsoids are scaled to 35 % probability level.

8.60 Å. One of the BODIPY units shows substantial deviation from planarity compared to the BODIPY monomer **TS35**. The two outer pyrrole nitrogens of this unit, N5 and N8 were found to be above and below the mean plane defined by the BODIPY core by a distance of 0.71 and 0.72 Å respectively. The other BODIPY unit shows comparatively less deviation from planarity. The two outer pyrrole nitrogens N1 and N4 were found to be above the mean plane defined by the BODIPY core by a distance of 0.28 and 0.13 Å respectively. As a result, each BODIPY unit is helically distorted and twist in the central 2,2′-bipyrrole units induces helicity in **TS37**. The non-planar arrangement of two BODIPY units even persists in solution state as evident from ^{1}H and ^{13}C NMR spectra of **TS37**. This in turn probably interrupts the electronic communication between the two units which is reflected in the absorption spectrum. Thus as mentioned earlier, absorption spectrum of **TS37** is only 42 nm red shifted compared to BODIPY monomer **TS35**, which is expected to be more in an otherwise planner arrangement.

6.3.10 Synthesis of naphthobipyrrole derived linear hexaphyrin TS38 and its corresponding BODIPY complex TS39

The photophysical properties of bis-naphthobipyrrolylmethene BODIPY **TS35** and its dimer **TS37** stimulated our interest for the synthesis of novel conformationally restricted BODIPYs, derived from naphthobipyrrole that absorb and emit in the NIR region. Keeping these views in mind, we chose to synthesize naphthobipyrrole derived linear hexaphyrin **TS38**. Scheme 6.5 depicts the synthesis of linear hexaphyrin derived from alkylated naphthobipyrrole derivatives. Reaction of two equivalent of alkylated naphthobipyrrole **TS20b** with naphthobipyrrole dialdehyde **TS21b** in presence of conc. HCl in EtOH leads to formation of

linear hexaphyrin **TS38** in 84 % yield. Compound **TS38** was isolated as its dihydrochloride salt and characterized by ^{1}H, ^{13}C NMR and high resolution mass spectrometry. Linear hexaphyrin derived from alkylated bipyrrole is previously known in literature and has been

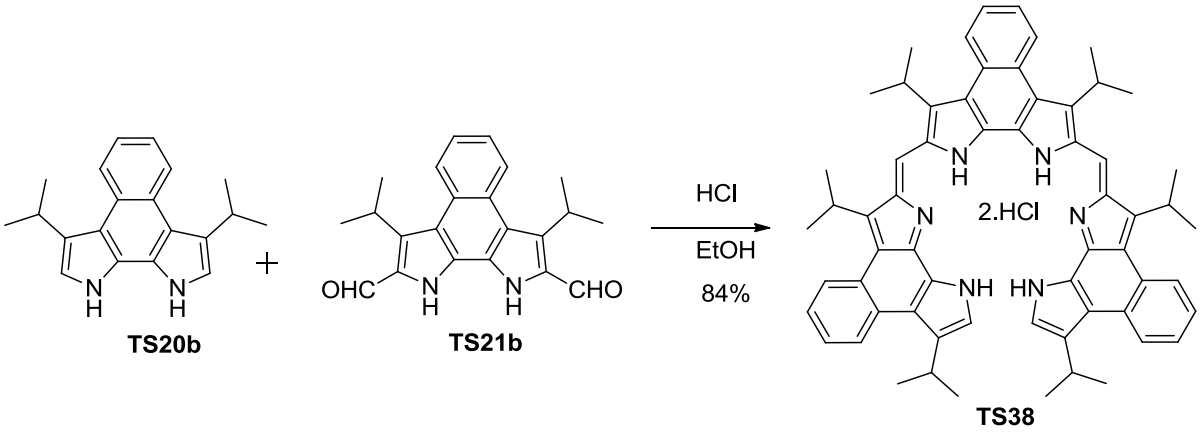

Scheme 6.5 Synthesis of linear hexaphyrin **TS38**.

employed to synthesize hexaphyrin(1.0.1.0.0.0).[44] However, owing to presence of fused bipyrrole **TS38** expected to possess a different chemistry. Compound **TS38** bearing two dipyrromethene units appear to be a suitable candidate for the synthesis of bis-BODIPY complex with rigid and extended π-conjugation. **TS38** upon treatment with $BF_3.OEt_2$ (23 equiv.) in presence of Et_3N (30 equiv.) at room temperature with stirring for 5 h, leads to formation of mono-BODIPY complex **TS39** in 29 % yield, along with the unreacted starting material. This compound was characterized by ^{1}H, ^{13}C NMR and HRMS analysis. Further increase in reaction time, $BF_3.OEt_2$ equivalent or reaction temperature did not allow us to

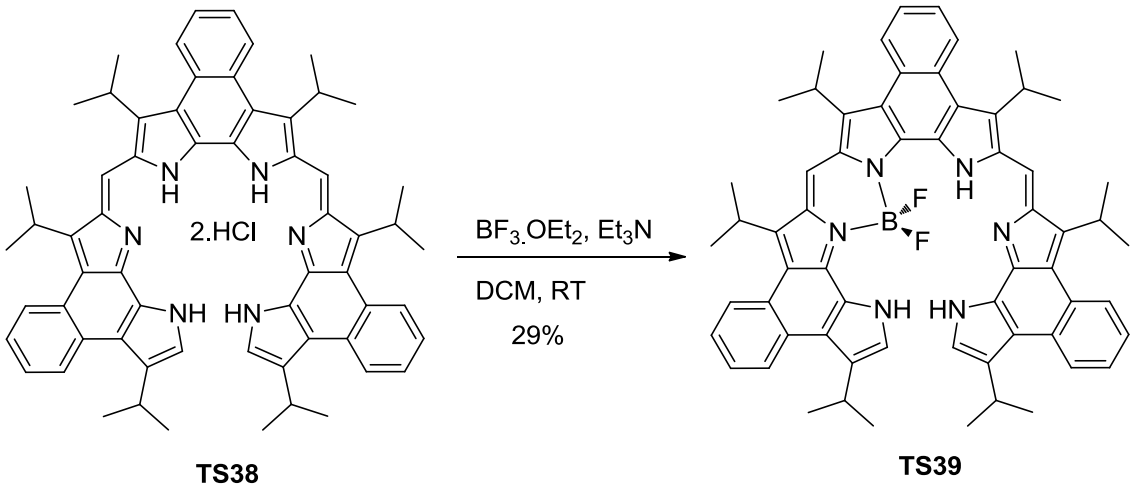

Scheme 6.6 Synthesis of BODIPY complex **TS39** from linear hexaphyrin **TS38**.

isolate either bis-BODIPY complex or even the mono-BODIPY complex **TS39**, rather we have isolated another blue colored compound which forms predominantly under all reaction conditions mentioned. ^{1}H NMR study of this compound shows highly complex nature and could not be assigned properly. However, ESI-HRMS analysis shows mass corresponding to a BF_3 complex of **TS38**. Very recently V. G. Anand and coworker reported isolation of BF_3 complex of an N-confused dipyrrin while attempting to synthesize BF_2-complex. They also mentioned complex nature of NMR spectra for this type of complex and was characterized through X-ray analysis.[45] Unfortunately we were unable to obtain any crystal for this compound so far, therefore could not confirm about this product at this moment. The failure to obtain bis-BODIPY complexes may be attributed to increase in steric hindrance inside the hexapyrrolic cavity.

6.3.11 Photophysical properties of TS38 and TS39

The extended π-conjugation in linear hexaphyrin **TS38** resulted in a rather intense absorption bands in the visible (533 nm) region, accompanied with a band in the near IR region (886 nm). These bands are 30 and 80 nm red shifted, respectively compared to the linear hexaphyrin analogue derived from alkylated bipyrrole (Figure 6.26).[44a] Absorption spectrum of mono-BF_2 complex **TS39** resembles more or less similar to the linear hexaphyrin **TS38**, displaying a slightly red-shifted absorption profile, with a strong visible band (536 nm), accompanied with a relatively less broad NIR band around 897 nm. Emission properties of BODIPY-monomer could not be evaluated at this moment due lack of instrumental facility.

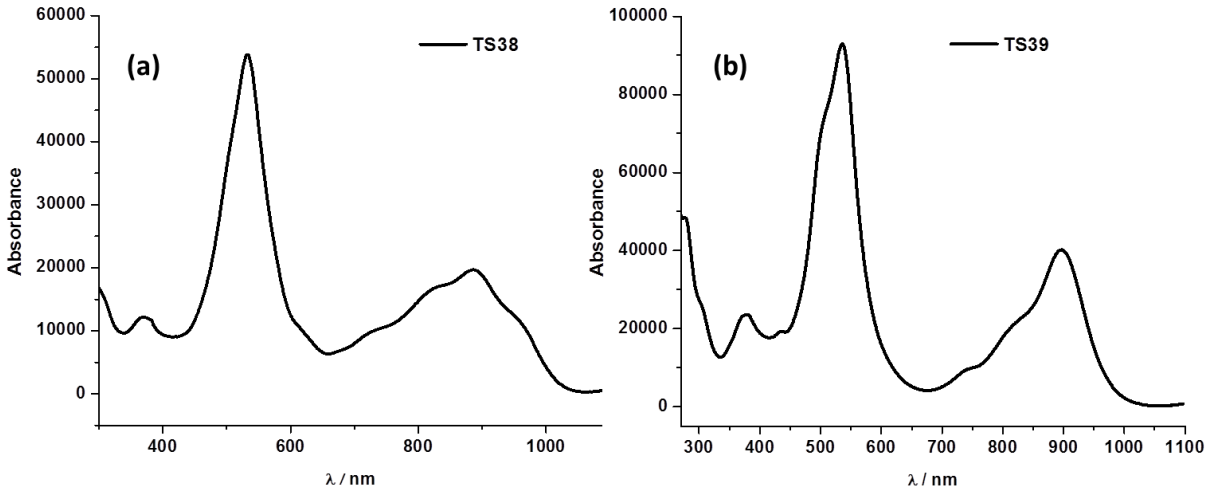

Figure 6.27 Absorption spectra of: (a) linear hexaphyrin **TS38** and (b) its BODIPY complex **TS39** in $CHCl_3$.

6.4 Conclusion

Successful synthesis and characterizations of naphthobipyrrole derived novel BODIPY dyes are presented. Bis-naphthobipyrrolylmethene-BODIPY **TS35** shows NIR absorption (730 nm) and emission (744 nm) with efficient quantum yield (ϕ_f = 0.65), exceptionally high extinction coefficient and good photostability. Further, formylation of bis-naphthobipyrrolylmethene BODIPY **TS35** leads to formation of the corresponding dialdehyde **TS36**. Dialdehyde **TS36** exhibits excellent photostability as well as enhancement in quantum yield compared to **TS35**, hence may find application as an efficient NIR dye. Besides, formylated BODIPY **TS36** can be used for preparing a variety of derivatives with further improved photophysical properties. BODIPY **TS35** and **TS36** can also be explored as a potential building block for synthesis of novel π-extended porphyrinoids.

BODIPY dimer **TS37** shows impressive absorption (λ_{max} = 769 nm) and emission (λ_{max} = 825 nm) in the NIR region. However, detail photophysical study is lacking at present. Moreover, solid state structure shows interesting helical arrangement of two monomers. Looking at the necessity in development of longer-chain oligopyrroles for new multinuclear single helicates that are stable against racemization, BODIPY dimer **TS37** with appropriate substituents may emerge as a potential candidate for further study in this direction.

Linear π-extended hexaphyrin **TS38** and its corresponding mono-BF_2 complex **TS39** show NIR absorption even beyond 900 nm. So far we were unsuccessful in synthesizing bis-BF_2 complex of **TS38**. Further detailed study, especially emission could not be presented at this moment due to lack of instrumental facility. Linear hexaphyrin **TS38** can also be used as a precursor for the synthesis of novel π-expanded as well as extended porphyrinoids. Efforts in directions are currently underway in our group.

6.5 Experimental Details

Synthesis of bis-naphthobipyrrolylmethene TS33

Di-isopropylnaphthobipyrrole **TS20b** (200 mg, 0.69 mmol) was dissolved in dichloromethane (20 mL) and placed in a 50 mL round bottom flask fitted with nitrogen inlet and stirring bar. To this solution, triethylorthoformate (0.116 mL, 0.69 mmol) was added, followed by addition of freshly distilled $POCl_3$ (0.032 mL, 0.34 mmol) and the reaction mixture was stirred for overnight at room temperature. Subsequently, the reaction mixture was washed with water, and dried over anhyd. Na_2SO_4; organic layer was evaporated under

reduced pressure. The dark green solid thus obtained was purified over a silica column using CH_2Cl_2 as eluent. Yield: 78 % (170 mg).

^{1}H NMR (400 MHz, $CDCl_3$, δ in ppm): 1.46 (d, J = 6.8 Hz, 12H, -CH_3 *i*-Pr), 1.79 (d, J = 7.2 Hz, 12H, -CH_3 *i*-Pr), 3.66 (m, 2H, -CH *i*-Pr), 4.35 (m, 2H, -CH *i*-Pr), 7.34 (s, 2H, α-CH Py), 7.50 (m, 4H, CH naph), 8.16 (s, 1H, CH *meso*), 8.38 (m, 4H, CH naph), 11.70 (s, 2H, NH), 12.60 (s, 2H, NH); ^{13}C NMR (100 MHz, $CDCl_3$, δ in ppm): 23.54, 23.95, 26.70, 27.50, 119.15, 120.65, 121.92, 124.66, 124.80, 125.15, 125.74,125.91, 126.07, 126.13, 129.30, 129.53, 129.71, 137.88, 149.22; HR-MS (ESI): m/z calcd for $C_{82}H_{86}ClN_8$: 1217.6664; found 1217.6664 $[2M\text{-}Cl]^+$.

Synthesis of bis-naphthobipyrrolylmethene-BODIPY complex TS35

To a solution of **TS33** (600 mg, 0.96 mmol) dissolved in dichloromethane (120 mL) was added triethylamine (4 mL, 28.7 mmol) and stirred for 10 min. $BF_3.OEt_2$ (5.4 mL, 43.2 mmol) was then added slowly. The reaction mixture was stirred for overnight at room temperature. Subsequently, the reaction mixture was diluted with dichloromethane (50 mL) and washed with 1N HCl. Organic layer was dried over anhyd. Na_2SO_4, evaporated to dryness and purified over a silica column using $CHCl_3$ as eluent. Yield: 496 mg (81 %).

^{1}H NMR (400 MHz, $CDCl_3$, δ in ppm): 1.47 (d, J = 6.8 Hz, 12H, -CH_3 *i*-Pr); 1.72 (d, J = 7.2 Hz, 12H, -CH_3 *i*-Pr), 3.68 (m, 2H, -CH *i*-Pr), 4.24 (m, 2H, -CH *i*-Pr), 7.30 (s, 2H, α-CH Py), 7.47 (m, 4H, CH naph), 8.12 (s, 1H, CH *meso*), 8.37 (m, 4H, CH naph), 9.99 (brs, 2H, NH); ^{13}C NMR (100 MHz, $CDCl_3$, δ in ppm): 23.72, 24.49, 26.83, 27.94, 122.15, 123.20, 124.54, 124.74, 125.02, 125.51, 125.70, 125.77, 127.00, 129.30, 129.64, 135.33, 139.62, 146.66; ^{11}B NMR (128 MHz, $CDCl_3$, δ in ppm): -6.58 (brs, 1B); ^{19}F NMR (376.4 MHz, $CDCl_3$, δ in ppm): -138.64 (brs, 2F). HR-MS (ESI): m/z calcd for $C_{41}H_{42}BF_2N_4$: 639.3471; found $[M+H]^+$ 639.3470.

Synthesis of BODIPY dialdehyde TS36

Dry DMF (1.44 mL, 15.5 mmol) was taken in a two necked round bottomed flask under N_2 atmosphere and cooled to 0°C, freshly distilled $POCl_3$ (1.2 ml, 15.5 mmol) was then added slowly to it with continuous stirring. After complete addition, the mixture was again stirred at room temperature for 1 h. Bis-naphthobipyrrolylmethene-BODIPY **TS35** (200 mg, 0.31 mmol) dissolved in 1,2-dichloroethane (20 mL), was added to the mixture of $POCl_3$-DMF and directly heated to reflux for 7 h on a preheated oil bath. Saturated solution of aqueous

NaOAc was added and refluxed for another 2 h. Reaction mixture was diluted with $CHCl_3$, and washed thoroughly with water. Organic layer was collected, dried over anhyd. Na_2SO_4 and evaporated on a rotary evaporator under reduced pressure. The green residue thus obtained was purified by column chromatography. (silica gel, ethyl acetate : hexane::1:10). Yield: 160 mg (73 %).

^{1}H NMR (400 MHz, $CDCl_3$, δ in ppm): 1.70 (m, 24H, -CH_3 *i*-Pr), 4.21 (m, 4H, -CH *i*-Pr), 7.51 (m, 4H, CH naph), 8.24 (s, 1H, CH *meso*), 8.36 (m, 4H, CH naph), 10.41 (s, 2H, CH aldehyde), 10.88 (brs, 2H, NH); ^{13}C NMR (100 MHz, $CDCl_3$, δ in ppm): 24.50, 25.07, 27.35, 27.96, 124.13, 124.47, 125.46, 125.52, 125.62, 125.94, 126.44, 126.49, 127.31, 129.17, 134.89, 136.40, 136.89, 139.76, 147.89, 180.98. ^{11}B NMR (128 MHz, $CDCl_3$, δ in ppm): 1.98 (brs, 1B); ^{19}F NMR (376.4 MHz, $CDCl_3$, δ in ppm): -139.14 (s, 2F). HR-MS (ESI): m/z calcd for $C_{43}H_{42}BF_2N_4O_2$: 695.3369; found $[M+H]^+$ 695.3388.

Synthesis of bis-naphthobipyrrolylmethene BODIPY dimer TS37

Bis-naphthobipyrrolylmethene BODIPY complex **TS35** (50 mg, 0.078 mmol) was dissolved in TFA (15 mL). Immediately, $Na_2Cr_2O_7.2H_2O$ (8.75 mg, 0.03 mmol)) dissolved in water (0.9 mL) was added. The resulting mixture was stirred for 24 h. Solvent was distilled off under reduced pressure. Residue was dissolved in $CHCl_3$, washed throughly with water before being evaporated to dryness. The crude product was purified using a nutral alumina column to obtain the desired product as the first fraction ($CHCl_3$:Hexane::1:10). Yield: 10 mg (20 %).

^{1}H NMR (400 MHz, $CDCl_3$, δ in ppm): 1.25 (m, 20H, -CH_3 *i*-Pr), 1.78 (m, 28H, -CH_3 *i*-Pr), 3.54 (m, 2H, -CH *i*-Pr), 3.94 (m, 2H, -CH *i*-Pr), 4.31 (m, 4H, -CH *i*-Pr), 7.12 (s, 2H, α-CH Py), 7.44 (m, 4H, CH naph), 7.58 (m, 4H, CH naph), 8.18 (s, 2H, CH *meso*), 8.27 (d, 2H, CH naph), 8.35 (d, 2H, CH naph), 8.48 (d, 2H, CH naph), 8.58 (d, 2H, CH naph), 9.86 (brs, 2H, NH), 10.09 (brs, 2H, NH); ^{13}C NMR (100 MHz, $CDCl_3$, δ in ppm): 11.04, 14.29, 22.85, 23.49, 24.51, 26.64, 26.89, 27.03, 27.90, 29.51, 30.32, 31.76, 32.08, 33.37, 121.74, 124.64, 124.75, 124.84, 125.51, 125.64, 125.86, 126.85, 127.38, 128.30, 128.48, 128.78, 129.32, 129.48, 135.75, 138.24, 140.31, 145.71, 147.50. ^{11}B NMR (128 MHz, $CDCl_3$, δ in ppm): -2.93 (brs, 2B). ^{19}F NMR (376.4 MHz, $CDCl_3$, δ in ppm): -136.61 (s, 2F), -137.64 (s, 2F). HR-MS (ESI): m/z calcd for $C_{82}H_{81}B_2F_4N_8$: 1275.6706; found $[M+H]^+$1275.6597.

Synthesis of naphthobipyrrole derived linear hexaphyrin TS38

Naphthobipyrrole **TS20b** (100 mg, 0.344 mmol) was dissolved in ethanol, acidified with conc. HCl (0.7 mL, 8.6 mmol), while dialdehyde **TS21b** (60 mg, 0.172 mmol) dissolved in ethanol was added drop wise over a period of 30 min with continuous stirring at room temperature. Reaction mixture turned pink after another 30 min and it was stirred for additional 4 h. Solvent was evaporated under reduced pressure. The residue was again dissolved in chloroform, washed with water to remove the excess acid. The organic layer was dried over anhyd. Na_2SO_4 and evaporated to dryness to obtain the product as its bis-hydrochloride salt. Further it was purified over a neutral alumina column using $CHCl_3$ as the eluent. Yield: 140 mg (84 %).

^{1}H NMR (400 MHz, $CDCl_3$, δ in ppm): 1.49 (d, 12H, J = 6.8 Hz, -CH_3 *i*-Pr), 1.84 (m, 24H, -CH_3 *i*-Pr), 3.74 (m, 2H, -CH *i*-Pr), 4.43 (m, 4H, -CH *i*-Pr), 6.54 (s, 2H, α-CH Py), 7.57 (m, 6H, CH naph and CH *meso*), 8.41 (m, 4H, CH naph), 8.49 (s, 4H, CH naph), 11.57 (s, 2H, NH), 11.77 (s, 2H, NH), 11.86 (s, 2H, NH); ^{1}H NMR (D_2O exchange, 400 MHz, $CDCl_3$, δ in ppm): 1.49 (d, 12H, J = 6.8 Hz, -CH_3 *i*-Pr), 1.84 (m, 24H, -CH_3 *i*-Pr), 3.74 (m, 2H, -CH *i*-Pr), 4.40 (m, 4H, -CH *i*-Pr), 6.54 (s, 2H, α-CH Py), 7.56 (m, 6H, CH naph and CH *meso*), 8.40 (m, 4H, CH naph), 8.47 (s, 4H, CH naph); ^{13}C NMR (100 MHz, $CDCl_3$, δ in ppm): 23.57, 24.43, 26.77, 27.37, 27.68, 121.75, 122.03, 122.03, 122.78, 123.85, 124.23, 125.42, 125.59, 125.93, 126.06, 126.88, 127.67, 129.53, 129.77, 138.90, 141.71, 142.17, 145.00, 146.68. HR-MS (ESI): m/z calcd for $C_{62}H_{64}ClN_6$: 927.4881; found $[M+H]^+$ 927.4843.

Synthesis of mono-BF_2 complex of linear hexaphyrin TS39

To a solution of **TS38** (50 mg, 0.053 mmol) in dichloromethane (15 mL), triethyl amine (225 μL, 1.60 mmol) was added. The reaction mixture was stirred at room temperature for 10 min, followed by slow addition of $BF_3.OEt_2$ (141 μL, 1.16 mmol) and was stirred for another 5 h. Reaction mixture was then diluted with chloroform, washed with 1N aqueous HCl, followed by thorough washing with water. Organic layer was collected and evaporated to dryness in a rotary evaporator under reduced pressure and purified over a neutral alumina column. First red fraction eluted with hexane was collected as the desired product. The second fraction collected was the unreacted starting material (eluted with $CHCl_3$). Yield: 14 mg (29 %).

^{1}H NMR (400 MHz, $CDCl_3$, δ in ppm): 1.26 (m, 12H, -CH_3 *i*-Pr), 1.79 (m, 24H, -CH_3 *i*-Pr), 3.50 (m, 1H, -CH *i*-Pr), 3.62 (m, 1H, -CH *i*-Pr), 4.30 (m, 4H, - CH *i*-Pr), 5.90 (s, 1H, α-CH Py), 6.21 (s, 1H, α-CH Py), 7.40 (m, 2H, CH naph), 7.51 (m, 4H, CH naph), 8.01 (s, 1H, CH *meso*), 8.11 (m, 1H, CH-naph), 8.25 (m, 2H, CH-naph and CH *meso*), 8.41 (m, 4H, CH-

naph), 9.10 (s, 1H, NH), 9.71 (s, 1H, NH), 13.38 (s, 1H, NH); ^{13}C NMR (100 MHz, $CDCl_3$, δ in ppm): 19.33, 23.40, 23.45, 24.38, 24.51, 26.76, 26.84, 27.17, 27.79, 28.05, 29.80, 31.75, 119.91, 120.51, 121.02, 121.43, 123.18, 123.62, 124.56, 124.87, 125.00, 125.23, 125.45, 125.63, 125.91, 126.05, 126.76, 126.87, 127.57, 127.84, 129.04, 129.19, 129.27, 129.38, 130.24, 131.48, 135.99, 136.24, 136.93, 137.05, 140.11, 144.81, 147.06, 151.68, 152.02, 155.41. ^{11}B NMR (128 MHz, $CDCl_3$, δ in ppm): -1.55 (brs, 1B). ^{19}F NMR (376.4 MHz, $CDCl_3$, δ in ppm): -138.23 (s, 2F). HR-MS (ESI): m/z calcd for $C_{62}H_{62}BF_2N_6$: 939.5097; found $[M+H]^+$ 939.4966.

6.6 Crystallographic details

Crystallographic data for **TS33**, **TS35** and **TS37** were collected on BRUKER SMART-APEX CCD diffractometer. Pertinent crystallographic data collection and refinement parameters are shown in the following table.

Table 6.4 Crystallographic parameters of crystals of **TS33**, **TS35** and **TS37**.

Crystal data	**TS33**	**TS35**	**TS37**
Formula unit	$C_{41}H_{43}ClN_4$	$C_{41}H_{41}BF_2N_4$	$C_{82}H_{80}B_2F_4N_8$
Formula wt.	627.24	638.59	1275.16
Crystal system	Orthorhombic	Monoclinic	Triclinic
T [K]	298(2)	298(2)	298(2)
a [Å]	36.284(7)	6.0643(4)	13.813(17)
b [Å]	14.401(3)	13.3784(8)	16.78(2)
c [Å]	13.156(3)	42.361(3)	19.73(2)
α [°]	90.00	90.00	94.938(17)
β [°]	90.00	93.7890(10)	107.806(17)
γ [°]	90.00	90.00	107.534(17)
volume [Å^3]	6874(2)	3429.3(4)	4070(9)
Space group	Cmca	P2(1)/n	P-1
Z′	0.5	1	1
Z	8	4	2

D_{calc} [g.cm^{-3}]	1.212	1.237	1.040
μ/mm^{-1}	0.146	0.080	0.067
Reflns collected	32572	38975	38578
Unique reflns	3218	8175	14303
Observed reflns	1446	6997	2500
R(int)	0.1313	0.0428	0.1643
R_1 [I > 2σ(I)],	0.0674	0.1299	0.0985
wR_2	0.2223	0.2745	0.2686
GOF	1.022	1.317	0.633

6.7 References

1. Frangioni, J. V. *Curr. Opin. Chem. Biol*. **2003**, *7*, 626.
2. (a) Boppart, S. A.; Oldenburg, A. L.; Xu, C. Y.; Marks, D. L. *J. Biomed. Opt*. **2005**, *10*, 041208. (b) Demos, S. G.; Radousky, H. B.; Alfano, R. R. *Opt. Exp*ress **2000**, *7*, 23. (c) Feng, L.; Yoo, K. M.; Alfano, R. R. *Appl. Opt*. **1993**, *32*, 554. (d) Boulnois, J.-L. *Lasers in Medical Science* **1986**, *1*, 47. (e) Susi, H.; Ard, J. S.; Carroll, R. J. *Biopolymers* **1971**, *10*, 1597. (f) Pansare, V. J.; Hejazi, S.; Faenza, W. J.; Prud'homme, R. K. *Chem. Mater*. **2012**, *24*, 812.
3. Chen, J.; Corbin, I. R.; Li, H.; Cao, W.; Glickson, J. D.; Zheng, G. *J. Am. Chem. Soc*. **2007**, *129*, 5798.
4. Malick, J.; Gryczynski, I.; Geddes, C. D.; Lakowicz, J. R. *J. Biomed. Opt*. **2003**, *8*, 472.
5. Ogawa, M.; Kosaka, N.; Choyke, P. L.; Kobayashi, H. *Cancer Res*. **2009**, *69*, 1268.
6. Ching-Hsuan, T.; Sebastian. B.; Umar, M.; Ralph, W. *Bioconjug. Chem*. **1999**, *10*, 892.

7. (a) Kiyose, K.; Kojima, H.; Urano, Y.; Nagano, T. *J. Am. Chem. Soc*. **2006**, *128*, 6548. (b) Tang, B.; Huang, H.; Xu, K.; Tong, L.; Yang, G.; Liu, X.; An, L. *Chem. Commun* **2006**, *34*, 3609. (c) Tang, B.; Cui, J. L.; Xu, H. K.; Tong, L. L.; Yang, W. G.; An, G. L. *ChemBioChem* **2008**, *9*, 1159. (d) Song, F.; Peng, X.; Lu Erhu, W. Y.; Zhou, W.; Fan, J. *Tetrahedron Lett.* **2005**, *46*, 4817.
8. Sasaki, E.; Kojima, H.; Nishimatsu, H.; Urano, Y.; Kikuchi, K.; Hirata, Y.; Nagano, T. *J. Am. Chem. Soc.* **2005**, *127*, 3684.
9. (a) Zhang, Z.; Achilefu, S. *Chem. Commun*. **2005**, *47*, 5887. (b) Tang, B.; Fabiao, Y.; Li, P.; Tong, L.; Duan, X.; Xie, T.; Wang, X. *J. Am. Chem. Soc*. **2009**, *131*, 3016.
10. Demchenko, A. P. *Introduction to fluorescence sensing*. **2009**, Springer, Amsterdam.
11. Chiara, A. B.; Giuseppe, C.; Barolo, C.; Viscardi, G.; Coluccia, S. *J. Fluoresc*. **2006**, *16*, 221.
12. Patsenker, L.; Tatarets, A.; Kolosova, O.; Obukhova, P. Y.; Fedyunyayeva, I.; Yermolenko, I.; Eewald, T. *Ann. N. Y. Acad. Sci*. **2008**, *1130*, 179.
13. (a) Tam, A. C. *Appl. Phys. Lett*. **1980**, *37*, 979. (b) Law, K.-Y. *Chem. Rev*. **1993**, *93*, 449.
14. (a) Dirk, C. W.; Herndon, W. C.; Cervantes-Lee, F.; Selnau, H.; Martinez, S.; Kalamegham, P.; Tan, A.; Campos, G.; Velez, M.; Zyss, I.; Ledoux, I.; Cheng, L.-T. *J. Am. Chem. Soc.* **1995**, *117*, 2214. (b) Ashwell, G. J.; Jefferies, G.; Hamilton, D. G.; Lynch, D. E.; Roberts, M. P. S.; Bahra, B. S.; Brown, C. R. *Nature* **1995**, *375*, 385. (c) Furuki, M.; Pu, L. S.; Sasaki, F.; Kobayashi, S.; Tani, T. *Appl. Phys. Lett.* **1998**, *21*, 2648.
15. (a) Iwamoto, M.; Shidoh, S. *Jpn. J. Appl. Phys*. **1990**, *29*, 2031. (b) Merrit, V. Y.; Hovel, H. J. *Appl. Phys. Lett*. **1976**, *29*, 414. (c) Morel, D. L.; Ghosh, A. K.; Feng, T.; Stogryn, E. L.; Purwin, P. E.; Shaw, R. F.; Fishman, C. *Appl. Phys. Lett*. **1978**, *32*, 495.
16. (a) Bonnett, R. *Chemical Aspects of Photodynamic Therapy*, Gordon and Breach, Amsterdam, **2000.** (b) Ramaiah, D.; Eckert, I.; Arun, K. T.; Weidenfeller, L.; Epe, B. *Photochem. Photobiol*. **2002**, *76*, 672. (c) Ramaiah, D.; Eckert, I.; Arun, K. T.; Weidenfeller, L.; Epe, B. *Photochem. Photobiol*. **2004**, *79*, 99.
17. Yohida, Z.; Shirota, Y. *Proceedings of the second international symposium on chemistry of functional dyes* **1993**, *2*.
18. Triebs, A.; Jacob, K. *Angew. Chem., Int. Ed. Engl*. **1965**, *4*, 694.

19. (a) Basheer, M. C.; Santhosh, U.; Alex, S.; Thomas, K. G.; Cherumuttathu, H. S.; Suresh, D. *Tetrahedron* **2007**, *63*, 1617. (b) Anatoliy, L. T.; Irina, A. F.; Tatyana, S. D.; Yevgeniy, A. P.; Andrey, O. D.; Ewald, A. T.; Leonid, D. P. *Anal. Chim. Acta* **2006**, *570*, 214. (c) Kalliat, T. A.; Danaboyina, R. *J. Phys. Chem. A* **2005**, *109*, 5571. (d) Keitaro, U.; Daniel, C.; Koji, S. *Anal. Sci.* **2008**, *24*, 213. (e) Keitaro, U.; Daniel, C.; Koji, S. *Chem. Lett.* **2007**, *36*, 1424. (f) Shigeyuki, Y.; Taishi, O.; Nobuo, A.; Hiroyuki, N. *Dyes Pigm.* **2008**, *77*, 525.
20. Ballou, B.; Ernst, L. A.; Waggoner, A. S. *Curr. Med. Chem*. **2005**, *12*, 795.
21. Treibs, A.; Kreuzer, F. H. *Justus Liebigs Ann. Chem*. **1968**, *718*, 208.
22. Arroyo, I. J.; Hu, R.; Merino, G.; Tang, B. Z.; Pena-Cabrea, E. *J. Org. Chem.* **2009**, *74*, 5719.
23. (a) Loudet, A.; Burgess, K. *Chem. Rev.* **2007**, *107*, 4891. (b) Haugland, R. P. In *The Handbook: A Guide to Fluorescent Probes and Labeling Technologies*, 10th ed.; Invitrogen Corp.: Eugene, OR, **2005**. (c) Ziessel, R.; Ulrich, G.; Harriman, A. *New J. Chem.* **2007**, *31*, 496. (d) Ulrich, G.; Ziessel, R.; Harriman, A. *Angew. Chem., Int. Ed.* **2008**, *47*, 1184.
24. Arbeloa, T. L.; Arbeloa, F. L.; Arbeloa, I. L.; Garcia-Moreno, I.; Costela, A.; Sastre, R.; Amat-Guerri, F. *Chem. Phys. Lett.* **1999**, *299*, 315.
25. (a) Brom, J. M. Jr.; Langer, J. L. *J. Alloys Compd.* **2002**, *338*, 112. (b) Lai, R. Y.; Bard, A. J. *J. Phys. Chem. B* **2003**, *107*, 5036. (c) Hepp, A.; Ulrich, G.; Schmechel, R.; Seggern, H. von; Ziessel, R. *Synth. Met.* **2004**, *146*, 11. (d) Jiao, C.; Wu, J. *Synlett.* **2012**, 171.
26. (a) Yamada, K.; Nomura, Y.; Citterio, D.; Iwasawa, N.; Suzuki, K. *J. Am. Chem. Soc.* **2005**, *127*, 6956. (b) Wang, J.; Qian, X. *Org. Lett.* **2006**, *8*, 3721. (c) Hudnall, T. W.; Gabbai, F. P. *Chem. Commun.* **2008**, 4596. (d) Domaille, D.W.; Zeng, L.; Chang, C. J. *J. Am. Chem. Soc.* **2010**, *132*, 1194. (e) Atilgan, E.; Ozdemir, E.; Akkaya, E. U. *Org. Lett.* **2010**, *12*, 4792. (f) Boens, N.; Leen, V.; Dehaen, W. *Chem. Soc. Rev.* **2012**, *41*, 1130. (g) Madhu, S.; Basu, S. K.; Jadhav, S.; Ravikanth, M. *Analyst* **2013**, *138*, 299. (h) Formica, M.; Fusi, V.; Giorgi, L.; Micheloni, M. *Coord. Chem. Rev.* **2012**, *256*, 170.
27. (a) Rousseau, T.; Cravino, A.; Bura, T.; Ulrich, G.; Ziessel, R.; Roncali, J. *Chem. Commun.* **2009**, 1673. (b) Kumaresan, D.; Thummel, R. P.; Bura, T.; Ulrich, G.; Ziessel, R. *Chem. Eur. J.* **2009**, *15*, 6335. (c) Kolemen, S.; Cakmak, Y.; Erten-Ela, S.;

Altay, Y.; Brendel, J.; Thelakkat, M.; Akkaya, E. U. *Org. Lett.* **2010**, *12*, 3812. (d) Bura, T.; Leclerc, N.; Fall, S.; Leveque, P.; Heiser, T.; Ziessel, R. *J. Am. Chem. Soc.* **2012**, *134*, 17404.

28. (a) Knaus, H.-G.; Moshammer, T.; Friedrich, K.; Kang, H. C.; Haughland, R. P.; Glossmann, H. *Proc. Natl. Acad. Sci. U.S.A.* **1992**, *89*, 3586. (b) Merino, E. J.; Weeks, K. M. *J. Am. Chem. Soc.* **2005**, *127*, 12766. (c) Meng, Q.; Kim, D. H.; Bai, X.; Bi, L.; Turro, N. J.; Ju, J. *J. Org. Chem.* **2006**, *71*, 3248. (d) Peters, C.; Billich, A.; Ghobrial, M.; Hoegenauer, K.; Ullrich, T.; Nussbaumer, P. *J. Org. Chem.* **2007**, *72*, 1842. (e) Li, Z.; Bittman, R. *J. Org. Chem.* **2007**, *72*, 8376. (f) Haugland, R. P. *Handbook of Fluorescent Probes and Research Chemicals*, 6th ed.; Molecular Probes: Eugene, OR, **1996**.
29. (a) Thivierge, C.; Bandichhor, R.; Burgess, K. *Org. Lett.* **2007**, *9*, 2135. (b) Dost, Z.; Atilgan, S.; Akkaya, E. U. *Tetrahedron* **2006**, *62*, 8484. (c) Rohand, T.; Qin, W.; Boens, N.; Dehaen, W. *Eur. J. Org. Chem.* **2006**, 4658. (d) Mei, Y.; Bentley, P. A.; Wang, W. *Tetrahedron Lett.* **2006**, *47*, 2447. (e) Rurack, K.; Kollmannsberger, M.; Daub, J. *Angew. Chem., Int. Ed.* **2001**, *40*, 385. (f) Rurack, K.; Kollmannsberger, M.; Daub, J. *New J. Chem.* **2001**, *25*, 289. (g) Yu, Y.-H.; Descalzo, A. B.; Shen, Z.; Röhr, H.; Liu, Q.; Wang, Y.-W.; Spieles, M.; Li, Y.-Z.; Rurack, K.; You, X.-Z. *Chem. Asian J.* **2006**, *1*, 176. (h) Lakshmi, V.; Ravikanth, M. *J. Org. Chem.* **2013**, *78*, 4993.
30. (a) Deniz, E.; Isbasar, G. C.; Bozdemir, O. A.; Yildirim, L. T.; Siemiarczuk, A.; Akkaya, E. U. *Org. Lett.* **2008**, *10*, 3401. (b) Rihn, S.; Erdem, M.; Nicola, A. D.; Retailleau, P.; Ziessel, R. *Org. Lett*. **2011**, *13*, 1916.
31. (a) Adarsh, N.; Avirah, R. R.; Ramaiah, D. *Org. Lett.* **2010**, *12*, 5720. (b) Hall, M. J.; McDonnell, S. O.; Killoran, J.; O'Shea, D. F. *J. Org. Chem.* **2005**, *70*, 5571. (c) Zhao, W.; Carreira, E. M. *Angew. Chem., Int. Ed.* **2005**, *44*, 1677. (d) Zhao, W.; Carreira, E. M. *Chem. Eur. J.* **2006**, *12*, 7254. (e) McDonnell, S. O.; O'Shea, D. F. *Org. Lett.* **2006**, *8*, 3493.
32. (a) Umezawa, K.; Nakamura, Y.; Makino, H.; Citterio, D.; Suzuki, K. *J. Am. Chem. Soc.* **2008**, *130*, 1550. (b) Umezawa, K.; Matsui, A.; Nakamura, Y.; Citterio, D.; Suzuki, K. *Chem. Eur. J.* **2009**, *15*, 1096. (c) Samuel, G. A.; Polreis, J.; Biradar, V.; You, Y. *Org. Lett.* **2011**, *35*, 3885. (d) Descalzo, A. B.; Xu, H.-J.; Xue, Z.-L.; Hoffmann, K.; Shen, Z.; Weller, M. G.; You, X.-Z.; Rurack, K. *Org. Lett.* **2008**, *10*, 1581. (e) Shen, Z.; Röhr, H.; Rurack, K.; Uno, H.; Spieles, M.; Schulz, B.; Reck, G.;

Ono, N. *Chem. Eur. J.* **2004**, *10*, 4853. (f) Ni, Y.; Zeng, W.; Huang, K-W.; Wu, J.; *Chem. Commun.* **2013**, *49*, 1217. (g) Wakamiya, A.; Murakami, T.; Yamaguchi, S. *Chem. Sci.* **2013**, *4*, 1002. (h) Jiao, C.; Huwang, K.-W.; Wu, J. *Org. Lett.* **2011**, *13*, 632. (i) Nakamura, M.; Tahara, H.; Takahashi, K.; Nagata, T.; Uoyama, H.; Kuzuhara, D.; Mori, S.; Okujima, T.; Yamada, H.; Uno, H. *Org. Biomol. Chem*. **2012**, *10*, 6840. (j) Hayashi, Y.; Obata, N.; Tamaru, M.; Yamaguchi, S.; Matsuo, Y.; Saeki, S.; Kureishi, Y.; Saito, S.; Yamaguchi, S.; Shinokubo, H. *Org. Lett.* **2012**, *14*, 866.

33. (a) Rogers, M. A. T. *J. Chem. Soc.* **1943**, 590. (b) Davies, W. H.; Rogers, M. A. T. *J. Chem. Soc.* **1944**, 126. (c) Knott, E. B. *J. Chem. Soc.* **1947**, 1196.
34. Sathyamoorthi, G.; Soong, M. L.; Ross, T. W.; Boyer, *J. H. Heteroat. Chem*. **1993**, *4*, 603.
35. (a) Killoran, J.; Allen, L.; Gallagher, J.; Gallagher, W.; O'Shea, D. *Chem. Commun.* **2002**, 1862. (b) Gorman, A.; Killoran, J.; O'Shea, C.; Kenna, T.; Gallagher, W. M.; O'Shea, D. F. *J. Am. Chem. Soc.* **2004**, *126*, 10619.
36. (a) Sarma, T.; Panda, P. K.; Anusha, P. T.; Rao, S. V. *Org. Lett*. **2011**, *13*, 188. (b) Roznyatovskiy, V.; Lynch, V.; Sessler, J. L. *Org. Lett.* **2010**, *12*, 4424. (c) Rao, S. V.; Prashant, T. S.; Swain, D.; Sarma, T.; Panda, P. K.; Tewari, S. P. *Chem. Phys. Lett.* **2011**, *514*, 98. (d) Sarma, T.; Panda, P. K. *Chem. Eur. J.* **2011**, *17*, 13987. (e) Roznyatovskiy, V. V.; Lim, J. M.; Lynch, V. M.; Lee, B. S.; Kim, D.; Sessler, J. L. *Org. Lett.* **2011**, *13*, 5620. (f) Kee, S.-Y.; Lim, J. M.; Kim, S.-J.; Yoo, J.; Park, J.-S.; Sarma, T.; Lynch, V. M.; Panda, P. K.; Sessler, J. L.; Kim, D.; Lee, C.-H. *Chem. Commun.* **2011**, *47*, 6813. (g) Ishida, M.; Kim, S.-J.; Preihs, C.; Ohkubo, K.; Lim, J. M.; Lee, B. S.; Park, J. S.; Lynch, V. M.; Roznyatovskiy, V. V.; Sarma, T.; Panda, P. K.; Lee, C. H.; Fukuzumi, S.; Kim D.; Sessler, J. L. *Nat. Chem*. **2013**, *5*, 15.
37. Sepulveda-Boza, S.; Breitmaier, E. *Liebigs Ann. Chem.* **1983**, 894.
38. Sarma, T.; Panda, P. K.; Setsune, J.-i. *Chem. Commun*. 2013, in press (DOI:10.1039/C3CC44834G).
39. (a) See http://omlc.ogi.edu/spectra/PhotochemCAD/html/011.html. (b) Mishra, A.; Behera, R. K.; Behera, P. K.; Mishra, B. K.; Behera, G. B. *Chem. Rev*. **2000**, *100*, 1973.
40. Sanyal, S.; Akselrod, M. S. *J. Appl. Phys.* **2005**, *98*, 033518/033511-033518/033512.
41. Kruk, M.; Ngo, T. H.; Savva, V.; Starukhin, A.; Dehaen, W.; Maes, W. *J. Phys. Chem. A* **2012**, *116*, 10704.

42. (a) Madhu, S.; Rao, M. R.; Shaikh, M. S.; Ravikanth, M. *Inorg. Chem.* **2011**, *50*, 4392. (b) Madhu, S.; Ravikanth, M. *Inorg. Chem*. **2012**, *51*, 4285.
43. Sessler, J. L.; Seidel, D.; Lynch, V. *J. Am. Chem. Soc.* **1999,** *121*, 11257.
44. (a) Sessler, J. L.; Weghron, S. J.; Lynch, V.; Fransson, K. *J. Chem. Soc., Chem. Commun.* **1994**, 1289. (b) Sessler, J. L.; Seidel, D.; Vivian, A. E.; Lynch, V.; Scott, B. L.; Keogh, D. W. *Angew. Chem. Int. Ed*. **2001**, *40*, 591.
45. Gadekar, S. C.; Reddy, B. K.; Anand, V. G. *Angew. Chem. Int. Ed.* **2013**, *52*, 7164.

CHAPTER 7

Conclusion

7.1 Summary

The thesis entitled "*Naphthobipyrrole derived novel π-extended porphyrinoids: Synthesis, structure and optical properties*" consists of seven chapters. It deals with the syntheses and characterizations of novel π-extended porphyrinoids derived from alkylated naphthobipyrroles developed in our group. These includes dinaphthoporphycenes, cyclo[4]naphthobipyrroles, naphthosapphyrins and various BODIPY dyes derived from naphthobipyrrole. These porphyrinoids have been further evaluated in terms of their optical properties, metal coordination properties and structural characterizations. In this chapter a very brief summary along with future scope of the work is presented.

Porphyrins that are known as pigments of life, plays a vital role in many of the biological process upon which life depends. Simultaneously, porphyrin displays very rich photochemistry and metal coordination chemistry. The fascinating properties of porphyrin made researcher to think beyond porphyrins and as a result a diverse area of research have been emerged that deals with contracted, isomeric and expanded porphyrins. Consequently a plethora of porphyrinoids have been synthesized and studied, many of them comes up with unique properties that were unprecedented in porphyrin chemistry. As a result search for new porphyrinoids with excellent properties still continues.

In this regard annulated porphyrins, wherein additional aromatic rings are fused on to the porphyrin periphery, have received much attention recently. Extension of π-conjugation through additional aromatic ring often leads to bathochromically shifted absorption spectra relative to their non-annulated counterpart. Thus these materials hold promise for various applications such as dye stuffs, optical materials, nonlinear optics, organic semiconductors, photosensitizers for photodynamic therapy (PDT), and dye-sensitized solar cells. However, π-extension in expanded and isomeric porphyrin is still in its infancy stage. Only a few examples appear very recently. Nonetheless these molecules show unprecedented optical and structural properties compared to their non-annulated counterpart. It has been well documented that electronic, optical and coordination properties of expanded porphyrins are dependent upon their conformations and hence control over their conformations is very crucial. Use of rigid fused bipyrrolic precursor or fusion of aromatic ring on periphery of expanded porphyrins has two-fold advantages as this not only increases π-conjugation but also imparts structural rigidification to the resulting macrocycle.

Incidentally we were interested to synthesize and explore novel π-extended porphyrinoids that are structurally rigid. In this context, we choose to synthesize naphthobipyrrole bearing alkyl substitutions at β-pyrrolic positions. One of the major concerns while synthesizing new porphyrinoids is solubility of the precursors as well as the resultant macrocycles in organic solvents. This is because most of the reactions and subsequent characterization and exploration of the resultant products deals mostly with organic solvents. Towards this we demonstrated a generalized route towards synthesis of alkylated naphthobipyrroles bearing alkyl chains at β-pyrrolic positions. This modification not only improves solubility but also increases its selectivity towards subsequent functionalization by blocking the β-pyrrolic positions hence preventing any other reactions at those positions. These novel alkylated naphthobipyrroles were utilized for synthesizing various novel π-extended porphyrinoids that possess unique properties. For instance, corresponding naphthobipyrrole dialdehydes were converted to novel π-extended porphycenes namely dinaphthoporphycenes, wherein two fused bipyrrolic units are involved in macrocyclization following the classical reductive McMurry coupling approach. As a result of extended π-conjugation dinaphthoporphycenes display dramatic improvement in their linear as well as nonlinear optical properties compared to normal porphycenes. Metal coordinating properties of dinaphthoporphycene have been studied with several metal ions, where Cu(II), Pd(II) and Ni(II) complexes could be realized successfully. These metal complexes showed a hitherto unknown square type N4-core upon metallation as inferred from X-ray structure analysis. Nonlinear optical studies reveal that these macrocycles show intensity dependent multi-photon absorbance possessing very high $\sigma^{(3)}$ and $\sigma^{(2)}$ values. Ultrafast excited state dynamics of dinaphthoporphycenes were also investigated using femtosecond and picosecond degenerate pump-probe techniques. It is worth mentioning that 2PA and 3PA studies in porphycene are very rare; in fact there exist only a single report regarding 2PA in porphycene prior to us.

We also described synthesis and characterization of cyclo[4]naphthobipyrroles, an unique example of cyclo[8]pyrrole possessing direct linkage between four naphthobipyrrole units through their α-carbon atoms. Strong NIR absorptions between 1273 to 1339 nm were observed for cyclo[4]naphthobipyrroles, obtained through acid-catalyzed oxidative coupling methods from β-dialkylnaphthobipyrroles. These molecules display a large red shift (161–228 nm) in their lowest energy bands relative to the reported alkylated cyclo[8]pyrrole, due to the induced

structural rigidification and extended π-conjugation. It was observed that the cyclo[8]pyrrole moiety is very sensitive to the nature of the substituents (even depending upon type of alkyl substituents) at its periphery, owing to the involvement of large number of nonbonding interactions. This is reflected not only on their photophysical properties but also in their synthesis from the corresponding bipyrroles. These cyclo[4]naphthobipyrroles, can be of great importance for practical application as NIR dyes, apart from their potential utility in light harvesting, dye-sensitized solar cells and bio imaging applications. Further, these macrocycles display large two-photon absorption cross-sections along with exciting solvent dependent behavior. Absorption spectra of cyclo[4]naphthobipyrroles in polar solvent such as DMSO undergoes a drastic change compared to the spectra in $CHCl_3$ or toluene. Precisely, intensity of NIR band reduces dramatically and appears as a very weak and broad band. This seems to be caused by two effects: (i) dissociation of the anion from the sulfate-stabilized complex possibly stabilized by specific interaction with the solvent and (ii) concomitant changes in geometry. Noticeable decrement in intensity of the NIR band was also observed for free base cyclo[4]naphthobipyrrole indicating the assumed geometrical change in absence of counter anion. Solvent sensitivity of the electronic spectra in combination with the absorption in the near IR range make cyclo[4]naphthobipyrroles promising objects for studying molecular recognition and ion transfer phenomenon. Further, in presence of acid, cyclo[4]naphthobipyrrole undergoes one electron oxidation thereby producing radical cation as evident from EPR measurement. This radical cation can be reduced back to its original state by treating with DBU. Perhaps this oxidation of cyclo[4]naphthobipyrrole in presence of acid is accompanied by reduction of dioxygen thereby producing H_2O_2. This aspects of cyclo[4]naphthobipyrrole is worth exploring in great detail as this type of proton-coupled electron transfer (PCET) is not only of biological interest but also of technological importance as fundamentals of fuel cells.

Another very interesting feature observed in case of cyclo[4]naphthobipyrrole is that both the free base and sulphate salts are found to be EPR active in solution as well as in solid state. This in turn indicates possible existence of close lying triplet state to HOMO of cyclo[4]naphthobipyrrole and hence its existence as a stable biradical at room temperature. Looking at the significance of stable organic radicals because of its numerous applications such as organic magnetic materials, electronic devices, optical materials etc.

cyclo[4]naphthobipyrroles in specific and cyclo[8]pyrroles in general, are highly promising to study in this direction.

Di-formylated naphthobipyrroles were also employed in synthesis of two novel *meso*-unsubstituted naphthosapphyrins, following rational [3 + 2] MacDonald type condensation. In one case all β-pyrrolic positions are substituted where as another having an unsubstituted pyrrole opposite to the bipyrrolic unit. Their comparative spectral analysis, including absorption and emission properties of diprotonated form prepared by treating with different acids has been discussed. Our ^{1}H NMR and UV-visible spectroscopic studies rules out presence of any inverted structure in these macrocycle at least in room temperature. The steric strain imposed by ring fusion is not sufficient enough to cause an inversion in pyrrole ring opposite to it, as observed in case of *meso*-tetraaryl and hetero sapphyrins analogues. We also synthesized a previously unknown octaalkylsapphyrin derivative derived from tetraethyl bipyrrole dialdehyde that possess an unsubstituted pyrrole ring opposite to the bipyrrolic unit. A comparative discussion of spectral properties of this molecule has been made with those of naphthosapphyrins. ^{1}H NMR spectrum of this latter system in presence of TFA indicates that in comparison to **TS31** this system is more flexible, probably resulting in one of the bipyrrolic pyrrole moiety going out of the plane to relieve the steric strain. Therefore it may be possible to observe new ways of ring inversion in a system where bipyrrole is more sterically crowded.

Further di-isopropylnaphthobipyrrole has been utilized for synthesis of novel π-extended BODIPY dyes. Reactions of this naphthobipyrrole with triethyl orthoformate in presence of $POCl_3$ led to the formation of bis-naphthobipyrrolylmethene. This was then further converted to its corresponding BODIPY complex. Bis-naphthobipyrrolyl BODIPY shows NIR absorption (730 nm) and emission (744 nm) with efficient quantum yield (ϕ_f = 0.65), exceptionally high extinction coefficient and good photostability. Further, formylation of bis-naphthobipyrrolyl BODIPY leads to formation of the corresponding dialdehyde. This dialdehyde exhibits excellent photostability as well as further enhancement in quantum yield. Photophysical properties of these molecules including the parent bis-naphthobipyrrolylmethene have been discussed. This dialdehyde in turn holds immense potential as a precursor leading to an array of conformationally restricted functionalized BODIPY dyes.

Bis-naphthobipyrrolyl BODIPY dimer synthesized from bis-naphthobipyrrolyl BODIPY, shows an impressive absorption (λ_{max} = 769 nm) and emission (λ_{max} = 825 nm) maxima in the NIR region. Moreover, solid state structure shows interesting helical arrangement of two monomers. Looking at the necessity in development of longer-chain oligopyrroles for new multinuclear single helicates that are stable against racemization, BODIPY dimer with appropriate substituents may be a potential candidate to study in this way.

Reaction between naphthobipyrrole dialdehyde and naphthobipyrrole leads to formation of linear π-extended hexaphyrin. This linear hexaphyrin was successfully converted to its corresponding mono-BF_2 complex that shows NIR absorption even above 900 nm. However, attempt to synthesize its bis-BF_2 complex is so far not successful.

In summary, an attempt has been made to synthesize and explore various conformationally rigid π-extended porphyrinoids derived from alkylated naphthobipyrroles. Dramatic improvements in both the linear and non-linear optical properties were observed in these porphyrinoids. These alkylated naphthobipyrroles and its linear analogues can also utilized for synthesizing many other π-extended porphyrinoids such as corrole, smaragdyrins, octaphyrins etc. Our initial findings also suggest possible exploration of naphthobipyrrole derived porphyrinoids in terms of organic magnetic material. We believe that these findings will be considered as important addition towards the emergent area of π-extended porphyrinoids.

Appendix

Appendix

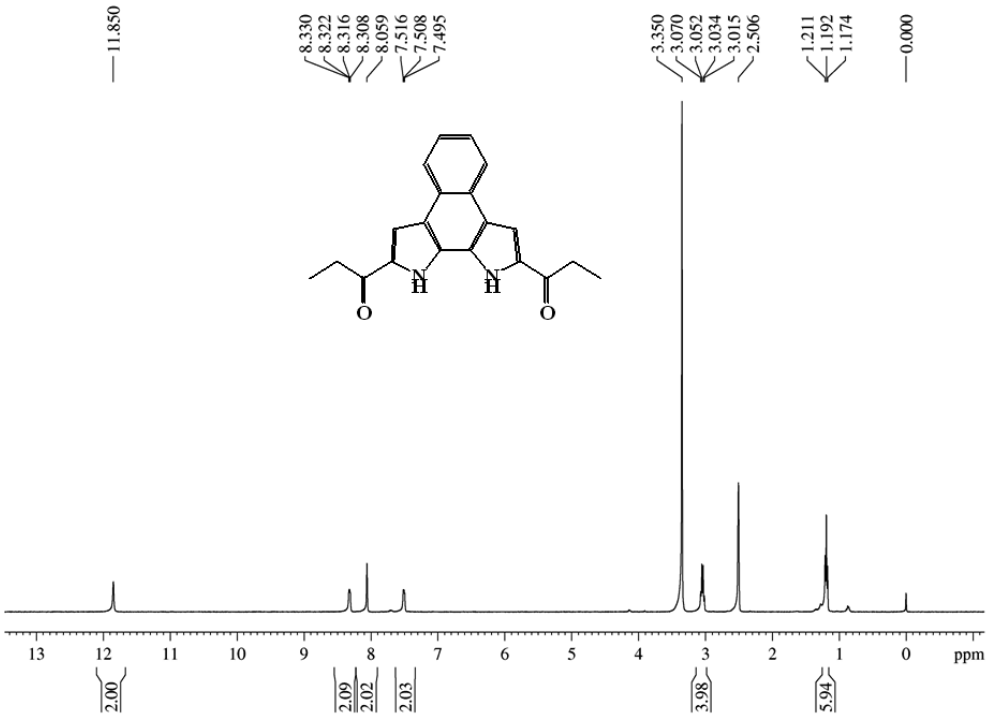

Figure A1 ^{1}H NMR spectrum of **TS15a** in DMSO-D_6.

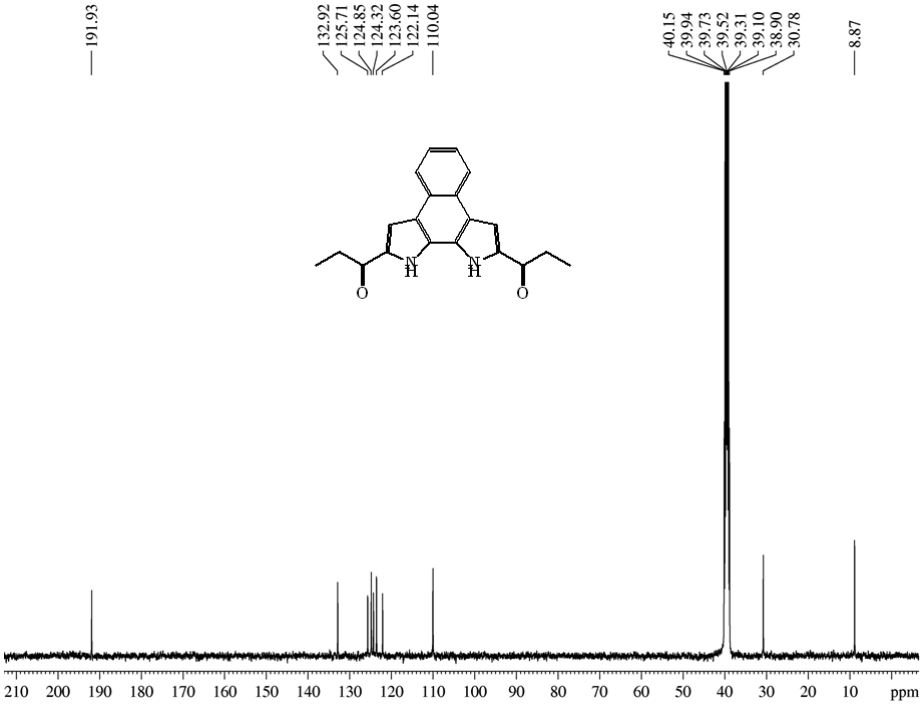

Figure A2 ^{13}C NMR spectrum of **TS15a** in DMSO-D_6.

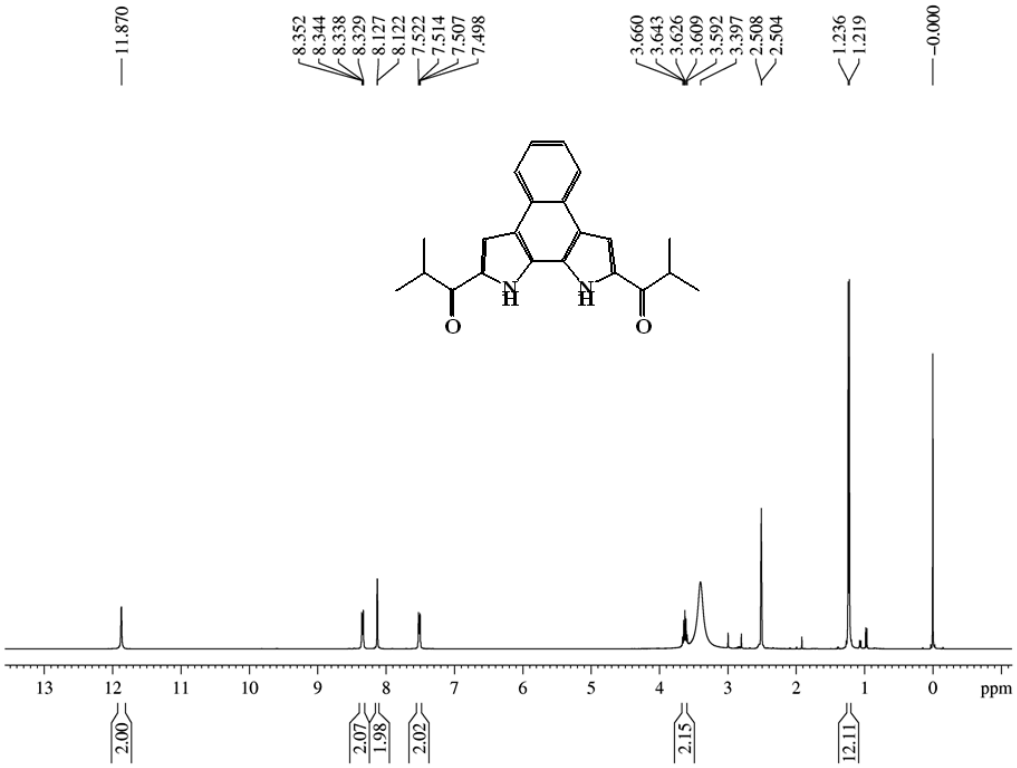

Figure A3 ^{1}H NMR spectrum of **TS15b** in DMSO-D_6.

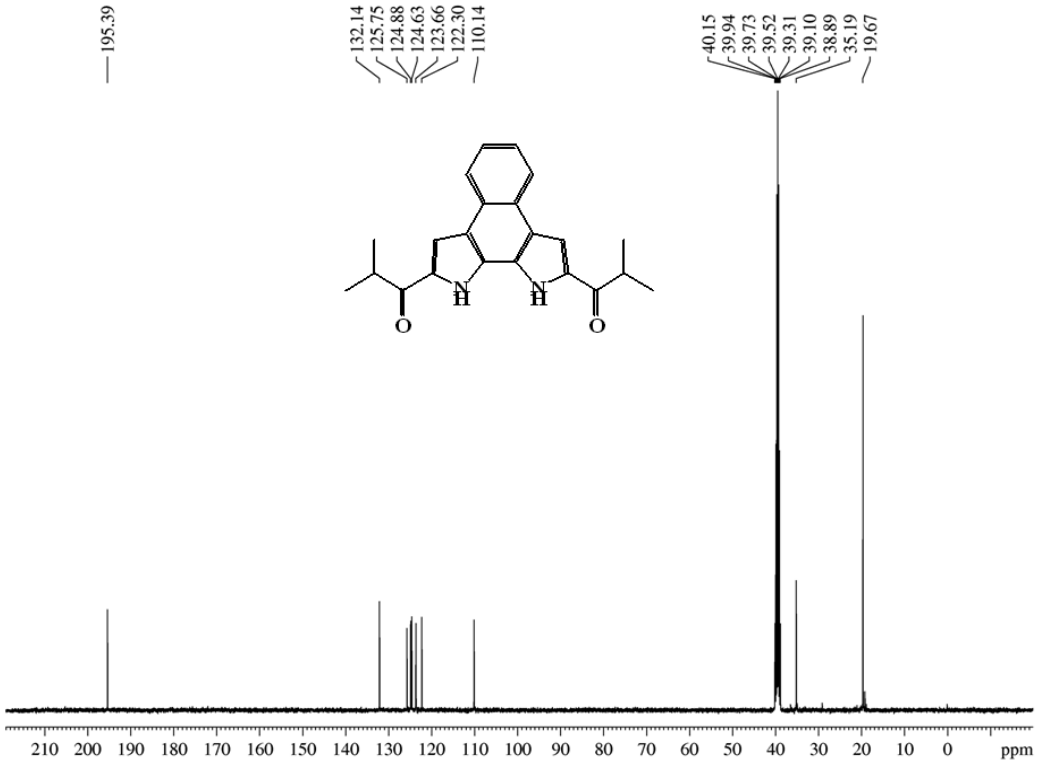

Figure A4 ^{13}C NMR spectrum of **TS15b** in DMSO-D_6.

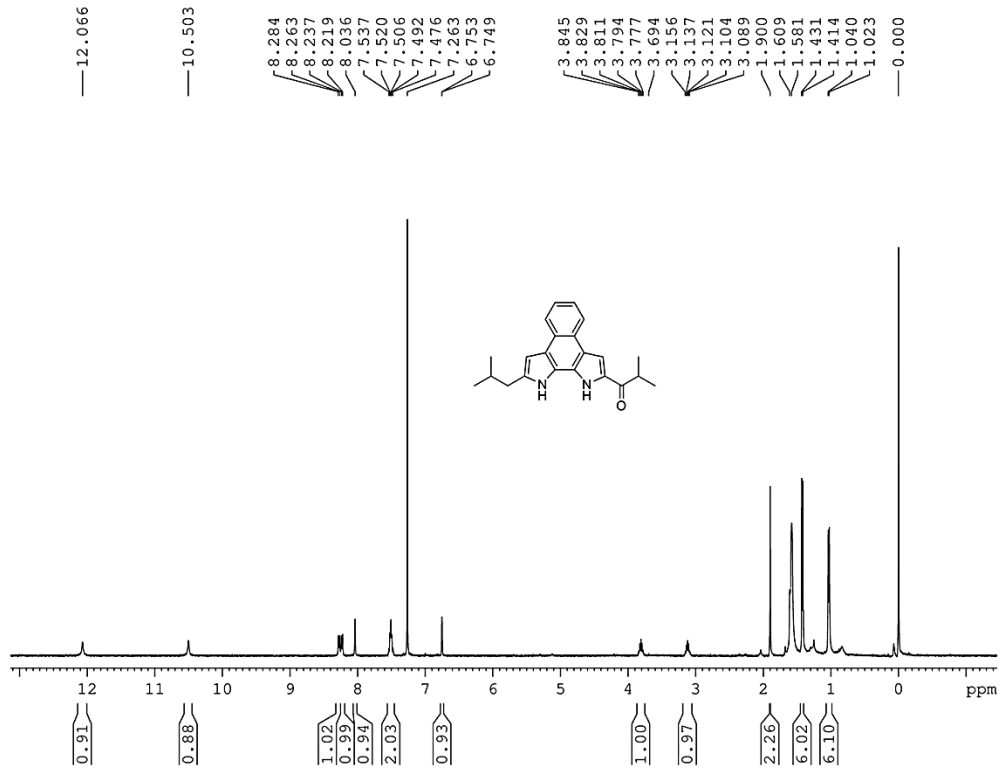

Figure A5 ^{1}H NMR spectrum of **TS16** in $CDCl_3$.

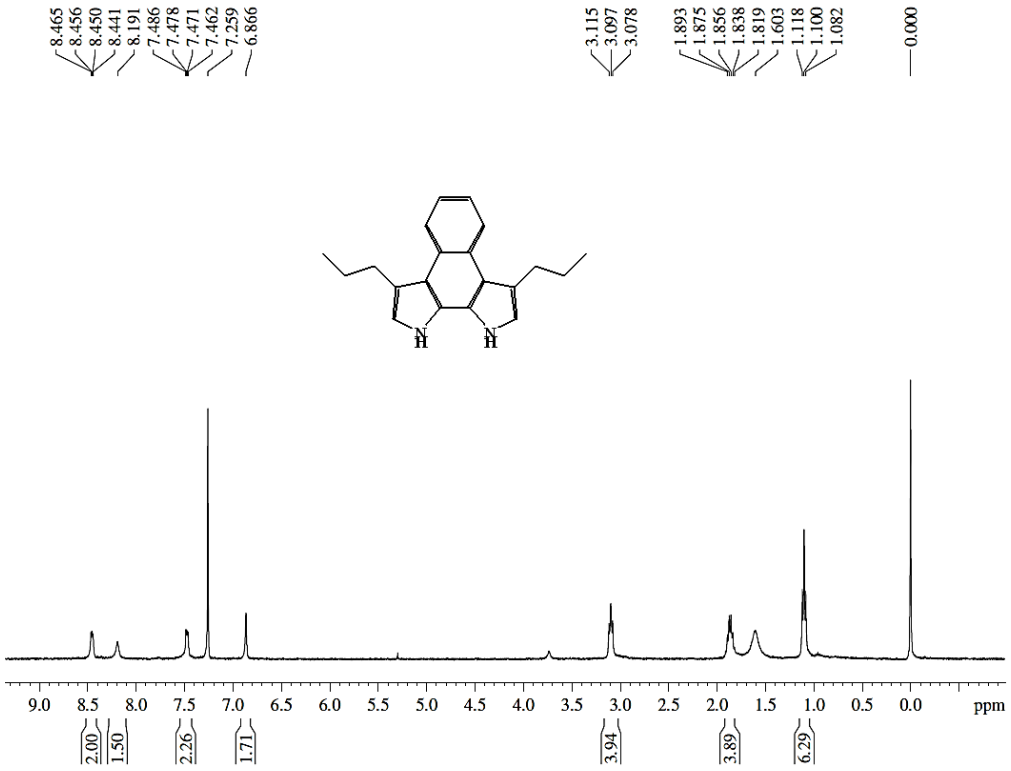

Figure A6 ^{1}H NMR spectrum of **TS20a** in $CDCl_3$.

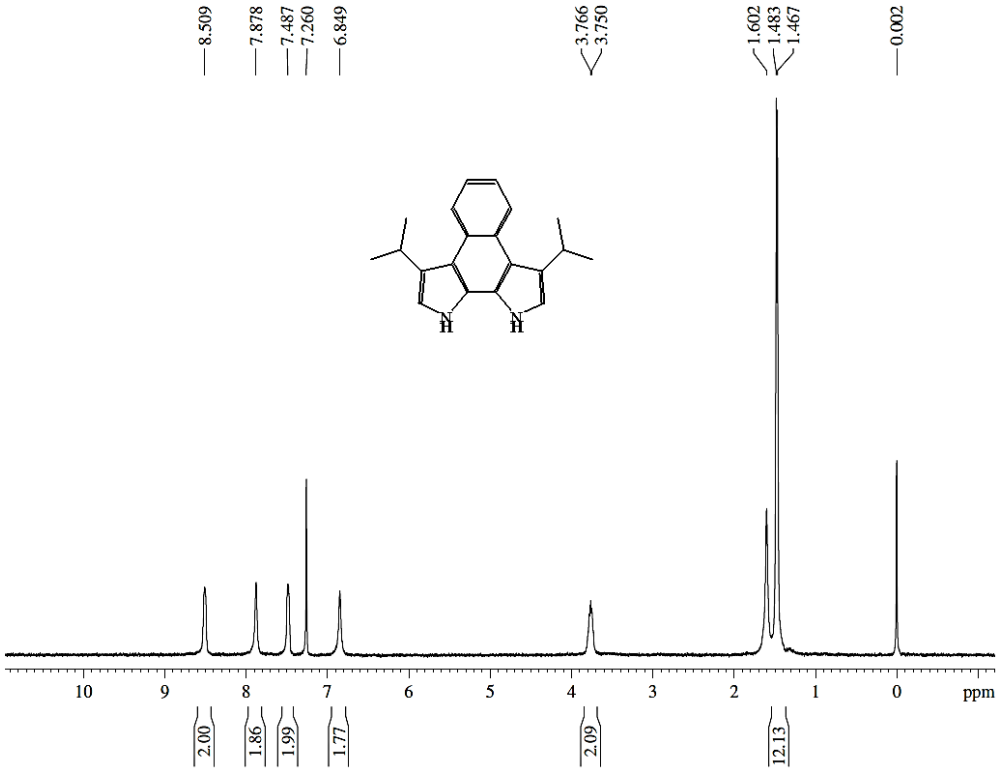

Figure A7 ^{1}H NMR spectrum of **TS20b** in $CDCl_3$.

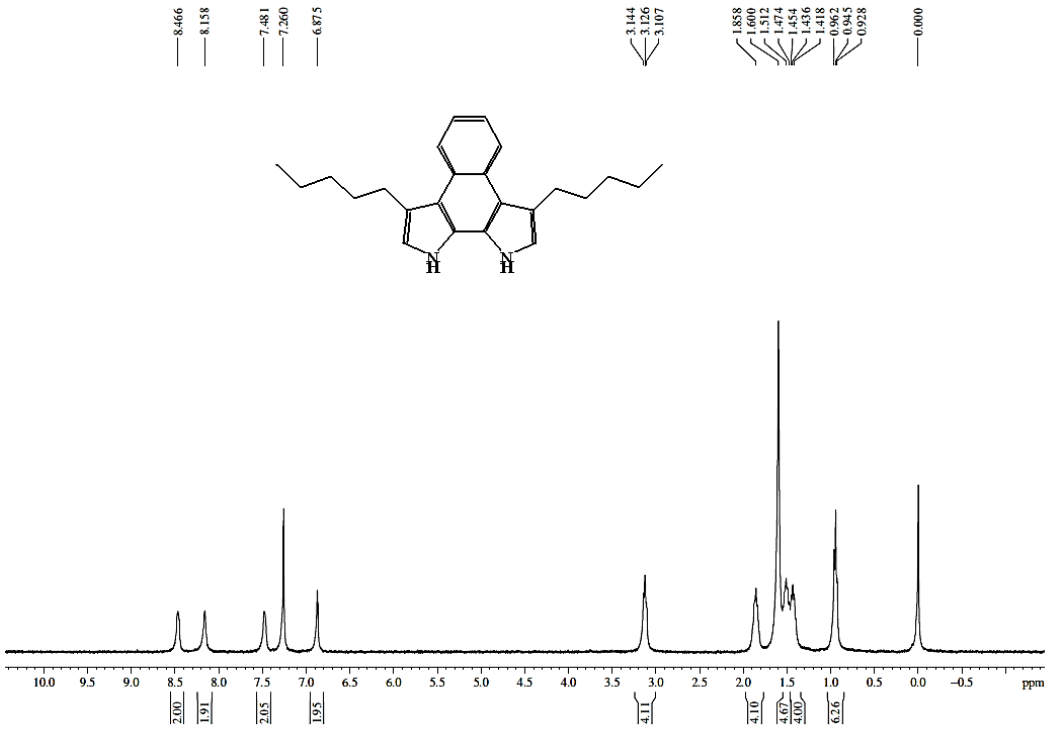

Figure A8 ^{1}H NMR spectrum of **TS20c** in $CDCl_3$.

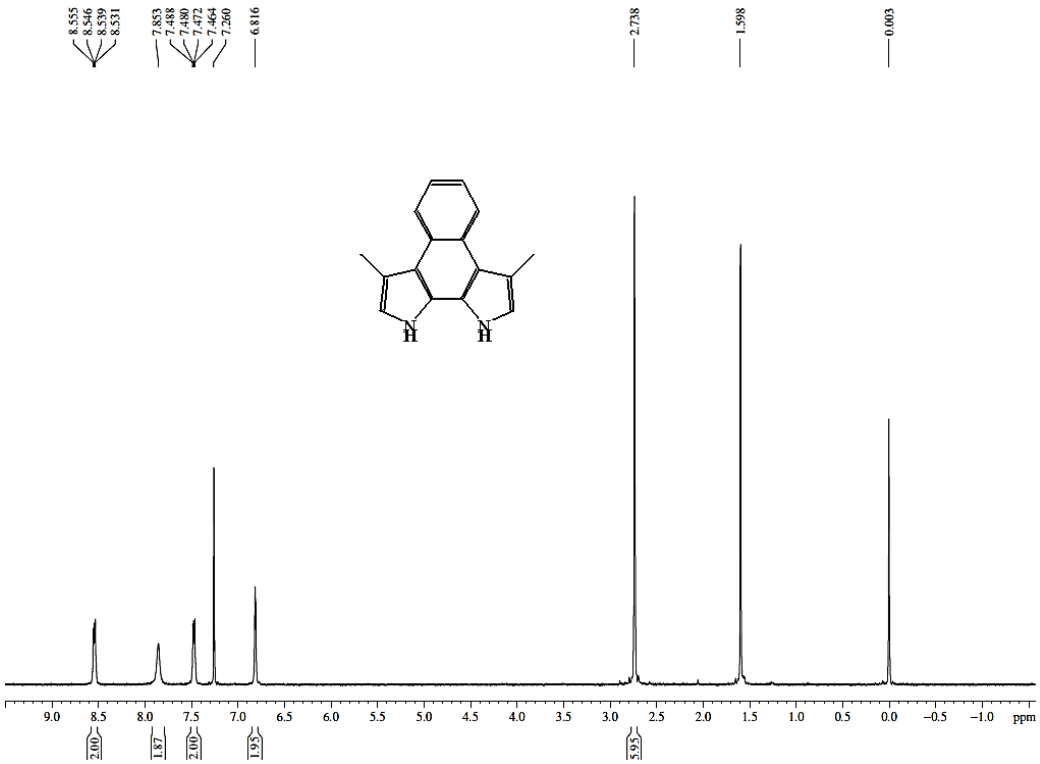

Figure A9 ^{1}H NMR spectrum of **TS20d** in $CDCl_3$.

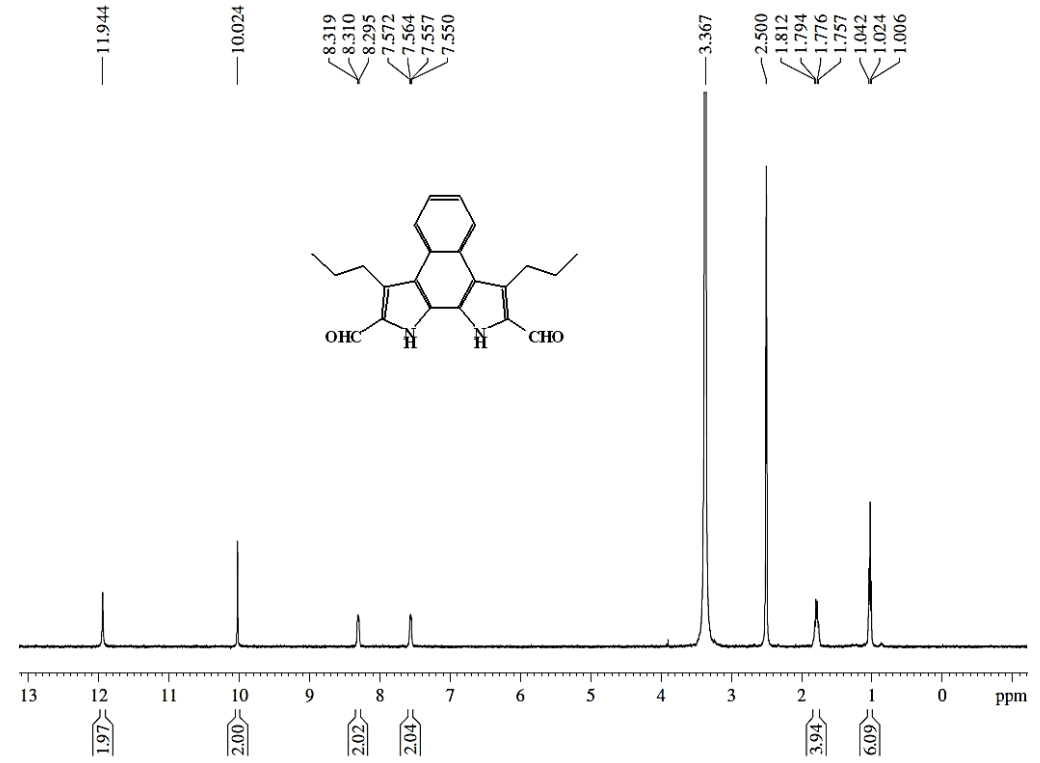

Figure A10 ^{1}H NMR spectrum of **TS21a** in DMSO-D_6.

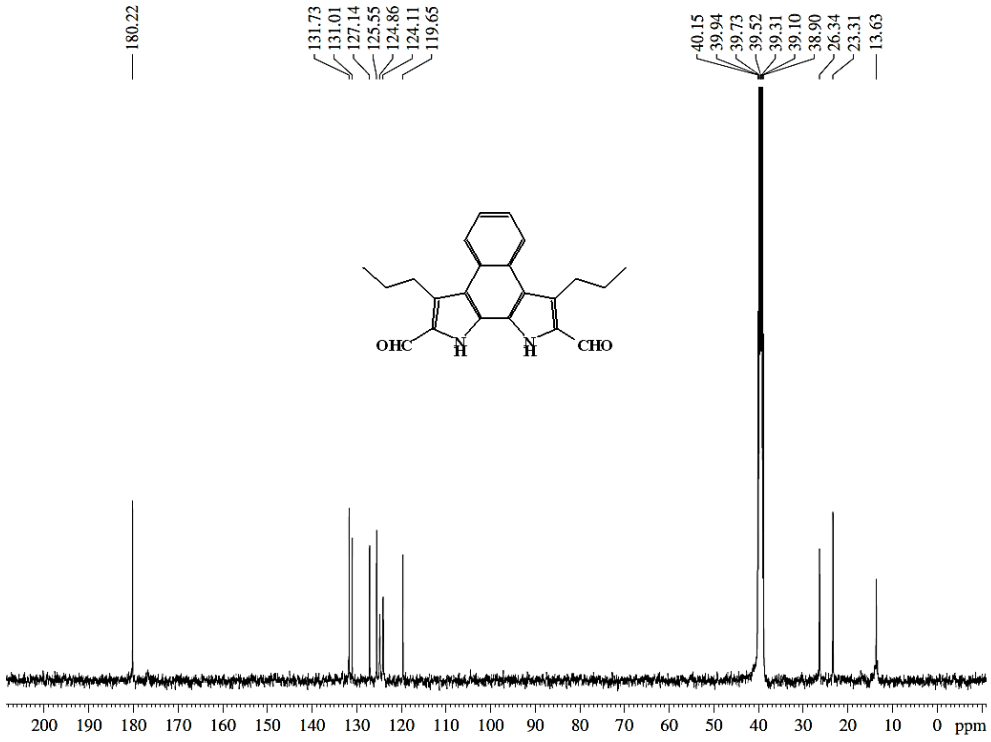

Figure A11 ^{13}C NMR spectrum of **TS21a** in DMSO-D_6.

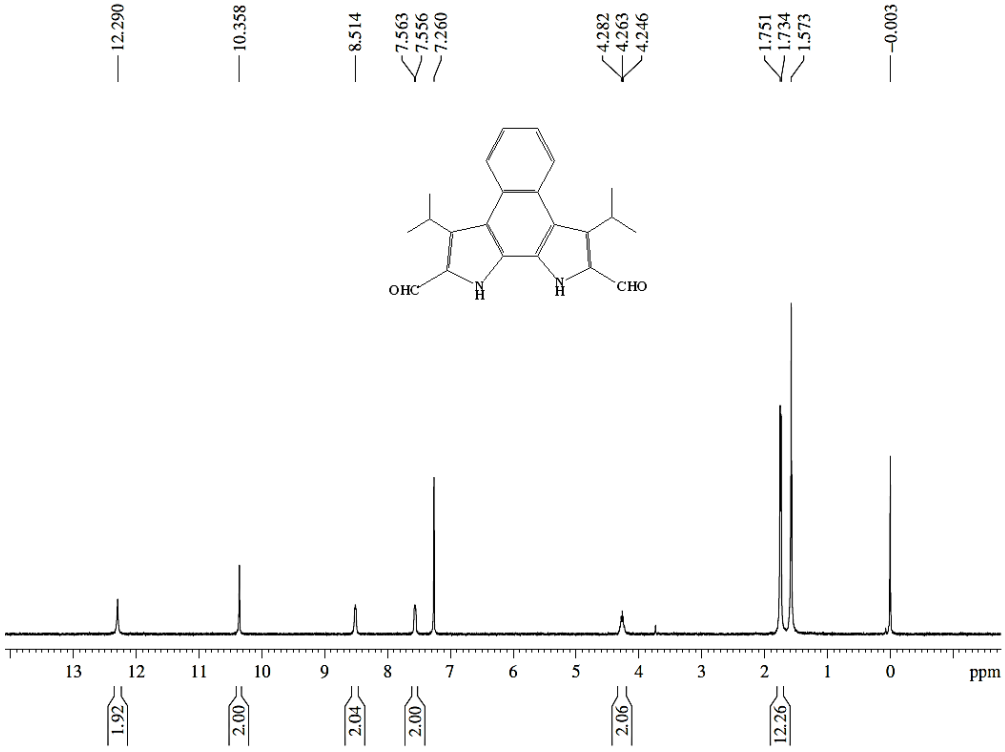

Figure A12 ^{1}H NMR spectrum of **TS21b** in $CDCl_3$.

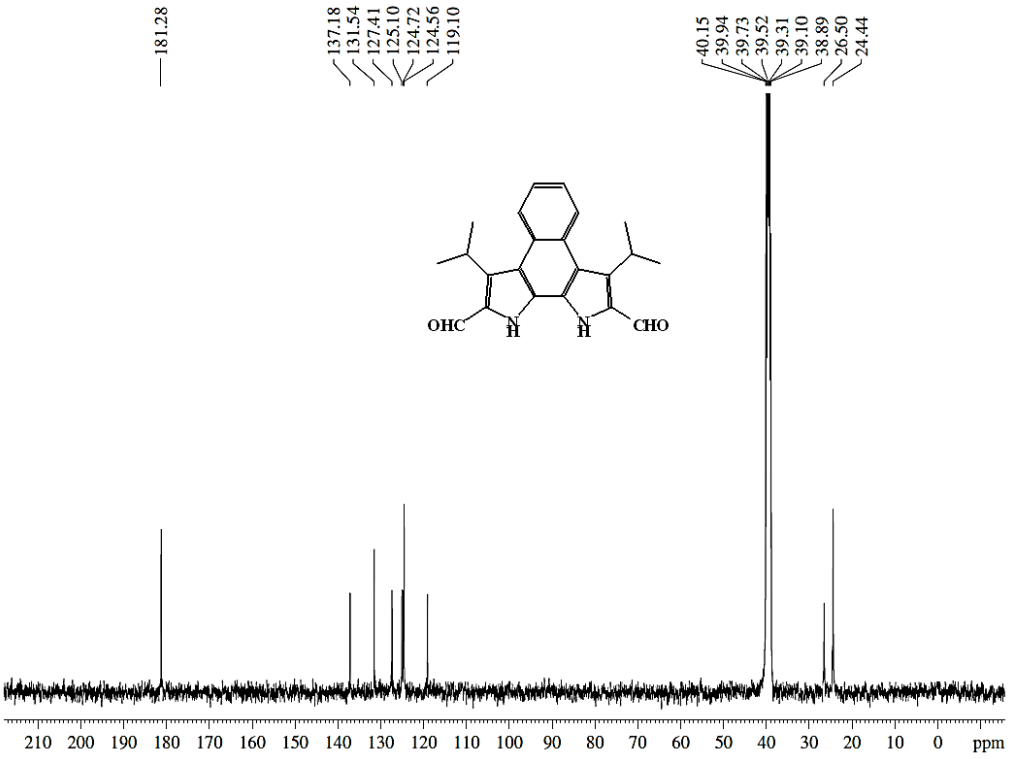

Figure A13 ^{13}C NMR spectrum of **TS21b** in $CDCl_3$.

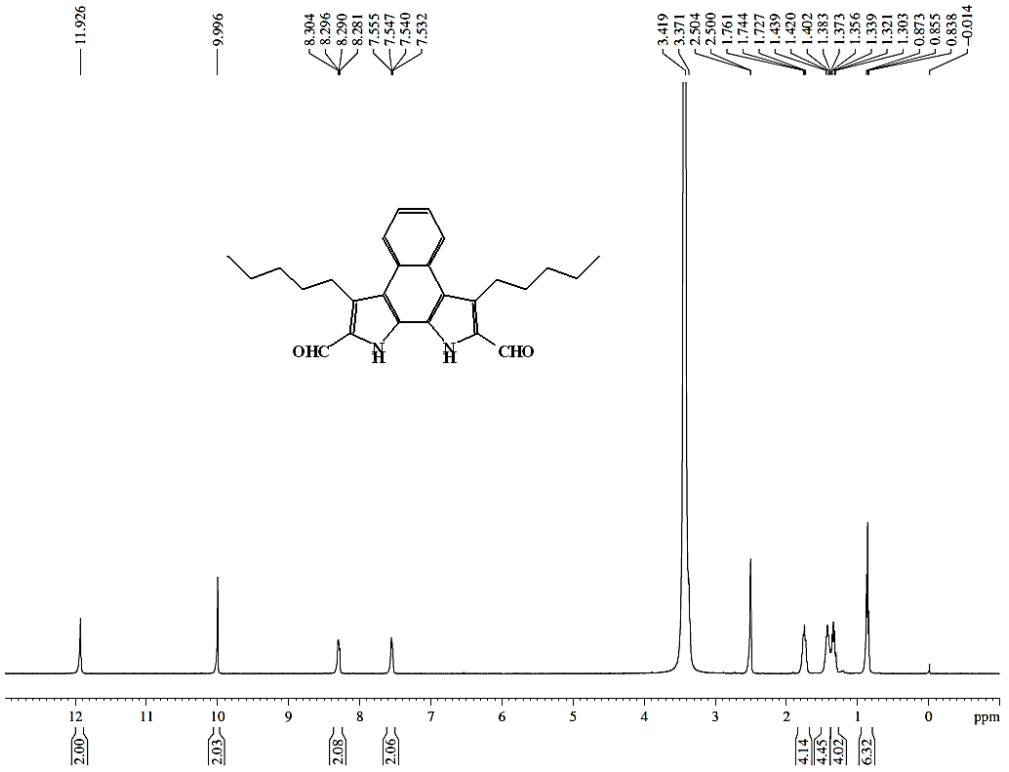

Figure A14 ^{1}H NMR spectrum of **TS21c** in DMSO-D_6.

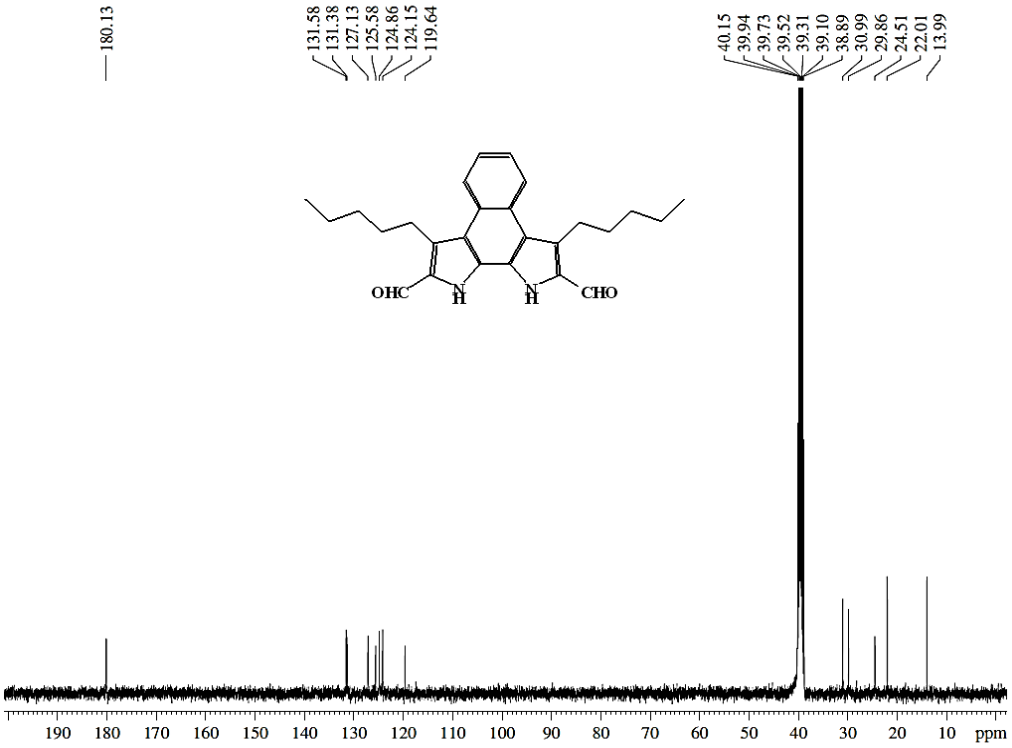

Figure A15 ^{13}C NMR spectrum of **TS21c** in DMSO-D_6.

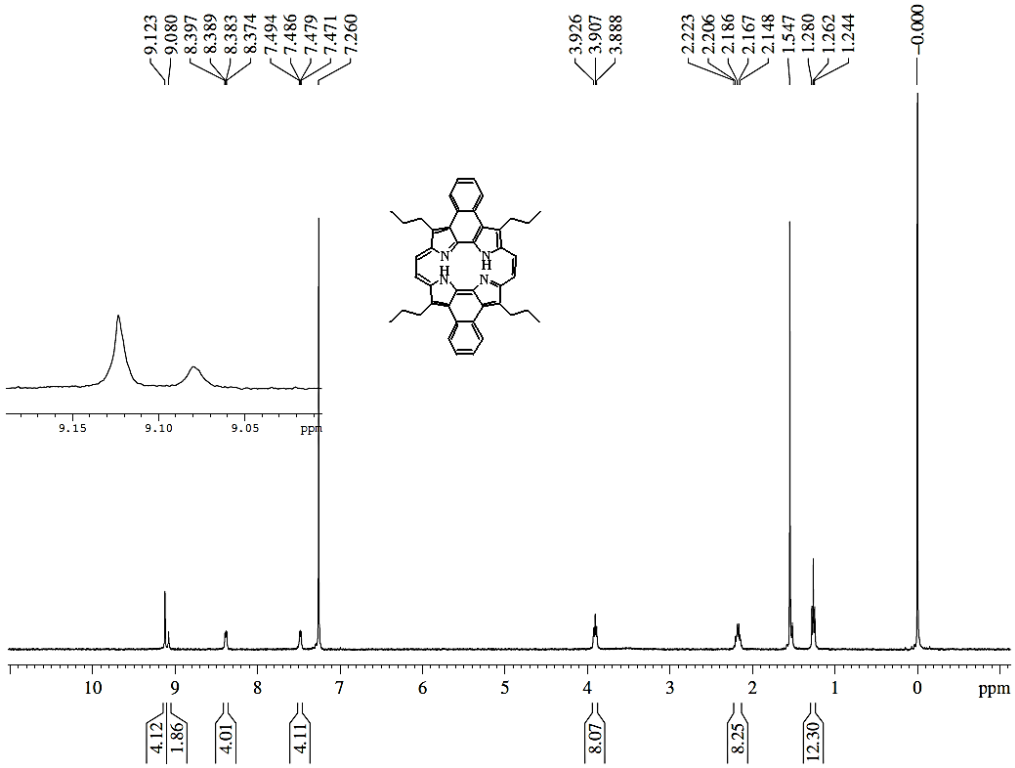

Figure A16 ^{1}H NMR spectrum of **TS22a** in $CDCl_3$.

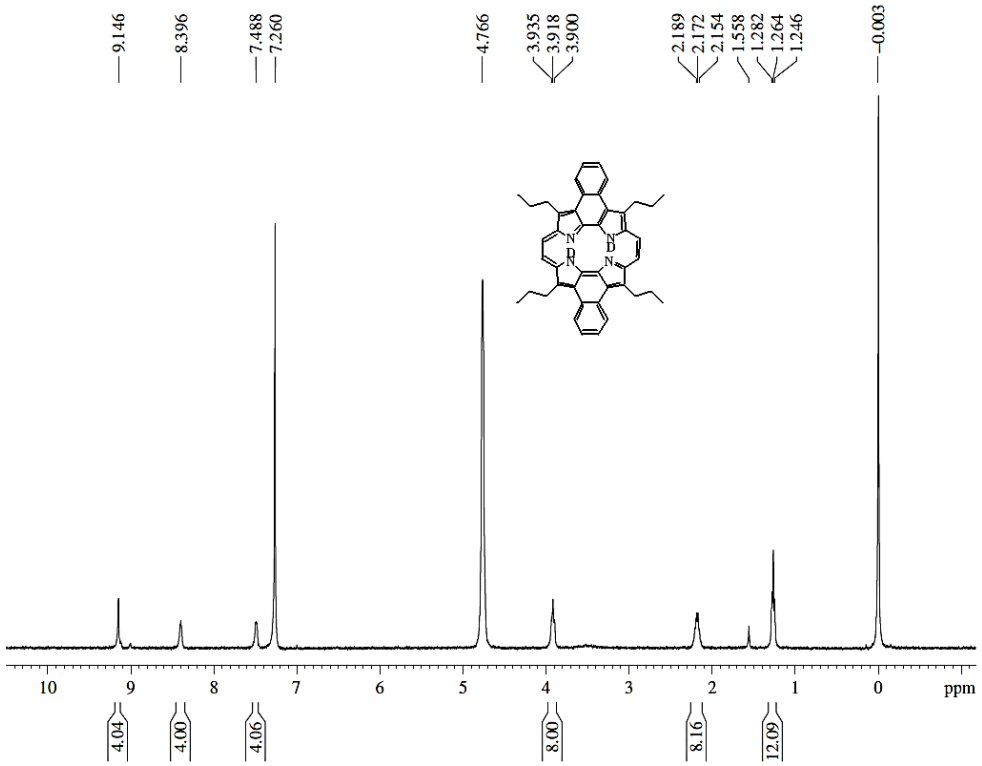

Figure A17 ^{1}H NMR spectrum of **TS22a** in $CDCl_3$-D_2O.

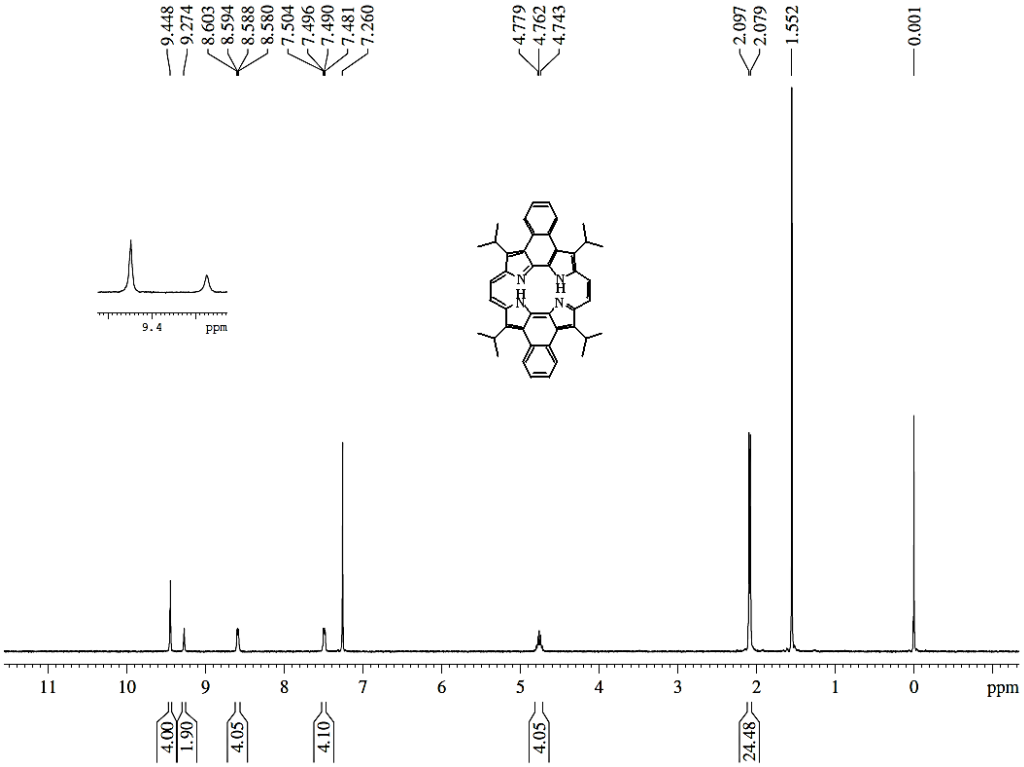

Figure A18 ^{1}H NMR spectrum of **TS22b** in $CDCl_3$.

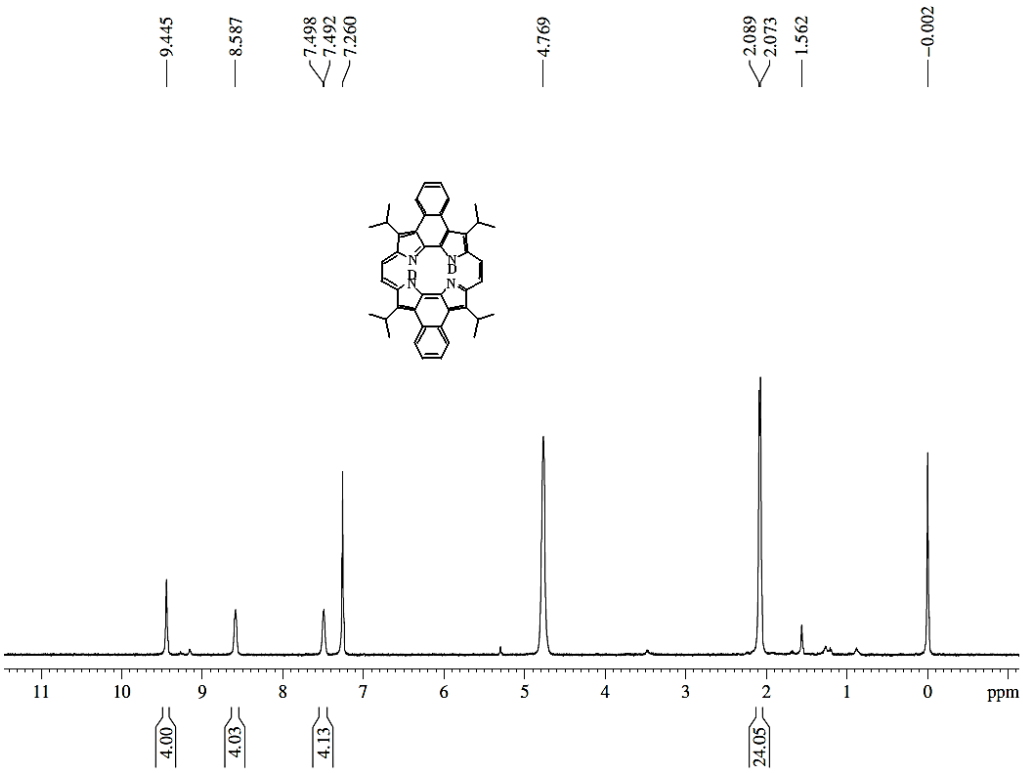

Figure A19 ^{1}H NMR spectrum of **TS22b** in $CDCl_3$-D_2O.

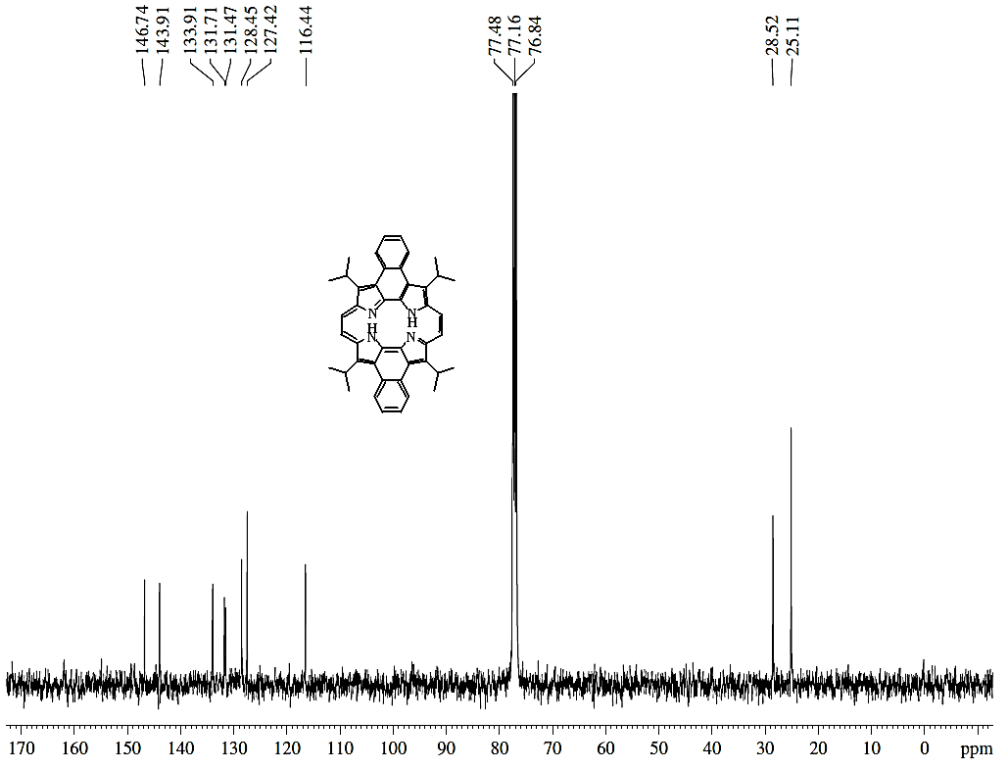

Figure A20 ^{13}C NMR spectrum of **TS22b** in $CDCl_3$.

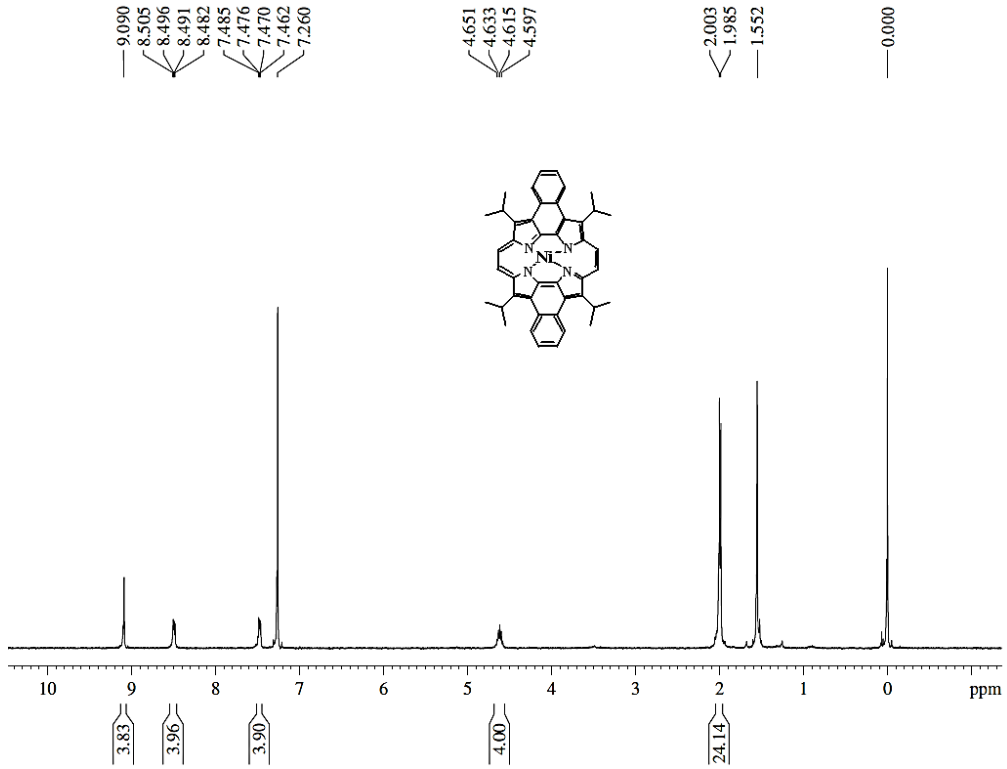

Figure A21 ^{1}H NMR spectrum of **TS23b** in $CDCl_3$.

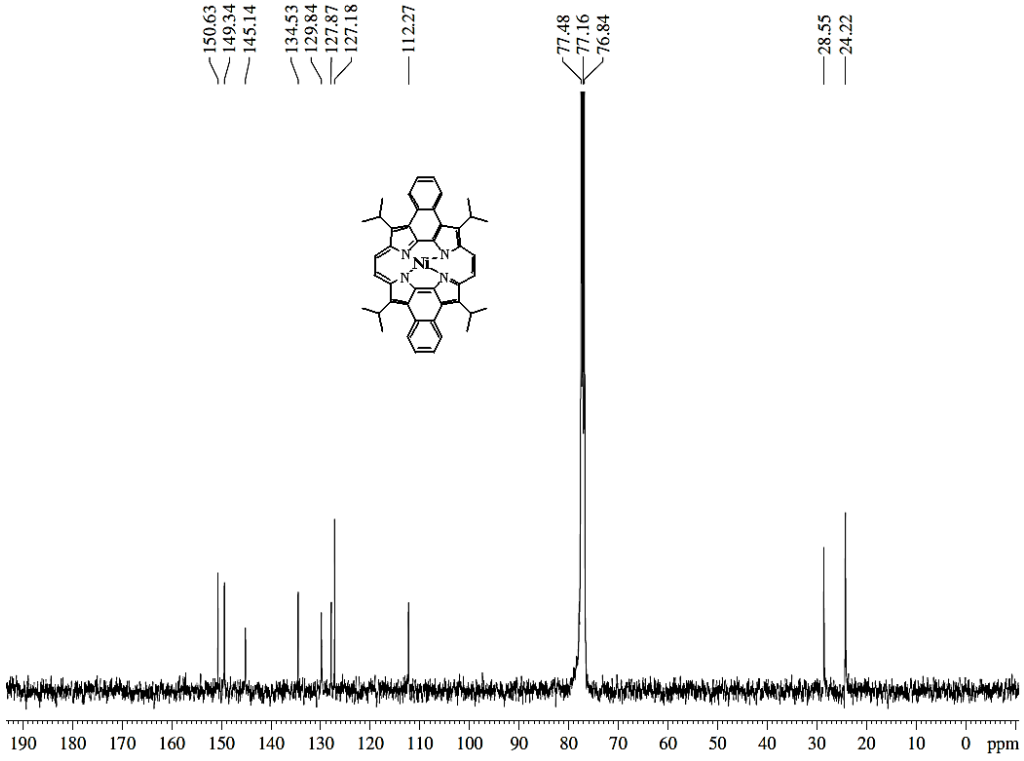

Figure A22 ^{13}C NMR spectrum of **TS23b** in $CDCl_3$.

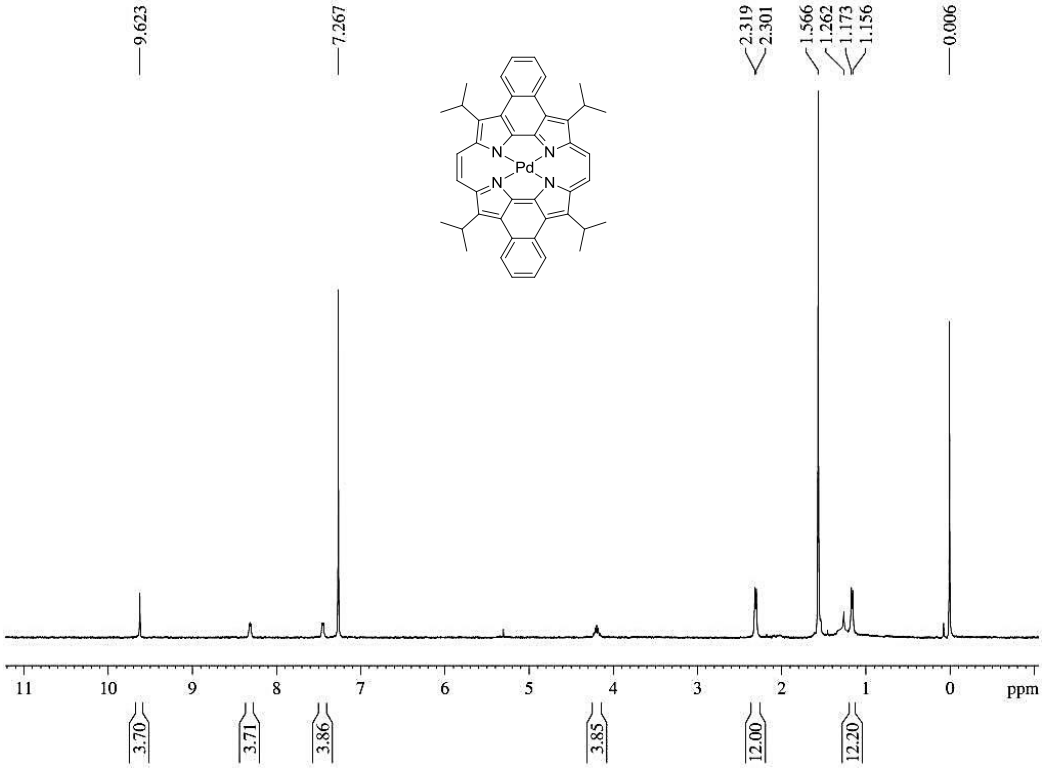

Figure A23 ^{1}H NMR spectrum of **TS25b** in $CDCl_3$.

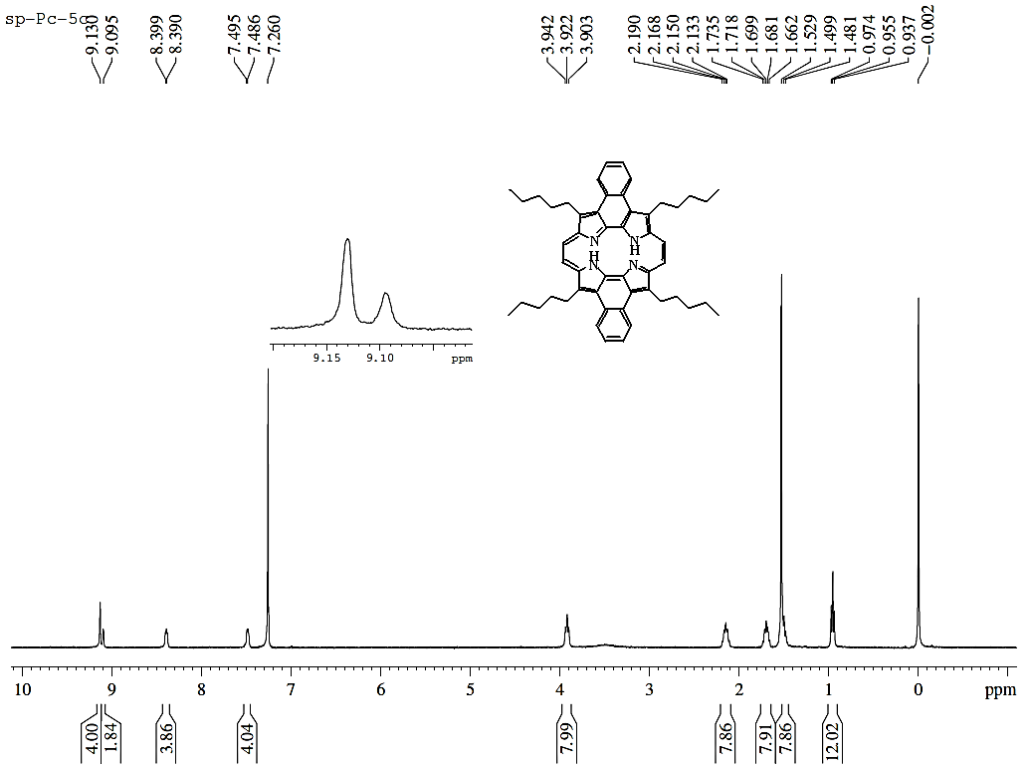

Figure A24 ^{1}H NMR spectrum of **TS22c** in $CDCl_3$.

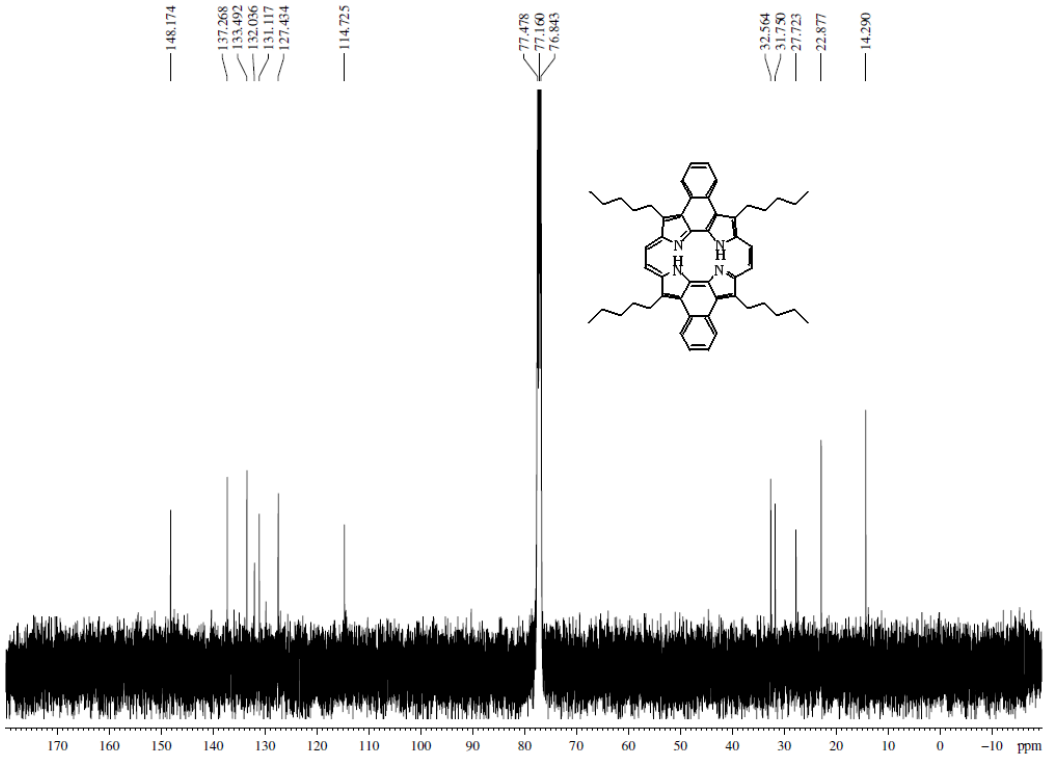

Figure A25 ^{13}C NMR spectrum of **TS22c** in $CDCl_3$.

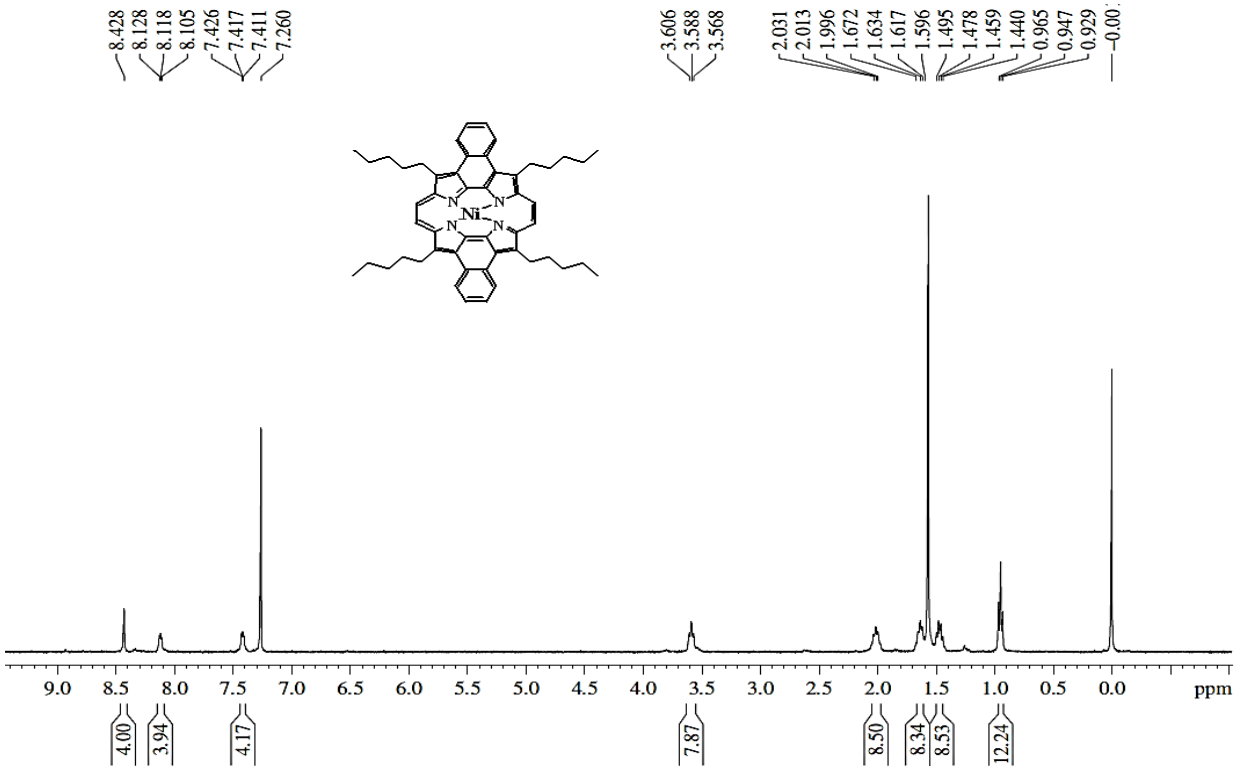

Figure A26 ^{1}H NMR spectrum of **TS23c** in $CDCl_3$.

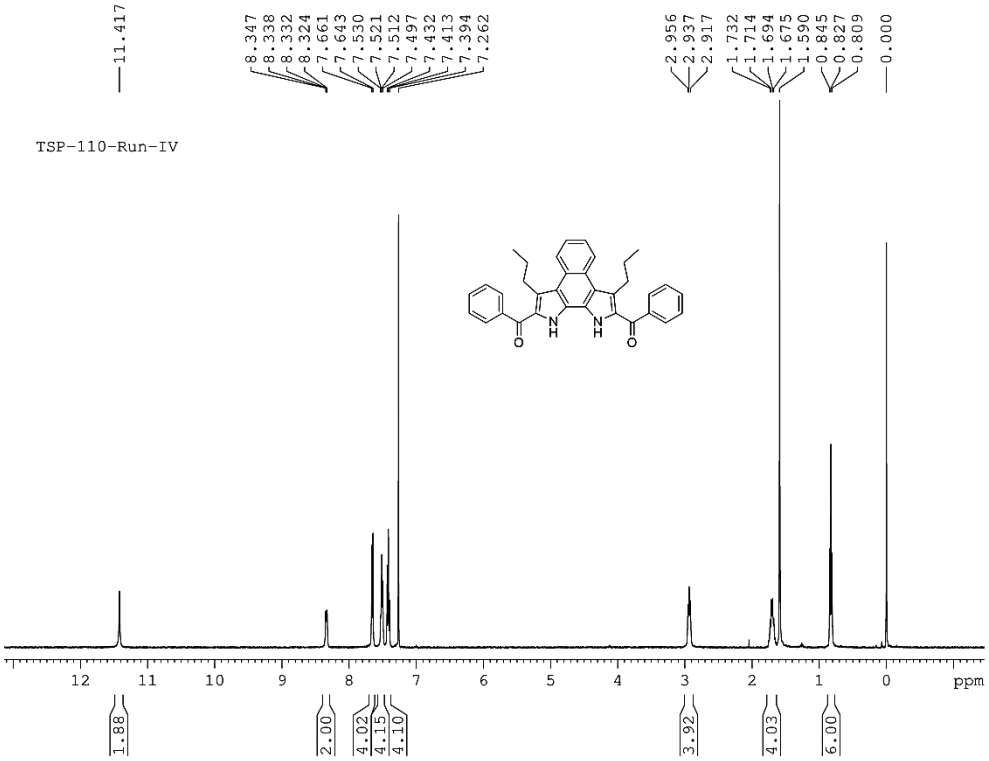

Figure A27 ^{1}H NMR spectrum of **TS26** in $CDCl_3$.

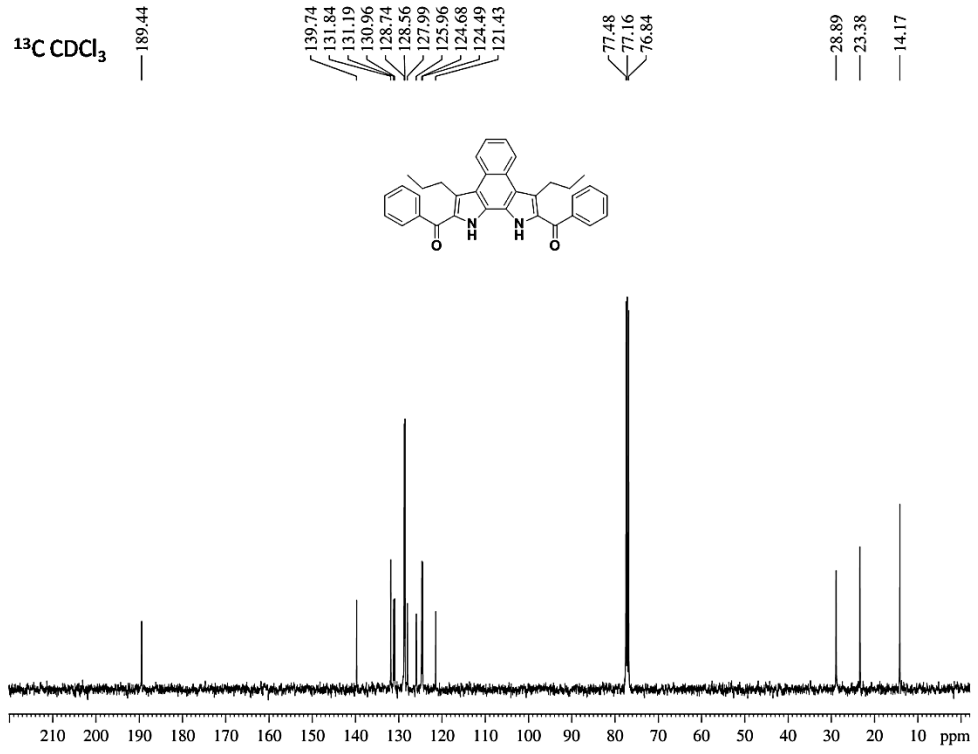

Figure A28 ^{13}C NMR spectrum of **TS26** in $CDCl_3$.

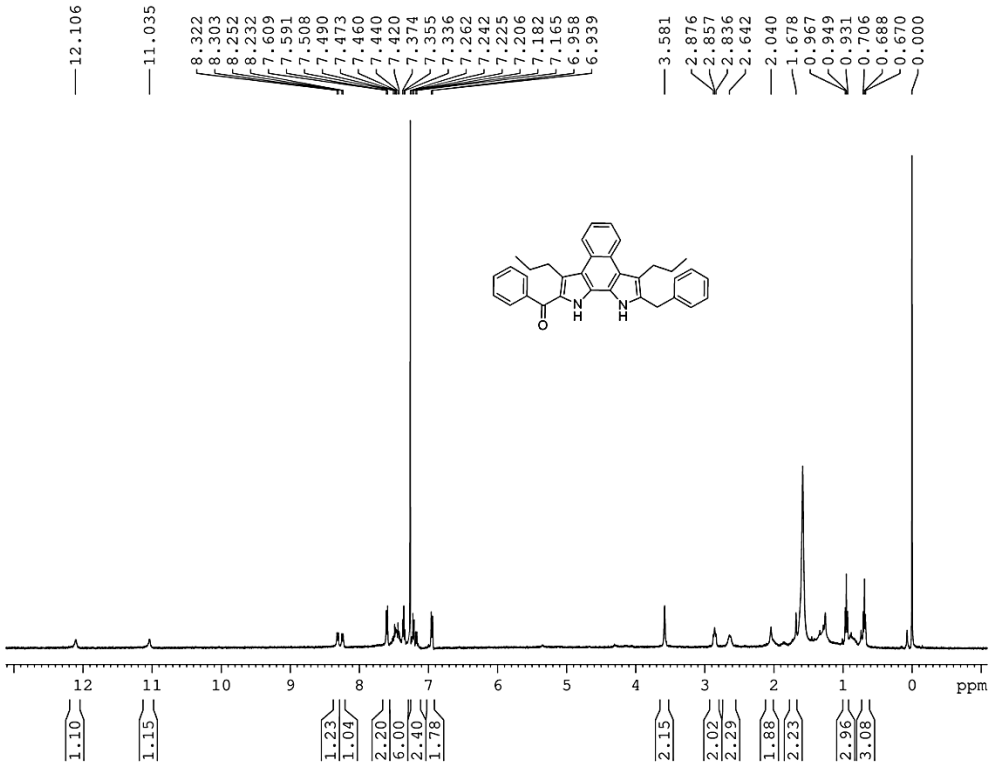

Figure A29 ^{1}H NMR spectrum of **TS27** in $CDCl_3$.

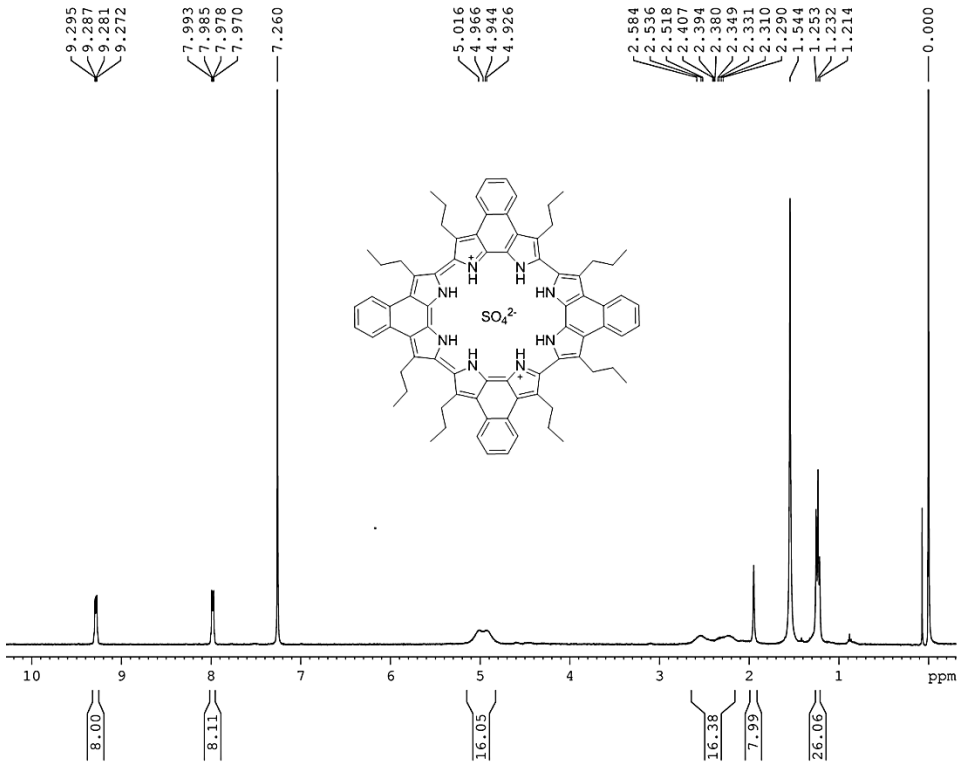

Figure A30 ^{1}H NMR spectrum of **TS29a** in $CDCl_3$.

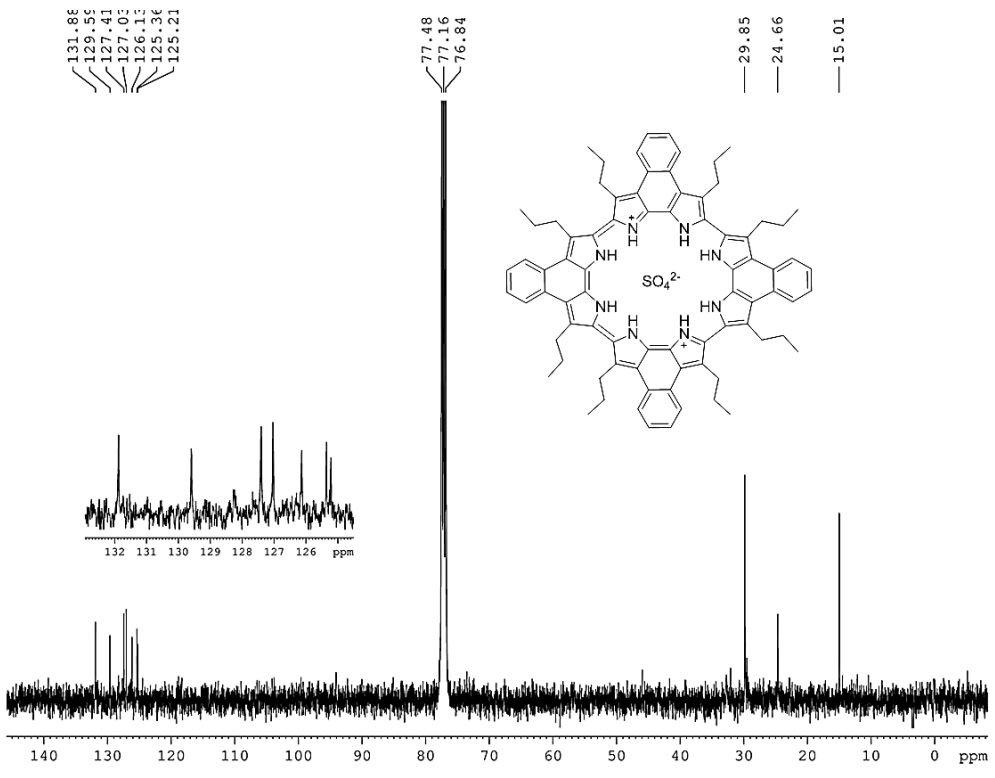

Figure A31 ^{13}C NMR spectrum of **TS29a** in $CDCl_3$.

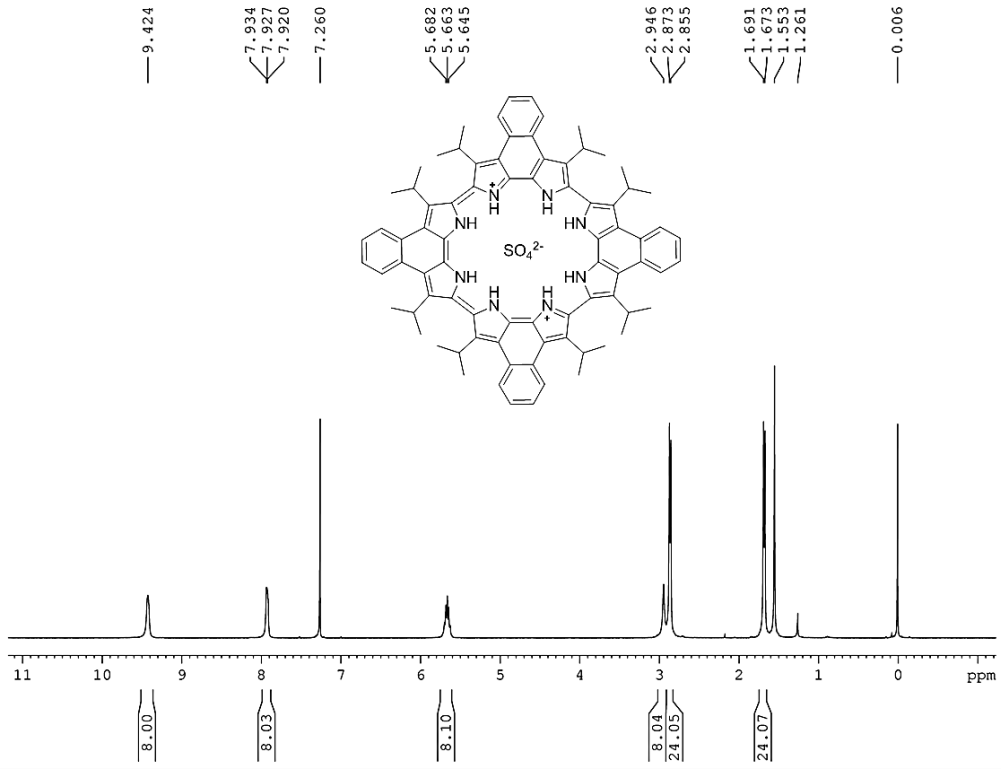

Figure A32 ^{1}H NMR spectrum of **TS29b** in $CDCl_3$.

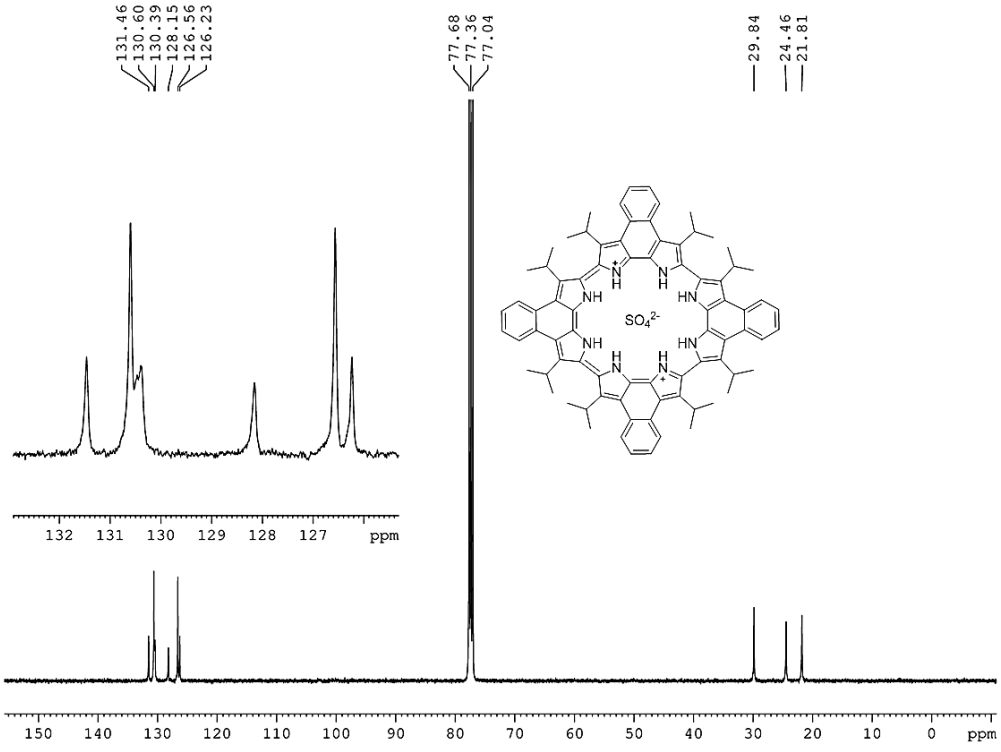

Figure A33 ^{13}C NMR spectrum of **TS29b** in $CDCl_3$.

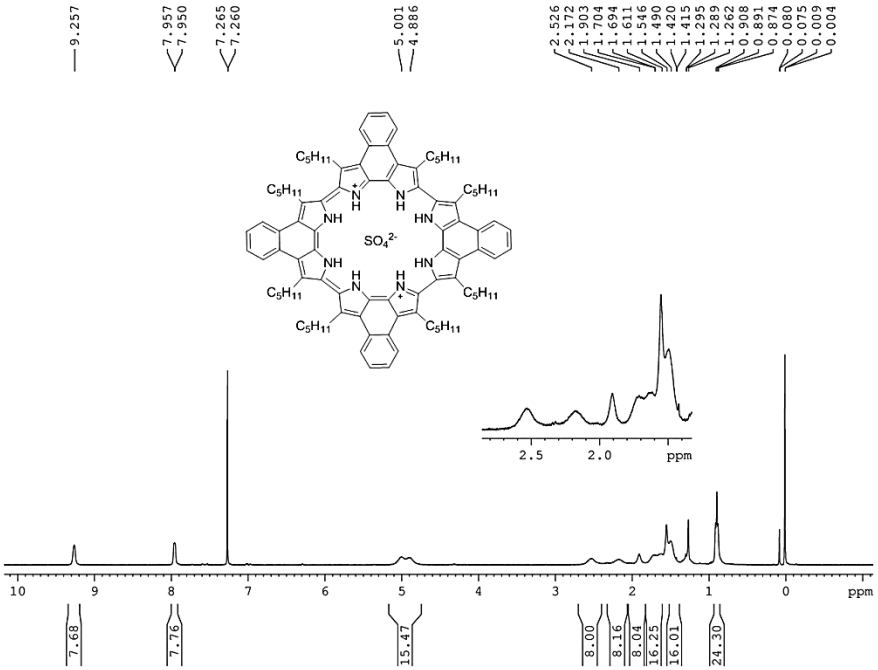

Figure A34 ^{1}H NMR spectrum of **TS29c** in $CDCl_3$.

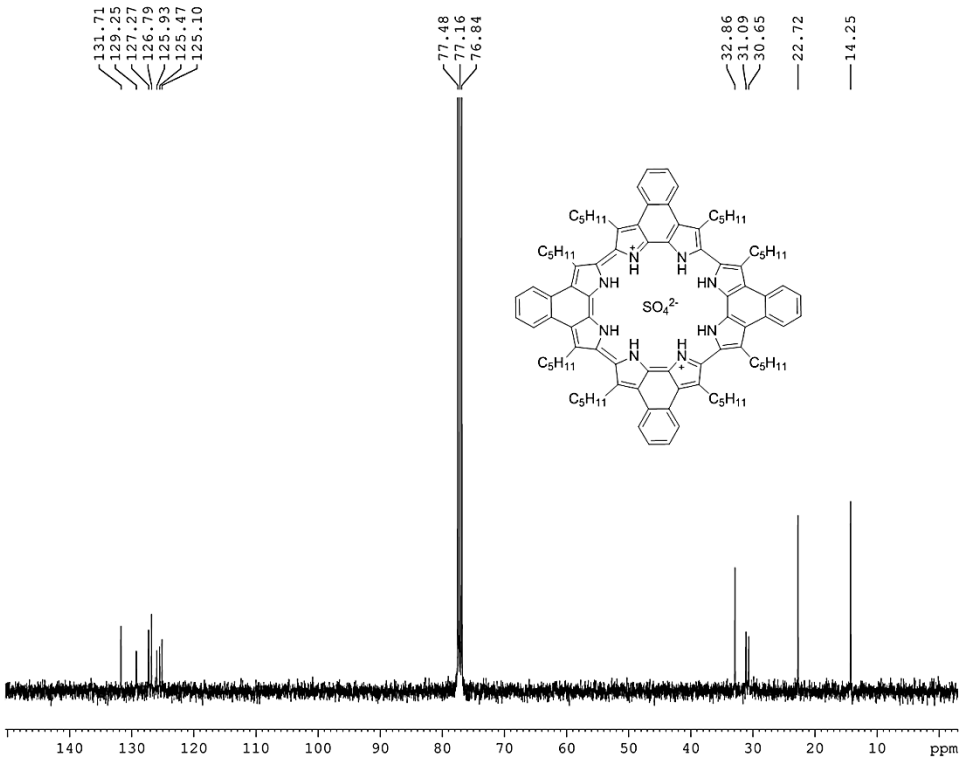

Figure A35 ^{13}C NMR spectrum of **TS29c** in $CDCl_3$.

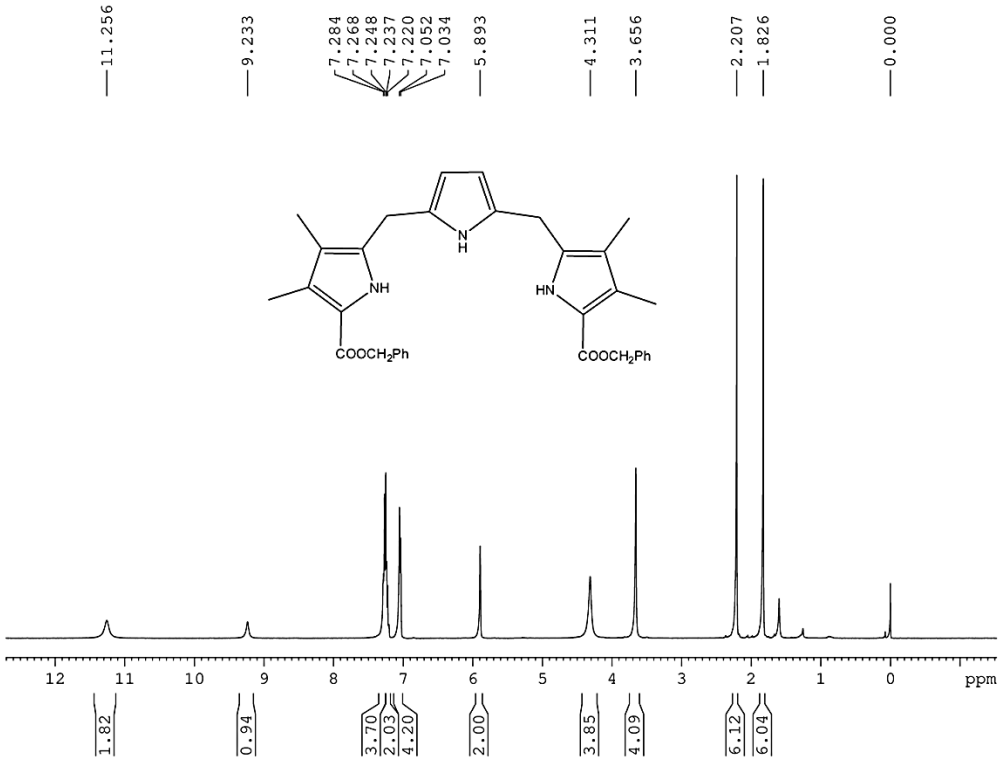

Figure A36 ^{1}H NMR spectrum of **TS33** in $CDCl_3$.

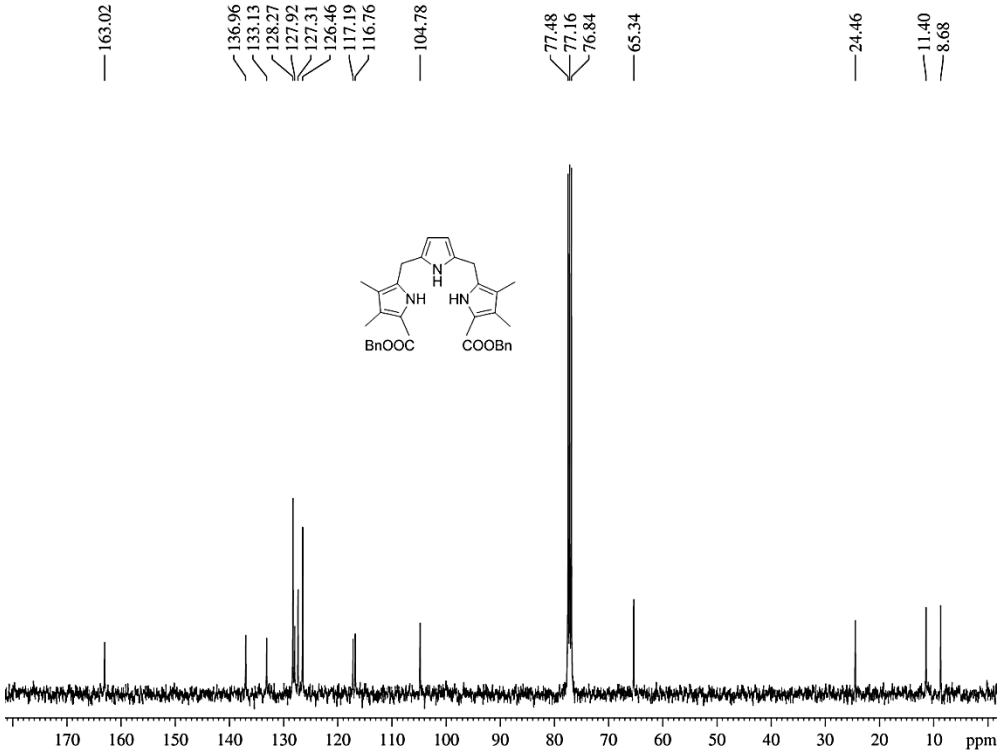

Figure A37 ^{13}C NMR spectrum of **TS33** in $CDCl_3$.

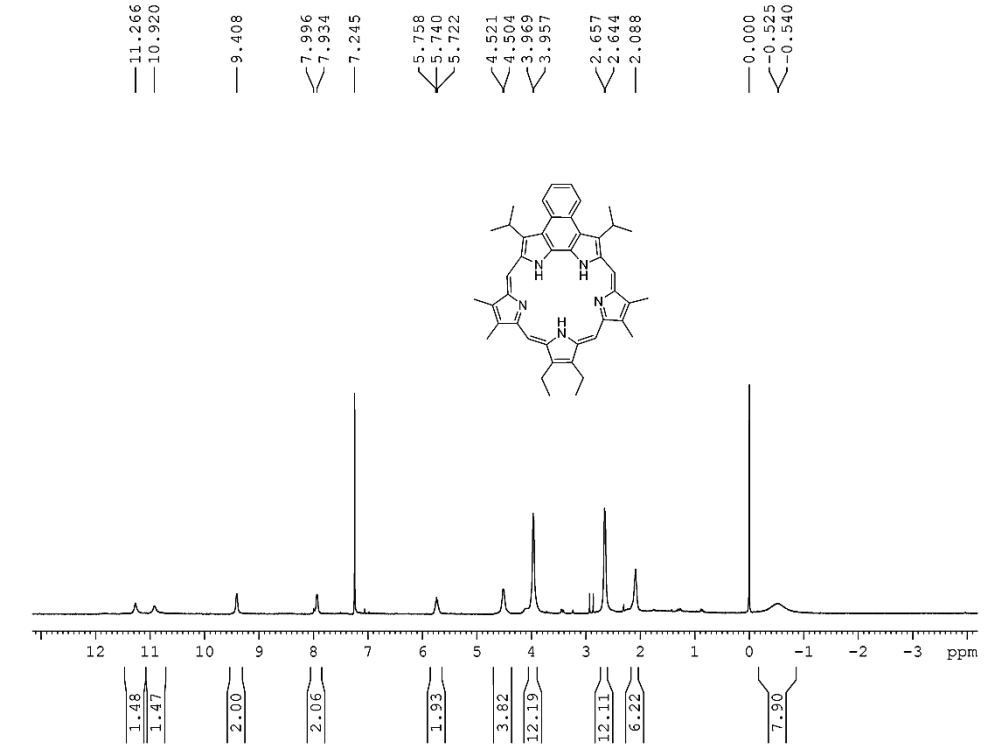

Figure A38 ^{1}H NMR spectrum of **TS30** in $CDCl_3$.

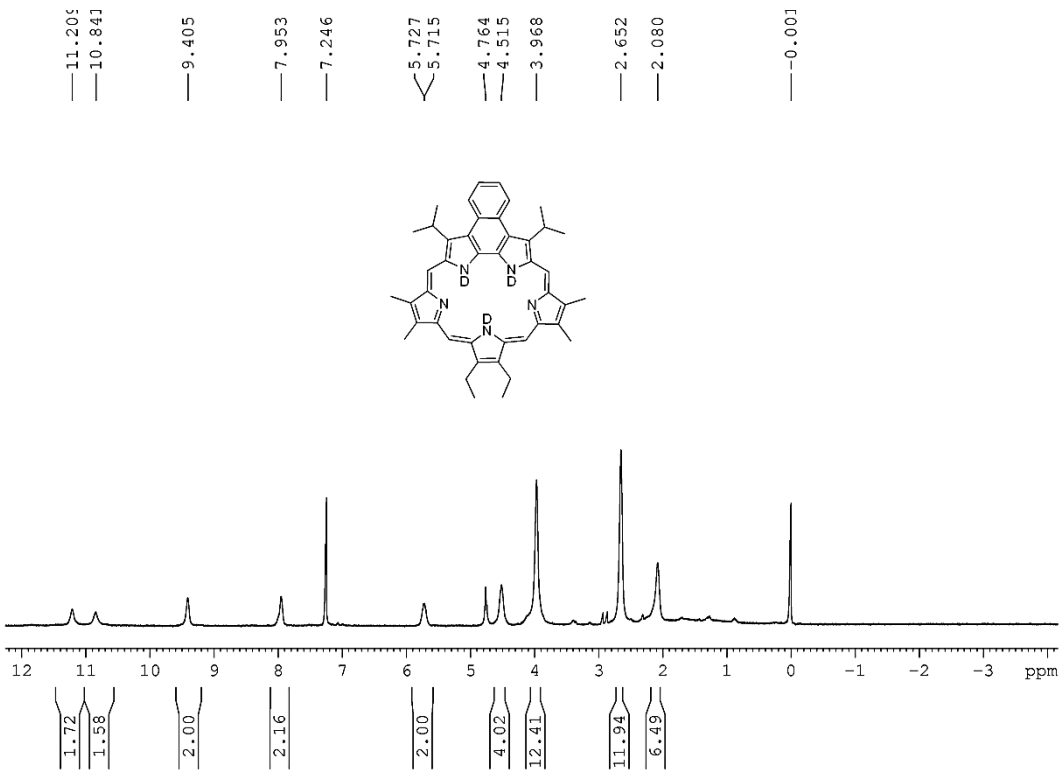

Figure A39 ^{1}H NMR spectrum of **TS30** in $CDCl_3$-D_2O.

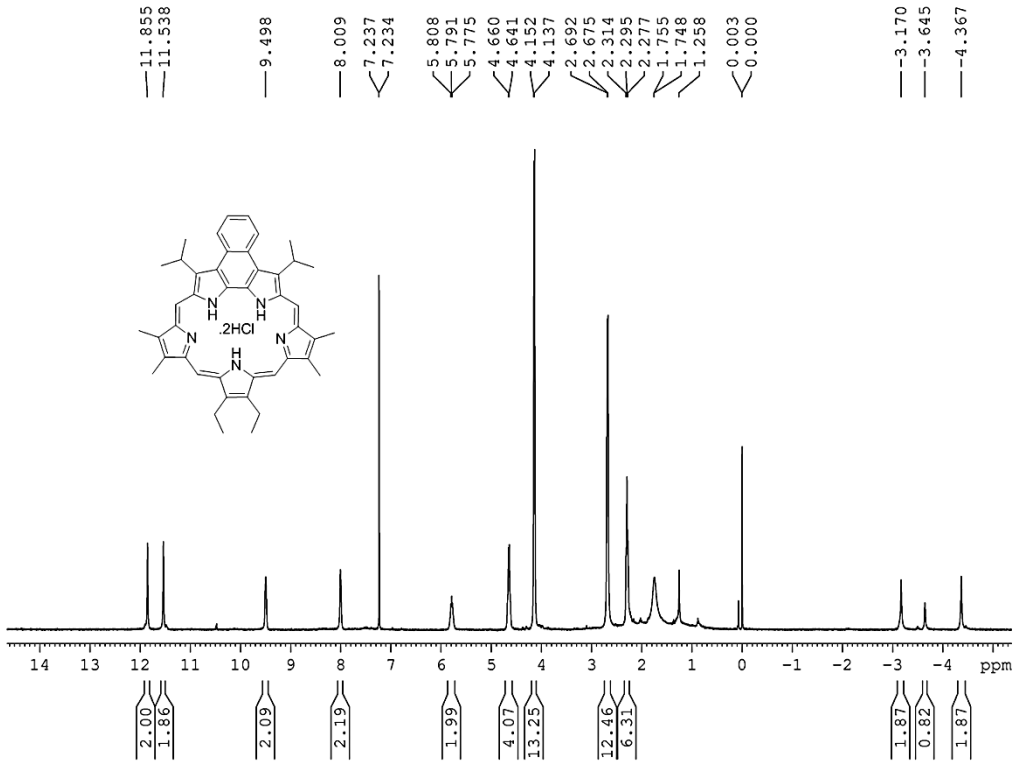

Figure A40 ^{1}H NMR spectrum of **TS30.2HCl** in $CDCl_3$.

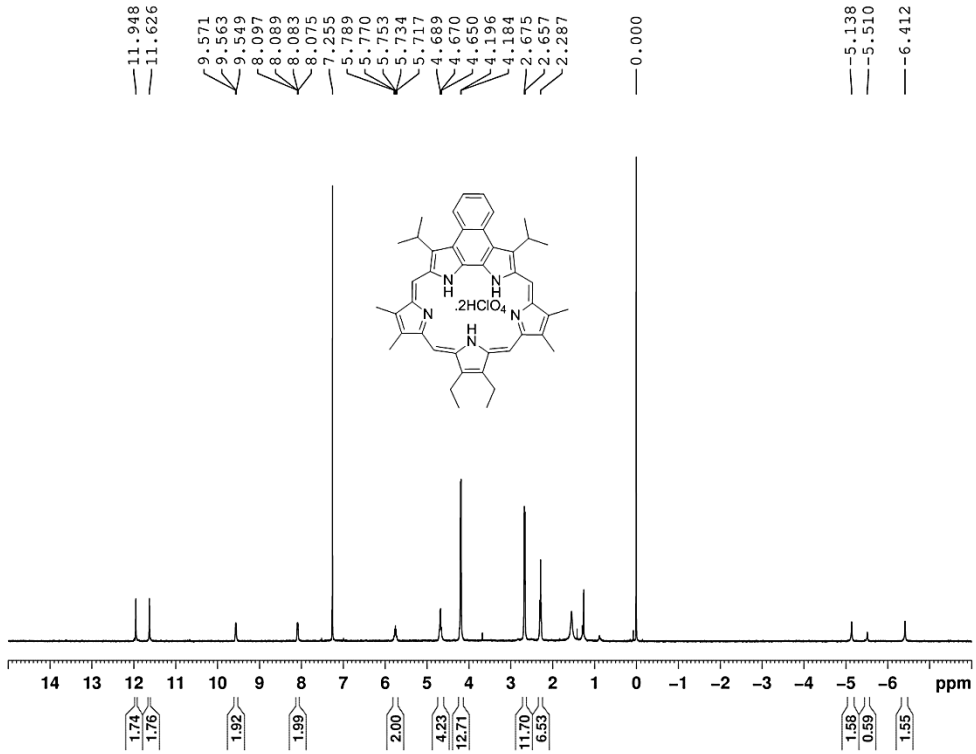

Figure A41 ^{1}H NMR spectrum of **TS30.2HClO$_4$** in $CDCl_3$.

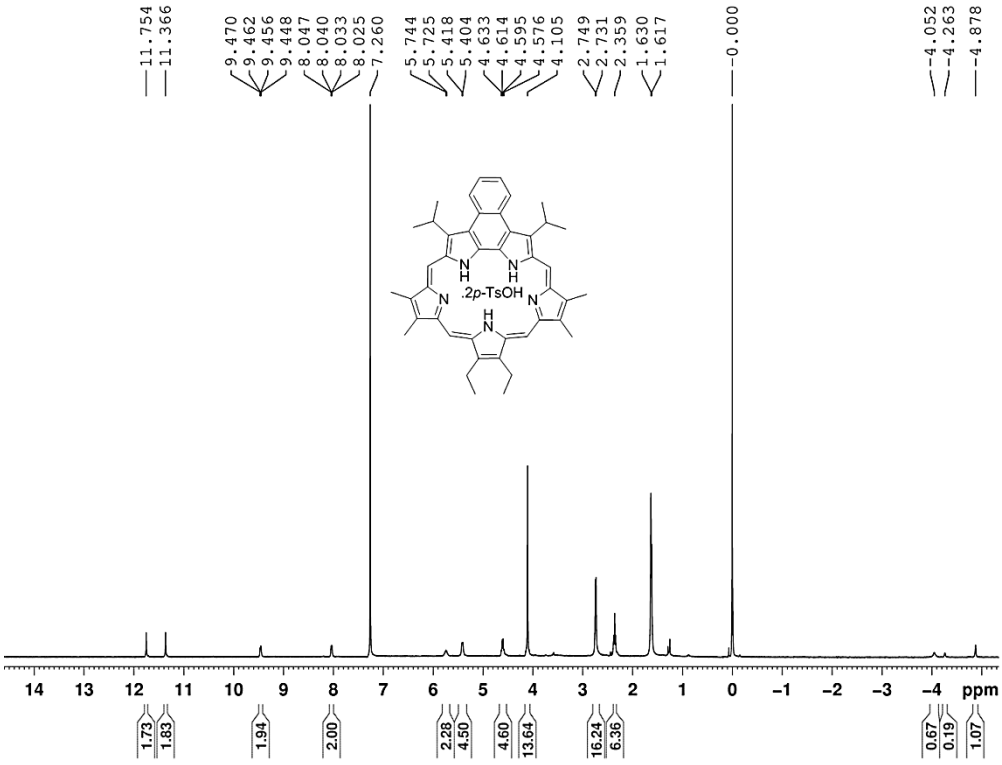

Figure A42 ^{1}H NMR spectrum of **TS30.2*p*-TsOH** in $CDCl_3$.

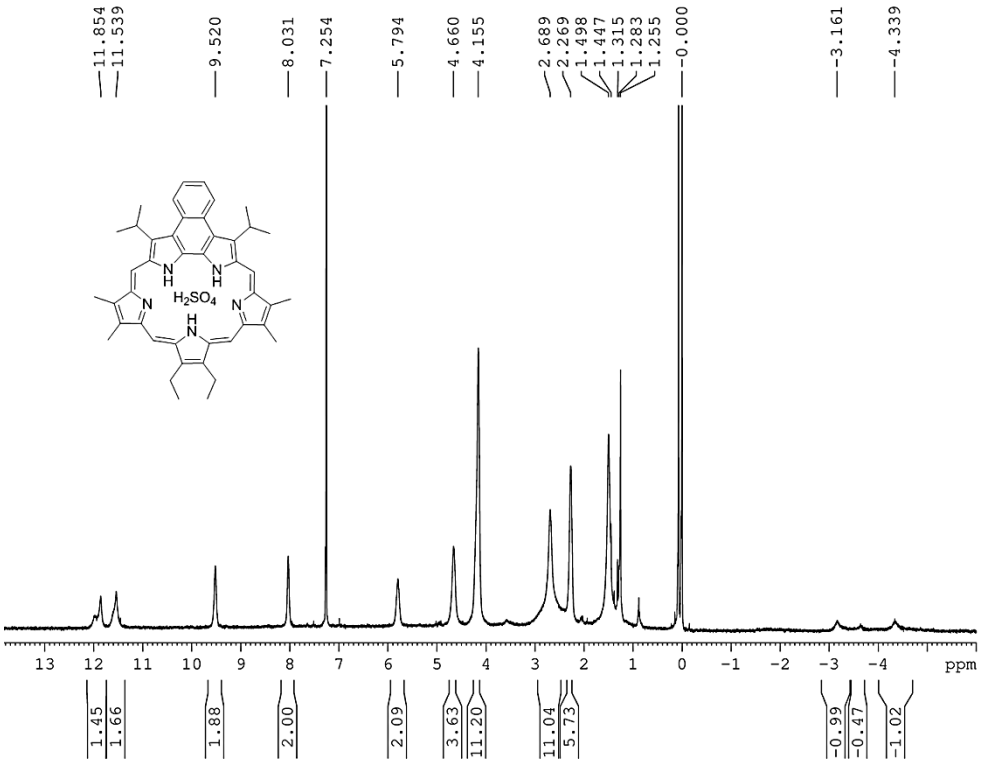

Figure A43 ^{1}H NMR spectrum of **TS30.H_2SO_4** in $CDCl_3$.

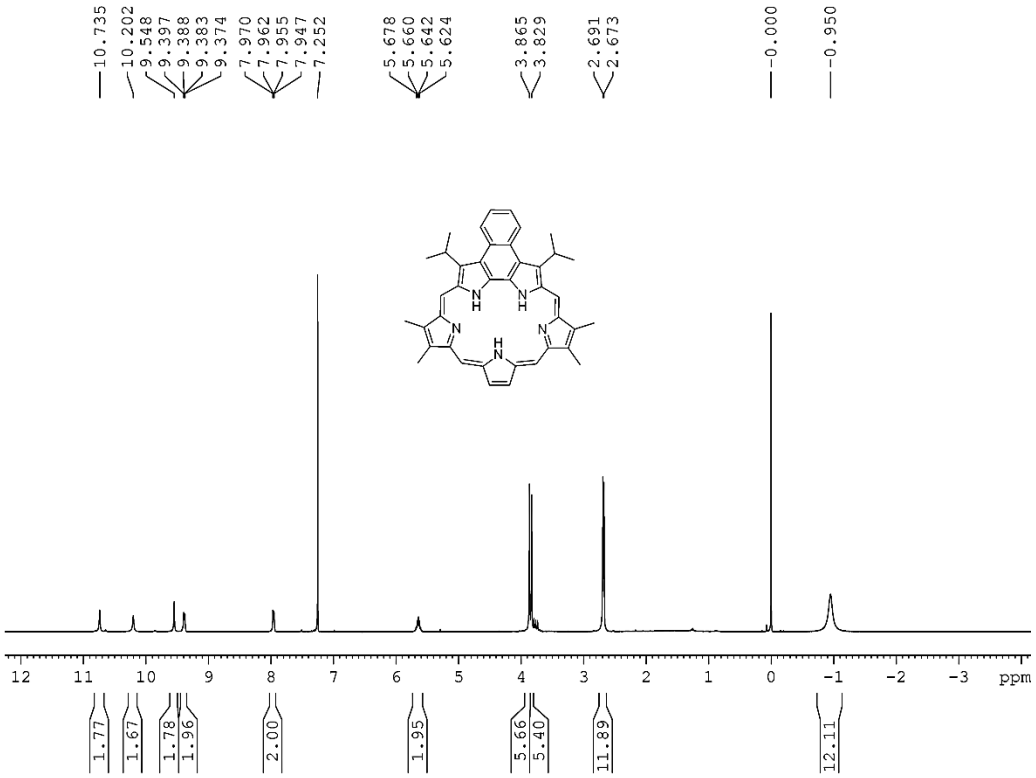

Figure A44 ^{1}H NMR spectrum of **TS31** in $CDCl_3$.

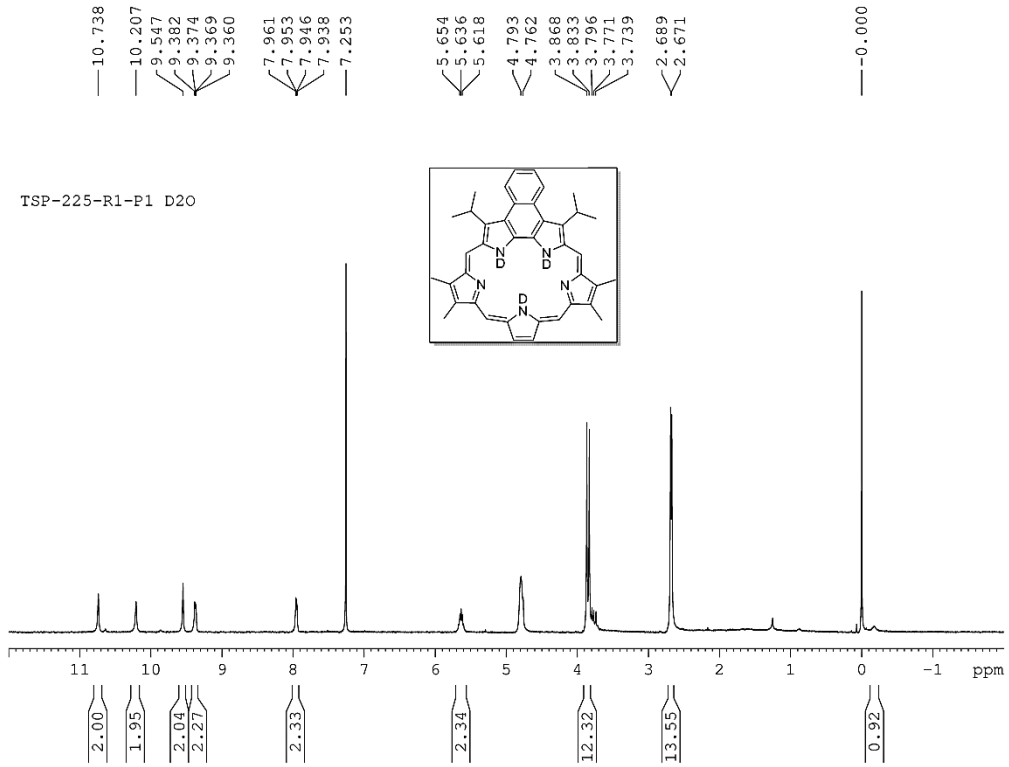

Figure A45 ^{1}H NMR spectrum of **TS31** in $CDCl_3$-D_2O.

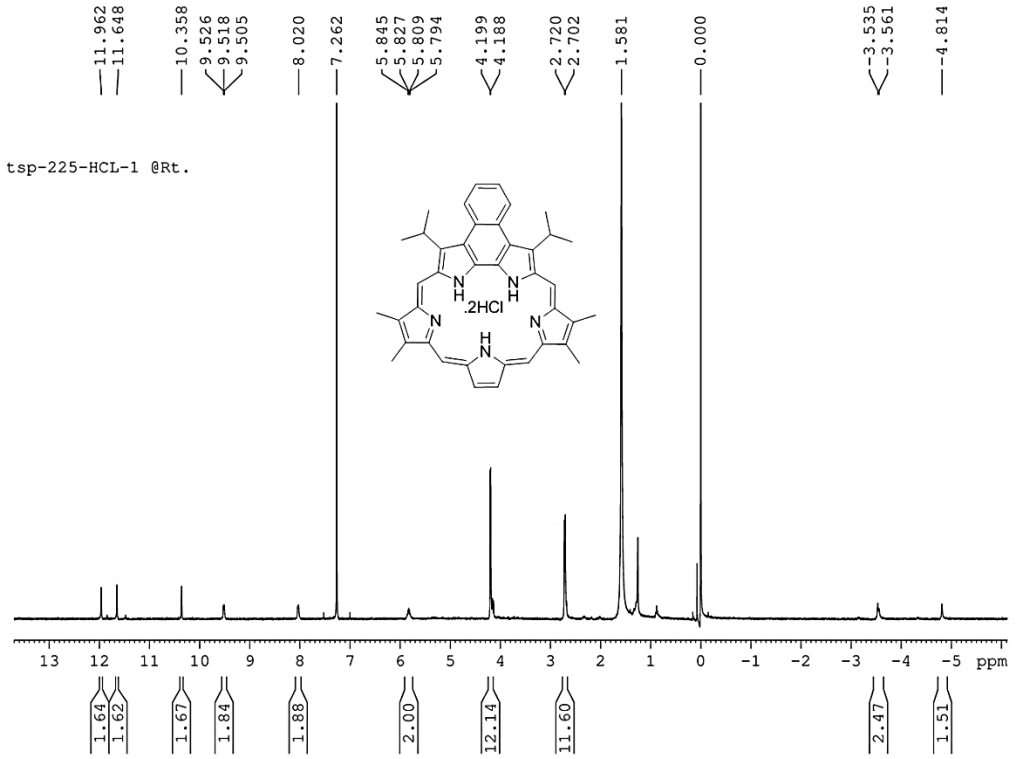

Figure A46 ^{1}H NMR spectrum of **TS31.2HCl** in $CDCl_3$.

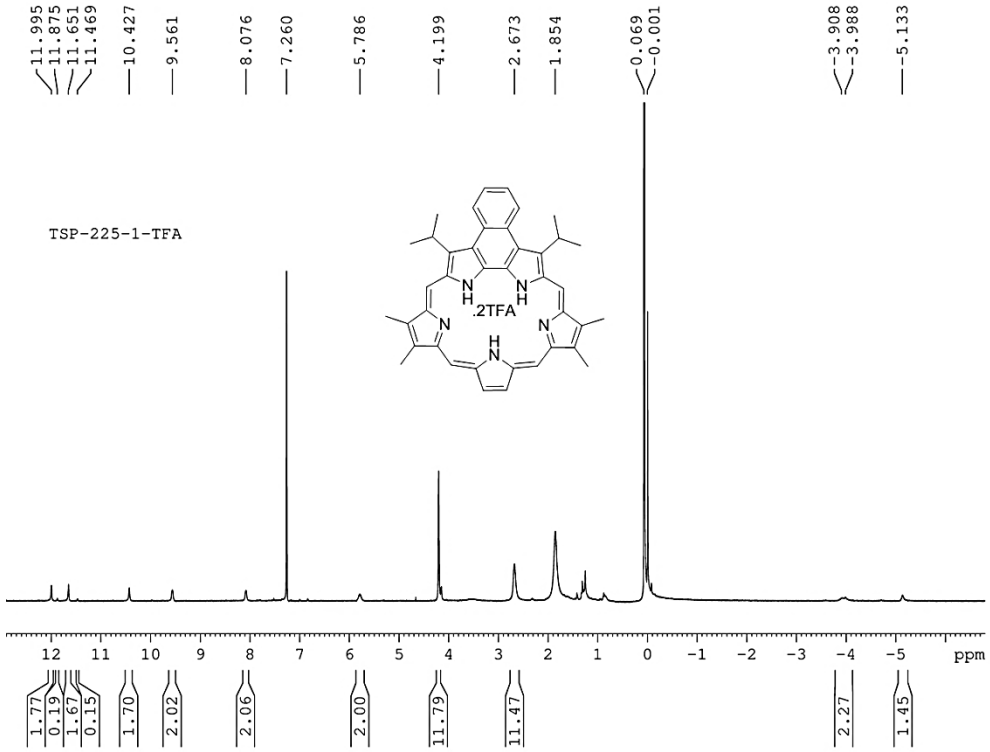

Figure A47 ^{1}H NMR spectrum of **TS31.2TFA** in $CDCl_3$.

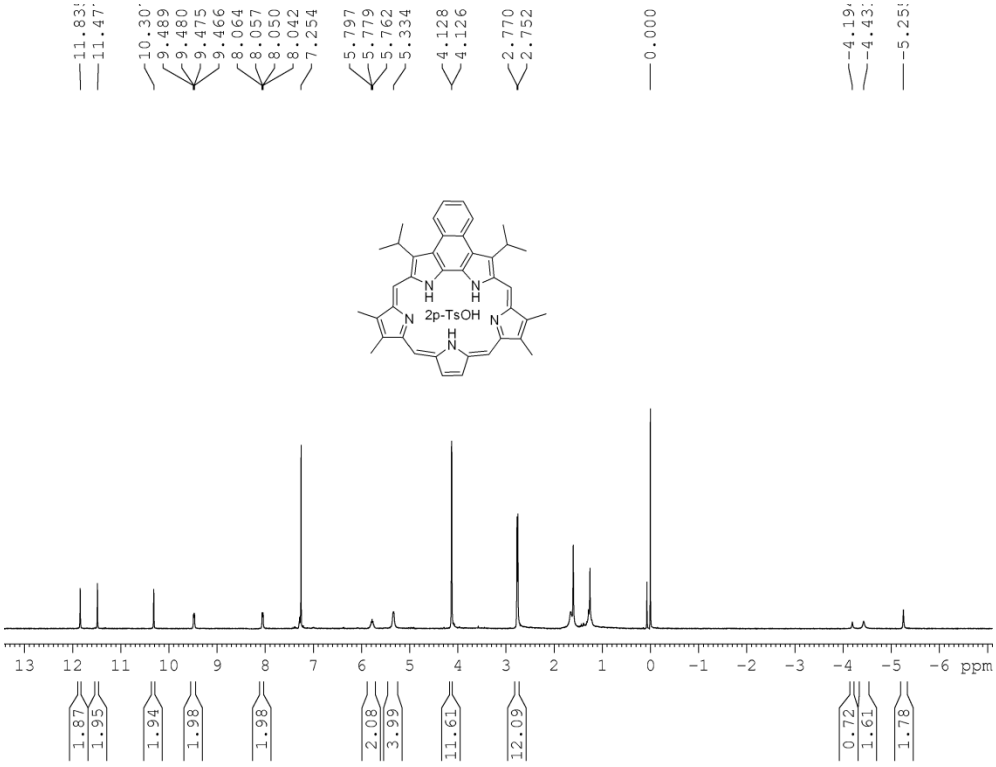

Figure A48 ^{1}H NMR spectrum of **TS31.2*p*-TsOH** in $CDCl_3$.

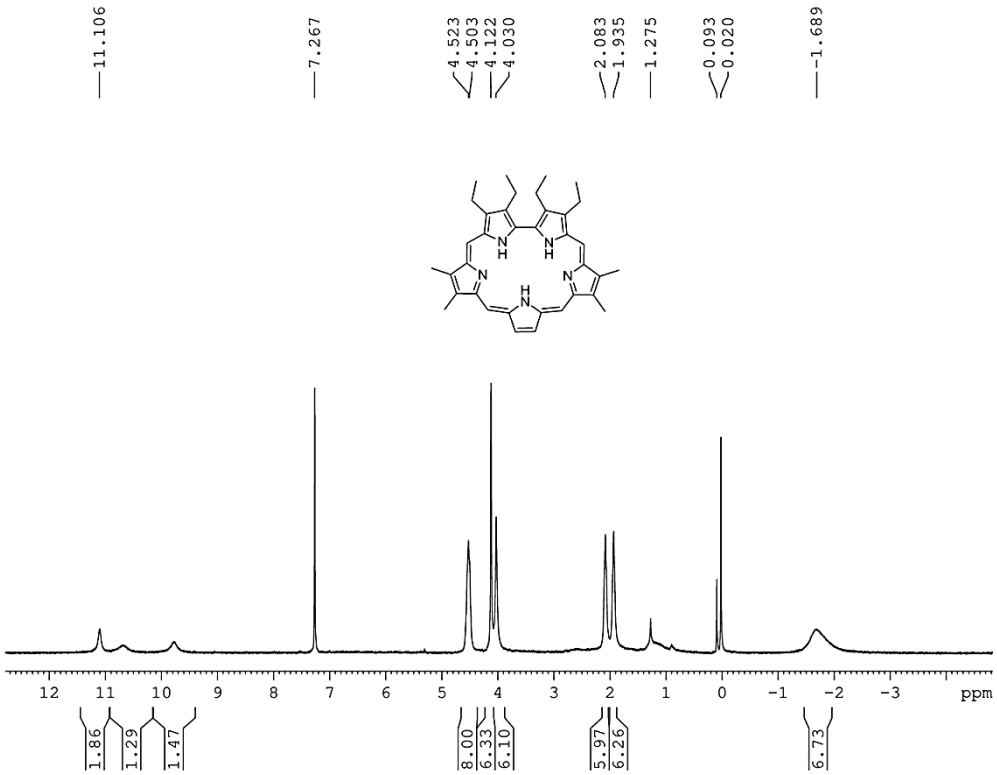

Figure A49 ^{1}H NMR spectrum of **TS32** in $CDCl_3$.

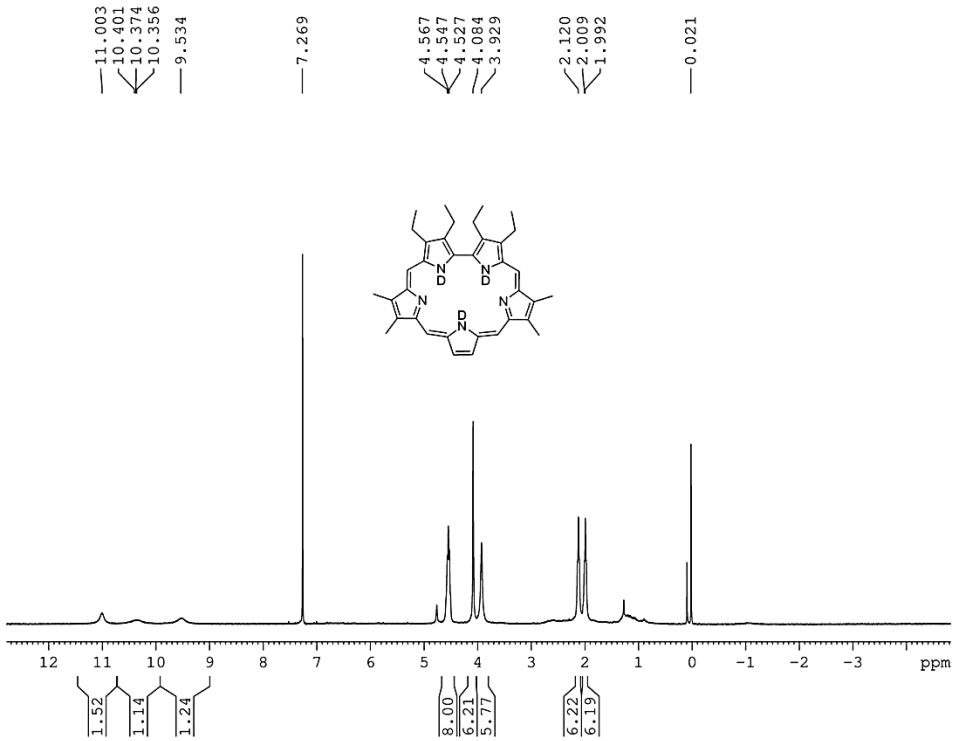

Figure A50 ^{1}H NMR spectrum of **TS32** in $CDCl_3$-D_2O.

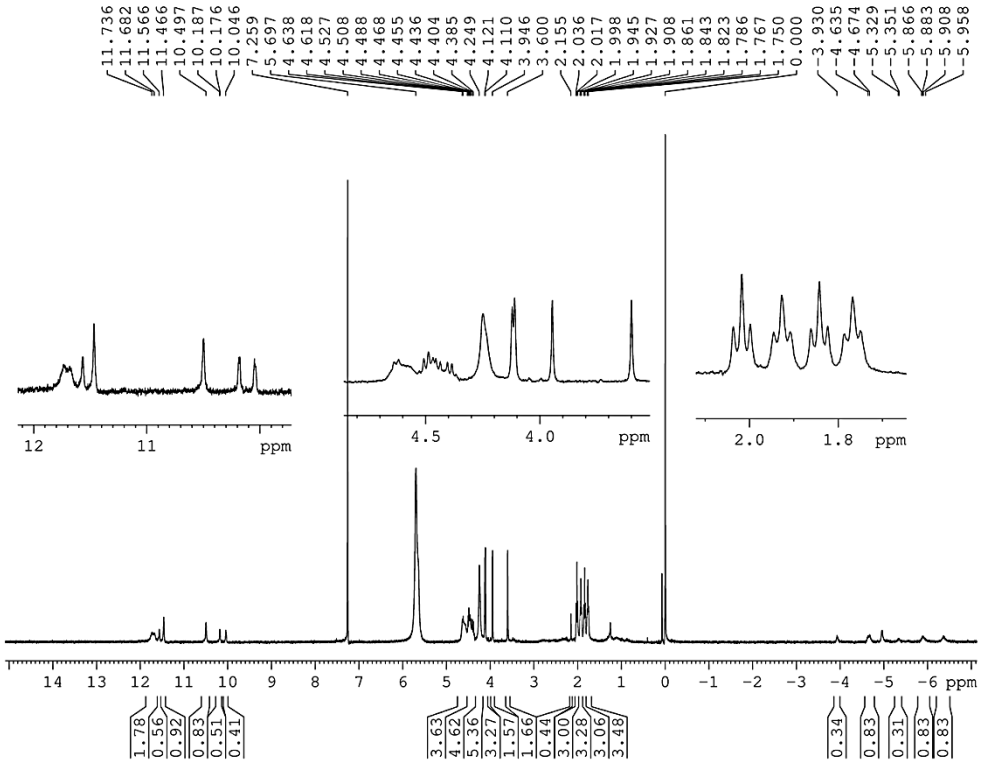

Figure A51 ^{1}H NMR spectrum of **TS32** in presence of excess TFA in $CDCl_3$.

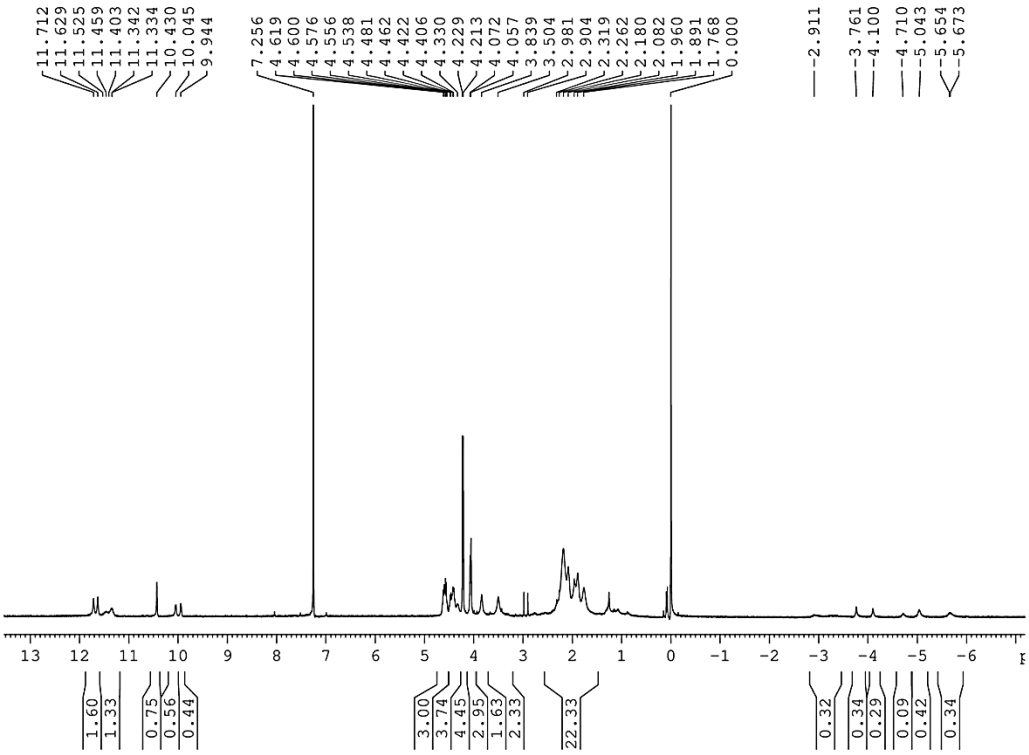

Figure A52 ^{1}H NMR spectrum of **TS32** after removal of excess TFA in $CDCl_3$.

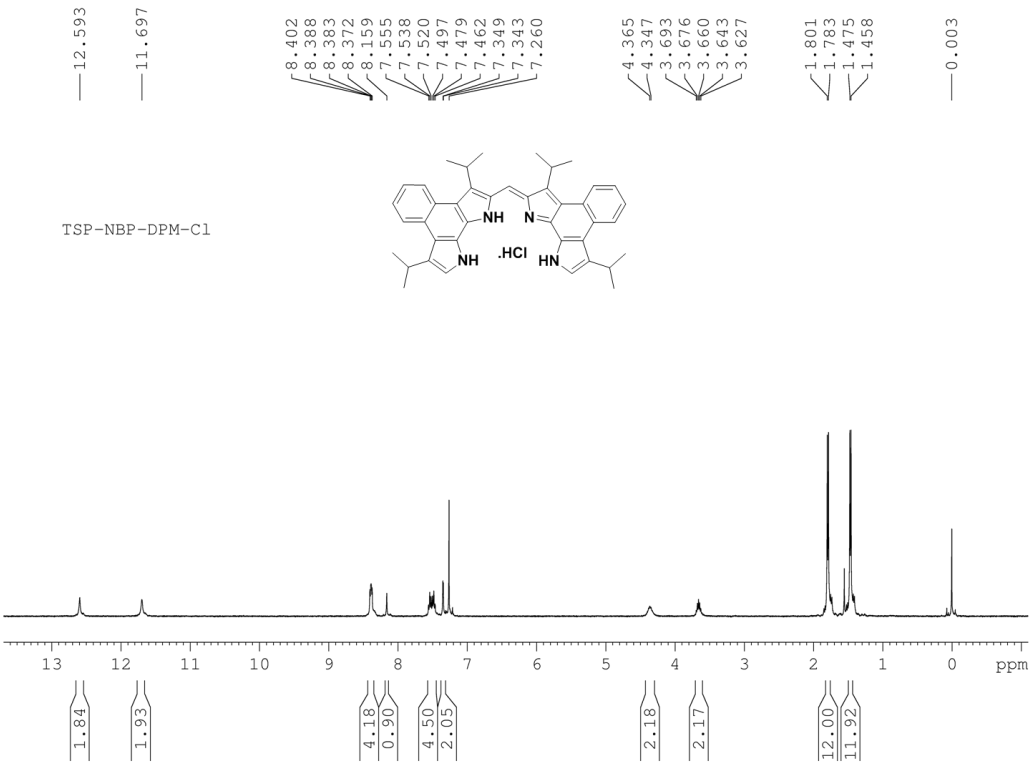

Figure A53 ^{1}H NMR spectrum of **TS33** in $CDCl_3$.

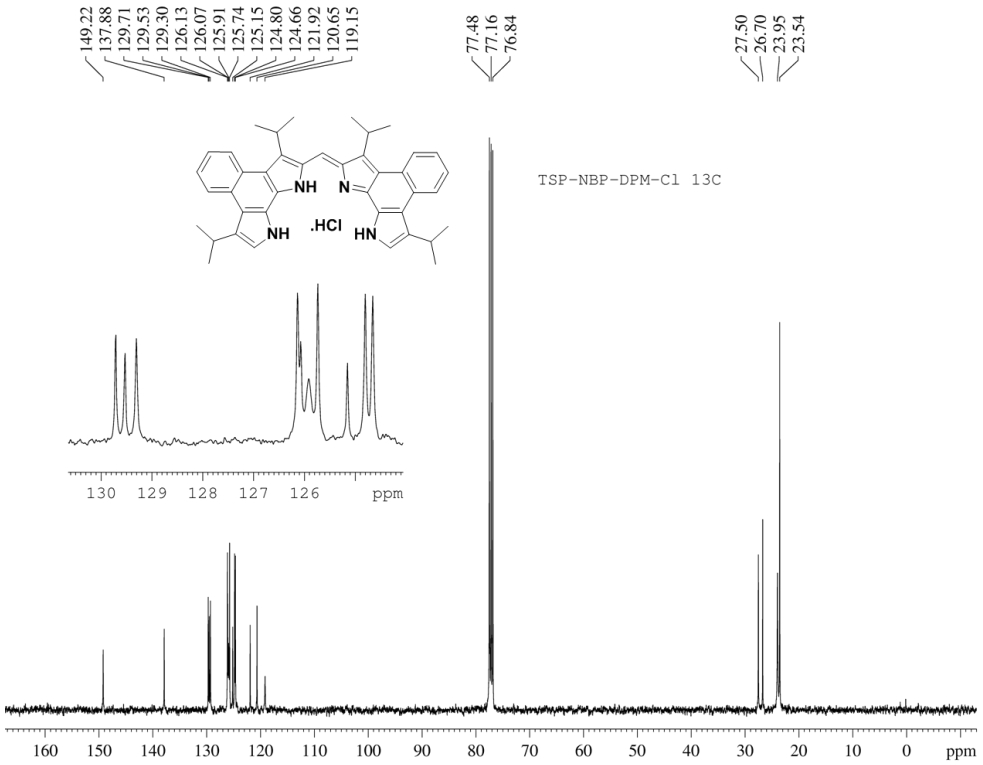

Figure A54 ^{13}C NMR spectrum of **TS33** in $CDCl_3$.

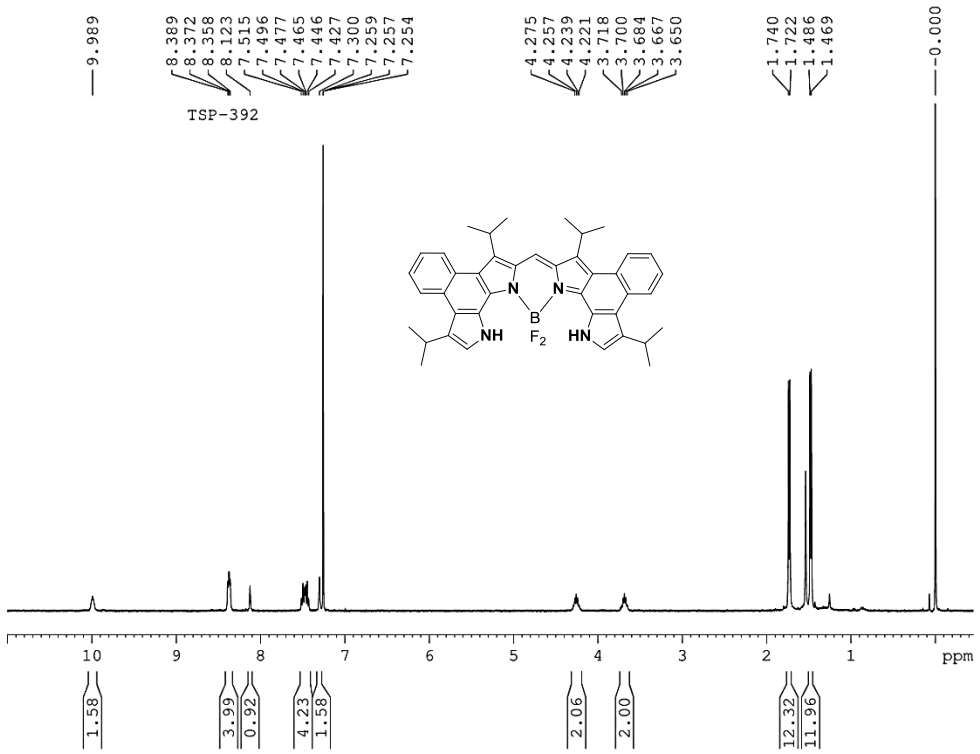

Figure A55 ^{1}H NMR spectrum of **TS35** in $CDCl_3$.

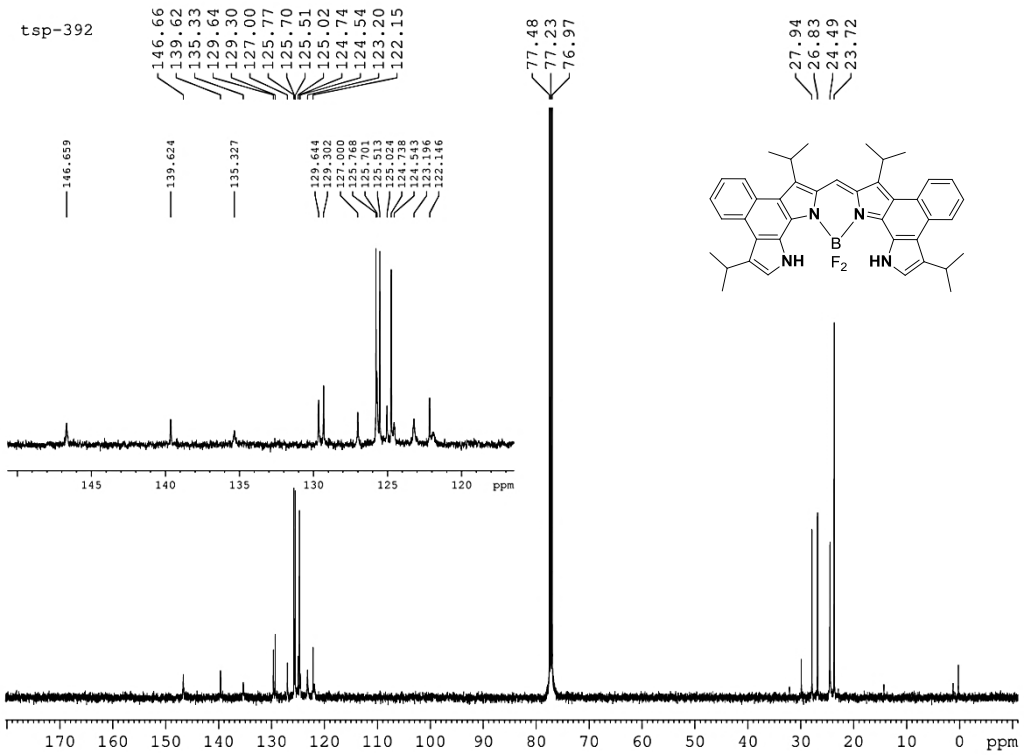

Figure A56 ^{13}C NMR spectrum of **TS35** in $CDCl_3$.

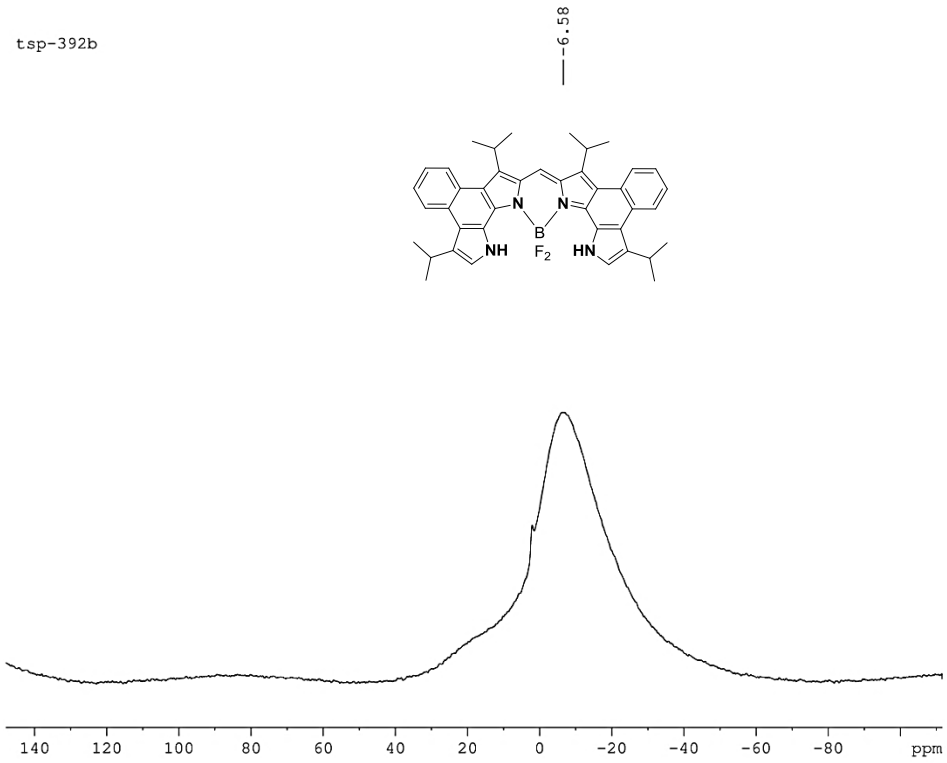

Figure A57 ^{11}B NMR Spectrum of compound **TS35** in $CDCl_3$.

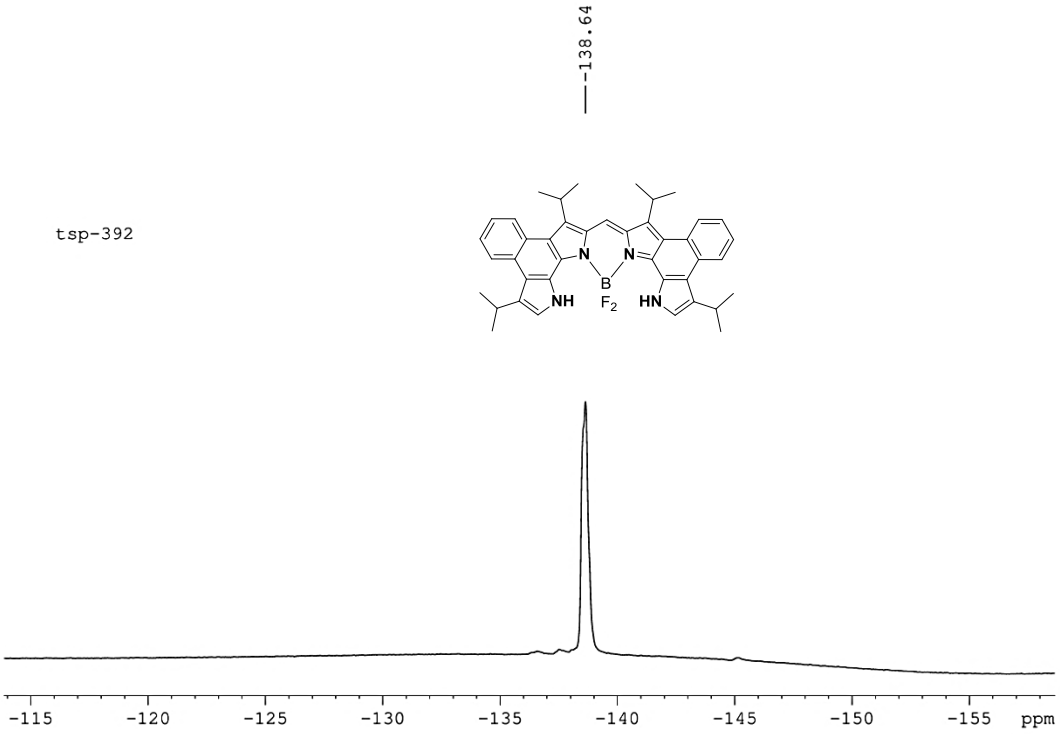

Figure A58 ^{19}F NMR Spectrum of compound **TS35** in $CDCl_3$.

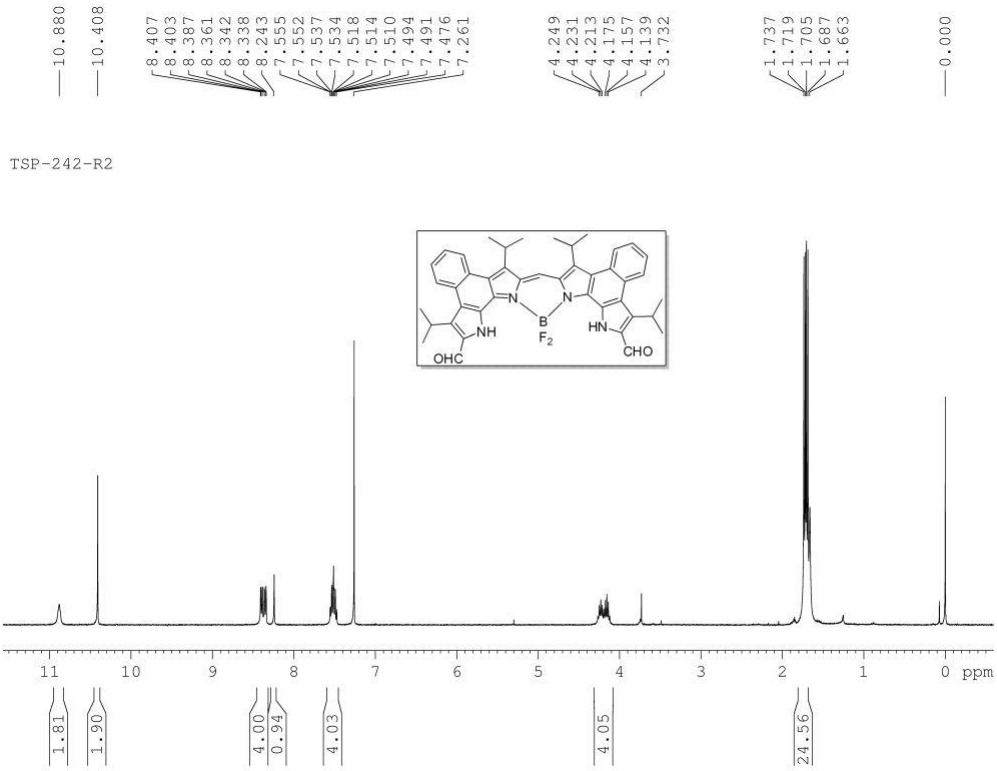

Figure A59 ^{1}H NMR spectrum of **TS36** in $CDCl_3$.

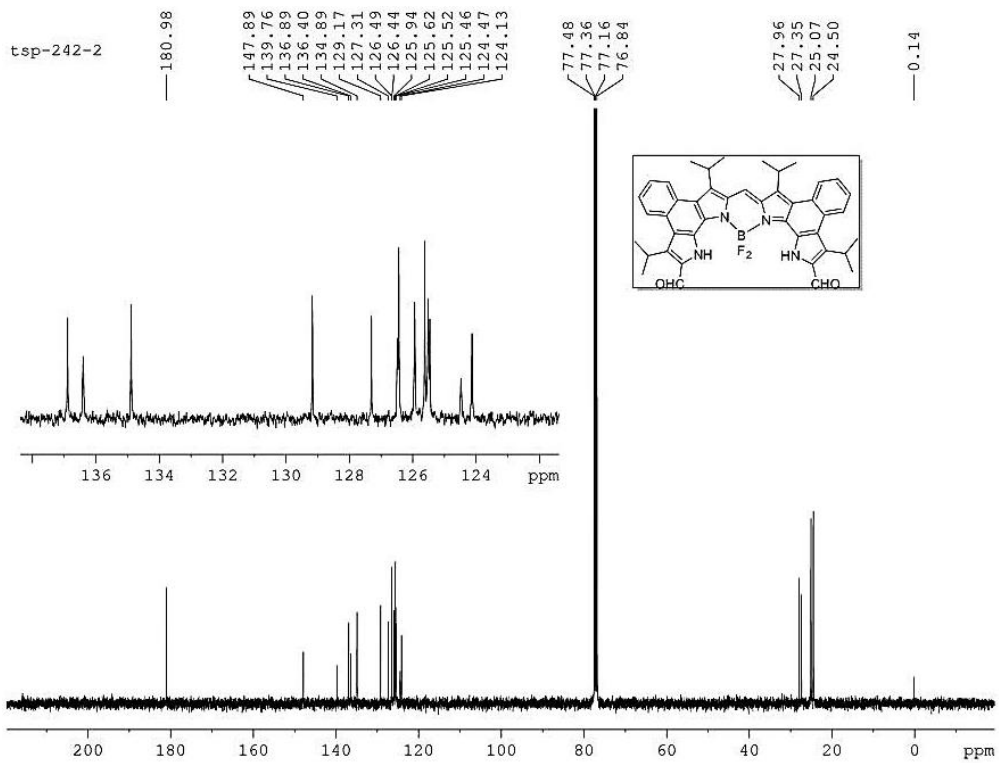

Figure A60 ^{13}C NMR spectrum of **TS36** in $CDCl_3$.

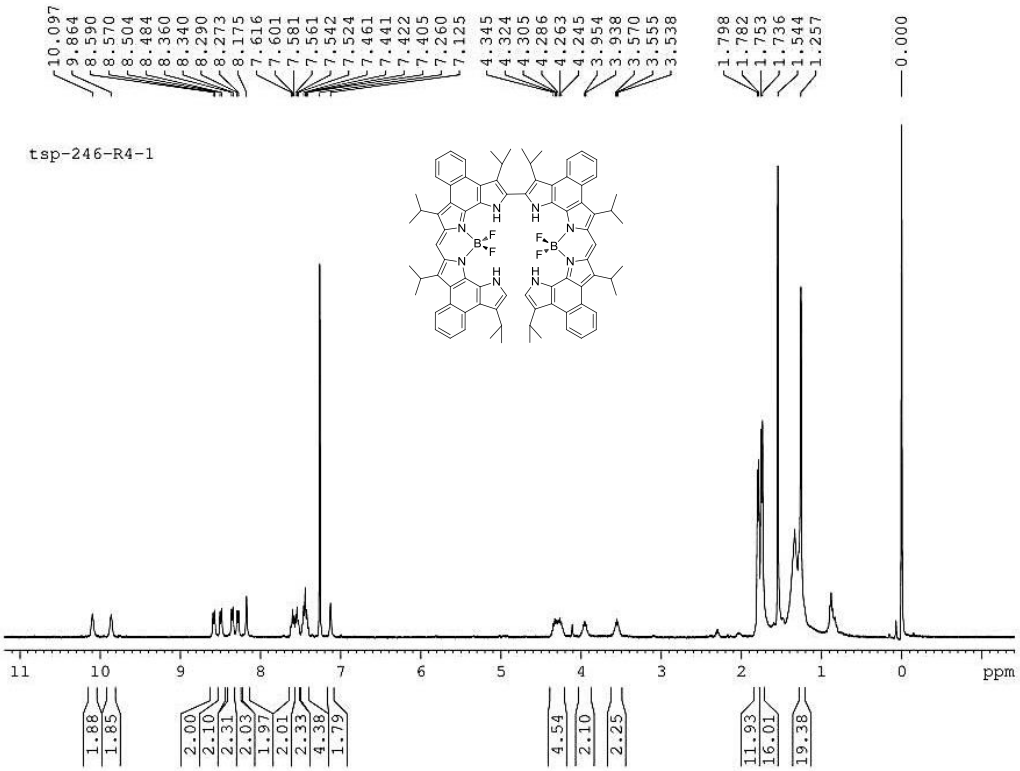

Figure A61 ^{1}H NMR spectrum of **TS37** in $CDCl_3$.

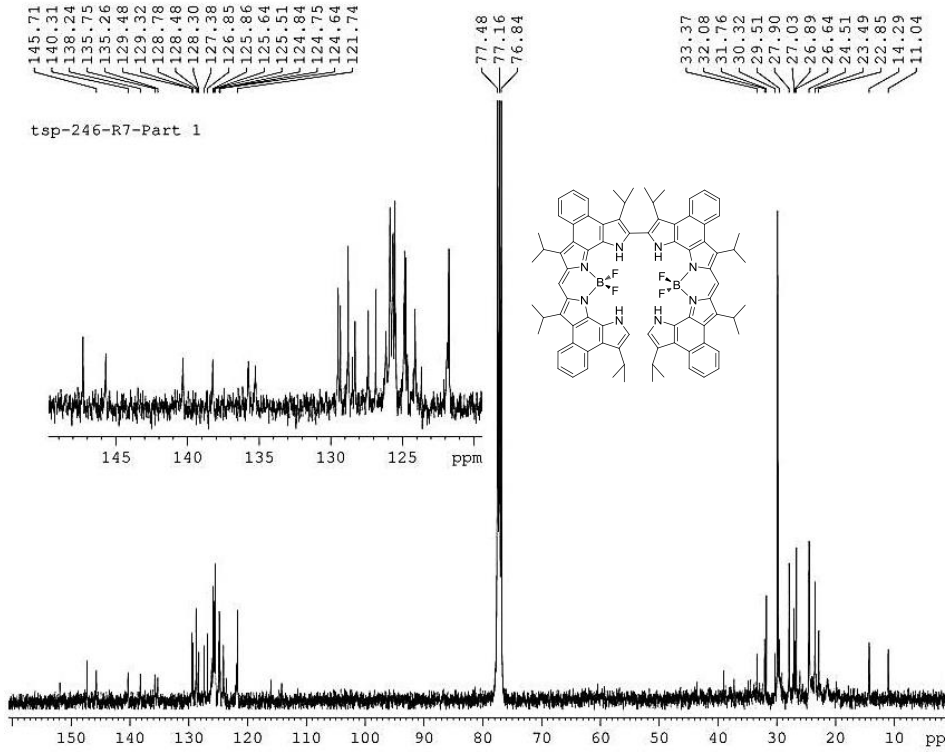

Figure A62 ^{13}C NMR spectrum of **TS37** in $CDCl_3$.

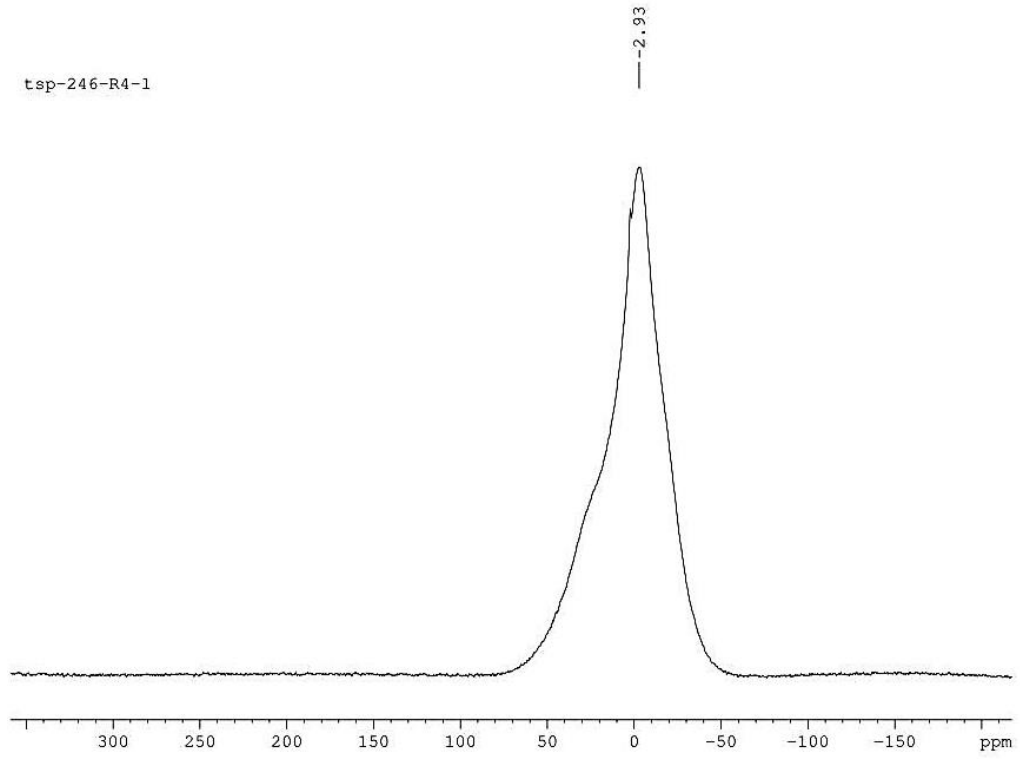

Figure A63 ^{11}B NMR Spectrum of compound **TS37** in $CDCl_3$.

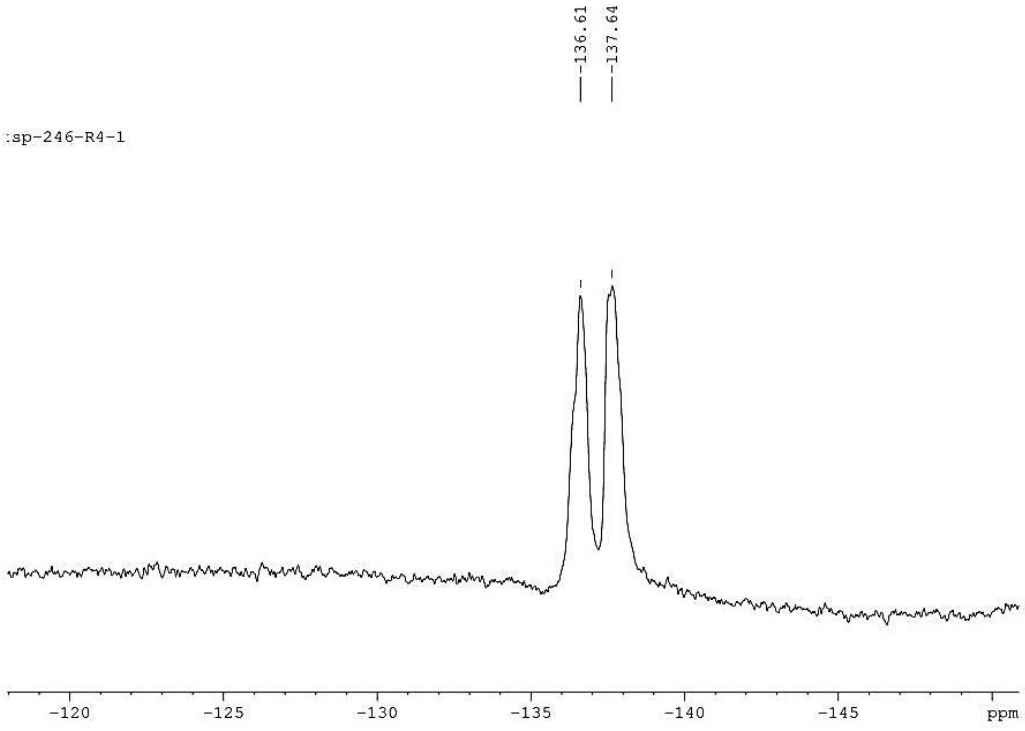

Figure A64 ^{19}F NMR Spectrum of compound **TS37** in $CDCl_3$.

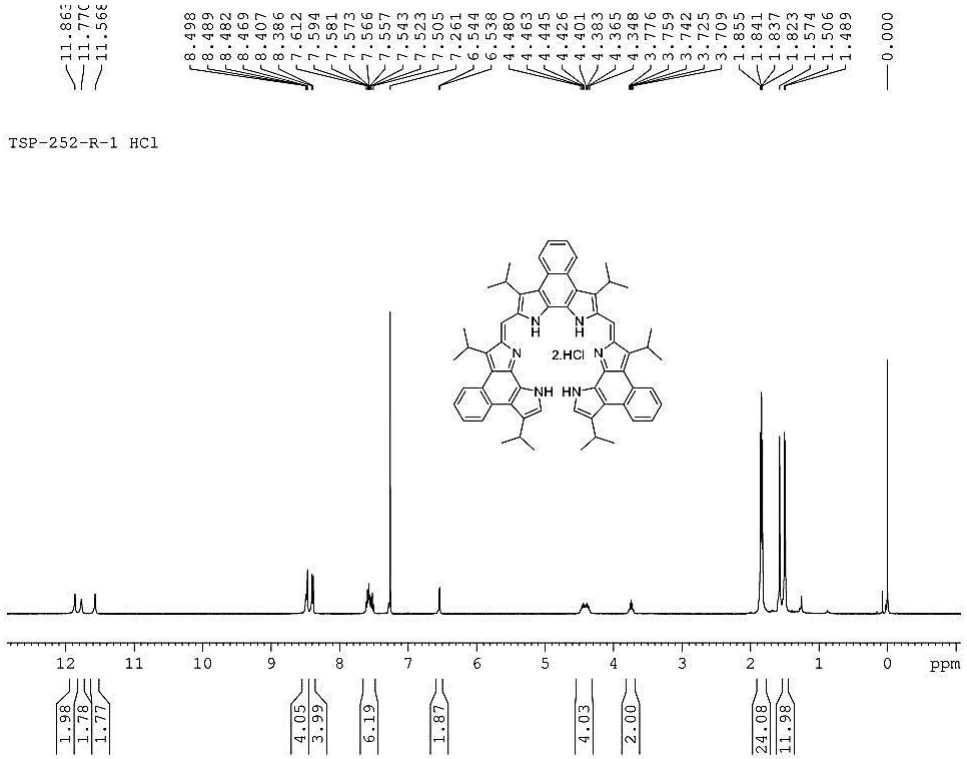

Figure A65 ^{1}H NMR spectrum of **TS38** in $CDCl_3$.

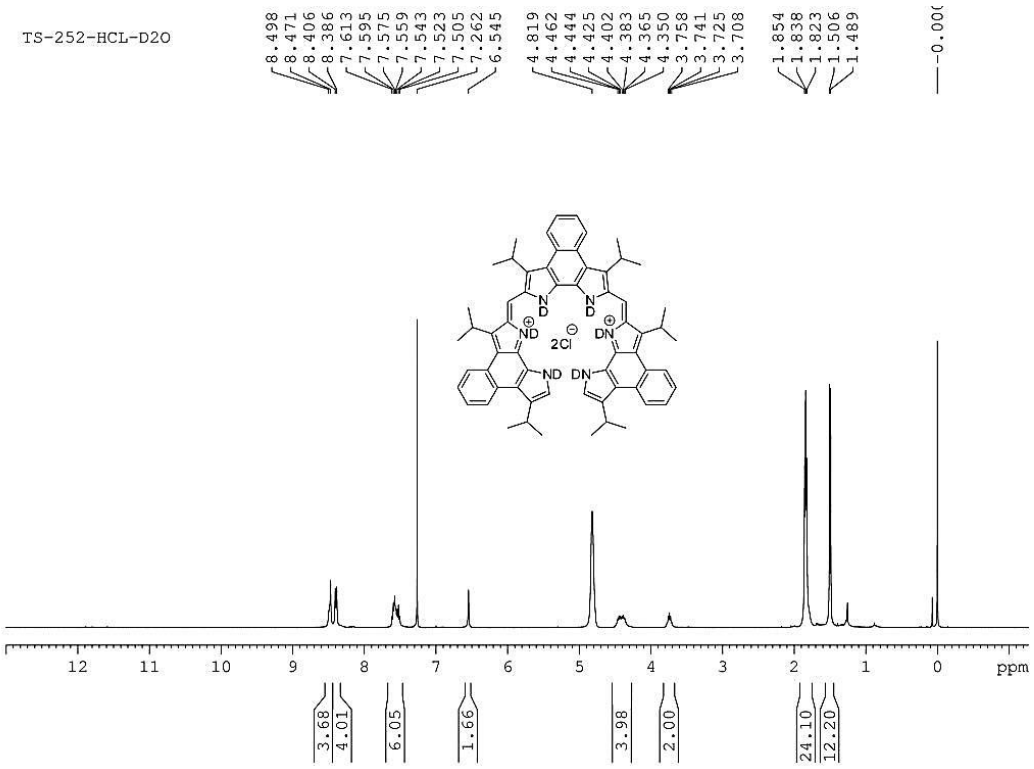

Figure A66 ^{1}H NMR spectrum of **TS38** in $CDCl_3$-D_2O.

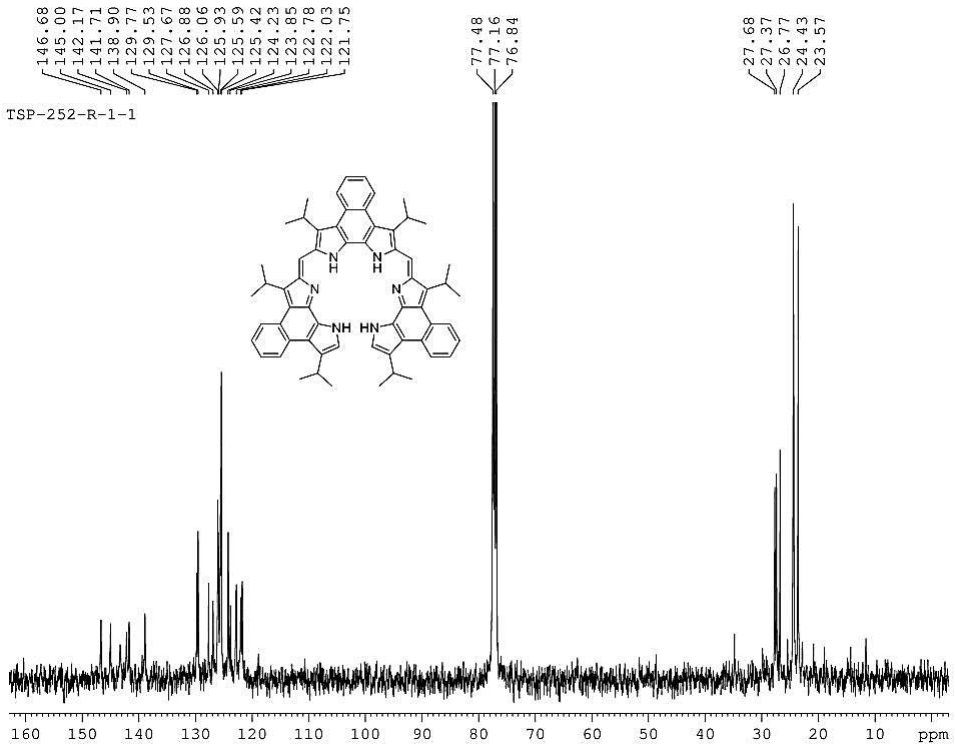

Figure A67 ^{13}C NMR spectrum of **TS38** in $CDCl_3$.

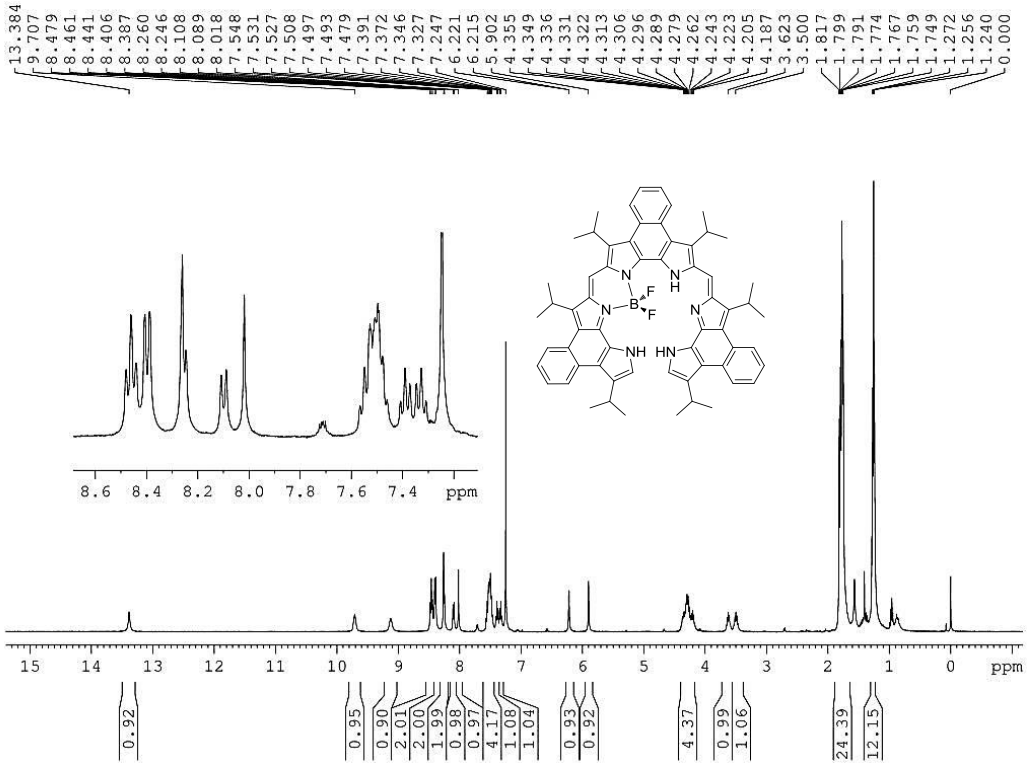

Figure A68 ^{1}H NMR spectrum of **TS39** in $CDCl_3$.

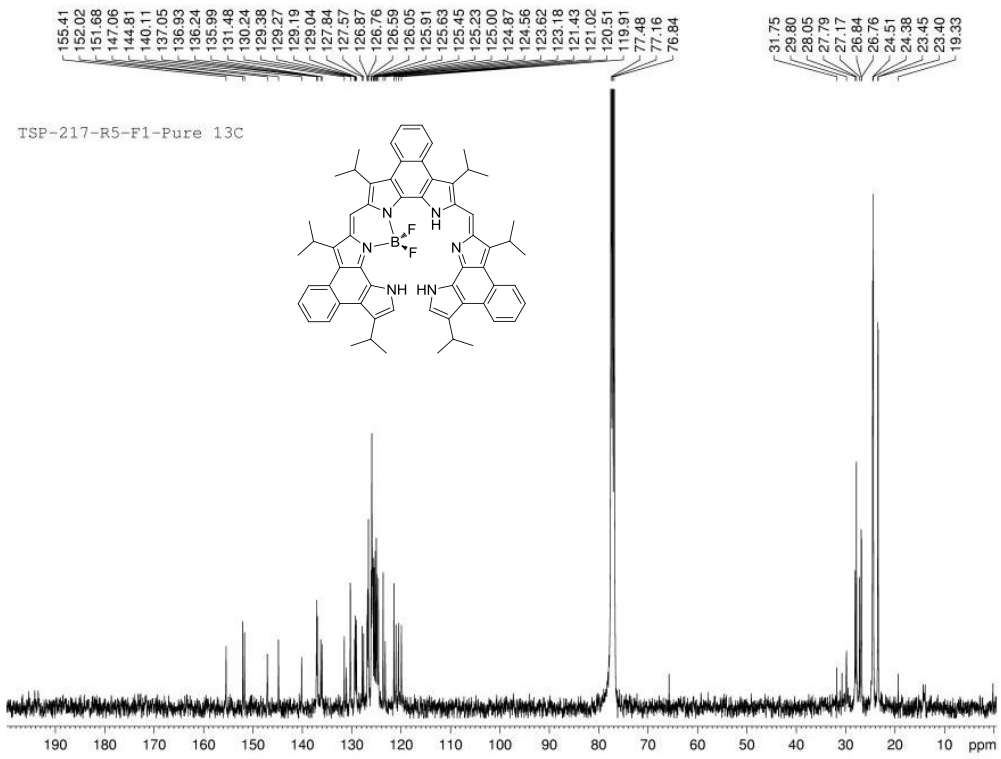

Figure A69 ^{13}C NMR spectrum of **TS39** in $CDCl_3$.

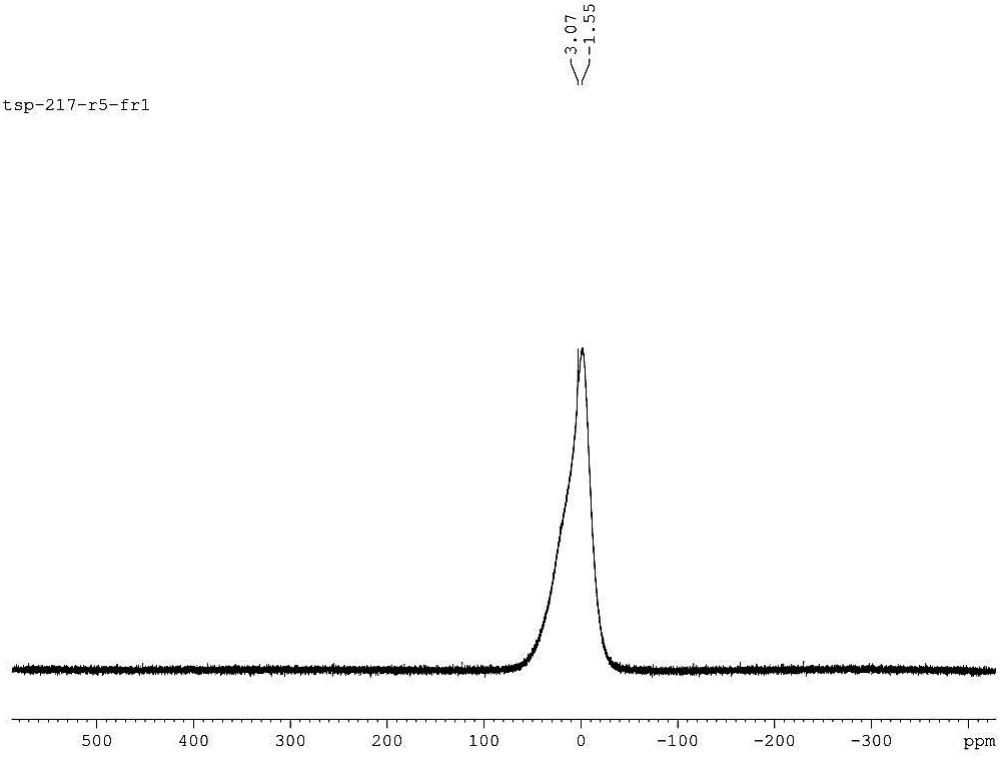

Figure A70 ^{11}B NMR Spectrum of compound **TS39** in $CDCl_3$.

Research Publications (Thesis)

1. Dinaphthoporphycenes: Synthesis and nonlinear optical studies, **Sarma, T**.; Panda, P. K.; Anusha, P. T.; Rao, S. V. *Org. Lett*. **2011**, *13*, 188.
2. Two-photon and three-photon absorption in dinaphthoporphycenes, Rao, S. V.; Prashant, T. S.; Swain, D.; **Sarma, T**.; Panda, P. K.; Tewari, S. P. *Chem. Phys. Lett.* **2011**, *514*, 96.
3. Cyclo[4]naphthobipyrroles: Naphthobipyrrole-Derived Cyclo[8]pyrroles with Strong Near-Infrared Absorptions, **Sarma, T**.; Panda, P. K. *Chem. Eur. J.* **2011**, *17*, 13987.
4. Ultrafast excited state dynamics and dispersion studies of nonlinear optical properties in dinaphthoporphycenes, Swain, D.; Anusha, P. T.; Prashant, T. S.; Tewari, S. P.; **Sarma, T**.; Panda, P. K.; Rao, S. V. *Appl. Phys. Lett*. **2012**, *100*, 141109.
5. Dispersion studies of optical nonlinearity and excited state dynamics in cyclo[4]naphthobipyrroles, Swain, D.; Anusha, P. T.; **Sarma, T**.; Panda, P. K.; Rao, S. V. *Chem. Phys. Lett.* **2013**, *580*, 73.
6. Bis-naphthobipyrrolylmethene derived BODIPY complex: an intense near-infrared fluorescent dye, **Sarma, T**.; Panda, P. K.; Setsune, J.-i. *Chem. Commun*. **2013**, in press (DOI:10.1039/C3CC44834G).

Conference Proceedings

7. Multiphoton Absorption Studies in Porphycenes Using Picosecond and Femtosecond Pulses, Swain, D.; Anusha, P. T.; Prashant, T. S.; Tewari, S. P.; **Sarma, T**.; Panda, P. K.; Rao, S. V. *AIP Conference Proceedings* **2011**, *1391*, 674.
8. Ultrafast nonlinear optical studies of cyclo[4]naphthobipyrroles, Anusha, P. T.; Swain, D.; Sarma, T.; Panda, P. K.; Rao, S. V. *Proc. of SPIE* 2012, *8434*, 84341D-1.

Research Publications (others)

9. Conformational and spectroscopic properties of π-extended, bipyrrole-fused rubyrin and sapphyrin derivatives, Kee, S.-Y.; Lim, J. M.; Kim, S.-J.; Yoo, J.; Park, J.-S.; **Sarma, T**.; Lynch, V. M.; Panda, P. K.; Sessler, J. L.; Kim, D.; Lee, C.-H. *Chem. Commun.* **2011**, *47*, 6813.
10. Protonation-coupled redox reactions in planar antiaromatic *meso*-pentafluorophenyl-substituted *o*-phenylene-bridged annulated rosarins, Ishida, M.; Kim, S.-J.; Preihs, C.;

Ohkubo, K.; Lim, J. M.; Lee, B. S.; Park, J. S.; Lynch, V. M.; Roznyatovskiy, V. V.; **Sarma, T**.; Panda, P. K.; Lee, C. H.; Fukuzumi, S.; Kim D.; Sessler, J. L. *Nat. Chem*. **2013**, *5*, 15.

Conference presentations

1. Poster presented on "Synthesis and characterization of dinaphthoporphycene and its metallo-derivatives", Modern Trend in Inorganic Chemistry, MTIC-XIII, December 07-10, **2009**, IISc, Bangalore.
2. Poster presented on "Synthesis and characterization of dinaphthoporphycene and its metallo-derivatives", 7th Annual In-House Symposium of the School of Chemistry, ChemFest-**2010**, University of Hyderabad.
3. Oral and poster presentation on "Cyclo[4]naphthobipyrroles: Naphthobipyrrole Derived Cyclo[8]pyrroles With Strong Near Infrared Absorptions:", Modern Trend in Inorganic Chemistry, MTIC-XIV, **2011**, University of Hyderabad.
4. Oral and poster presentation on "Naphthobipyrrole derived novel π-extended porphyrinoids", 9th Annual In-House Symposium of the School of Chemistry ChemFest-**2012**, University of Hyderabad.